MONASH University

The Structural and Functional Characterization of the Antigenic Domains on Hepatitis C Virus Glycoprotein E2

Jun Gu

Doctor of Philosophy

A thesis submitted for the degree of *Doctor of Philosophy* at
Monash University in 2018

Department of Microbiology,
Faculty of Medicine, Nursing and Health Sciences
Conducted in
The Viral Entry and Vaccines Laboratory, Life Sciences, Burnet Institute

Copyright notice

Declaration

This thesis contains no material which has been accepted for the award of any other degree or diploma at any university or equivalent institution and that, to the best of my knowledge and belief, this thesis contains no material previously published or written by another person, except where due reference is made in the text of the thesis.

Signature:  …

Print Name: ……Jun Gu…….

Date: ……12/7/2018…….

Preface

This is to acknowledge work conducted by others or in collaboration (in order of appearance in the thesis):

- Mouse monoclonal antibody production and isolation was performed by CSL Ltd (Parkville, Australia).
- Mouse monoclonal antibody characterization, except for reactivity towards E2 proteins with single point mutations, was conducted by Dr Yousef Alhammad and Dr Patricia Vietheer (Burnet Institute, Melbourne, Australia).
- Guinea pig immunization was conducted by CSL Ltd. in collaboration with Dr Patricia Vietheer (Burnet Institute, Melbourne, Australia).
- The expression and purification of recombinant WT E2 and D123 proteins were performed by CSL Ltd.
- The high throughput sequencing of HCVcc quasispecies was performed by Dr Silvana Gaudieri and Dr Abha Chopra (Institute for Immunology and Infectious Diseases, Murdoch University, Murdoch, Australia).
- The neutralization assay of HCVcc mutants was performed by Ms Irene Boo (Burnet Institute, Melbourne, Australia).
- The crystal structure of MAb24-peptide complex was solved by A/Prof Fasséli Coulibaly and Mr Joshua Hardy (Department of Biochemistry and Molecular Biology, Monash University, Clayton, Australia).
- The blood samples of chronic HCV subjects were obtained from Dr Mandvi Bharadwaj (Department of Microbiology and Immunology, University of Melbourne, Parkville, Australia) and Dr Peter Higgs (Burnet Institute, Melbourne, Australia).
- Phage library work was conducted in collaboration with Dr Stewart Nuttall (Biomedical Manufacturing, CSIRO Parkville, Australia).

Publications

Journal articles arising from this thesis include:

Alhammad, Y., Gu, J., Boo, I., Harrison, D., McCaffrey, K., Vietheer, P. T., Edwards, S., Quinn, C., Coulibaly, F., Poumbourios, P. & Drummer, H. E. (2015). Monoclonal Antibodies Directed toward the Hepatitis C Virus Glycoprotein E2 Detect Antigenic Differences Modulated by the N-Terminal Hypervariable Region 1 (HVR1), HVR2, and Intergenotypic Variable Region. *Journal of Virology* **89**, 12245-12261.

Vietheer, P. T., Boo, I., Gu, J., McCaffrey, K., Edwards, S., Owczarek, C., Hardy, M. P., Fabri, L., Center, R. J., Poumbourios, P. & Drummer, H. E. (2017). The core domain of hepatitis C virus glycoprotein E2 generates potent cross-neutralizing antibodies in guinea pigs. *Hepatology* **65**, 1117-1131.

Gu, J.*, Hardy, J.*, Boo, I.*, Vietheer, P., McCaffrey, K., Alhammad, Y., Chopra, A., Gaudieri, S., Poumbourios, P., Coulibaly, F. & Drummer, H. E. (2018). Escape of Hepatitis C virus from epitope I neutralization increases sensitivity of other neutralization epitopes. *Journal of Virology*. Accepted manuscript posted online 21 February 2018, doi:10.1128/JVI.02066-17 (*Authors contributed equally)

Conference Proceedings arising from this thesis include:

Gu, J., Nuttall, S., Hellard, M., Pantelis, P. & Drummer, H. E. (2013). Mapping broadly neutralizing antibody specificity from an individual chronically infected with HCV genotype 6a using phage display technology. In *20th International Symposium on Hepatitis C Virus and Related Viruses*. Melbourne, Victoria, Australia.

Gu, J., Alhammad, Y., Boo, I., Vietheer, P., Poumbourios, P. & Drummer, H. (2014). The presence of hypervariable regions in HCV glycoprotein E2 modulates antigen recognition and accessibility to E2 specific monoclonal antibodies. In *HCV2014: 21st International Symposium on Hepatitis C and Related Viruses*. Banff, Alberta, Canada.

Gu, J., Vietheer, P., Alhammad, Y., Boo, I., Poumbourios, P. & Drummer, H. (2014). Hepatitis C virus can accumulate mutations that confer resistance to a novel broadly neutralizing antibody MAb24. In *9th Australasian Viral Hepatitis Conference*. Alice Springs, Northern Territory, Australia.

Acknowledgement

I would like to express my deepest gratitude to my supervisors, A/Prof Heidi Drummer and Dr Andy Poumbourios for giving me the opportunity to work on such a challenging and interesting project in the Viral Entry and Vaccine laboratory, for providing financial support in my early PhD years, for their invaluable advice on my experiments, project progress and directions, conference and thesis preparation, and for their continued support, guidance and supervision during my candidature.

I would also like to thank past and present members of the lab, particularly Dr Kathleen McCaffrey, Dr Patricia Vietheer, Dr Yousef Alhammad, and Ms Irene Boo for their amazing ground work on D123; Dr Robert Center for lab advice and thesis draft revision; Ms Irene Boo, again, for providing me with enormous amount of assistance in the lab and more than sufficient amounts of chocolate and snacks in the office.

It has also been my great privilege to conduct collaborative work with brilliant minds like A/Prof Fasséli Coulibaly, Mr Joshua Hardy, Dr Silvana Gaudieri, Dr Abha Chopra, and Dr Stewart Nuttall, all of whom are true experts in their respective fields. Thanks, Fasséli and Joshua for solving the crystal structure and giving me a “eureka” moment to enjoy; Silvana and Abha for numerous Skype calls to explain NGS to me; Stewart, and colleagues at CSIRO Parkville campus, Ms Lesley Pearce, Dr Greg Coia, and Dr Timothy Adams for accommodating me in the Parkville campus, giving me lab space, reagents, equipment as well as office space for the phage library work.

I am very grateful to colleagues at Burnet Institute who had provided me with training and/or excellent resources, Ms Devy Santoso and Ms Kylie Milne from 360biolabs for training me how to properly process PBMCs, Dr Rachel Sack-Davies and Dr Peter Higgs from Population Health for providing me with valuable information on samples. I am also grateful to Ms Sherrie Young at Department of Microbiology at Monash, who patiently took care of all my requests for various administrative paperwork.

I would like to acknowledgement funding organizations that provided travel grants during my PhD, including ASHM Junior Research Support Awards, Micromon Travel Grant (both national and international), travel grant from Monash Institute of Graduate Research, and a travel award from the organizing committee of the 21st International Symposium on Hepatitis C virus and Related viruses (HCV2014).

Lastly, to my family and friends, especially my mum and my two dearest friends, Cathy and Linda Xu, thank you for your continued support and counselling, even in my darkest time.

Table of Content

Abstract

It is estimated that in 2015, 71 million people worldwide were infected with hepatitis C virus (HCV). Whilst ~25% of HCV cases are acute and spontaneously resolve, ~75% will progress to chronic infection, if untreated, and can lead to cirrhosis and hepatocellular carcinoma. As an RNA virus, HCV exhibits enormous genetic diversity, which greatly impedes its control and prevention. Although direct acting antivirals (DAAs) have begun to greatly reduce the number of HCV infections in countries that have adopted and accelerated the use of DAA therapy, the prevention and elimination of HCV still requires a universal vaccine, which is not available. One of the key criteria for an effective antibody-based HCV vaccine is the ability to potently elicit broadly reactive neutralizing antibodies that inhibit early events in viral entry.

The entry of HCV into hepatocytes is primarily mediated by the HCV glycoprotein E2, which forms heterodimers with glycoprotein E1. During HCV infection, E2 directly interacts with the host cell receptor CD81, and the CD81 binding site is a major target of neutralizing antibodies (NAbs). The receptor binding domain (RBD) of E2 is comprised of the N-terminal 278 residues of E2 and contains three hypervariable regions (HVRs). When the RBD is expressed in isolation, the three HVRs can be deleted to produce the E2 core domain (D123) whilst maintaining key functions of CD81 binding and retaining major NAb epitopes. Additionally, the isolated E2 RBD and D123 inherently fold into multiple disulfide-linked oligomeric forms. Structural studies of the truncated monomeric E2 core domain show that it adopts a compact globular structure with a flexible neutralizing face, consisting of four known cross-reactive neutralizing epitopes (I-IV), which also overlaps with the proposed CD81 binding surface.

This study found that the each of the three HVRs contributed to modulating the antibody recognition of E2 while D123 showed enhanced immunogenicity of at least two cross-reactive neutralizing epitopes (epitope I and III) in guinea pigs. In addition, the high order oligomeric forms of D123 were able to elicit higher titres of cross-reactive antibodies towards epitope I and III than the monomeric counterpart. These findings suggested that the HVRs of E2 play a pivotal role in the

immunogenicity of cross-reactive neutralizing epitopes, and the high order oligomeric forms of D123 are improved candidates for a universal vaccine. Isolated from mice immunized with D123, monoclonal antibody MAb24 recognizes epitope I, a major cross NAb epitope, and is broadly neutralizing. Structural studies performed here showed that epitope I adopts a β-hairpin conformation when complexed with MAb24, whilst long-term *in vitro* passaging of HCV with MAb24 demonstrated that HCV was able to rapidly escape MAb24 neutralization by two distinct mechanisms involving changes at residue N415. The resistant mutations greatly increased the sensitivity of HCV to NAbs targeting other regions on E2 and the E1E2 heterodimer. A poly-specific immune response to a vaccine candidate such as D123 is therefore required to prevent HCV escape. Lastly, using *in vitro* neutralization assay screening, this study identified individuals who had potent cross NAbs amongst a small cohort of chronic HCV patients and characterized the antibody repertoire of one subject. Future investigation into the structural and functional roles of E1E2 heterodimers and the isolation and characterization of novel broadly neutralizing antibodies are needed for the design of an effective HCV vaccine.

List of Tables

List of Figures

Appendix I Abbreviations

ADCC	antibody-dependent cellular cytotoxicity
ALT	alanine aminotransferase
apo	apolipoprotein
BCR	B cell receptor
brNAb	broadly neutralizing antibody
CDC	complement-dependent cytotoxicity
cDNA	complementary DNA
CDR	complementarity determining region
C_H	the constant region of the heavy chain
CHO	Chinese hamster ovary
C_L	the constant region of the light chain
CLDN1	claudin-1
DAA	direct acting antiviral
DC-SIGN	dendritic cell-specific intercellular adhesion molecule 3-grabbing non-integrin
DMEM	Dulbecco's Modified Eagle Medium
DNA	deoxyribonucleic acid
EBV	Epstein Barr virus
EGFR	epidermal growth factor receptor
EL	extracellular loop
ELISA	enzyme linked immunosorbent assay
EphA2	ephrin receptor type A2
ER	endoplasmic reticulum
Fab	antigen binding fragment
FDA	Food and Drug Administration
FR	frame region
GAG	glycosaminoglycan
GNA lectin	*Galanthus nivalis* lectin
GWASs	genome wide association studies
HBV	hepatitis B virus
HC	heavy chain
HCC	HCV-related hepatocellular carcinoma

HCV	hepatitis C virus
HCVcc	cell culture-derived HCV
HCVpp	pseudotyped HCV particle
HDL	high-density lipoprotein
HEK	human embryonic kidney
HIV	human immunodeficiency virus
HMAb	human monoclonal antibody
HMW	high molecular weight
HRP	horseradish peroxidase
HSPG	heparan sulfate proteoglycan
HVRs	hypervariable regions
HVR1	hypervariable region 1
HVR2	hypervariable region 2
IC_{50}	50% inhibitory concentration
IC_{80}	80% inhibitory concentration
ID	inhibitory dose
IDL	intermediate-density lipoprotein
IDU	injecting drug user
IFA	immunofluorescence assay
IFN	interferon
Ig	immunoglobulin
igVR	intergenotypic region
IPTG	isopropyl ß-D-1-thiogalactopyranoside
IRES	internal ribosome entry site
ISGs	interferon-stimulated genes
L-SIGN	liver/lymph node-specific intercellular adhesion molecule 3-grabbing integrin
LC	light chain
LDL	low density lipoprotein
LDLR	low density lipoprotein receptor
LEL	large extracellular loop
LVP	lipoviroparticle
MAb	monoclonal antibody
MBP	maltose-binding protein

MHC	major histocompatibility complex
MPHR	membrane proximal heptad repeat
MWCO	molecular weight cut-off
NAb	neutralizing antibody
NOB	neutralization of binding
NPC1L1	Niemann-Pick C1-like 1
NS	non-structural protein
OD	optical density
OLDN	occludin
PBMC	peripheral blood mononuclear cell
PBS	phosphate buffered saline
PCR	polymerase chain reaction
PD-1	programmed cell death-1
PEG	polyethylene glycol
PEI	polyethylenimine
PFU	plaque forming unit
PGS	protein G sepharose
RBD	receptor binding domain/ectodomain
RNA	ribonucleic acid
RT	room temperature
RT-PCR	reverse transcription polymerase chain reaction
scFv	single chain variable fragment
SDS-PAGE	sodium dodecyl sulfate polyacrylamide gel electrophoresis
SEL	short extracellular loop
siRNA	small interfering RNA
SR-BI	scavenger receptor B type I
SVR	sustained virologic response
TBEV	tick-borne encephalitis virus
TfR1	transferrin receptor 1
TLR	toll-like receptor
TMB	3,3’,5,5’-tetramethylbenzidine
TMD	transmembrane domain
TNF	tumor necrosis factor
UTR	untranslated region

VLDL	very low-density lipoprotein
V_H	the variable region of the heavy chain
V_L	the variable region of the light chain
VLP	virus-like particle
WHO	World Health Organization
μ	micro
Å	angstrom

Appendix II The epitope maps of published HMAbs

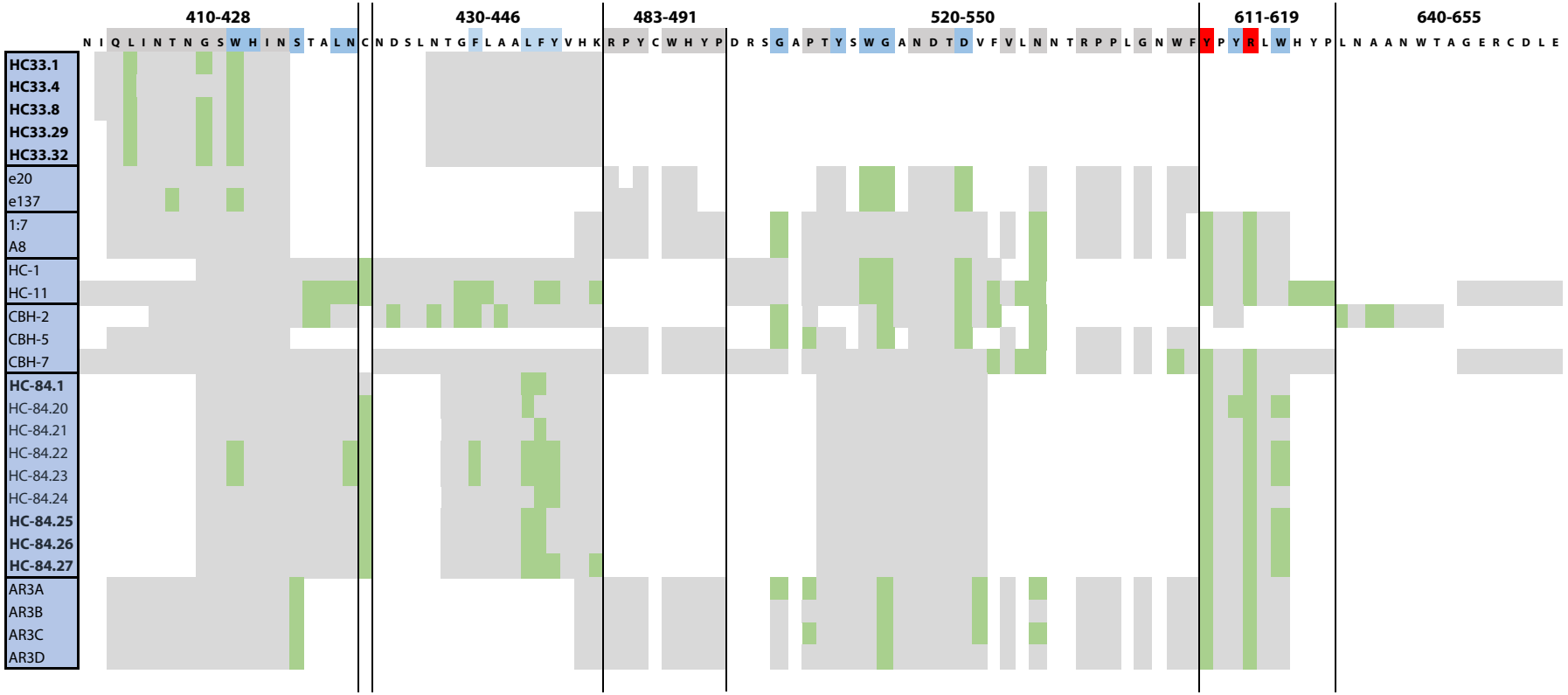

HMAbs in bold: recognize linear peptides; residues in blue: involved in E2-CD81 binding; residues in grey: MAb-E2 binding characterized but do not affect MAb-E2 binding; residues in green: mutations at these residues reduce HMAb-E2 binding to less than 25% of HMAb-WT E2 binding.

The epitopes of HC33-related HMAbs were mapped by Keck *et al*. (2013). The epitopes of HMAbs e20 and e137 were described in Mancini *et al.* (2009) and Perotti *et al.* (2008), respectively. The epitopes of HMAbs 1:7 and A8 were characterized by Johansson *et al.* (2007). The epitopes of HMAbs HC-1, HC-11, CBH-2, CHB-5, CBH-7 were determined by Keck *et al.* (2008) and Keck *et al.* (2011). The epitopes of HC84-related HMAbs listed here were reported by Keck *et al.* (2012). The AR3A, AR3B, AR3C and AR3D epitope maps were published in Law *et al.* (2008) and Kong *et al.* (2013)

Chapter 1 Introduction

1.1 HCV: a silent epidemic

Transfusion-associated non-A, non-B hepatitis was first reported in the 1970s (Feinstone *et al.*, 1975). It was not until 1989 that hepatitis C virus (HCV) was identified as the causative agent (Choo *et al.*, 1989). HCV is classified into the genus *Hepacivirus* of the *Flaviviridae* family and is distantly related to flaviviruses such as tick-borne encephalitis virus (TBEV) and dengue virus. It is primarily transmitted via parenteral exposure, including transfusion of contaminated blood products, which remains the major mode of transmission in developing countries. In developed countries, HCV disproportionately affects injecting drug users (IDUs), although accidental exposure associated with invasive medical procedures, needle stick injuries, haemodialysis as well as tattooing and piercing have been reported but are less common (Smith *et al.*, 2012). About 55-85% of HCV-infected individuals become asymptomatic chronic carriers of the virus (WHO, 2016). If untreated, about 16% of chronic carriers will develop cirrhosis or hepatocellular carcinoma which eventually progresses into end stage liver failure (Thein *et al.*, 2008). This makes HCV the major cause for liver transplantation in developed countries. In Australia, adult liver transplants associated with HCV have increased from 3% to 29% between 1989 and 2013 whilst HCV-related mortality in the US has surpassed 60 other infectious diseases combined including HIV (Ly *et al.*, 2016; Lynch & Balderson, 2014).

By 2013, 92-149 million people globally have had HCV infection and it is estimated that 71 million people were living with HCV in 2015 (Gower *et al.*, 2014; WHO, 2017). Developing countries recorded the highest prevalence of HCV. In Egypt, 10.3%-18% of the population are seropositive for HCV whilst 7%-12.2% are RNA positive which is indicative of active HCV infection. China recorded the highest HCV prevalence with an estimated 13-17 million cases of viraemic infection (Gower *et al.*, 2014; Messina *et al.*, 2015). The HCV epidemic is further complicated by the genetic diversity of the virus. To date, HCV has been classified into 7 genotypes (Genotype 1-7, or G1-7) and further divided into 67 confirmed subtypes,

20 provisional and 21 unassigned novel subtypes (Smith *et al.*, 2014). At the nucleotide level, the intra-genotypic and inter-genotypic differences are 20-25% and >30%, respectively (Simmonds *et al.*, 2005). As the major genotype responsible for the HCV epidemic, G1 is found in most parts of the world including Australasia, North America and Europe and accounts for 46% of the infections worldwide, followed by G3 (30.1%) (Messina *et al.*, 2015). In contrast, G4 and G6 are endemic in Central Africa and Southeast Asia, respectively, contributing to 13.7% of HCV cases globally. While countries such as Egypt are predominantly affected by a single genotype, significant genotypic diversity is observed in countries such as China and Australia. These differences in HCV genotypes and geographical distribution contribute to obstacles for HCV control and eradication.

Recent epidemiological data indicate that the prevalence of HCV is declining, possibly due to successful public health interventions and the release of new antiviral treatments. However, given the asymptomatic nature of HCV infections and the lack of routine screening, cases of HCV are often underreported. For instance, in the US, 50%-75% of the infected individuals are unaware of their HCV status. As a result, one of the major US risk groups, the1945-1965 birth cohort, is likely to contribute over 1 million new HCV cases (Rein *et al.*, 2012; Smith *et al.*, 2012). Therefore, HCV still poses a major threat to the global health system. In 2016, the World Health Assembly called for the elimination of viral hepatitis, mainly hepatitis B and C as a public health threat by 2030, and aims to "reduce new infections by 90% and mortality by 65%" (WHO, 2017).

The elimination of HCV cannot be achieved without a thorough understanding of HCV virology, and efforts to develop and implement effective treatment and prevention strategies. This chapter will give a brief overview of *in vitro* and *in vivo* models developed to study HCV and the present knowledge on HCV virology. Current understanding of HCV infection and immunity and current research efforts on the prevention strategies in the control of the HCV epidemic will then be discussed. Together, these form the theoretical framework and rationale for this thesis.

1.2 HCV study models

1.2.1 In vitro models

Until the discovery of the Japanese fulminant hepatitis C virus strain, JFH-1 (G2a), and the production of its full-length infectious clone in 2005, it was not possible to replicate patient-derived viruses in hepatoma cells (Kato *et al.*, 2001; Wakita *et al.*, 2005; Zhong *et al.*, 2005). This greatly impeded the characterization of HCV virions and the study of HCV entry and replication. To overcome this limitation, pseudotyped retroviral particles incorporating the envelope proteins E1 and E2 (HCVpp) and heterologous overexpression of glycoproteins were used to identify HCV entry factors and characterize the functional elements of E1 and E2. Initial HCV studies examined the biochemical characteristics and biogenesis of truncated soluble forms of E2 (Michalak *et al.*, 1997) and E1E2 glycoprotein complexes (Dubuisson *et al.*, 1994; Ralston *et al.*, 1993). This later led to the discovery of two essential HCV host cell coreceptors, CD81 and SR-BI (Pileri *et al.*, 1998; Scarselli *et al.*, 2002). The interaction between E2 and CD81 has since been studied extensively. To further determine the structure and antigenic features of HCV surface proteins in the context of whole virions, HCV virus-like particles (VLPs) expressed in insect cell lines using the Baculovirus expression system were developed (Baumert *et al.*, 1998; Clayton *et al.*, 2002; Owsianka *et al.*, 2001). These systems provided early findings on structural and antigenic differences in soluble E2, HCV E1E2 proteins as well as HCV VLPs (Clayton *et al.*, 2002; Owsianka *et al.*, 2001).

To elucidate the early events in HCV entry, infectious retroviral particles bearing HCV structural glycoproteins E1 and E2 (HCVpp, G1a and G1b) were expressed in human embryonic kidney cell line HEK293T cells (Bartosch *et al.*, 2003b; Drummer *et al.*, 2003; Hsu *et al.*, 2003). HCVpp can initiate entry into several human hepatoma cell lines including Huh7 and its derivatives. The development of this pseudotyping system enabled studies on the role of the E1E2 complex in viral entry as well as the role of neutralizing antibodies that inhibit entry (Bartosch *et al.*, 2003a). Most importantly, two additional HCV host cell coreceptors, claudin-1 and occludin were identified using HCVpp (Evans *et al.*, 2007; Ploss *et al.*, 2009). However, limited numbers of patient-derived E1E2 sequences can produce infectious

HCVpp particles (Owsianka *et al.*, 2005; Tarr *et al.*, 2011). Many isolates resulted in defective E1E2 expression or incorporation of nonfunctional E1E2 complexes. In addition, HCVpp can only serve as a surrogate system for HCV entry since the biogenesis of HCVpp is distinctly different from native HCV (Catanese & Dorner, 2015). The former occurs on post-Golgi compartments in HEK293T cells that lack lipid metabolism, whereas the later occurs in the endoplasmic reticulum (ER) and is closely associated with host cell lipoprotein biogenesis.

Following the isolation of the highly efficient JFH-1 subgenomic replicons, cell culture-derived HCV virus (HCVcc) was generated in hepatocytes transfected with the full-length RNA and was shown to replicate efficiently *in vitro* (Wakita *et al.*, 2005; Zhong *et al.*, 2005). The HCVcc system was further complemented with the development of a highly permissive human hepatoma cell line Huh7.5 (Blight *et al.*, 2002). This enabled the entire replication cycle of HCV to be studied both *in vitro* and in the only animal model of HCV infection, the chimpanzee (Lindenbach *et al.*, 2005; Lindenbach *et al.*, 2006; Wakita *et al.*, 2005). Since then, various intragenotypic and intergenotypic chimeras containing structural components from all 7 genotypes have been constructed containing the nonstructural regions of JFH-1 (Gottwein *et al.*, 2009; Lindenbach *et al.*, 2005; Lindenbach *et al.*, 2006; Pietschmann *et al.*, 2006). These provide a useful platform for screening pan-genotypic entry inhibitors or broadly neutralizing antibodies.

Recently, more novel techniques to culture full-length HCV from different genotypes, strains and clinical isolates *in vitro* have been developed. For instance, highly efficient full-length G1a (strains TN, H77 and HCV1) and 2b HCVcc were constructed (Li *et al.*, 2012; Li *et al.*, 2015b; Ramirez *et al.*, 2014). Furthermore, a host factor SEC14L2 was found to allow pan-genotypic replication of HCV *in vitro* without adaptive mutations and support replication of patient-derived viruses (Saeed *et al.*, 2015).

1.2.2 Animal models

To fully understand HCV infection, animal models need to be used to recapitulate the complete HCV replication cycle within the host (Beld *et al.*, 1999). Chimpanzees are the only animal model for HCV studies as they can be

experimentally infected with HCV, either through intrahepatic injection of HCV RNA or by intravenous inoculation of HCV particles. Early studies on the viral kinetics, liver pathology, infection outcomes, and protective immune responses of HCV relied primarily on the use of chimpanzees (Bukh, 2004). Once infected, chimpanzees tend to present a milder disease than humans, with distinct cytoplasmic tubular structures in liver biopsies (Alter *et al.*, 1978; Feinstone *et al.*, 1981).

In recent years, more studies have been directed to alternative small animal models because of the high cost and ethical restrictions associated with chimpanzee experiments. Mice are not naturally susceptible to HCV infection. However, several murine models were developed to circumvent this, including immunodeficient uPA-SCID mice transplanted with human hepatocytes (Mercer *et al.*, 2001), transgenic mice with human host coreceptors CD81 and occludin (Dorner *et al.*, 2011; Dorner *et al.*, 2013) and mice with human immune systems and hepatocytes (Bility *et al.*, 2012; Washburn *et al.*, 2011). Rhesus macaques have also recently been evaluated as an alternative non-human primate model for the study of HCV replication (Scull *et al.*, 2015).

1.3 HCV genome

HCV is a positive-sense, single-stranded RNA virus with a genome size of ~9.6kb (Choo *et al.*, 1991). The viral RNA is flanked by two conserved untranslated regions (UTRs), the 5'-UTR and the 3'-UTR. The 5'-UTR contains the internal ribosome entry site (IRES) responsible for initiating translation of the HCV genome, and both UTRs are important in replication (Han *et al.*, 1991; Kolykhalov *et al.*, 1996). The HCV genome encodes a single polyprotein precursor (~3000 amino acids in size) that is co- and post-translationally cleaved by viral or host signal peptidases, into 10 mature proteins including the N-terminal structural proteins (core, glycoproteins E1 and E2) and the C-terminal non-structural proteins (p7, NS2, NS3, NS4A, NS4B, NS5A and NS5B), as shown in Figure 1.1A. Whilst the core protein forms the integral part of the viral nucleocapsid encapsulating the viral RNA, the two type I transmembrane proteins, E1 and E2, are embedded in the viral membrane, mediate HCV entry and are targets of the humoral immune response (Figure 1.1B). HCV replication relies on the non-structural proteins such as NS3/4A, a serine protease responsible for the cleavage of the polyprotein and NS5B, a low-fidelity

RNA-dependent RNA polymerase. These non-structural proteins are not incorporated into virions. In addition, an alternative reading frame of HCV which overlaps the core gene was also reported (Walewski *et al.*, 2001). It encodes for a novel product, protein F whose exact role is yet to be defined.

1.4 HCV virions

An average of ~10^{12} HCV virions can be produced daily from the liver of an infected individual and these viral particles are present in the circulating blood (Neumann *et al.*, 1998). Cell culture-derived HCV particles are spherical and pleomorphic with the particle size ranging from 40nm to 100nm (Catanese *et al.*, 2013; Gastaminza *et al.*, 2010; Wakita *et al.*, 2005). Characterization of both patient and cell culture-derived HCV showed that the virions consist of lipoviroparticles (LVPs, illustrated in Figure 1.1C), which are rich in triglycerides and cholesteryl esters (Merz *et al.*, 2011; Petit *et al.*, 2005). For instance, present in HCV particles derived from primary hepatocytes are apolipoprotein (apo) A-I, a high-density lipoprotein (HDL) component, as well as low-density lipoprotein (LDL), intermediate-density lipoprotein (IDL) and very low-density lipoprotein (VLDL)-associated apoB (Catanese *et al.*, 2013). In addition, apoE, found mostly in VLDL, is more abundant on the virion than the envelope glycoprotein E2, as the anti-ApoE antibody showed a 10-fold higher capacity to capture RNA-containing HCV particles than the anti-E2 antibody, and is important for HCV infectivity (Hishiki *et al.*, 2010). The close association of lipoproteins with HCV, particularly LDLs and VLDLs, is thought to contribute to the low buoyant density observed in patient-derived HCV, ranging from 1.03 g/mL to 1.10g/mL (André *et al.*, 2002; Kanto *et al.*, 1994; Kanto *et al.*, 1995; Miyamoto *et al.*, 1992; Nielsen *et al.*, 2006; Thomssen *et al.*, 1992; Thomssen *et al.*, 1993). While the low-density fraction is highly infectious, the high-density component is less infectious and consists of HCV-antibody complexes (André *et al.*, 2002; Bradley *et al.*, 1991; Dienstag *et al.*, 1979; Hijikata *et al.*, 1993; Kanto *et al.*, 1994).

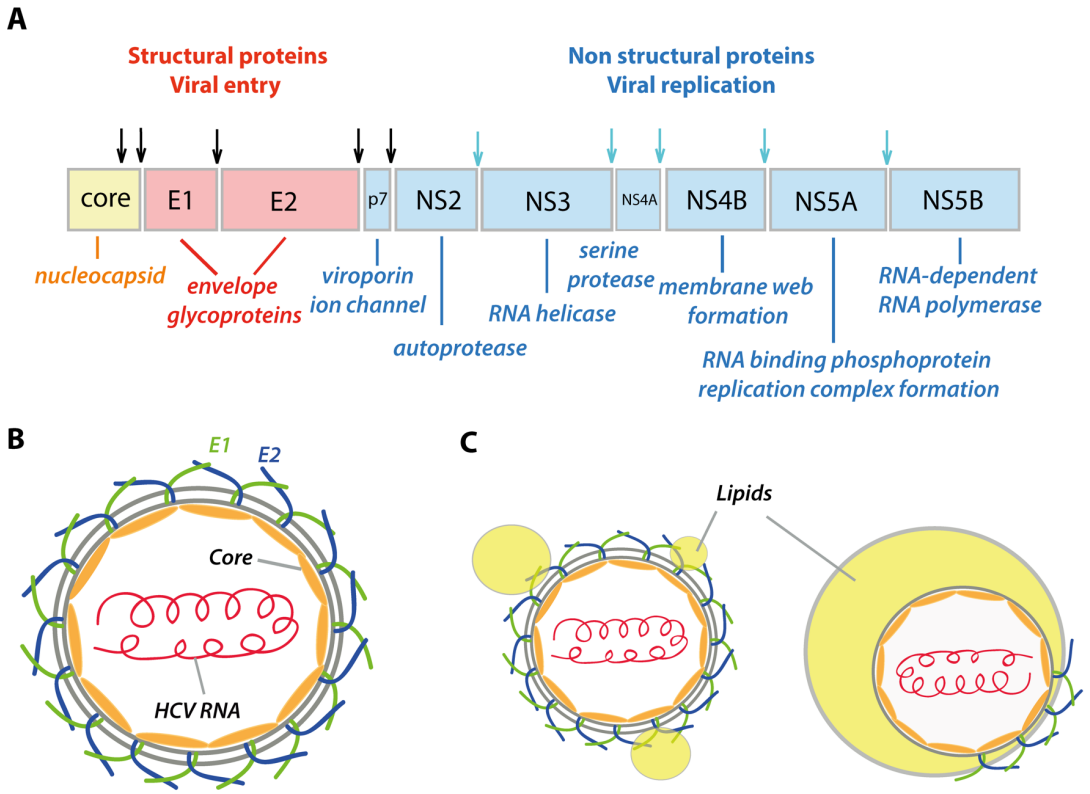

Figure 1.1 The HCV virion. (A) The genome organization of HCV. The HCV polyprotein is cleaved by host peptidases (black arrows) and viral proteases (blue arrows) into 3 structural proteins (yellow and red) and 7 non-structural proteins (blue). (B) Schematic diagram of the HCV particle. The envelope glycoproteins E1 (green) and E2 (dark blue) form heterodimers on the lipid bilayer while the viral RNA is encapsulated by a nucleocapsid made of core proteins. (C) Alternative models of the HCV lipoviroparticle. The HCV particle is decorated with small droplets of lipids (left). Or, the majority of the HCV surface is shielded with a large lipid droplet (right) (Lindenbach & Rice, 2013).

1.5 HCV entry

The entry of HCV into hepatocytes is a multi-step process that involves multiple host cell coreceptors as well as other entry factors. It is mediated by the envelope proteins E1 and E2 that attach the virions to host cell coreceptors and function in fusion of the viral and cellular membrane.

1.5.1 HCV entry: the envelope glycoproteins E1 and E2

The E1E2 heterodimers

The HCV envelope glycoproteins E1 (residues 191-383) and E2 (residues 384-746) form essential structural components of infectious particles and are sufficient and necessary for HCV entry into hepatocytes (Bartosch *et al.*, 2003b; Drummer *et al.*, 2003; Hsu *et al.*, 2003). E2 is involved in HCV receptor binding, and interacts with host coreceptors CD81 and SR-BI (Pileri *et al.*, 1998; Scarselli *et al.*, 2002). Using heterologous expression systems, co-immunoprecipitation using E1 or E2-specific antibodies showed that intracellularly-expressed E1E2 forms both non-covalent heterodimers and disulfide-linked high molecular weight complexes (Dubuisson *et al.*, 1994; Grakoui *et al.*, 1993; Ralston *et al.*, 1993). While the disulfide-linked complexes were considered misfolded aggregates that underwent nonproductive folding, the noncovalently-linked E1E2 heterodimers were thought to be the functional complexes, as they are the predominant species produced intracellularly as well as found on the HCVpp surface, and are capable of binding to CD81 and mediate HCVpp entry (Deleersnyder *et al.*, 1997; Drummer *et al.*, 2003; Op De Beeck *et al.*, 2004). However, recent characterization of HCVcc demonstrated that E1E2 heterodimers are present as disulfide-linked high molecular weight complexes on the virion surface (Vieyres *et al.*, 2010). Together, these findings highlighted the differences between the two *in vitro* models and indicated that during the assembly of HCV particles, the E1E2 heterodimers possibly undergo a transition from intracellular noncovalently-associated complexes to disulfide-linked high order forms on mature virions.

Both E1 and E2 are type I transmembrane proteins with an N-terminal ectodomain (E1 residues 192-353; E2 residues 384-715) and a C-terminal transmembrane domain (TMDs, E1 residues 354-383; E2 residues 716-746), as shown

in Figure 1.2. The hydrophobic TMDs serve as ER retention signals that anchor both proteins to the ER membrane during their biogenesis, and are also key determinants for E1E2 heterodimerization (Cocquerel *et al.*, 1998; Cocquerel *et al.*, 1999; Cocquerel *et al.*, 2002; Duvet *et al.*, 1998; Op De Beeck *et al.*, 2000). Truncation or mutation of the TMDs abrogate heterodimer formation and result in the cell surface expression of E1 and E2 (Cocquerel *et al.*, 1998). In addition, the TMD of E2 is involved in E1 folding (Patel *et al.*, 2001). Other key determining factors for E1E2 heterodimerization include the hydrophobic membrane proximal heptad repeat (MPHR) region, hypervariable region-2 (HVR2) and intergenotypic region (igVR) of the E2 ectodomain (Drummer & Poumbourios, 2004; McCaffrey *et al.*, 2011).

The biogenesis of E1E2 heterodimers is a slow and intricate process, and involves several events in the ER, including extensive protein folding, disulfide bond formation and glycosylation (Dubuisson *et al.*, 1994). E1 and E2 contain 8 and 18 strictly conserved cysteine residues, respectively (Figure 1.2), and these cysteines play a critical role in the disulfide pairing and proper folding of the E1E2 heterodimer. While mutation of any one E2 cysteine residue abolishes viral entry of HCVpp and HCVcc, specific E2 cysteines affect the correct folding of E2 in the E1E2 complexes, the formation of E1E2 heterodimers and the ability of the E1E2 heterodimer to interact with host cell coreceptor CD81 (McCaffrey *et al.*, 2012; Wang *et al.*, 2014). By contrast, cysteines in E1 are mostly involved in maintaining the structural stability of HCV particles and have less drastic effects on HCVcc infectivity as mutations only mildly attenuated HCVcc *in vitro* (Wahid *et al.*, 2013). In addition, free thiols groups have been detected in both E1 and E2 and have been shown to be essential in HCVcc infectivity (Fraser *et al.*, 2011).

Early expression studies showed that E1E2 heterodimer biogenesis is closely associated with lectin-binding chaperones in the ER such as calnexin, calreticulin and BiP, and the glycosylation of E1 and E2 is pivotal for the formation of properly folded E1E2 heterodimers (Choukhi *et al.*, 1998; Dubuisson & Rice, 1996). There are up to 5 and 11 N-linked glycosylation sites on E1 and E2, respectively (Figure 1.2) (Goffard & Dubuisson, 2003). In E1, glycan N250 is only found in G1b and G6 sequences but is 97% and 100% conserved in these two genotypes, respectively. The remaining 4 glycans on E1 (N196, N209, N234, N305) are conserved in >95% of

HCV sequences. In E2, glycans constitute one-third of its mass, and 9 out of the 11 sites (N417, N423, N430, N448, N532, N556, N576, N623, N645) are conserved in almost all genotypes (>99%). Intracellularly expressed E1E2 heterodimers are found to have mainly high mannose carbohydrates whereas complex or hybrid glycans are present on HCVpp (Drummer *et al.*, 2003; Vieyres *et al.*, 2010). A more heterogeneous glycan pattern was observed in HCVcc. Whilst the glycans on HCVcc E1 are mostly high mannose, a combination of complex or hybrid and high mannose glycans is found on E2 (Vieyres *et al.*, 2010). Mutations in the glycosylation sites on E1 and E2 affect the expression, folding and incorporation of correctly folded E1E2 into HCVpp, and removal of glycosylation sites in combination significantly reduces the expression of soluble E2 (Goffard *et al.*, 2005; Meunier *et al.*, 1999; Slater-Handshy *et al.*, 2004). Furthermore, glycans of E2 have been shown to influence the capacity of E2 to bind to host cell coreceptor CD81, affect the infectivity of HCVpp and HCVcc, as well as modulate viral sensitivity to neutralizing antibodies (Falkowska *et al.*, 2007; Helle *et al.*, 2007; Helle *et al.*, 2010).

The E1 glycoprotein

In the prototypic strain H77c, E1 is 192 amino acids in length with 4 N-glycosylation sites and 8 cysteines, as shown in Figure 1.2. During the expression of the E1E2 heterodimer, E1 is closely involved in E2 folding. The folding of E1 is slow, and is highly dependent on coexpression of the full-length E2, which acts as a chaperone (Brazzoli *et al.*, 2005; Dubuisson & Rice, 1996; Michalak *et al.*, 1997). In the absence of E2, E1 is misfolded and therefore must be co-expressed with E2 to examine its structural and functional characteristics. On HCVcc and HCVpp, E1 forms trimers, and its cysteine residues are important in maintaining the structural stability of HCVcc particles (Falson *et al.*, 2015; Wahid *et al.*, 2013). Although the crystal structures of regions of E1, including its N-terminal end (residues 192-272) and a C-terminal motif that is targeted by the neutralizing antibody IGH526 (residues 314-324), have been solved, the exact folding arrangement of E1 remains unclear (El Omari *et al.*, 2014a; El Omari *et al.*, 2014b; Kong *et al.*, 2015). While the precise functional role of E1 is not known, it is implicated in the early events of HCV replication such as entry and fusion, as anti-E1 antibodies can neutralize HCVpp entry (Meunier *et al.*, 2008). Furthermore, in addition to the free thiols detected on E1 that are necessary for entry, E1 may also be indirectly involved in virion-receptor

interaction as mutations in E1 cysteines can modulate the CD81 binding surface on virion-associated E2 (Fraser *et al.*, 2011; Wahid *et al.*, 2013).

The E2 glycoprotein: the receptor binding domain

In the prototypic strain H77c, E2 is 363 amino acids in length with 11 N-glycosylation sites and 18 cysteines, as shown in Figure 1.2. It consists of the receptor binding ectodomain (RBD: residues 384-661), the stem region (residues 662-714) and the transmembrane domain (TMD: residues 715-746). Whilst the TMD of E2 anchors E2 to the ER membrane and facilitates E1E2 heterodimerization, the amphipathic helical stem region links the TMD and the E2 ectodomain and is essential for HCVcc infectivity (Albecka *et al.*, 2011). The E2 RBD (residues 384-661) can be expressed as soluble proteins while maintaining a native conformation that competitively inhibits HCVcc infection *in vitro* (Michalak *et al.*, 1997; Whidby *et al.*, 2009).

Following the characterization of antibodies that inhibit E2 binding to CD81, several putative CD81 binding motifs on E2 were proposed, including residues 412-423, 480-493, 528-535 and 544-551 (Flint *et al.*, 1999a; Owsianka *et al.*, 2001). Site-directed mutagenesis studies later revealed that the CD81 binding face on E2 involves residues from four distinct regions including W^{420}H-S^{424}-L^{427}N (Boo *et al.*, 2012; Kong *et al.*, 2013; Owsianka *et al.*, 2006), G^{436}WL-G^{440}LFY (Drummer *et al.*, 2006; Kong *et al.*, 2013), G^{523}-P^{525}-Y^{527}-W^{529}G-D^{535} (Kong *et al.*, 2013; Owsianka *et al.*, 2006) , Y^{613}R-W^{616}HY (Roccasecca *et al.*, 2003; Rothwangl *et al.*, 2008). While mutations at these residues significantly reduce the ability of E1E2 to bind to CD81, it is likely that some of these residues are indirectly involved E2-CD81 binding by maintaining the local environment required for E2-CD81 interaction.

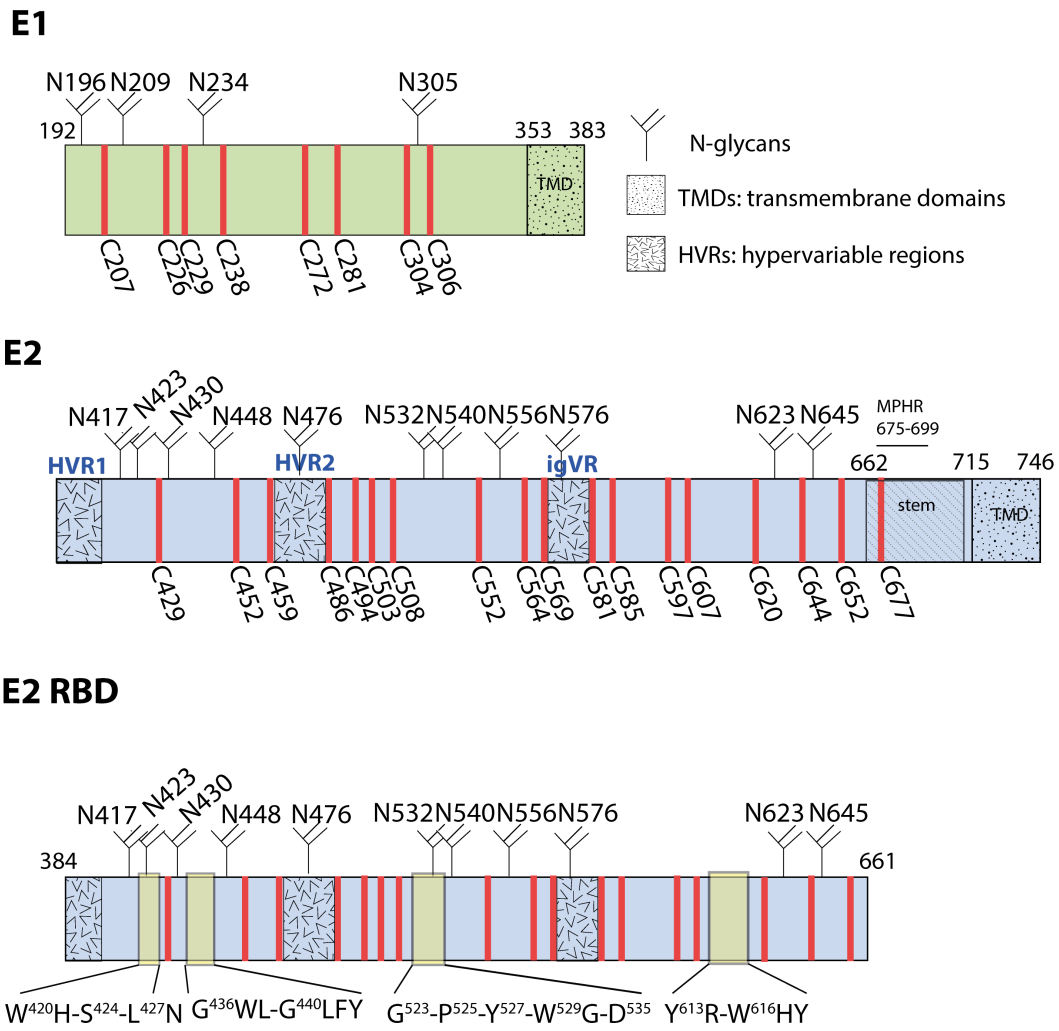

Figure 1.2 The domain organization of HCV glycoproteins E1 and E2 of the prototypic HCV strain H77c (G1a). Strictly conserved cysteine residues are highlighted in red (McCaffrey *et al.*, 2012; Wahid *et al.*, 2013). The four discontinuous CD81 binding motifs on the receptor binding domain of E2 (E2 RBD, bottom) are highlighted in yellow.

Hypervariable regions of the E2 glycoprotein

Sequence alignment of different HCV isolates showed that the E2 RBD contains three hypervariable regions (HVRs), HVR1 (residues 384-411), HVR2 (residues 460-485) and the intergenotypic region igVR (residues 570-580) (Kato *et al.*, 1992; McCaffrey *et al.*, 2007) (Figure 1.2). Analysis of patient isolates also suggested an additional HVR (HVR3: residues 431-466) that was under intra-host selective pressure (Troesch *et al.*, 2006). However, residue changes in this region are conservative and do not alter its overall hydropathy. Flanked by conserved cysteine residues, the HVR2 and igVR, along with HVR1 form flexible, surface exposed loops on E2 and can be deleted individually or in combination and replaced with a flexible linker without affecting the overall conformation of E2 (McCaffrey *et al.*, 2007).

Located at the N-terminus of E2, HVR1 is the most variable region in the HCV genome and is highly immunogenic, generating strong antibody responses in natural infection (Weiner *et al.*, 1991). Despite the high degree of sequence variation, it maintains a basic stretch with positively charged residues located at conserved positions (Penin *et al.*, 2001). These conserved basic residues are possibly responsible for the interaction of HVR1 with the negatively charged glycosaminoglycans on the cell surface, facilitating nonspecific cell attachment of HCV during early entry processes. This is supported by the findings that a synthetic peptide representative of HVR1 binds to heparin with high affinity while an increased number of positively charged residues is associated with an increased level of HCVpp entry (Basu *et al.*, 2004; Callens *et al.*, 2005). Although not required for E2 folding or the formation of E1E2 heterodimers, HVR1 is involved in maintaining the biophysical characteristics of infectious virions including the low buoyant density and native apoE-association (McCaffrey *et al.*, 2011; Meola *et al.*, 2015; Prentoe *et al.*, 2014). One of the key functions of HVR1 is to modulate the exposure or the conformation of CD81 binding motifs on E2 as deletion of HVR1 enhances E2-CD81 binding (Bankwitz *et al.*, 2010; Roccasecca *et al.*, 2003). In addition, HVR1 is essential in the binding of soluble E2 to SR-BI and is involved in the enhancement of HCVpp entry through the HDLs, possibly facilitated by SR-BI (Bartosch *et al.*, 2005; Scarselli *et al.*, 2002). While HVR1-deleted virus can still bind to cellular SR-BI, it exhibits a decrease in SR-BI usage for infection (Bankwitz *et al.*, 2010; Prentoe *et al.*, 2014). The functional importance of HVR1 is further demonstrated in its role in viral

infectivity. Characterization of JFH-1 chimeric viruses containing structural proteins of different genotypes showed that while removal of HVR1 does not affect the infectivity of G2a, G5a, G6a viruses *in vitro*, it severely attenuates G1a, G1b, G2b, G3a and G4a viruses, suggesting a genotype-specific modulation of HCV infectivity by HVR1 (Prentoe *et al.*, 2011). Although HVR1 deletion attenuates some HCV strains *in vitro* as well as in chimpanzees and human liver chimeric mice, viral infectivity can be fully restored by adaptive mutations in other regions of the HCV genome including HVR2 (Forns *et al.*, 2000; McCaffrey *et al.*, 2011; Prentoe *et al.*, 2016).

Compared to HVR1, HVR2 is relatively stable with intragenotypic variations ranging from 7% (G5a) to 39% (G1a and G1b) (McCaffrey *et al.*, 2007). In the case of the igVR, initial studies suggested that sequence change is only observed across genotypes but is conserved within a genotype (McCaffrey *et al.*, 2007). While no evidence suggests the HVR2 and igVR are under immune pressure, considerable changes in both HVR2 and igVR were observed in an individual with chronic G3a over a 108-week period whereas in a patient with acute G3a, mutations were only found in igVR, suggesting an intra-host selective pressure on HVR2 and the igVR (Alhammad *et al.*, 2015b). Although both HVR2 and the igVR are dispensable for the overall folding or CD81 binding capability of isolated recombinant E2 RBD, deletion of HVR2 and/or the igVR completely abolishes the incorporation of noncovalently associated E1E2 heterodimers into HCVpp (Albecka *et al.*, 2011; McCaffrey *et al.*, 2007; McCaffrey *et al.*, 2011). Furthermore, during the biogenesis of E1E2 heterodimers, the presence of HVR2 and the igVR is crucial in maintaining the proper folding of CD81 binding motifs and the arrangement of the immunogenic domains of E2. Together with HVR1, HVR2 and the igVR play an important role in the early steps of HCV entry by modulating the CD81 binding sites on E2 as well as HCV infectivity *in vitro* and *in vivo* (Albecka *et al.*, 2011; McCaffrey *et al.*, 2007; Prentoe *et al.*, 2014; Prentoe *et al.*, 2016; Roccasecca *et al.*, 2003).

The E2 glycoprotein: the structure of the E2 ectodomain

Given the phylogenetic similarity of HCV to the flaviviruses, early studies using computational modeling proposed that E2 is a Class II fusion protein similar to the E protein of the flavivirus TBEV, and was therefore predicted to have an extended structure with predominantly β turns (Yagnik *et al.*, 2000). Using comparative mass spectroscopy and N-terminal sequencing of trypsin-cleaved, reduce or non-reduced E2e (E2 with TMD deleted) from three strains (G1a, H77, G2a, JFH-1 and G2b UKN2b_2.8), Krey and colleagues determined 8 disulfide bridges within E2 and assigned the remaining two cysteines (C13-C15) as the 9th bond, shown in Figure 1.3A (Krey *et al.*, 2010). In combination with secondary structures predicted by circular dichroism, Fourier transform infrared spectroscopy as well as computer modelling, Krey *et al* organized E2 into an elongated Class II fusion protein that has a three-domain architecture (DI, DII and DIII, as shown in Figure 1.3B). The central DI consists of the HVR1 region and a β-sandwich while the DII contains HVR2 and a putative fusion loop (residues 502-520) and connects to DI via the two top sheets of the β-sandwich (D_0 and E_0). Linked by the igVR, DI and DIII are responsible for CD81 engagement, while DIII is located adjacent to the stem region that anchors the ectodomain to the TMD.

The three-domain model was challenged by negative staining of full-length E2 (residues 384-717) in complex with the antigen-binding fragment (Fab) of the neutralizing antibody AR3C. Electron microscopy of the complex showed that instead of having an extended structure found in class II fusion proteins, the estimated length of E2 is ~60Å (Kong *et al.*, 2013). Crystal structure of AR3C Fab-bound E2 core protein (G1a, strain H77, residues 412-645; PDB: 4MWF, Figure 1.3C) further revealed that the E2 core protein adopts a compact globular structure, consistent with the E2 core structure (G2a, strain J6, residues 456-656, non-glycosylated; PDB: 4WEB, Figure 1.3D) solved with the Fab of non-neutralizing antibody 2A12 by another group (Khan *et al.*, 2014; Kong *et al.*, 2013). Despite the differences in E2 truncation (illustrated in Figure 1.3A) and Fab target sites between the two structures, the E2 core proteins display a common fold, with a central β-sandwich flanked by front and back layers of random loops, α helices and β sheets. As shown in Figure 1.3C, the central β-sandwich has an immunoglobulin (Ig)-like fold, consisting of four

inner sheets (g, f, c, c') and two outer sheets (b, e) connected by small turns and loops while the N-terminus of E2 forms the front layer containing loops, α helices and a small β sheet. Negative staining of CD81-bound E2 and mutagenesis and deletion studies indicate that the larger flexible loop connecting e and c' sheets of the sandwich (termed "CD81 loop") together with α helix (α1) at the front layer forms the CD81 binding interface on E2, shown in Figure 1.3C and Figure 1.4C (Drummer *et al.*, 2006; Khan *et al.*, 2014; Kong *et al.*, 2013; McCaffrey *et al.*, 2012; Owsianka *et al.*, 2006). This region exhibits a relatively high degree of conservation and is also described as the neutralizing face as antibodies to this region such as AR3C inhibit HCVcc entry by competitively blocking E2-CD81 binding. The back layer of the E2 core is composed of two large β sheets with novel folds as well as random loops. The C-terminal back layer forms the occluded face of E2, linking the E2 ectodomain to the stem region (shown in Figure 1.4B), and antibodies targeting this region such as 2A12 are non-neutralizing. Surrounded by the central β sheets and the two β sheets from the back layer is a hydrophobic core which is predicted to be the site of E1E2 association, depicted in Figure 1.4D.

Despite the common fold, the disulfide arrangement of E2 differs between the two structures. While Kong's construct contains 16 cysteines with 7 disulfide bonds solved in the structure, Khan's structure has 5 cysteine pairs and 4 unresolved cysteines, shown in Figure 1.3A. Common to both E2 core structures are three disulfide bonds, C5-C9 and C7-C8 that are located in the central β sandwich, and C14-C16 that is responsible for stabilizing the two β sheets at the back layer, highlighting the structural importance of both regions in E2 core protein. This also corroborates the results of the E2 RBD mutagenesis studies which showed that alanine replacement of any of these 6 cysteine residues either abrogate or reduce the binding of E2 to the conformational antibody H53 (McCaffrey *et al.*, 2012). Except for the three common disulfide bonds, cysteine pairing differs significantly between the structures of Kong's and Khan's, and mutations in these cysteines do not affect E2 conformation. In addition, free thiol groups have been detected in both E1 and E2 on HCVcc and HCVpp (Fraser *et al.*, 2011). Together, these findings suggest that E2 cysteines are possibly involved in flexible intramolecular pairing or intermolecular bonding with E1 where free cysteines are also present. Another missing structural

feature on the E2 core are the glycans, which were enzymatically removed in Khan's construct and mostly disordered in Kong's structure. However, using small angle X-ray scattering, Khan and colleagues found that glycans constitute a third of the E2 mass and determined the approximate distribution of glycans. Glycan modeling on the E2 core further predicts that most of the glycans lie proximal to the occluded back layer of E2, forming a highly glycosylated face (Figure 1.4D). Lastly, the exact details of E2 HVRs (HVR1 and HVR2) are not available on current E2 structures. The highly flexible HVR1, although not included in either E2 core constructs, is thought to be in close proximity to the CD81 loop/neutralizing face, together with the adjacent disordered 412-419 region. By contrast, the disordered HVR2 is predicted to be at the occluded face of E2, adjacent to the igVR within the E2 monomer.

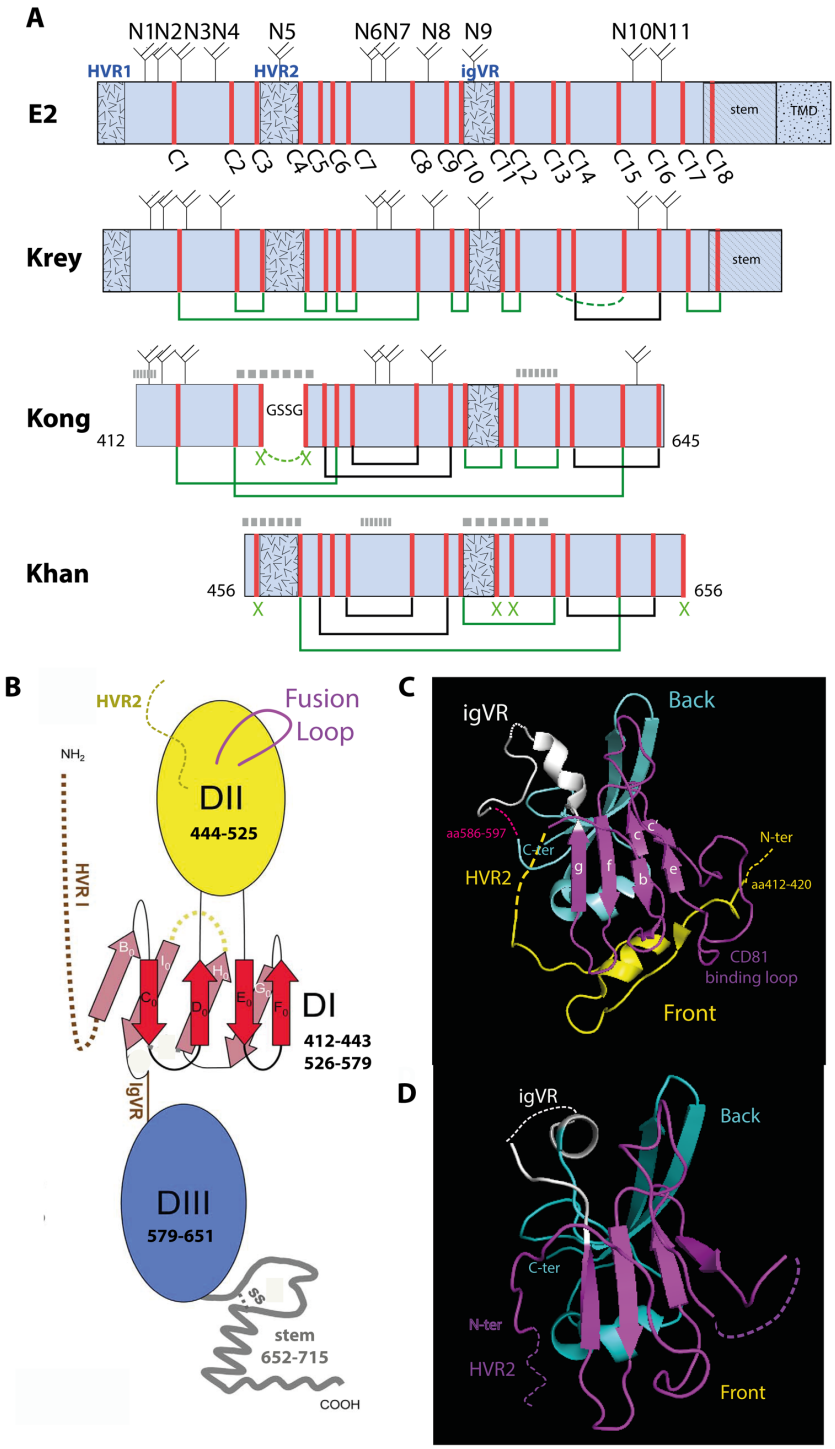

Figure 1.3 The structure of HCV E2 ectodomain. (A) Schematic diagram depicting the differences in truncation, disulfide pairing (as green/black connecting lines, with cysteines in red and unsolved cysteines labeled as X), glycosylation (as branched sticks) and HVRs amongst the full-length E2, the proposed E2 model by Krey *et al* (2010) and the crystal structures of E2 by Kong *et al* (2013) and Khan *et al* (2014). Unsolved regions in the crystal structures are indicated as grey dash lines. (B) The three-domain model of E2 proposed by Krey *et al* (2010). (C) The crystal structure of E2 core (PDB: 4MWF) (Kong *et al.*, 2013). (D) The crystal structure of E2 core (PDB: 4WEB) (Khan *et al.*, 2014).

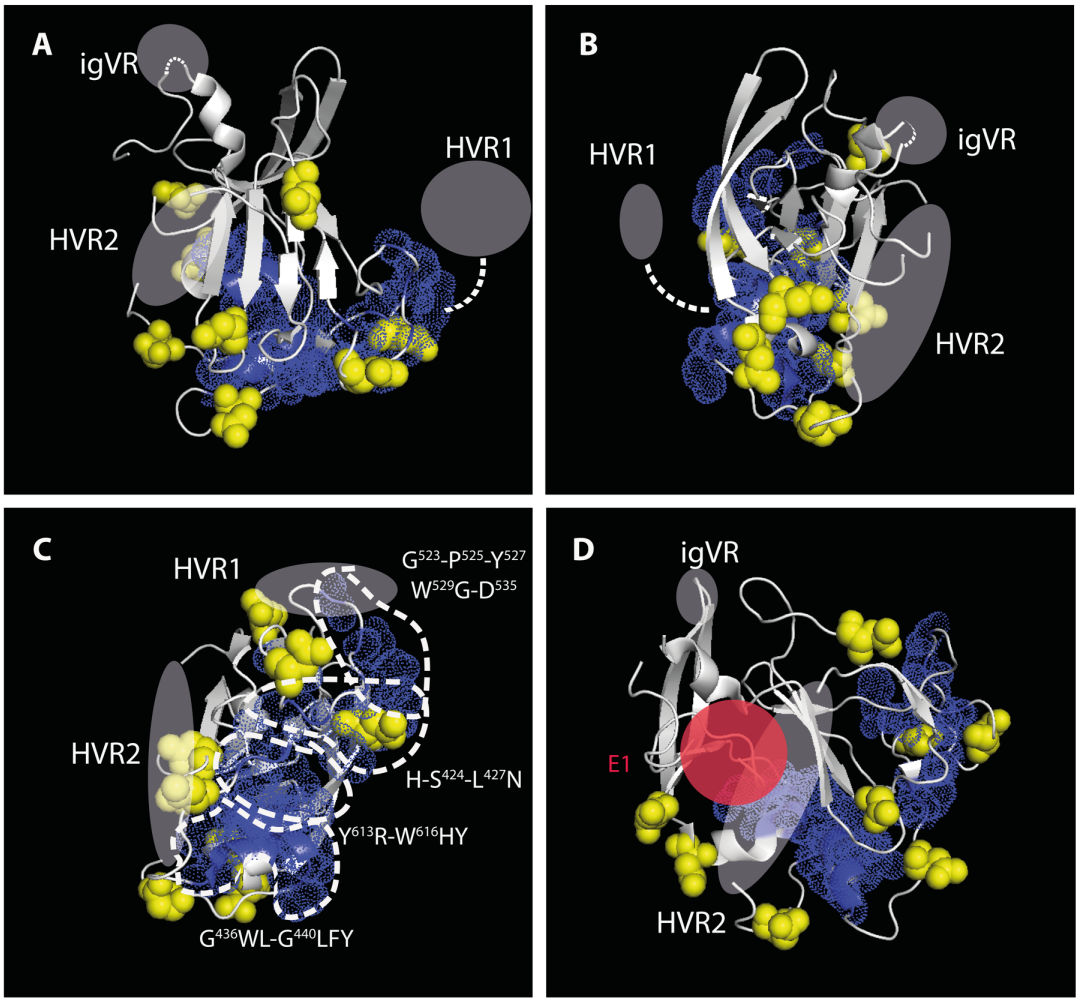

Figure 1.4 The key structural features on the E2 core solved by Kong *et al* (2013). The CD81 binding residues are illustrated as blue dotted spheres and the positions of the HVRs and glycans are indicated as white ovals and yellow spheres respectively. (A) The E2 core with the novel Ig-like β-sandwich positioned in the center. (B) The occluded face of E2. (C) The neutralizing face of E2 with the four CD81 binding motifs also indicated. (D) The glycosylated face of E2 with the hydrophobic core likely to be the site of E1 association also shown.

1.5.2 HCV entry: host cell coreceptors

CD81

CD81 was the first host cell receptor identified for HCV and its role in HCV entry has since been well characterised (Pileri *et al*., 1998). It was discovered from the screening of a complementary DNA (cDNA) library based on a human T-cell lymphoma cell line that has high affinity for HCV glycoprotein E2. CD81 belongs to the tetraspanin superfamily and is expressed in all nucleated cells. It is comprised of four transmembrane domains and two extracellular loops: a short extracellular loop (SEL) and a large extracellular loop (LEL), as shown in Figure 1.6A.

Soluble E2, or E2 in the context of E1E2 heterodimers or HCV VLPs, binds directly to cell surface expressed CD81 via its LEL region, and such interaction is species-specific and can be inhibited by anti-CD81 antibodies (Flint *et al.*, 1999a; Petracca *et al.*, 2000; Triyatni *et al.*, 2002). X-ray crystallographic studies showed that the CD81-LEL forms homodimers and adopts a mushroom-like structure as shown in Figure 1.5 (Kitadokoro *et al*., 2001). CD81-LEL dimerization is required for binding to E2 (Drummer *et al.*, 2005; Kong *et al.*, 2013). Each LEL subunit in the homodimer consists of 5 α-helices making up the stalk and head subdomains, with the head domain responsible for interaction with E2. Mutagenesis studies on CD81-LEL fusion proteins and cell surface expressed CD81 revealed that mutations in residues L162, I182, N184, F186 within the LEL region significantly reduce the binding of E2 to CD81 (Bertaux & Dragic, 2006; Drummer *et al*., 2002; Higginbottom *et al*., 2000). The residue F186 in particular, is critical for the binding of E2 to both soluble CD81-LEL and cellular CD81. In addition, in cellular CD81, mutations in its C-terminal domain, transmembrane domain and intracellular domain affect HCVpp entry (Bertaux & Dragic, 2006).

Numerous studies have demonstrated that CD81 is essential for HCV entry into hepatocytes. Ectopic expression of CD81 in non-permissive liver cell lines, which have little or no CD81 expression, renders the cells permissive to HCVpp infection (Cormier *et al*., 2004; Flint *et al*., 2006; McKeating *et al.*, 2004; Zhang *et al*., 2004). In addition, soluble CD81-LEL competes for E2 binding with cellular CD81 and inhibits HCVpp entry (Flint *et al*., 2006; Hsu *et al*., 2003; Petracca *et al*.,

2000). Antibodies or small interfering RNAs (siRNAs) targeting cellular CD81 abrogate the infection of HCVpp, HCVcc and serum-derived HCV (Bartosch *et al.*, 2003b; Cormier *et al.*, 2004; Flint *et al.*, 2006; Molina *et al.*, 2008; Wakita *et al.*, 2005; Zhang *et al.*, 2004; Zhong *et al.*, 2005). Interaction with CD81 occurs following the initial HCV attachment to cells, as anti-CD81 antibody can block virus entry after HCVpp binds to cells (Bertaux & Dragic, 2006). In human liver uPA-SCID mice, anti-CD81 antibodies effectively protect animals from HCV infection (Meuleman *et al.*, 2008).

Interestingly, several studies examined the entry level of HCVpp into different human liver cell lines, and found that there is no correlation between CD81 expression and HCVpp entry (Bartosch *et al.*, 2003b; Hsu *et al.*, 2003; Zhang *et al.*, 2004). Cellular tropism of HCV is limited to certain human liver cell lines while many human hepatic cell lines expressing high levels of CD81 do not support HCVpp infection. Furthermore, CD81 alone does not affect HCV species tropism. Mouse cell lines transfected with human CD81 remain non-permissive to HCVpp and expression of human CD81 in transgenic mice alone does not support HCV infection (Cormier *et al.*, 2004; Masciopinto *et al.*, 2002). These suggest that CD81 is necessary but not sufficient for HCV entry.

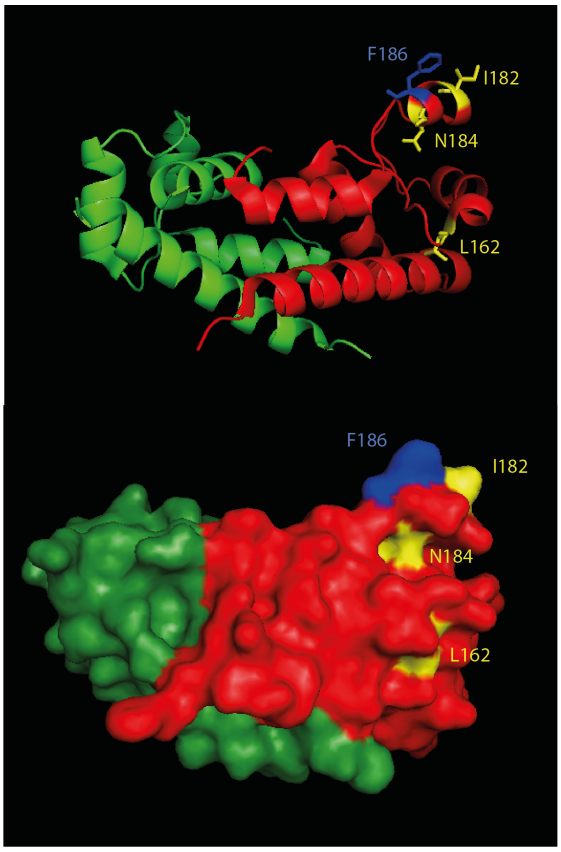

Figure 1.5 The crystal structure of HCV coreceptor CD81-LEL homodimer (1.6Å, PDB:1G8Q). Each subunit (in green and red) consists of 5 α-helices (shown in the top cartoon representation) that are arranged into the stalk and head subdomains. The distribution of the four residues important in CD81-E2 interactions (I182, N184, L162 in yellow and F186 in blue) on CD81-LEL surface is depicted in the bottom surface representation (Kitadokoro *et al.*, 2001).

Scavenger receptor class B type I (SR-BI)

The human hepatoma cell line HepG2, which has no detectable CD81 expression and yet bind E2 with high affinity, was used to identify scavenger receptor class B type I (SR-BI), also known as CLA-1, as an essential HCV entry factor (Scarselli *et al.*, 2002). It is 509 amino acids in length and adopts a horseshoe-like structure that is extensively glycosylated, illustrated in Figure 1.6B (Acton *et al.*, 1996). It is highly expressed in the liver and steroidogenic tissues and is responsible for the transfer of cholesterols and uptake of HDLs.

An increased level of SR-BI expression in the permissive Huh7.5 cells is associated with increased HCVcc infectivity (Grove *et al.*, 2007). SR-BI-interfering agents, such as siRNA, antibodies directed to SR-BI and small molecule antagonists can inhibit infection of different strains of HCVpp and HCVcc (Catanese *et al.*, 2007; Kapadia *et al.*, 2007; Lavillette *et al.*, 2005b; Syder *et al.*, 2011; Zeisel *et al.*, 2007). Kinetic studies of monoclonal antibodies specific to SR-BI showed that similar to anti-CD81 antibodies, they potently block HCV infection before HCV attaches to cells (Catanese *et al.*, 2010; Dreux *et al.*, 2006; Zeisel *et al.*, 2007). This indicates that SR-BI serves as a capture receptor for HCV and may be temporally linked to interactions with CD81. In addition, only human cellular SR-BI can bind to E2, indicating a species-specific interaction between E2 and SR-BI (Scarselli *et al.*, 2002). Although there is no direct evidence showing the binding between HVR1 and SR-BI, HVR1 is a key determinant in E2-SR-BI interaction, as deletion of HVR1 ablates SR-BI binding to soluble E2 and anti-HVR1 antibodies block E2 binding to cellular SR-BI (Scarselli *et al.*, 2002). However, HVR1-deleted HCVcc is able to bind to cellular SR-BI, indicating that additional regions on the virions are involved in HCV-SR-BI interaction (Bankwitz *et al.*, 2010). Although the exact region of SR-BI that interacts with E2 is not known, modification of its cytoplasmic tail was reported to affect HCV entry (Dreux *et al.*, 2009). It is hypothesised that SR-BI serves as a multi-functional receptor in HCV entry, by mediating lipid transfer as well as interacting with HCV glycoprotein E2 (Voisset *et al.*, 2005). Ectopic expression of SR-BI in addition to CD81, however, does not render non-hepatic cells such as Chinese hamster ovary (CHO) cells permissive to HCV entry, suggesting additional coreceptors for HCV (Bartosch *et al.*, 2003c).

Claudin-1 (CLDN1)

Claudin-1 was identified through screening a lentiviral cDNA library from the highly permissive Huh7.5 cells for genes that makes HEK293T cells expressing CD81 and SR-BI permissive to HCV infection (Evans *et al.*, 2007). It was the first host cell factor identified to confer HCV permissiveness to non-hepatic cells. Claudin-1 is a tight junction protein that is predominantly expressed in epithelial tissues and is responsible for the paracellular transport of ions, solutes and water (Krause *et al.*, 2008). It is 211 amino acids in length and consists of two extracellular loops, four transmembrane helices and three intracellular domains, shown in Figure 1.6C (Furuse *et al.*, 1998). Extracellular loop 1 (EL1) is involved in tight junction pore formation whilst extracellular loop 2 (EL2) is responsible for the formation of oligomeric claudin-1 at tight junctions (Krause *et al.*, 2008).

In overexpression systems, claudin-1 forms a complex with both E1 and E2, CD81 and low density lipoprotein receptor (LDLR) (Yang *et al.*, 2008). Although there is no evidence of a direct interaction between claudin-1 and HCV virions, the formation of claudin-1-CD81 complexes is required for HCV entry (Evans *et al.*, 2007; Harris *et al.*, 2010). Ectopic expression of claudin-1 in non-hepatic cells that do not have endogenous claudin-1 expression confers susceptibility to HCVpp entry, and silencing of claudin-1 expression in Huh7.5 cells significantly impairs HCVpp and HCVcc infection (Evans *et al.*, 2007). Polyclonal antibodies raised to claudin-1 block the binding of E2 to permissive cells, and inhibit HCVcc infection *in vitro* alone or synergistically with anti-CD81 and anti-SR-BI antibodies (Krieger *et al.*, 2010). Monoclonal antibodies targeting either the EL1 or EL2 of claudin-1 can prevent HCV infection of different genotypes both *in vitro* and in the human uPA-SCID mouse model, possibly by blocking the CD81 and claudin-1 complex interaction (Fofana *et al.*, 2010; Fukasawa *et al.*, 2015; Mailly *et al.*, 2015; Paciello *et al.*, 2016). Domain swapping of claudin-1 with claudin-7, a related claudin family member that is not involved in HCV entry, reveals that the N-terminal region of EL1 (residues I32 and E48) is essential for HCV infection whereas the intracellular domains are not required for HCV entry (Evans *et al.*, 2007). Mutagenesis studies further indicate that the highly conserved hydrophobic W^{30}-GLW^{51}-C^{54}-C^{64} motif and residues I32 and D38 within the EL1 domain are essential for HCV infection, as they maintain the integrity

of cell-cell contact and claudin-1 localization necessary for HCV entry (Cukierman *et al.*, 2009).

Occludin (OLDN)

Numerous cell lines that endogenously express CD81, SR-BI and claudin-1 are non-permissive to HCV, suggesting the presence of additional entry factor(s) for HCV infection (Evans *et al.*, 2007). Occludin was discovered from retrovirus-based screening of a cDNA library derived from the highly permissive Huh7.5 cells that made the mouse embryonic fibroblast cell line NIH3T3 overexpressing CD81, SR-BI and claudin-1, permissive to HCV infection (Ploss *et al.*, 2009). Occludin is a 60kDa tight junction protein, and adopts a similar membrane topology as claudin-1 with four transmembrane domains, two extracellular loops and intracellular regions, as shown in Figure 1.6D (Furuse *et al.*, 1994). Compared to claudin-1, occludin has a more extensive C-terminal intracellular domain, which facilitates the localization of occludin to tight junctions and interacts directly with ZO-1, a membrane peripheral protein closely associated with the actin cytoskeleton (Chiba *et al.*, 2008). Moreover, the C-terminal intracellular domain contains motifs for phosphokinases, which are responsible for downstream signal transduction.

The knockdown of occludin expression in hepatoma cells partially inhibits HCVpp entry and HCVcc infection while ectopic expression of occludin in mouse cells results in a 120-fold increase in HCVpp entry (Liu *et al.*, 2009; Ploss *et al.*, 2009). It has been shown that deletion of its second extracellular loop (EL2) significantly impairs HCVpp entry and replacement of EC2 with that of mouse origin also abolishes HCVpp entry, indicating that HCV-occludin interaction is species-specific and the EC2 of occludin is involved in mediating HCVpp entry (Liu *et al.*, 2010b; Michta *et al.*, 2010; Ploss *et al.*, 2009). The exact interaction between occludin and HCV particles remains unclear. Studies have shown that occludin forms complexes with HCV E2 in infected cells and HCV infection ultimately affects the cellular expression and distribution of occludin (Liu *et al.*, 2009). Furthermore, kinetic studies suggested that occludin, like claudin-1, is involved in post-binding steps of HCV entry (Benedicto *et al.*, 2009). Occludin, together with CD81 determines the species tropism of HCV, as CD81 and occludin of human origin are the minimal requirement for HCVpp entry in non-hepatic cells and HCVcc infection

in transgenic mice (Dorner *et al.*, 2011). To date, CD81, SR-BI, claudin-1 and occludin are considered the four essential coreceptors that define the liver tropism of HCV in humans.

Other entry factors

In addition to the four essential coreceptors, HCV entry involves other host factors including glycosaminoglycans (GAGs) and C-type lectins. Present on the cell surface, GAGs are involved in the initial low-affinity interaction between HCV and liver cells. The direct binding of HCV VLPs and soluble E2 to heparin is facilitated by the presence of basic residues on HCV particles including those in the HVR1 region (Barth *et al.*, 2003; Basu *et al.*, 2004). While heparin competitively inhibits HCV attachment to cells, enzymatic degradation of heparan sulfate proteoglycans (HSPGs) significantly reduces the absorption of patient-derived HCV into peripheral blood mononuclear cells (PBMCs) and human hepatocarcinoma cells (Cribier *et al.*, 1998; Germi *et al.*, 2002). Additionally, C-type lectins such as dendritic cell-specific intercellular adhesion molecule 3-grabbing non-integrin (DC-SIGN, or CD209) and liver or lymph node-specific intercellular adhesion molecule 3-grabbing integrin (L-SIGN, or CD209L) are implicated in HCV entry, possibly through their interactions with the glycans present on the envelope proteins. L-SIGN in particular, is expressed on liver sinusoidal endothelial cells, and is likely to play a role in the capture and delivery of HCV particles into the liver. Serum-derived HCV, HCVpp or soluble E2 can bind to DC-SIGN and L-SIGN with high affinity (Gardner *et al.*, 2003; Lozach *et al.*, 2003; Lozach *et al.*, 2004; Pöhlmann *et al.*, 2003). The association of HCV particles with LDL and VLDL also led to the proposal that LDL receptor (LDLR) is an entry receptor for HCV, and it has been demonstrated that free LDL and soluble LDLR peptide competitively inhibit the cellular attachment of HCV whilst siRNA and antibodies specific to LDLR reduce HCVcc infectivity *in vitro* (Albecka *et al.*, 2012; Molina *et al.*, 2007; Monazahian *et al.*, 1999). Responsible for the cellular uptake of lipoproteins, LDLR maintains an intracellular lipid composition optimal for HCV replication and assembly, and is associated with the nonproductive uptake of HCV as it preferentially interacts with lipoprotein lipase-modified HCV particles that have reduced infectivity (Albecka *et al.*, 2012). Other host factors that are associated with enhanced HCV entry include epidermal growth factor receptor (EGFR), ephrin receptor type A2 (EphA2), cholesterol absorption receptor Niemann-Pick C1-like 1

(NPC1L1), and transferrin receptor 1 (TfR1), although their exact roles remain unclear (Lupberger *et al.*, 2011; Martin & Uprichard, 2013; Sainz *et al.*, 2012).

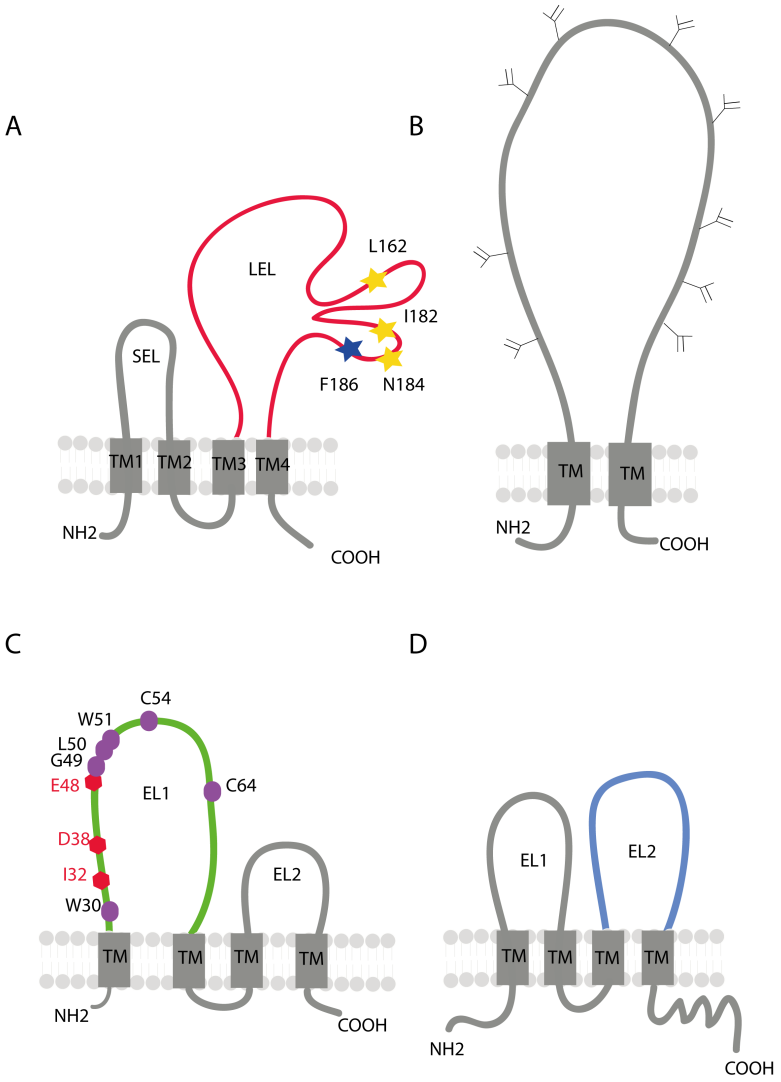

Figure 1.6 The membrane topology of the four HCV host coreceptors, CD81, SR-BI, claudin-1 and occludin. (A) The tetraspanin CD81 consists of two extracellular loops, large extracellular loop (LEL, red) and small extracellular loop (SEL, grey), four transmembrane domains (TMs) and intracellular domains. The LEL is involved in E2 binding through at least four residues, L162, I182, N184 (yellow) and F186 (blue). (B) The glycoprotein SR-BI has 9 glycans (branched sticks). (C) The tight junction protein claudin-1 (bottom left) is composed of two extracellular loops (EL1 and EL2), four transmembrane domains (TMs) and intracellular regions. EL1 (green) is involved in HCV entry. The residues I32, D38, E48 (in red) and the conserved W^{30}-GLW^{51}-C^{54}-C^{64} motif (in magenta) within EL1 are critical for mediating HCV entry. (D) The tight junction protein occludin has two extracellular loops (EL1 and EL2), four transmembrane domains (TMs) and intracellular regions. EL2 (in blue) is involved in mediating HCV entry. The extensive C-terminal intracellular region of occludin is implicated in downstream cell signaling pathways.

1.5.3 Early steps of HCV entry and viral fusion

The entry of HCV into hepatocytes initially involves non-specific virion capture by host factors including GAGs, DC-SIGN, L-SIGN, and SR-BI (Douam *et al.*, 2015; Lindenbach & Rice, 2013). The lipid transfer activity of SR-BI then induces structural modifications of the HCV particles and exposes the CD81 binding regions on E2, resulting in the subsequent high-affinity interaction between HCV E2 and CD81. The engagement of CD81 activates Rho GTPase family members, and mediates the actin-dependent relocalisation and lateral movement of HCV-CD81 complexes towards the tight junctions, where the virion interacts with tight junction proteins, claudin-1 and occludin (Figure 1.8) (Brazzoli *et al.*, 2008; Harris *et al.*, 2010).

The subsequent stages of HCV entry involve clathrin-mediated endocytosis of virions followed by the slow internalization of HCV into endosomes (Blanchard *et al.*, 2006; Codran *et al.*, 2006; Lavillette *et al.*, 2006; Tscherne *et al.*, 2006). Whilst low pH is required for HCV entry as treatment of cells with inhibitors of ATPase or ammonium chloride prevent entry, the conformational changes associated with HCV fusion, the location of the fusion peptide and the post fusion structure of E1E2 are unknown. Given the phylogenetic relatedness of HCV to flaviviruses such as TBEV, HCV E2 was proposed to be a class II fusion protein. Class II fusion proteins, such as the E proteins of the flaviviruses and the E1 protein of the alphavirus, have ectodomains that are organized into three domains and are made of mainly ß sheets (Modis *et al.*, 2004; Rey *et al.*, 1995). They have an internal hydrophobic fusion motif that is 16-26 amino acids in length and a stem region that connects their TMDs and ectodomains (Kielian & Rey, 2006). Both the fusion peptide and the stem regions are critical in viral entry as well as the heterodimerization of the fusion protein with its closely associated companion envelope protein.

The exact fusion mechanisms and the glycoprotein responsible for HCV fusion remain elusive. Both E1 and E2 have been proposed to be the glycoprotein responsible for membrane fusion, and putative fusion motifs have been described in both E1 and E2, as shown in Figure 1.7. Early envelope glycoprotein sequence analyses using computer algorithms showed that the motif within HCV E1 (residues

264-290 or residues 272-281) shares a degree of sequence homology with the fusion motifs of class II fusion proteins such as the E protein of TBEV (Flint *et al.*, 1999b; Garry & Dash, 2003). Biophysical analyses later suggested that peptides representing two hydrophobic regions in E1 (residues 265-296 and residues 310-331) interact with phospholipid model membranes, and therefore have the potential to mediate fusion and hemifusion (Pérez-Berná *et al.*, 2006; Pérez-Berná *et al.*, 2009). However, the length of E1 is shorter than previously described class II fusion proteins. It was therefore proposed that E1 is a truncated class II protein that lacks domain III and the stem region critical in the class II fusion and hemifusion processes. Functional studies later showed that E1 is unlikely to contain the fusion loop since most mutations in its putative fusion motif (residues 272-304) do not alter E1E2 expression and heterodimerization or HCVpp entry, although some residues are implicated in viral entry (Drummer *et al.*, 2007; Lavillette *et al.*, 2007; Li *et al.*, 2009).

Mutagenesis studies showed that HCVpp carrying mutations in two regions of E2 (residues 416-430 and residue 600-620) retain the ability to bind to CD81 but cannot mediate the entry of HCVpp into hepatocytes, possibly due to a defect in membrane fusion (Lavillette *et al.*, 2007). Also, E2 has been shown to have hydrophobic regions (residues 430-449, residues 543-560 and residues 603-624) that interact with liposomes, suggesting a possible role in HCV fusion (Pacheco *et al.*, 2006). Furthermore, the MPHR of E2 (residues 675-699) has both structural and functional analogy to the glycoprotein E of flaviviruses as it is an essential determinant of E1E2 heterodimerization and viral entry (Drummer & Poumbourios, 2004). Lastly, the resolution of the two crystal structures of the truncated E2 ectodomains revealed an Ig-like fold that resembles the domain III of the flavivirus glycoprotein E contradicting the model proposed by Yagnik *et al* (Khan *et al.*, 2014; Kong *et al.*, 2013; Yagnik *et al.*, 2000). Gel filtration chromatographic analyses indicated that the structure of the E2 core does not undergo a conformational rearrangement after low pH treatment (Khan *et al.*, 2014). However, to fully determine whether E2 is the fusion protein, the exact effect of low pH on full-length E2 or E2 in the context of infectious particles needs to be investigated. Alternatively, HCV may utilise a novel fusion mechanism distinct from the three classes of fusion mechanisms described to date (Li & Modis, 2014). It is possible that both E1 and E2 are required to supply the hydrophobic fusion peptide and stem-TMD region to drive

the apposition of viral and cellular membranes, although detailed structural information on E1E2 heterodimers is needed to confirm this theory.

By analogy to fusion mechanisms common to all three classes, low pH is likely to induce a major conformational change within the E1E2 heterodimer such that the fusion loop is inserted into the cell membrane (Li & Modis, 2014). Subsequently, cell and viral membranes are brought together through the formation of hairpin structures, resulting in hemifusion and fusion pore formation. Viral RNA is then released into the cytoplasm through the fusion pore. This is followed by viral RNA replication and viral protein synthesis, which is closely associated with cellular lipid metabolism and occurs in the ER (Pawlotsky *et al.*, 2007). Once assembled and packaged, HCV virions are matured and released.

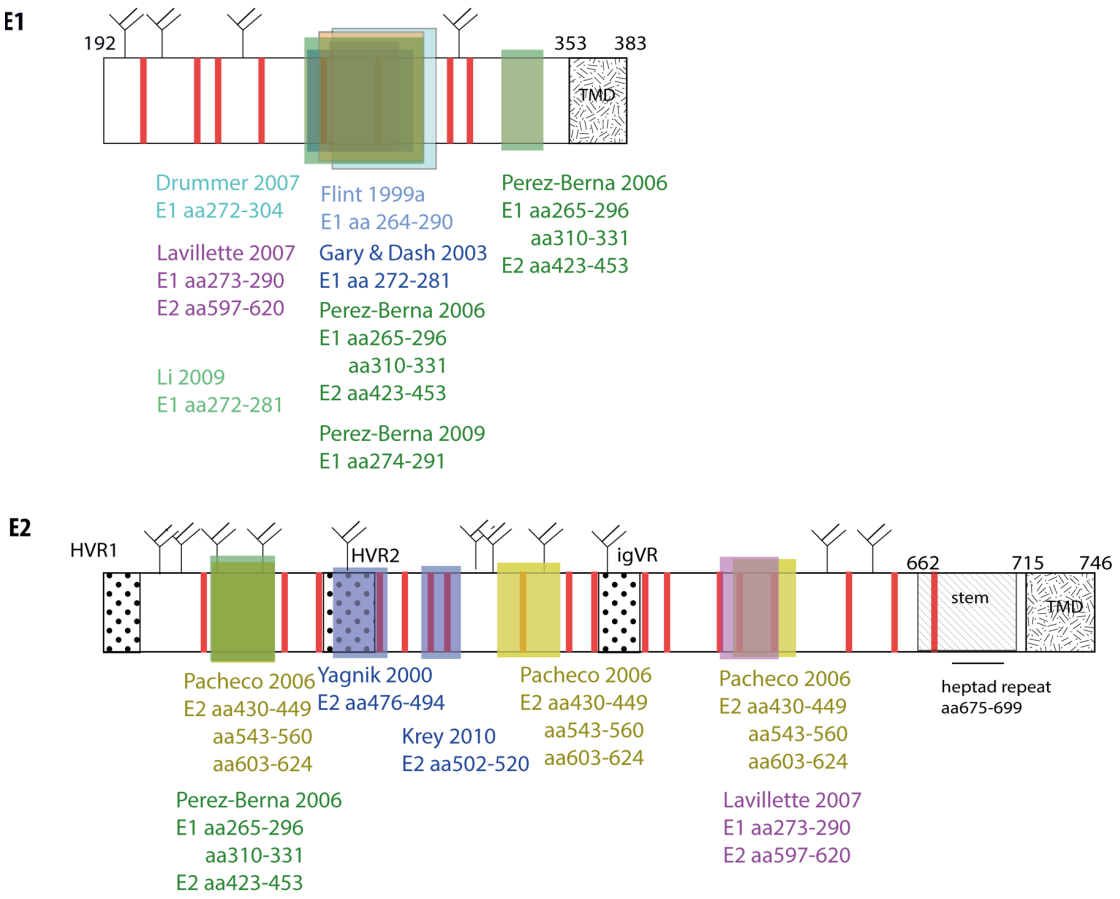

Figure 1.7 The putative fusion motifs proposed in HCV glycoproteins E1 and E2. E1 and E2 are numbered according to HCV strain H77 consensus sequence. Regions of putative fusion loops are highlighted by colored boxes and numbered according to the original publications.

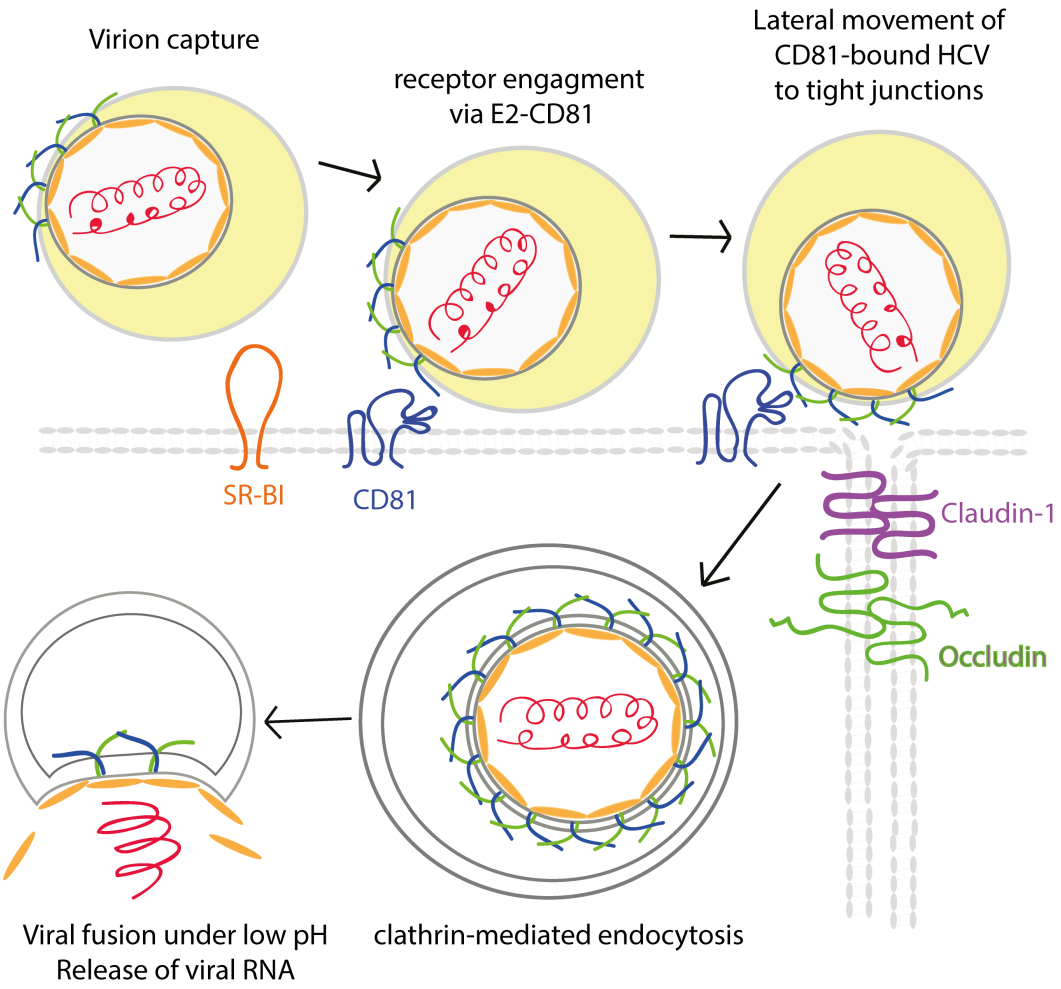

Figure 1.8 The early steps in HCV entry. HCV entry is initiated by host factor interaction via LDLR and SR-BI, and this is followed by CD81-E2 interaction. The association of HCV with CD81 results in the lateral movement of the complex towards tight junctions, further interacting with tight junction proteins, claudin-1 and occludin. The virus then enters the hepatocyte via clathrin-mediated endocytosis before viral fusion in the acidified endosome and RNA release into the ER (Lindenbach & Rice, 2013).

1.6 HCV infection

Natural HCV infections have diverse clinical outcomes and lack a defined clinical progression, resulting in either an acute infection that is asymptomatic and self-resolving within 3-6 months, or a chronic HCV infection that persists for decades (Abe *et al.*, 1992; Alter & Seeff, 2000). The clinical outcome associated with HCV is likely to be the result of a combination of host factors (age at the time of infection, gender, coinfection with HIV or HBV, daily alcohol consumption, and genetics) and viral factors (genotypes, viral load and quasispecies) (Seeff, 2002).

1.6.1 Acute HCV infection with spontaneous clearance

Within the first 6 months, HCV infection presents little or no specific clinical symptoms (Hajarizadeh *et al.*, 2012). In chimpanzees experimentally infected with HCV, viremia occurs in the first 1-2 weeks with serum viral RNA detectable as early as 3 days post-exposure (Farci *et al.*, 1991; Shimizu *et al.*, 1990). This is often accompanied by elevated serum alanine aminotransferase (ALT) levels, possibly due to immune-mediated liver damage (Dahari *et al.*, 2005). In humans, changes in viral RNA in serum occurs in three phases, the pre-ramp up phase, the ramp up phase and the plateau phase (Glynn *et al.*, 2005). During the acute HCV, viral RNA levels can reach up to 10^8 copies/mL (Rehermann, 2009). Similar to HCV infection in chimpanzees, this is followed by elevated serum ALT and seroconversion. However, ALT and antibody levels can vary significantly between infected individuals (Hajarizadeh *et al.*, 2012). Thus, the presence of viral RNA in serum is considered the earliest marker for an active HCV infection (Cox *et al.*, 2005; Farci *et al.*, 1991).

During acute HCV infection, acute liver failure or fulminant hepatitis rarely occurs. Following acute infection, it is estimated that an average 25% of infected individuals spontaneously clear their infection, with the clearance rate higher in females than males (Micallef *et al.*, 2006). Some studies reported a spontaneous clearance rate of 46%-52% in cohorts with a higher risk of infection (Gerlach *et al.*, 2003; Seaberg *et al.*, 2015). Compared to humans, chimpanzees show a higher rate of spontaneous viral clearance (Bassett *et al.*, 1998).

1.6.2 HCV Reinfection following clearance

When challenged with homologous or heterologous HCV, chimpanzees that had previously cleared their HCV infection still develop viremia, suggesting a lack of sustained protective immunity after viral clearance (Farci *et al.*, 1992; Prince *et al.*, 1992). Compared to primary infection, reinfections in chimpanzees are associated with more rapid control of viral replication and are more likely to resolve than to progress into chronicity (Bassett *et al.*, 2001; Major *et al.*, 2002). Some studies also found that previous clearance of HCV or intrahepatic inoculation of viral RNA in chimpanzees can confer protection when they are subsequently challenged with low doses of heterologous viruses (Lanford *et al.*, 2004; Weiner *et al.*, 2001). However, such protection is limited and inconsistent among chimpanzees as some can still develop chronic infection (Bukh *et al.*, 2008).

Similarly, in humans, reinfection is common, especially amongst high risk groups such as IDUs (van de Laar *et al.*, 2009). Early studies indicated that IDUs who had HCV infection have a lower risk of reinfections (Grebely *et al.*, 2006; Mehta *et al.*, 2002). However, in later studies where more frequent HCV testing was performed, a higher rate of reinfection was detected in those who had previous HCV infections (Aitken *et al.*, 2008; Micallef *et al.*, 2007). Nevertheless, it is clear that in humans, previous HCV infection(s) provide limited protective immunity against reinfection. Interestingly, a higher rate of HCV clearance is also observed in reinfected individuals, and some individuals were described as "elite controllers", and are able to clear multiple episodes of HCV reinfections and remain RNA negative (Cox *et al.*, 2005; Grebely *et al.*, 2012; Osburn *et al.*, 2010). Overall, similar to chimpanzee reinfections, HCV reinfections in humans are generally shorter in duration and less likely to become chronic infections (Mehta *et al.*, 2002).

1.6.3 Chronic HCV infection

Approximately 75% of acute HCV infections develop into persistent infections, with serum viral RNA detectable for >6 months. Chronic HCV infections are responsible for most of the morbidity and mortality associated with HCV. Two thirds of chronic HCV infections are mild and non-progressive, while one third of people with chronic HCV develop progressive chronic liver diseases such as fibrosis, cirrhosis and HCV-related hepatocellular carcinoma (HCC) (Alter & Seeff, 2000; Zaltron *et al.*, 2012). Additionally, spontaneous resolution of chronic HCV infections has also been reported (Raghuraman *et al.*, 2012; Scott *et al.*, 2006; Watanabe *et al.*, 2003). The exact mechanism associated with the progression of HCV-related liver disease is not known. However, several risk factors have been identified, including age, gender, duration of HCV infection, alcohol consumption and coinfection with HIV or HBV. Similar to acute HCV infection, serum RNA levels in chronic HCV infection fluctuate (Cox *et al.*, 2005). In addition, ALT levels are transient in both humans and chimpanzees chronically infected with HCV, and is associated with liver damage (Abe *et al.*, 1992; Major *et al.*, 1999).

In progressive chronic HCV infection, the commonly associated liver pathology includes liver inflammation and tissue necrosis, which further progresses into liver fibrosis and blockage of hepatic veins which ultimately impairs liver function (Afdhal, 2004). This is often followed by hepatic decompensation and cirrhosis. Prior to the release of HCV-specific direct acting antivirals (DAAs), the prevalence of HCV-related cirrhosis varies significantly, from 0.3% to 55%, depending on the sampled population, study design and follow-up period (Seeff, 2009). As infection persists, the risk of cirrhosis increases almost three-fold, from 16% after 20 years of infection to 41% after 30 years of infection (Thein *et al.*, 2008). Moreover, progression of cirrhosis is exponential, and further increases the risk for HCC (1-6% per year) and liver failure (2-3% per year) (Grebely & Dore, 2011). Without effective treatment, over 10% of clinically compensated cirrhosis develops into hepatocellular carcinoma (Hamada *et al.*, 2002). Currently, liver transplantation is the only solution for HCV-associated end stage liver failure.

To date, there is no definitive biomarker to identify or distinguish between acute and chronic HCV infection. Detection of serum viral RNA remains the only indicator for an active HCV infection. Due to the asymptomatic nature and extensive period of infection, identification and characterization of natural HCV infection remains difficult and requires vigorous testing for viral RNA.

1.6.4 Treatment for HCV infection

Prior to the release of HCV-specific DAAs, the conventional treatment regimens for HCV are pegylated interferon-α and ribavirin combination therapy, which has limited efficacy and are often associated with severe side effects (Chatel-Chaix *et al.*, 2012). In 2011, telaprevir (Vertex Pharmaceuticals) and boceprevir (Merck & Co) became the first two HCV-specific DAAs approved by the US Food and Drug Administration (FDA). Both DAAs target HCV NS3/4 serine protease and inhibit the processing of the HCV polyprotein. Since then, DAAs targeting a range of HCV non-structural proteins including second generation protease inhibitors, inhibitors to NS5A (daclatasvir, Bristol-Myers Squibb) and NS5B (sofosbuvir, Gilead) have become available. Some of these highly potent DAAs have pan-genotypic efficacy with sustained virologic response (SVR) of >95% and low toxicity, and they are now gradually replacing the conventional interferon/ribavirin therapies as the standard of care for HCV.

1.7 Immune response against HCV

The diverse outcomes in HCV infection are largely determined by the dynamic and intricate interplay between the host immune response and HCV replication. The quality of the immune response in natural HCV infection plays a major role in clinical outcome with a delayed response of narrow specificity resulting in a chronic infection. By contrast, a rapid, strong and broadly reactive immune response involving both innate and adaptive immunity is associated with the control of HCV infection and possibly viral clearance.

1.7.1 Innate Immunity

Upon HCV infection, viral RNA is detected by host cell toll-like receptors (TLRs) and RIG-like receptors. This activates the transcription of interferon (IFN), leading to the activation of IFN-stimulated genes (ISGs) which mediate antiviral activities as well as the activation of adaptive immunity (Schoggins & Rice, 2013). IFNs such as IFN-α and IFN-γ play important roles in innate immune responses against HCV (Heim, 2013). In addition, IFN-λ is a key mediator in HCV clearance. Multiple genome wide association studies (GWASs) showed that IL28B gene polymorphisms are a key determinant in the spontaneous resolution of HCV and the viral clearance following interferon/ribavirin therapy (Rauch *et al.*, 2010; Thomas *et al.*, 2009; Tillmann *et al.*, 2010). Individuals carrying the homozygous favored IL28B alleles are three times more likely to spontaneously clear HCV than those with the risk alleles (Thomas *et al.*, 2009). The favored IL28B allele is associated with increased levels of IFN-λ3 production, which enhances antiviral activities and inhibits of HCV replication *in vitro* (Tanaka *et al.*, 2009). The alternative risk allele was found to be associated with IFN-λ4 production which impairs HCV clearance (Prokunina-Olsson *et al.*, 2013).

1.7.2 Cellular immunity

Cell-mediated immune responses primarily target non-structural components of HCV. Studies on acute HCV infection in chimpanzees showed that a rapid, broad and sustained HCV-specific T cells, involving both $CD4^+$ and $CD8^+$ T cells, are necessary to control and clear HCV (Cooper *et al.*, 1999; Nascimbeni *et al.*, 2003; Prince *et al.*, 2005; Shoukry *et al.*, 2003). However, such responses are often delayed

in natural HCV infections (Post *et al.*, 2004). Following infection, a memory T cell repertoire is generated and plays an important role in the quick resolution of reinfection (Bassett *et al.*, 2001). In chimpanzees, memory T cells can persist for over seven years and play a key role in protection from reinfection (Major *et al.*, 2002; Shoukry *et al.*, 2003).

CD4$^+$ T cells

$CD4^+$ helper T cells recognize viral peptide-bound MHC class II molecules on antigen presenting cells and can produce proinflammatory cytokines such as IFN-γ (Neumann-Haefelin & Thimme, 2013). Depletion of $CD4^+$ T cells using anti-CD4 monoclonal antibody in chimpanzees results in HCV persistence (Grakoui *et al.*, 2003). Broadly specific $CD4^+$ T cells are present in individuals that clear the infection but absent in those whose infection persists (Day *et al.*, 2003; Diepolder *et al.*, 1995; Lucas *et al.*, 2007; Schulze zur Wiesch *et al.*, 2012; Tester *et al.*, 2005; Ulsenheimer *et al.*, 2006). These findings suggest that a rapid $CD4^+$ T cell response plays a key role in the early control of HCV. Furthermore, $CD4^+$ T cell responses need to be sustained to prevent viral rebound. Loss of proliferative activity, followed by rapid depletion and exhaustion of $CD4^+$ T cells can lead to viral recurrence (Gerlach *et al.*, 1999; Schulze zur Wiesch *et al.*, 2012). Some evidence also indicates that a switch from a Th1 response to a Th2 response occurs when infection progress into chronicity (Tsai *et al.*, 1997). In chimpanzees, a strong and sustained proliferation of $CD4^+$ T cells and IFN-γ production is associated with viral control after multiple homologous challenges (Bukh *et al.*, 2008; Nascimbeni *et al.*, 2003).

CD8$^+$ T cells

$CD8^+$ cytotoxic T cells limit viral replication via cytolytic and non-cytolytic mechanisms, either directly killing the infected cells via Fas-Fas ligand interaction, or expression of cytokines IFN-γ and tumor necrosis factor (TNF)-α (Neumann-Haefelin & Thimme, 2013; Thimme *et al.*, 2001). The direct cytolysis by $CD8^+$ T cells significantly reduces viral load by eliminating infected cells, although this also contributes to HCV-related pathology such as liver injuries (Thimme *et al.*, 2001). $CD8^+$ T cell responses occur 6-8 weeks following exposure (Shin *et al.*, 2011; Thimme *et al.*, 2001; Thimme *et al.*, 2002). Similar to $CD4^+$ T cells, depletion of $CD8^+$ T cells in chimpanzees results in viral persistence (Shoukry *et al.*, 2003). It is

well established that an early, strong broadly specific $CD8^+$ T cell response towards multiple HCV epitopes coupled with production of IFN-γ is associated with clearance (Cooper *et al.*, 1999; Lauer *et al.*, 2004; Lechner *et al.*, 2000b; Thimme *et al.*, 2002). A weak $CD8^+$ T cell response that is short-lived and targets limited epitopes is often associated with progression into chronic infection (Lauer *et al.*, 2004; Lechner *et al.*, 2000a; Tester *et al.*, 2005; Tsai *et al.*, 1997). As infection persists, $CD8^+$ cells become dysfunctional and express elevated levels of programmed cell death-1 (PD-1) on the cell surface. This makes CD8+ T cells more susceptible to apoptosis and also impairs their ability to proliferate and produce IFN-γ (Radziewicz *et al.*, 2008; Urbani *et al.*, 2006; Wedemeyer *et al.*, 2002). Reversal of such dysfunction is associated with the spontaneous clearance of chronic HCV infection (Raghuraman *et al.*, 2012).

1.7.3 Humoral immunity

Antibody response during HCV infection

HCV particles isolated from infected individuals are often found as immune complexes, associated with IgG or IgM, suggesting a HCV-specific antibody response (André *et al.*, 2002; Dienstag *et al.*, 1979; Hijikata *et al.*, 1993; Kanto *et al.*, 1995). Similar to cellular immune responses, the development of anti-HCV antibodies is delayed, although most of the infected individuals (>97%) develop anti-HCV antibodies within 6 months of infection. Upon exposure, a core or NS3-specific IgM response is elicited followed by class switching to an IgG response that targets a more diverse range of antigens including core, E1, E2, NS3, NS4 and NS5 proteins (Beld *et al.*, 1999; Netski *et al.*, 2005; Nikolaeva *et al.*, 2002; Yamaguchi *et al.*, 2000). Seroconversion, or the development of antibodies to HCV core and NS5 proteins, does not occur until 8-9 weeks following exposure (Workowski & Bolan, 2015). In addition, isotyping of anti-core, E2, NS3, NS4 and NS5 antibodies derived from HCV positive patients showed that this IgG-mediated response is mostly limited to isotypes IgG1 and IgG3 (Chen *et al.*, 1999). This may potentially restrict the Fc-mediated effector functions such as antibody-dependent cellular cytotoxicity (ADCC), complement-dependent cytotoxicity (CDC) or antibody-dependent phagocytosis.

Antibody responses against HCV play an important role in the control of infection. Early studies showed that pre-exposure transfusion of immunoglobulin preparations containing HCV-specific antibodies delays HCV infection and the onset

of hepatitis (Conrad & Lemon, 1987; Knodell *et al.*, 1976; Krawczynski *et al.*, 1996; Sanchez-Quijano *et al.*, 1988; Sugg *et al.*, 1985). Individuals with agammaglobulinaemia, an immunodeficiency resulting in compromised antibody production, showed a more rapid disease progression during HCV infection, with end stage liver disease developing as early as 18 months of infection, which would otherwise take 20-30 years in individuals with normal antibody levels (Björkander *et al.*, 1988; Bjoro *et al.*, 1994; Christie *et al.*, 1997). Furthermore, B cell depletion following immunosuppressive treatment significantly increases the viral loads in HCV patients (Ennishi *et al.*, 2008).

In early HCV studies, it was unclear whether antibodies are needed for HCV clearance and prevention, as anti-HCV antibodies were often undetectable in individuals who cleared their infection (Post *et al.*, 2004). Similarly, in chimpanzees, there is a poor correlation between viral load and antibody titre, and animals that resolved infection have low titres of HCV-specific antibodies (Abe *et al.*, 1992; Cooper *et al.*, 1999). However, most of these studies examined the infection outcomes in the context of the general antibody response, mainly seroconversion towards core and non-structural proteins, and this may not directly reflect the exact protective roles of antibodies. More recent studies have examined the protective antibody responses and their role in the HCV prevention and clearance.

Neutralizing antibody response against HCV

One of the key parameters to determine and predict the protective effects of the antibody response to viral infections is the presence of neutralizing antibodies, which target structural proteins on virion surface and prevent virus from entering the cells via either the inhibition of virus-receptor binding, virus-cell membrane fusion or other post attachment events. Early studies characterizing the neutralizing antibody response against HCV showed that individuals who resolve the acute infection rapidly develop high titres of antibodies that are able to neutralize HCVpp carrying autologous envelope sequences (Dowd *et al.*, 2009; Lavillette *et al.*, 2005a; Pestka *et al.*, 2007). In addition, the presence of neutralizing antibodies is associated with a reduced viral load during acute HCV (Lavillette *et al.*, 2005a). However, little or no antibodies that can neutralize prototypic strains of unmatched HCVpp *in vitro* were found (Bartosch *et al.*, 2003a; Kaplan *et al.*, 2007; Logvinoff *et al.*, 2004; Meunier *et*

al., 2005; Netski *et al.*, 2005). Together, these studies suggest that isolate-specific neutralizing antibodies are elicited in acute resolvers and an early neutralizing antibody response is associated with viral clearance. Whether these neutralizing antibodies are sufficient to achieve the clearance of acute HCV or whether they act in concert with cellular responses remains unclear. Nevertheless, in animal models, polyclonal antibodies isolated during the acute phase of HCV are able to neutralize homologous virus and prevent infections in chimpanzees and human liver chimeric mice (Farci *et al.*, 1994; Vanwolleghem *et al.*, 2008).

Most chronically infected HCV patients have low titres of neutralizing antibodies during the first 6-8 months of infection (Bartosch *et al.*, 2003a; Dowd *et al.*, 2009; Lavillette *et al.*, 2005b; Logvinoff *et al.*, 2004; Meunier *et al.*, 2005; Pestka *et al.*, 2007; von Hahn *et al.*, 2007). However, as infection persists, they develop high titres of cross neutralizing antibodies that neutralize heterologous strains. In patient H who had chronic HCV and was monitored for 26 years, isolate-specific neutralizing antibodies appeared at 7 weeks post-exposure, whereas cross neutralizing antibodies did not appear until week 33 (Logvinoff *et al.*, 2004; Meunier *et al.*, 2005; von Hahn *et al.*, 2007). In human liver chimeric uPA-SCID mice, these cross neutralizing antibodies are protective against different genotypes of HCV when passively transferred prior to viral challenge (Meuleman *et al.*, 2011). However, *in vitro* neutralization assays suggested that despite the presence of cross reactive neutralizing antibodies, antibodies from chronic sera failed to neutralize concurrent strains of HCVpp (Dowd *et al.*, 2009; Farci *et al.*, 1994; Logvinoff *et al.*, 2004; Shimizu *et al.*, 1994; von Hahn *et al.*, 2007). This led many to propose that cross neutralizing antibodies had little effect on the control of HCV since HCV is able to mutate rapidly, circulating in an infected host as a dynamic pool of genetic variants, or quasispecies that contain neutralization resistant variants. However, it is also possible that cross neutralizing antibodies play a role in HCV control but their effects are masked by high titres of antibodies to immunodominant epitopes that are non-neutralizing and/or interfering.

E2: the major target of neutralizing antibodies during HCV infection

While both E1 and E2 elicit neutralizing antibodies during HCV infection, the immunogenicity of E1 remains unknown. In contrast, E2, particularly its N-terminal HVR1 region, is a major target of neutralizing antibodies. Single source outbreak studies found that the presence of high titres of HVR1-specific antibodies in the early phase of infection is associated with viral clearance (Allander *et al.*, 1997; Zibert *et al.*, 1997). In addition, hyperimmune sera raised against a HVR1 peptide protects chimpanzees from homologous viruses (Farci *et al.*, 1996). Although both the N-terminal and C-terminal regions of HVR1 are able to elicit antibodies, only antibodies specific to its C-terminus (residues 396-407) are able to neutralize autologous strains of HCVpp and HCVcc *in vitro*, by interfering with post attachment events other than E2-CD81 and HCV-GAG interactions (Farci *et al.*, 1996; Flint *et al.*, 1999a; Guan *et al.*, 2012; Owsianka *et al.*, 2001; Vieyres *et al.*, 2011).

It is well documented that during chronic HCV infection, HVR1 undergoes rapid sequence changes and multiple HVR1 variants can be found within an infected individual (Farci *et al.*, 1994; Farci *et al.*, 2000; Kato *et al.*, 1994; Kurosaki *et al.*, 1993; Ogata *et al.*, 1991; Weiner *et al.*, 1992). Sequence analyses of envelope proteins from G1a and 1b revealed that HVR1 contains the most nonsynonymous substitutions, suggesting that it is under positive selection pressure, mainly by antibodies (Tarr *et al.*, 2015). Furthermore, when compared to HCV positive individuals with hypogammaglobuliemia whose HVR1 sequences can remain unchanged for 2.5 years, those with normal antibody production have an over 20-fold increase in HVR1 amino acid diversity (Booth *et al.*, 1998; Kumar *et al.*, 1994). In one subject, HVR1 remained unchanged for 21 months until the appearance of antibodies (Liu *et al.*, 2010a).

Given the sequence diversity and structural flexibility of HVR1, anti-HVR1 antibodies have limited cross-reactivity and does not provide protection against heterologous challenge (Farci *et al.*, 1996; Kato *et al.*, 1993). As an immune epitope that elicits high titres of isolate-specific antibodies and rapidly selects for escape variants, HVR1 is one of the major contributing factors in HCV persistence and is responsible for the type-specific neutralizing antibody response observed in HCV infection. HVR1 also shields the exposure of conserved neutralization epitopes on E2

as deletion of HVR1 increases the sensitivity of HCVpp and HCVcc to neutralizing antibodies targeting other regions of E2 (Bankwitz *et al.*, 2010; Bartosch *et al.*, 2005; Prentoe *et al.*, 2011; Prentoe *et al.*, 2016). When bound to E2, HVR1-specific antibodies inhibit the binding of neutralizing antibodies to an adjacent region (residues 412-423) and reduce their ability to neutralize HCVcc (Keck *et al.*, 2016). Together, these finding suggest that the lack of correlation between neutralizing antibody response and the control and clearance of HCV is partly due to the presence of HVR1-specific antibodies, which not only provide limited protection but also interfere with the protective effects of other neutralizing antibodies.

1.8 Broadly neutralizing monoclonal antibodies to HCV E1 and E2

1.8.1 Isolation of monoclonal antibodies from natural HCV infections

One of the approaches to fully dissect and examine the role of neutralizing antibodies (NAbs) in HCV infection is to isolate monoclonal antibodies (MAbs) from infected individuals. To date, several panels of HCV-specific human monoclonal antibodies (HMAbs) have been isolated, using either Epstein Barr virus (EBV)-immortalized B cells (Hadlock *et al.*, 2000; Keck *et al.*, 2005; Keck *et al.*, 2008), phage display libraries (Allander *et al.*, 2000; Burioni *et al.*, 1998; Giang *et al.*, 2012; Johansson *et al.*, 2007; Law *et al.*, 2008; Schofield *et al.*, 2005), or yeast display libraries (Keck *et al.*, 2012; Keck *et al.*, 2013), shown in Table 1.1. While most of the HMAbs showed little or limited cross neutralization, some HMAbs such as the HC84 group and AR3/AR4 groups are broadly neutralizing, with potent *in vitro* 50% inhibitory concentrations (IC_{50}) to some HCV strains in the ng/mL range, as shown in Table 1.2. However, the exact breadth of neutralization of HMAbs cannot be fully determined given the limited set of *in vitro* isolates currently available.

In human liver chimeric mice, pre-transfusion of AR3A or AR3B prior to heterologous quasispecies challenge significantly reduces viral load, with viral rebound occurring immediately following antibody decay (Law *et al.*, 2008). Subsequent studies using adenovector-delivered AR3A, AR3B and AR4A antibodies indicate that a sustained level of broadly neutralizing antibodies is able to provide complete protection against low dose of H77c infectious clone (de Jong *et al.*, 2014). In primary hepatocytes with established HCVcc infection, AR3A, AR3B and AR4A alone or in combination inhibits viral replication, while in combination, they completely suppress viral RNA in transgenic mice with established HCVcc J6/JFH-1. However, the efficacy of AR3A, AR3B and AR4A are less pronounced in mice with established H77 quasispecies infection, with a delayed viral load suppression followed by immediate viral rebound (de Jong *et al.*, 2014). These findings underscored the significance of broadly neutralizing antibodies (brNAbs) in the

prevention of HCV. Investigations into novel brNAbs, particularly their target epitopes, will therefore shed some light on the development of antibody-based immunotherapies and vaccines.

Table 1.1 HCV-specific monoclonal antibodies isolated from humans

HMAbs	Isolation	Reference
e20 & e137	Phage library derived from the bone marrow RNA of G1b; selected for reactivity to E2 388-644 G1a	(Burioni *et al.*, 1998)
CBH-related HMAbs	EBV-immortalized peripheral B cells of a chronic G1b that showed high serum neutralization of binding (NOB) titre; screened by immunofluorescence assay (IFA) of Sf9 cells expressing E2 (G1a)	(Hadlock *et al.*, 2000; Keck *et al.*, 2005)
HCV#-related HMAbs	Phage library derived from bone marrow RNA of an asymptomatic chronic G1a (patient H in 1999); screened with E2 (G unknown)	(Schofield *et al.*, 2005)
HCV-Ab^{XTL}68	EBV-immortalized peripheral B cells of an HCV positive patient (G unknown); screened with E1E2 (G1a, strain H)	(Eren *et al.*, 2006)
HC-related HMAbs	EBV-immortalized peripheral B cells from a chronic G1a that had high titres of antibodies to E2 and neutralizes HCVpp (G1a); screened against E2 (G1a and G1b)	(Keck *et al.*, 2008)
AR-related HMAbs	Phage library derived from bone marrow mononuclear cell RNA of a chronic G1a; screened with E2 (G1a) followed by masked E2 or E1E2	(Giang *et al.*, 2012; Law *et al.*, 2008)
HC84-related HMAbs	Yeast display single chain variable fragment (scFv) library derived from peripheral B cells of a chronic G2b that showed high titres of antibodies to E2 and neutralized HCVpp H77c and HCVcc JFH-1; Selected against E2 Y623A and D535A as well as cross-reactivity to E2 from all 6 genotypes	(Keck *et al.*, 2012)
HC33-related HMAbs	Yeast display scFv library derived from peripheral B cells from chronic G2b that showed high titres of antibodies to peptide 410-425 and neutralized HCVcc JFH-1; selected against E2 peptide 410-425	(Keck *et al.*, 2013)

Table 1.2 The breadth and potency of HCV-specific human monoclonal antibodies *in vitro*

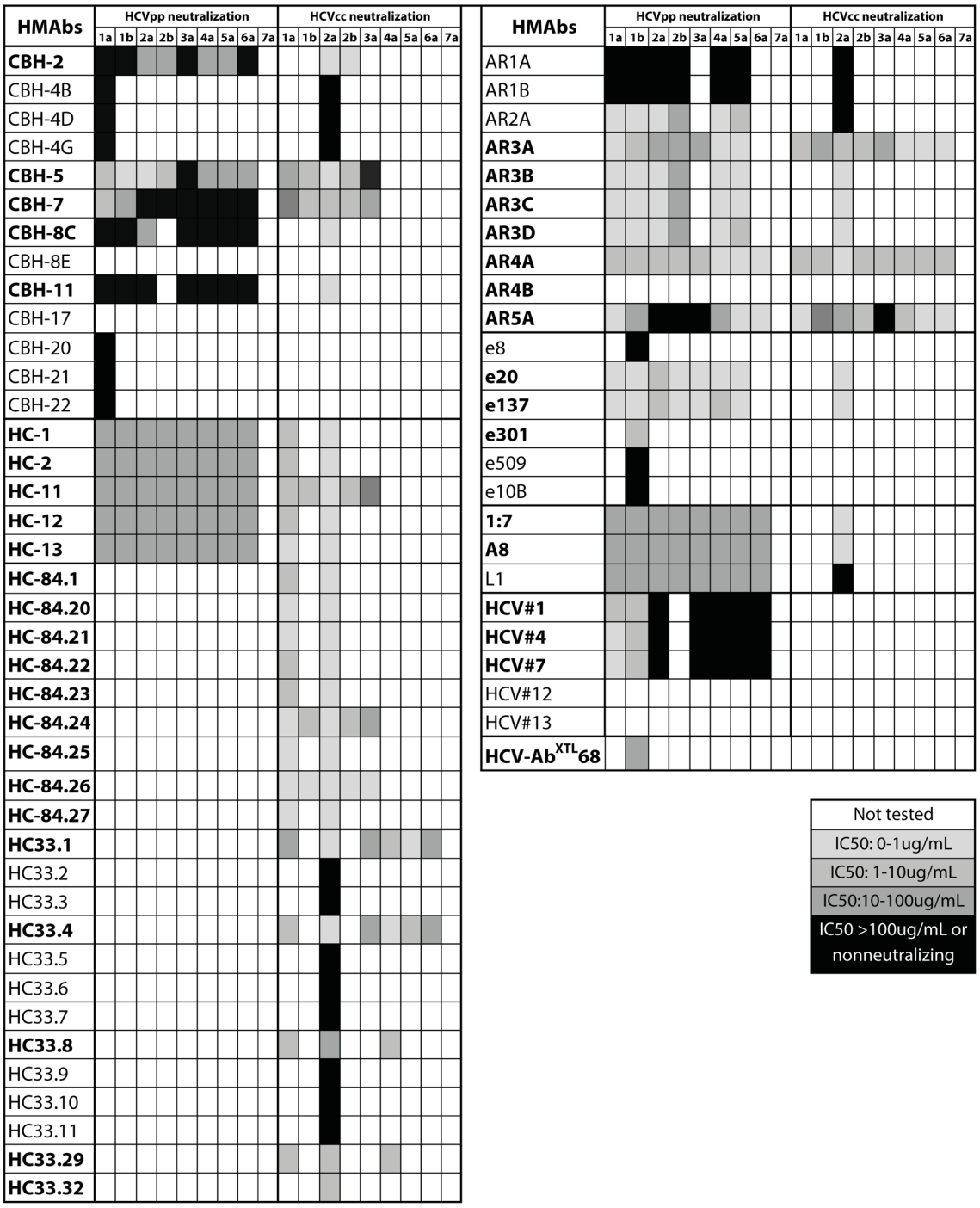

Figure 1.9 Targets of neutralizing antibodies on HCV E1 and E2. (A) Neutralizing

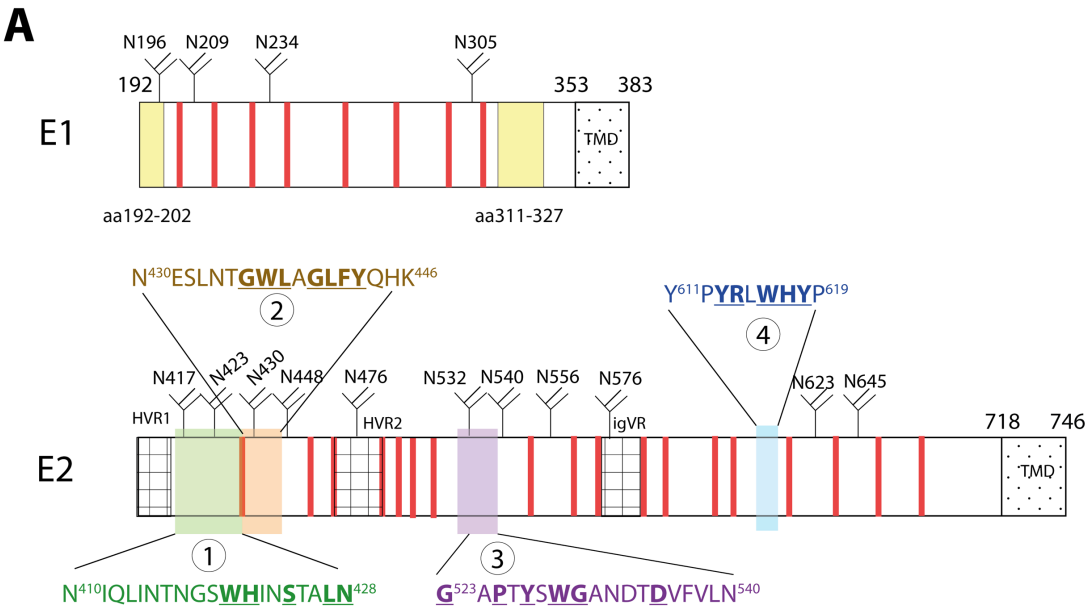

B

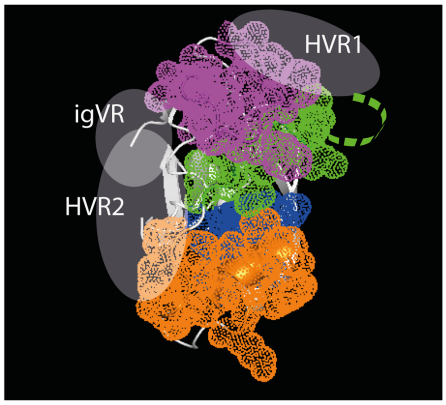

C

	HMAbs	1	2	3	4
domain E	HC33.1	+			
	e20			+	
antigenic region 3	e137	+		+	
	AR3C	+	+	+	
	1:7			+	
	A8			+	
domain B	HC-1			+	
	HC-11	+	+	+	+
	CBH-2	+	+	+	
	CBH-5			+	
domain C	CBH-7			+	
domain D	HC84.21		+		+
	HC84.27		+		+

antibody epitopes on E1 (in yellow) and E2. The E2 Epitopes, I (1), II (2), III (3) and IV (4) are highlighted in green, orange, magenta and blue respectively. The CD81 binding residues on E2 are in bold and underlined. (B) The distribution of the four neutralizing epitopes on the neutralizing face of the E2 core structure solved by Kong *et al* (2013). (C) The epitope I-IV recognition by well characterized neutralizing HMAbs specific to E2.

1.8.2 Targets of cross neutralizing antibodies on E1

Characterization of HMAbs (H-111, IGH526 and IGH520) revealed two neutralizing epitopes on E1, residues 192-202 and residues 311-327, as shown in Figure 1.9A (Keck *et al.*, 2004b; Meunier *et al.*, 2008). *In vitro* neutralization studies further suggested that all of them exhibit cross-neutralizing potential. When bound to the monoclonal antibody IGH526, the 311-327 region adopts an α-helical conformation (Kong *et al.*, 2015). However, the exact mechanism involved in E1-specific neutralization is not understood.

1.8.3 Targets of cross neutralizing antibodies on E2

Early competitive inhibition analyses of neutralizing and non-neutralizing HMAbs suggested that E2 contains multiple immunogenic domains including the antibody domains (Domain A-E) assigned by Foung *et al*, and the antigenic regions (AR1-5) proposed by Law *et al* (Giang *et al.*, 2012; Keck *et al.*, 2004a; Keck *et al.*, 2008; Keck *et al.*, 2012; Keck *et al.*, 2013; Law *et al.*, 2008). Using alanine mutagenesis of the E1E2 proteins, the exact E2 residues responsible for each HMAb recognition were later determined. Thus far, four cross-reactive NAb epitope regions on E2 are identified (detailed residue mapping as shown in Appendix II). These include epitope I (residues 412-428), epitope II (residues 430-446), epitope III (residues 523-540), and epitope IV (residues 611-619), as shown in Figure 1.9A. Epitope I and epitope II are often referred to as linear continuous epitopes, since MAbs to these two regions, such as HMAbs HC33.1 and HC84.27, can recognize the peptide analogues of the epitopes. In contrast, epitope III and epitope IV are described as discontinuous conformational epitopes, as the MAbs to these two epitopes often require the tertiary organization of E2 ectodomains and does not recognize denatured E2. Together, the four neutralizing epitopes constitute the proposed neutralizing face on E2 core structure, which also overlaps with the CD81 binding face on E2, as shown in Figure 1.9B and C.

Epitope I and epitope II

Epitope I (residues 412-428, also described as domain E or antigenic site AS412) is one of best characterized neutralizing epitopes on E2. It is well conserved and is essential for the entry of HCVcc and HCVpp (Meola *et al.*, 2015). Several MAbs to this region have been isolated from E2-immunized animals and infected humans, including mouse MAbs AP33 and MAb24, rat 3/11, HMAbs HCV1 and HC33.1, all of which are cross reactive against E2 of various genotypes, and can competitively inhibit E2-CD81 binding and cross neutralize diverse strains of HCVcc and HCVpp *in vitro* (Alhammad *et al.*, 2015a; Broering *et al.*, 2009; Flint *et al.*, 1999a; Owsianka *et al.*, 2001; Pantua *et al.*, 2013; Sabo *et al.*, 2011). MAb characterization also suggested that glycosylated at N417 and N423, the 412-423 region is highly accessible on E2, E1E2 heterodimers and VLPs and has a flexible structure which was disordered in the E2 core structure (Alhammad *et al.*, 2015a; Clayton *et al.*, 2002; Keck *et al.*, 2013; Kong *et al.*, 2013; Morin *et al.*, 2012; Owsianka *et al.*, 2001). In natural HCV infection, the immunogenicity towards the 412-423 region is low, with an estimated seroprevalence of 2.5%-15% in HCV-positive individuals (Keck *et al.*, 2013; Tarr *et al.*, 2007). Despite this low prevalence, HMAbs to this region, such as HC33.1, have been isolated from humans (Keck *et al.*, 2013).

In chimpanzees, HCV1, the epitope I-specific HMAb isolated from transgenic mice with human antibody genes, prevents HCV infection when administered prior to homologous challenge (Morin *et al.*, 2012). In acutely and chronically infected chimpanzees, transfusion of HCV1 transiently reduces viral load followed by viral rebound due to the acquisition of HCV1 resistance. Similar observations were obtained in humans receiving a 7-day HCV1 monotherapy from the day of liver transplant, with viral rebound occurring as early as 14 days post transplantation (Chung *et al.*, 2013). Long term *in vitro* passaging of G1a or G2a HCV suggested that other epitope I-specific MAbs, AP33 and HMAb HC33.1 can select for escape mutants. Although sharing only two common epitope residues, AP33 and HCV1 selected for surprisingly similar resistant mutants *in vitro* and *in vivo*, with changes at the residue N415 and the glycan N417, neither of which compromised viral fitness (Broering *et al.*, 2009; Tarr *et al.*, 2006). Structural studies showed that despite differences in paratopes, the conformation of both HCV1 and AP33-bound epitope I

peptide adopt a β-hairpin structure with N415 critical in maintaining the epitope conformation (Figure 1.10A) (Kong *et al.*, 2012a; Kong *et al.*, 2012b; Potter *et al.*, 2012). Furthermore, epitope I can adopt two other distinct extended structures when complexed with rat MAb 3/11 and HMAb HC33.1 (Figure 1.10B) (Li *et al.*, 2015a; Meola *et al.*, 2015).

Epitope II (residues 430-446, also referred to as domain D or antigenic site AS434) is a key component of the neutralizing face on E2 which is recognized by brNAbs such as HC84.27 and AR3C, and has also been described as an epitope for $CD4^+$ and $CD8^+$ T cells (Kong *et al.*, 2013; Tarr *et al.*, 2012; von Hahn *et al.*, 2007). Early reports proposed that antibodies to epitope II are non-neutralizing and interfering, as depletion of epitope II antibodies from chronic plasma or E1E2-immunized humans enhance the cross-neutralization potential of the immune serum *in vitro* (Kachko *et al.*, 2015; Zhang *et al.*, 2007; Zhang *et al.*, 2009). However, work conducted by others found that antibodies that were affinity purified to epitope II from chronic sera are able to neutralize HCVpp and HCVcc, and when combined with epitope I antibodies, demonstrated additive neutralization (Tarr *et al.*, 2012). In addition, conformational HMAbs specific to this regions, HC84.1 and HC84.27 exhibit potent broad neutralization *in vitro* and synergistically neutralize HCVcc when combined with epitope I-specific HMAbs such as HC33.1 (Keck *et al.*, 2012). Although the exact mechanisms associated with the observed neutralization enhancement as a result of epitope II-antibody depletion is not known, it is clear that epitope II can elicit neutralizing antibodies. As an α-helix at the front layer of E2 (Figure 1.10 C and D), epitope II is involved in CD81 binding and is functionally essential as *in vitro* passaging of HCVcc G2a in the presence of HC84.1 failed to select for escape mutants (Drummer *et al.*, 2006; Keck *et al.*, 2012; Kong *et al.*, 2013; Krey *et al.*, 2013).

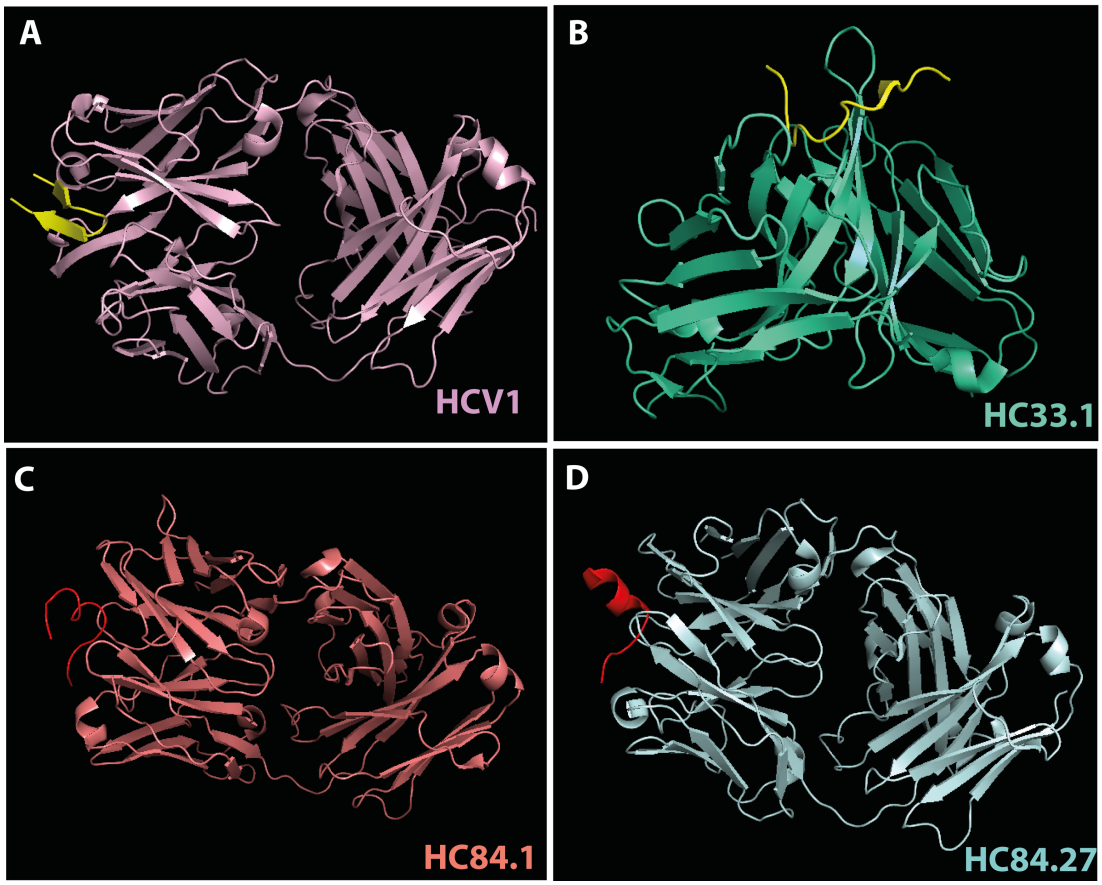

Figure 1.10 The structures of cross-NAb epitopes I and II on E2 when complexed with HMAbs. (A) The 412-423 peptide (epitope I, yellow) when bound to HCV1 Fab (PDB: 4DGY, C2 form, light purple) (Kong *et al.*, 2012b). (B) The 412-423 peptide (epitope I, yellow, with an additional Arg residue at N-terminus) when complexed with HC33.1 scFv (PDB: 4XVJ, green) (Li *et al.*, 2015a). (C) The 435-446 peptide (epitope II, red) when bound to HC84.1 Fab (PDB: 4JZN, orange red) (Krey *et al.*, 2013). (D) The 436-446 peptide (epitope II, red) when bound to HC84.27 Fab (PDB: 4JZO, light blue) (Krey *et al.*, 2013). All the structures are shown as cartoon representation using PyMOL.

Figure 1.11 The tertiary organization of cross-NAb epitopes on the AR3C-E2 complex (PDB: 4MWF) (Kong et al., 2013). HMAb AR3C and E2 are shown as light purple and white cartoon representations, respectively. The cross-NAb epitopes are highlighted in green (epitope I), orange (epitope II), dark purple (epitope III) and blue (epitope IV). The N-terminus of epitope (residues 412-419) I is disordered and not shown.

Epitope III and epitope IV

As a crucial component of the neutralizing face on E2, epitope III (residues 523-540) is required for the recognition of E2 by most conformational HMAbs including domain-B, -C, -D and AR3 antibodies, as shown in Figure 1.9C and Figure 1.11, and its N-terminus forms the flexible CD81 binding loop on E2. In contrast, epitope IV is not directly associated with the neutralizing face of E2. Located towards the back layer of the E2 core structure, epitope IV forms close contacts with the α-helical structure of epitope II, and replacement or mutations in this region abolish E2-CD81 binding and significantly reduce HC84-like HMAbs binding to E2 (Boo *et al.*, 2012; Keck *et al.*, 2012; Roccasecca *et al.*, 2003; Rothwangl *et al.*, 2008).

In summary, the isolation of HMAbs as well as the current E2 ectodomain structures have provided us a working template for the investigation into the neutralizing epitopes on E2. Further characterization of the cross-NAb epitopes on E2 as well as E1E2 heterodimers is required to fully understand the neutralizing mechanisms of brNAbs, particularly the HMAbs AR4/AR5 that recognize E1E2 heterodimers. Furthermore, studies into the isolation of new HMAbs to novel epitopes as well as the structural basis of E2-CD81 complex and E1E2 heterodimers are needed.

1.9 HCV vaccines

Despite the >95% cure rate achieved with DAAs, multiple issues limit the use of DAAs in the control of HCV. With 50-75% of HCV-positive people unaware of their infection, which additionally serves as a source for further transmission, widespread screening is required for the diagnosis and treatment of HCV (Smith *et al.*, 2012). Yet, there is no cheap, technology-free point of care test available for the detection of viral RNA, especially in resource-constrained settings where HCV is most prevalent. Furthermore, the cost barriers to DAA access and the care cascade required for DAAs (testing, diagnosis, treatment and cure or chronic infection management) remain two of the major obstacles for DAA use in HCV elimination. Additionally, DAAs do not provide long-lasting protection, which makes cured individuals vulnerable to reinfections. Therefore, an effective vaccine that elicits protective immunity is essential in controlling the HCV epidemic and achieving the elimination targets set by the WHO.

The major impediment to developing an effective vaccine for HCV is its genetic diversity. An ideal vaccine candidate needs to offer potent, long-lasting sterilizing immunity that confers pan-genotypic protection and prevents immune escape. Given the positive correlation between strong T-cell responses and HCV clearance, many vaccine candidates have focused on eliciting strong T cell responses towards HCV components, mostly the core and non-structural proteins which are relatively conserved, by using either adjuvants that promote T cell responses, incorporation of viral sequences into viral vectors for delivery or DNA electroporation (Barnes *et al.*, 2012; Drane *et al.*, 2009; Folgori *et al.*, 2006; Klade *et al.*, 2008; Polakos *et al.*, 2001; Swadling *et al.*, 2014; Wedemeyer *et al.*, 2009; Youn *et al.*, 2008; Yutani *et al.*, 2009). As one of the most promising HCV vaccine candidates, the ChAd3/MVA-NSmut vaccine (ChAd3, chimpanzee adenoviral vector and MVA, modified vaccinia Ankara vector, G1b) developed by Oxford University, used a heterologous prime/boost regimen to deliver multiple HCV non-structural proteins (NS3-NS5B) and has demonstrated potent, long-lasting and multi-specific immunogenicity in both $CD4^+$ and $CD8^+$ T cell responses in healthy volunteers, suggesting that it is a promising component of a prophylactic vaccine for HCV (Swadling *et al.*, 2014). This vaccine is currently in a Phase II trial to determine safety and efficacy in naïve

volunteers (ClinicalTrials.gov Identifier: NCT01436357). However, recent human clinical trial results suggest that its efficacy in patients with chronic HCV, when used as a therapeutic vaccine to cure or reduce viral load, is low (Kelly *et al.*, 2016; Swadling *et al.*, 2016). The $CD4^+$ T cell response, in particular, was almost undetectable. Thus, overcoming the low efficacy associated with T cell exhaustion in chronic infections remains a major challenge for developing an effective T cell based therapeutic vaccine for HCV.

A meta-analysis of chimpanzee vaccine trials conducted prior 2010 suggested that vaccines incorporating non-structural components that induce T-cell responses effectively control viremia, but confer little protection (Dahari *et al.*, 2010). Vaccines containing HCV glycoproteins E1 and E2 on the other hand, effectively induces E1E2-specific antibodies that are correlated with protection. This highlighted the importance of HCV E1E2 and E1E2-specific antibody response in HCV vaccine design. Most of the currently licensed vaccines rely primarily on eliciting a protective antibody response to prevent infections. One of the conventional approaches to elicit protective antibody responses is to immunize with whole virus that is either inactivated or attenuated. UV-inactivated, cell culture-derived HCV particles (J6/JFH1 chimeric HCVcc, G2a, with adjuvant) demonstrated high immunogenicity in mice and were able to induce cross neutralizing antibodies that protect uPA-SCID mice from low dose homologous viral challenge (Akazawa *et al.*, 2013). However, parallel vaccination experiments suggested that whole virus vaccines elicit less anti-E2 antibodies in mice compared to E2 immunization. In addition, the need to use bovine serum albumin to produce HCV virions and the relatively low yield remain the key technical issues to overcome in the large-scale production of such a vaccine.

As an alternative to the whole virus vaccines, recombinant forms of HCV E1E2 proteins can be expressed at high yield and are therefore ideal candidates for antibody-based vaccines. Chimpanzee immunization studies showed that the gpE1/gpE2 protein (G1a, strain HCV1, with MF59 as the adjuvant) is immunogenic and is able to elicit high antibody titres, which correlates with protection against homologous challenges in chimpanzees (Choo *et al.*, 1994). In goats, gpE1/E2 was able to elicit antibodies that compete with known neutralizing antibodies for binding to E1E2 (Wong *et al.*, 2014). However, a delay in seroconversion towards

gpE1/gpE2 (24-36 weeks) was observed in chimpanzees and the magnitude of the antibody response varied between animals (Choo *et al.*, 1994). Also, *in vitro* neutralization studies showed that the antibodies induced by gpE1/gpE2 in chimpanzees and humans in Phase I clinical trials exhibited limited cross-neutralizing capacity against other genotypes of HCVpp and HCVcc (Meunier *et al.*, 2011; Stamataki *et al.*, 2011). Although immunization with E1E2 partially delays viremia in immunized chimpanzees challenged with homologous virus, persistent infection still develops (Puig *et al.*, 2004). In Phase I clinical trials, only one of 16 vaccinated humans had cross reactive antibodies that at 1/50 dilution, achieved >50% neutralization against heterologous viruses (G1b, G4a, G5a and G6a) (Law *et al.*, 2013). Lastly, gpE1/gpE2 was shown to elicit HVR1-specific antibodies, which are known to be type-specific and associated with the generation of immune escape variants (Ray *et al.*, 2010). Therefore, the ability to elicit broadly neutralizing antibodies against HCV glycoproteins E1 and E2 remains the key criteria in determining the efficacy of a universal antibody-based vaccine for HCV.

Whilst the relatively conserved E1 immunogen cannot be expressed alone as a recombinant protein, investigations into a VLP-based E1 vaccine (G1b, strain BE11) demonstrated its immunogenicity in inducing both T cell and antibody responses in healthy and chronically infected individuals (Leroux-Roels *et al.*, 2004; Leroux-Roels *et al.*, 2005; Maertens *et al.*, 1996; Nevens *et al.*, 2003; Verstrepen *et al.*, 2011). In addition, it protects chimpanzees from infection by a heterologous virus of the same genotype (Verstrepen *et al.*, 2011). Nevertheless, there is limited knowledge of E1-specific neutralizing antibodies and their role in protection *in vitro* and *in vivo*. In contrast, the RBD of E2 can be readily expressed as a soluble protein in cell culture and is highly immunogenic in natural HCV infection. Antibodies specific to E2 are able to recognize conserved regions of E2 that mediate broad neutralization against diverse strains of HCV both *in vitro* and *in vivo* (de Jong *et al.*, 2014; Law *et al.*, 2008). E2 is therefore an ideal vaccine candidate for eliciting neutralizing antibodies specific to HCV.

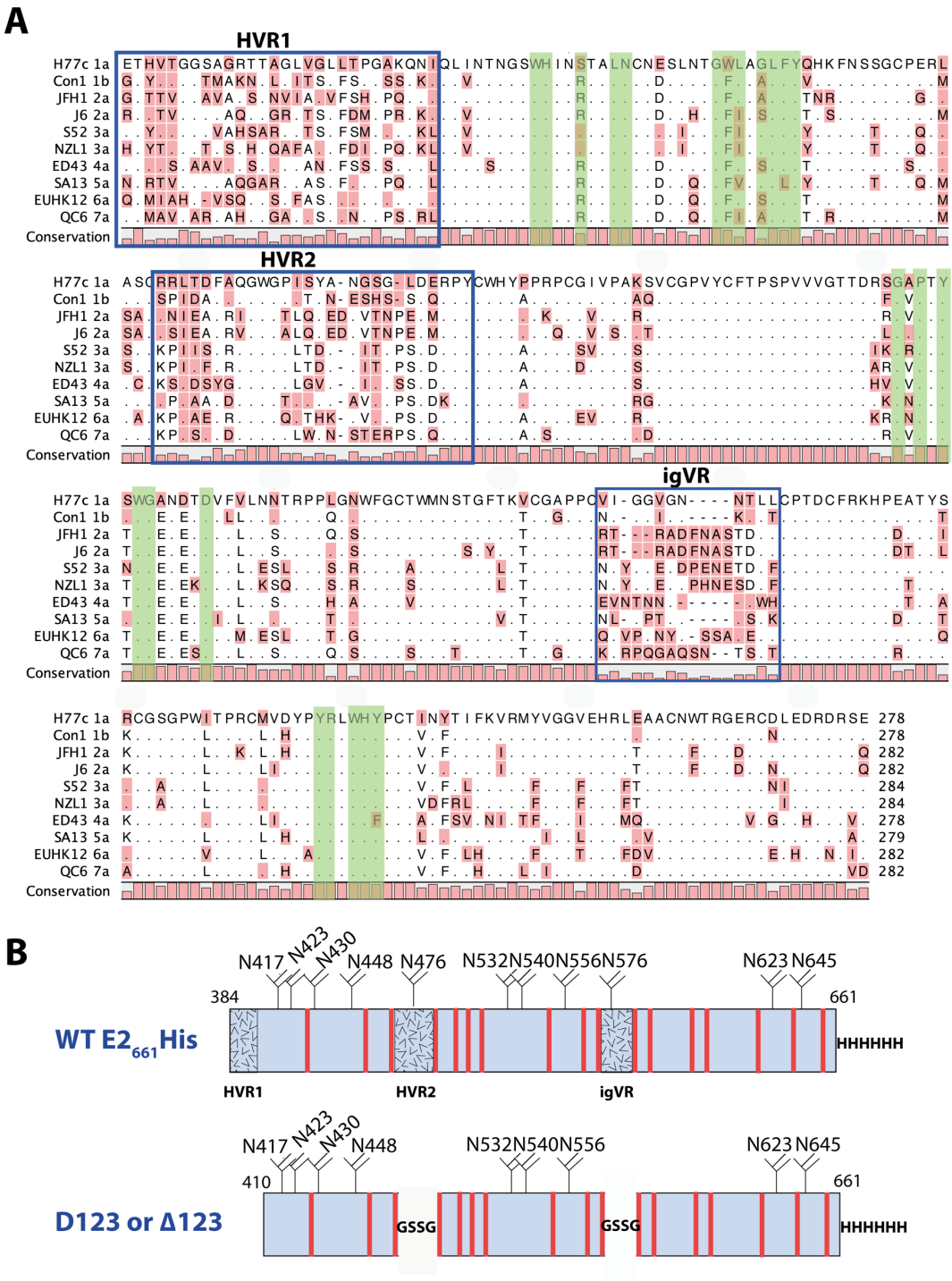

Figure 1.12 The receptor binding domain of HCV E2. (A) Sequence alignment of E2 RBD from prototypic strains of 7 HCV genotypes (CLC Main Workbench v7). CD81 binding residues are highlighted in green. Hypervariable regions (HVR1, HVR2 and igVR) of E2 are boxed. Matching residues are shown as dots. (B) Schematic diagram of WT RBD and D123 proteins. The HVRs of D123 were replaced with GSSG linkers. Glycosylation sites are indicated as tree diagrams. Conserved cysteine residues are highlighted as red bars. The poly-HIS tag of both proteins is shown as HHHHHH.

Table 1.3 Percent identity matrix of WT E2 (top) and D123 (bottom) from prototypic strains of HCV (created by Clustal2.1)[1].

WT E2	H77c, G1a	Con1, G1b	JFH-1, G2a	J6, G2a	S52, G3a	NZL1, G3a	ED43, G4a	SA13, G5a	EUHK2, G6a	QC6, G7a
H77c, G1a	100	78.42	71.84	71.84	73.38	71.94	72.2	76.62	72.2	73.38
Con1, G1b		100	75.45	73.65	75.18	72.66	72.56	**78.06**	72.2	77.34
JFH-1, G2a			100	84.4	70.46	70.46	70.04	73.38	70.25	73.48
J6, G2a				100	70.82	68.68	**67.87**	72.3	68.46	72.4
S52, G3a					100	**87.32**	71.58	72.04	72.34	69.5
NZL1, G3a						100	70.14	70.25	70.57	69.86
ED43, G4a							100	68.35	70.76	69.42
SA13, G5a								100	73.38	74.55
EUHK2, G6a									100	71.17
QC6, G7a										100

D123	H77c, G1a	Con1, G1b	JFH-1, G2a	J6, G2a	S52, G3a	NZL1, G3a	ED43, G4a	SA13, G5a	EUHK2, G6a	QC6, G7a
H77c, G1a	100	87.5	83.48	81.7	82.14	81.25	80.36	85.27	81.25	82.14
Con1, G1b		100	87.05	84.82	82.59	81.25	82.14	**87.5**	83.04	87.05
JFH-1, G2a			100	88.39	79.91	79.46	81.25	83.48	82.59	85.71
J6, G2a				100	79.02	**77.68**	79.46	80.8	79.91	81.7
S52, G3a					100	**93.75**	78.57	80.36	82.14	79.02
NZL1, G3a						100	79.46	79.02	79.91	80.36
ED43, G4a							100	78.57	81.25	79.91
SA13, G5a								100	81.7	83.48
EUHK2, G6a									100	81.7
QC6, G7a										100

[1]The lowest and highest (intra and inter-genotypic) % identity is highlighted in orange and green respectively.

1.10 Hypotheses and Aims

1.10.1 Hypotheses

The key challenge facing E2 immunogen design is that it exhibits substantial sequence diversity, with amino acid residues varying up to 32.13% amongst representative strains of HCV from 7 genotypes and this diversity is predominately found in the three HVRs (Table 1.3, ED43 G4a vs J6 G2a, and Figure 1.12A). McCaffrey *et al* (2007) proposed that the three HVRs form surface exposed flexible structures on E2 and found that they can be readily replaced with short linkers composed of glycine and serine residues (GSSG linkers) without significant changes in E2 conformation. The resulting HVRs-deleted E2 RBD (D123, residues 410-661, shown in Figure 1.12B), which also contains a C-terminal HIS tag for the ease of purification and detection, was found to retain high levels of glycoprotein secretion and a conformation similar to WT E2 RBD (residues 384-661, shown Figure 1.12B), as assessed with panels of conformational neutralizing and non-neutralizing HMAbs and recombinant CD81-LEL (McCaffrey *et al.*, 2007).

The efficacy of a preventative universal antibody-based HCV vaccine candidate such as D123 is contributed by its ability to elicit broadly neutralizing antibodies, which 1) target multiple conserved NAb epitopes within the E1E2 glycoprotein complex; 2) prevents the generation of escape variants; and 3) provides long-lasting immunity. Here, it is hypothesised that 1) the HVRs modulate the recognition of E2 by NAbs and that by deleting the HVRs the immune response will be re-directed towards conserved regions of E2; 2) Highly conserved NAb epitopes on E2 within the 412-423 region are essential for HCV infectivity and viral escape mutants are suppressed; 3) Chronic HCV infection results in the generation of broadly reactive antibodies that recognize a conserved core domain of E2 such as D123.

1.10.2 Aims

The overall aim of this thesis is to further our understanding of antigenic domains of HCV envelope glycoprotein E2 and to increase knowledge on the immunogenic features of D123 to aid the design and development of a universal antibody-based preventative vaccine for HCV.

Aim 1: To determine the role of the hypervariable regions of E2 in antibody recognition and generation

Chapter 3 will investigate the role of HVRs in the exposure and immunogenicity of NAb epitopes on E2. The antibody specificities elicited by WT E2 and D123, and their oligomeric forms will be characterized and compared in two small animals, mice and guinea pigs.

Aim 2: To elucidate the broad neutralization mechanisms of MAb24 and investigate the escape pathways associated with MAb24

Chapter 4 will involve the forced evolution of HCV *in vitro* under MAb24, a murine broadly neutralizing antibody to epitope I. The escape pathways associated with MAb24 resistance will be investigated and the structural basis of MAb24 neutralization and resistance will be characterized.

Aim 3: To characterize the neutralizing antibody response in chronic HCV

Chapter 5 will examine the cross-neutralization profiles of individuals with chronic HCV and dissect the B cell repertoire of an individual with high titres of cross neutralizing antibodies and isolate D123-specific broadly reactive antibodies.

Chapter 2 Materials and Methods

2.1 Cell lines

Human embryonic kidney cell line HEK293T cells were maintained in DMF10 media, which contains Dulbecco's Modified Eagle Medium (DMEM, Invitrogen, Thermo Fisher Scientific, Waltham, MA, USA) supplemented with 10% heat-inactivated fetal bovine serum (Invitrogen), 2mM L-glutamine (Invitrogen), 16.8mM HEPES buffer (Invitrogen), 1μg/mL minocycline hydrochloride salt (Sigma-Aldrich, St Louis, MO, USA) and 40μg/mL gentamicin (Gibco, Thermo Fisher Scientific). Human hepatocellular carcinoma cell line Huh7.5 cells were kindly provided by Professor Charles Rice (Rockefeller University, USA) (Blight *et al.*, 2002), and maintained in DMF10 media supplemented with 100mM Eagle's minimum essential medium non-essential amino acids (Gibco) (DMF10NEA). Both cell lines were maintained in a humidified incubator at 37˚C with 5% CO_2.

2.2 Expression vectors

The E2 RBD expression vectors, pcoE2 and pcoD123, encode for the codon-optimised sequences of WT E2 and D123 respectively (G1a H77c strain, residues 384-661, synthesized by GeneArt, Invitrogen), which were subcloned into the pcDNA3.1 vector (Invitrogen) (Alhammad *et al.*, 2015a). Both sequences contain an N-terminal trypsinogen activator leader sequence for efficient glycoprotein cleavage and secretion, and a C-terminal poly-histidine (6×HIS) tag for rapid detection and ease of purification. Alternatively, the expression vector pE2 was used for E2 RBD expression. The pcDNA3 (Invitrogen)-based pE2 vector was generated previously and encodes for a non-codon optimised E2 RBD sequence (G1a H77c strain, residue 384-661, GenBank Accession No. AF009606) with an N-terminal tissue plasminogen activator leader sequence (tPA) and a C-terminal 6×HIS tag (McCaffrey *et al.*, 2007). The D123 expression vector pD123 was also generated previously, using overlap extension polymerase chain reaction (PCR) and pE2 as template to replace HVR1, HVR2 and igVR with the GSSG linkers (McCaffrey *et al.*, 2007). The $E2_{661}$myc expression vector and the related mutants ($E2_{661}$myc G436A, W437A, L438A, A439P, A439S, G440A, L441A and F442A) were generated and described

previously, and contain non-codon optimised WT E2 sequences with the N-terminal tPA leader and a C-terminal myc tag (Drummer *et al.*, 2006).

The HCV E1E2 expression vectors, pH77cE1E2, pHE1E2 and pCon1E1E2 were generated previously by cloning the E1E2 sequences from HCV strains H77c (G1a, GenBank Accession No. AF009606), H (G1a, GenBank Accession No. M67463) and Con1 (G1b, GenBank Accession No. AJ238799) into pcDNA4HisMax (Invitrogen) vector (Drummer *et al.*, 2003). The HIV-1 luciferase reporter vector pNL4-3.LUC.R-E- was obtained from Dr Nathaniel Landau through the NIH AIDs Reagent Program, Division of AIDS, NIAID, NIH (Connor *et al.*, 1995; He *et al.*, 1995). It encodes full-length HIV-1 sequence with defective Env/Nef/Vpr that expresses *Firefly* luciferase and is capable of only a single round of replication for use in pseudotyping assays. Together, the HCV E1E2 expression vectors and the HIV-1 luciferase reporter vector were used in the generation of HCVpp.

The HCVcc vector pJC1FLAG2 (p7-NS-GLUC2A) and the pJC1FLAG2 (p7-NS-GLUC2A) GND mutant were both kind gifts from Professor Charles Rice. The pJC1FLAG2 (p7-NS-GLUC2A) plasmid encodes for a highly-infectious, full-length J6/JFH-1 chimeric HCVcc clone (J6-derived core, E1, E2, p7 and partial NS2 sequences and JFH-1-derived partial NS2, NS3, NS4A/B, NS5A/B sequences) (Lindenbach *et al.*, 2005). The *Gaussia* luciferase reporter gene was inserted into the NS2 region (Marukian *et al.*, 2008). Mutated at the active site of the RNA-dependent RNA polymerase NS5B, the GND plasmid encodes for a replication-defective HCVcc and was used as a negative control in this study.

The expression vectors for HMAbs HCV1, HC84.1 and HC84.27 were generated by cloning the variable regions (V_H and V_L) of HCV1 (PDB No. 4DGV) (Kong *et al.*, 2012b), HC84.1 (PDB No. 4JZN) and HC84.27 (PDB No. 4JZO) (Krey *et al.*, 2013) into pcDNA3-tpa-HC and pcDNA3-tpa-LC vectors, which contain the constant region of IgG1 heavy chain and kappa light chain respectively, as well as an N-terminal tPA signal peptide (Alhammad *et al.*, 2015a).

2.3 Protein and peptide reagents

The D123 proteins used in the direct binding enzyme-linked immunosorbent assay (ELISA, Section 2.8.3) and the biopanning of the 5032 phage libraries (Section 2.11.2) was prepared by CSL Ltd (Parkville, VIC, Australia), as previously described (Vietheer *et al.*, 2017). Briefly, either one of the D123 expression vectors pD123 or pcoD123 was transfected into Freestyle 293F cells using 293fectin transfection reagent (Invitrogen). The secreted proteins were then purified from the tissue culture fluid using nickel-affinity chromatography followed by size exclusion chromatography. Fractions containing high molecular weight (HMW)-1, HMW2 or monomeric species of WT E2 or D123 were collected and buffer exchanged into phosphate-buffered saline (PBS, pH 6.8). The peptides used in the direct binding ELISA assays (Section 2.8.3) were synthesized by Auspep Pty Ltd (Tullamarine, VIC, Australia) or GenScript (Piscataway, NJ, USA). Each peptide contains a biotin tag at its N-terminus and an amide group at its C-terminal end. The amino acid sequences of the peptides are shown in Table 2.1.

Table 2.1 Synthetic peptides used in this study.

Peptides		**Sequence**
408-428	H77c	biotin-**KQNIQLINTNGSWHINSTALN**-NH_2
	J6	biotin-**RQKIQLVNTNGSWHINRTALN**-NH_2
430-451	H77c	biotin-**NESLNTGWLAGLFYQHKFNSSG**-NH_2
	J6	biotin-**NDSLHTGFIASLFYTHSFNSSG**-NH_2
523-549	H77c	biotin-**GAPTYSWGANDTDVFVLNNTRPPLGNW**-NH_2
	J6	biotin-**GAPTYTWGENETDVFLLNSTRPPLGSW**-NH_2

2.4 Monoclonal antibodies

2.4.1 Antibodies

The HCV E2-specific conformation-dependent mouse MAb H53 was a kind gift from Dr Jean Dubuisson (Institut Pasteur de Lille, France) (Deleersnyder *et al.*, 1997). The HCV E2-specific conformation-dependent domain-B HMAb CBH-5 was kindly gifted by Professor Steven Foung (Stanford University, USA) (Keck *et al.*, 2004a). The HMAb targeting the antigenic region-3 of HCV E2, AR3C was kindly provided by Associate Professor Mansun Law (The Scripps Research Institute, USA) (Law *et al.*, 2008). The rat MAb 3/11 specific to the E2 412-423 region was kindly provided by Professor Jane McKeating (University of Birmingham, UK) (Flint *et al.*, 1999a). The mouse anti-NS5A antibody 9E10 was a kind gift from Professor Charles Rice (Lindenbach *et al.*, 2005). Other antibodies used in this study were commercially available.

Mouse hybridoma clones were generated and isolated by Dr Patricia Vietheer (Burnet Institute, Melbourne, VIC, Australia) in collaboration with CSL Ltd (Alhammad *et al.*, 2015a). MAb1, 6, 7, 10, 12, 13, 14, 16 and 20 were isolated from BALB/c mice immunized with a single dose of 20µg WT E2 protein in the ISCOMATRIX adjuvant. MAb22, 23, 25, 26, 33. 36, 39 and 44 were isolated from mice immunized with a single dose of 20µg D123 protein in ISCOMATRIX. MAb24 was isolated from mice immunized first with a single dose of 20µg D123 protein in ISCOMATRIX followed by two more doses of 20µg D123 protein in alum and one dose of 20µg D123 protein in saline. Concentrated hybridoma culture fluids containing MAb IgG were harvested using the miniPERM bioreactors (CSL Ltd). MAb24 was also produced by harvesting the tissue culture fluid of MAb24 hybridoma cells maintained long-term in CD hybridoma medium (Invitrogen) supplemented with 15% fetal calf serum, or by a commercial source (the Antibody Services at Walter and Eliza Hall Institute Biotechnology Centre, Melbourne, VIC, Australia).

HMAbs HCV1, HC84.1 and HC84.27 were expressed by co-transfecting the heavy and light chain vectors (pHC and pLC) containing the appropriate gene inserts into HEK293T cells pre-seeded in 6-well plates or 10mm^2 tissue culture round dishes,

using polyethylenimine (PEI, Polysciences Inc., Warrington, PA, USA). After 4 hours, the transfection mix was replaced with Opti-MEM reduced serum media (Gibco). The HMAb-containing cell culture supernatant was collected after three days and clarified with a 0.45µM filter. Alternatively, the vectors were transfected into FreeStyle 293F suspension cells in flasks using 293fectin before harvest and filtration (Ms Irene Boo, Burnet Institute) (Alhammad *et al.*, 2015a).

2.4.2 Antibody purification and Fab preparation

The antibody-containing tissue culture fluid or miniPERM solution was affinity-purified using Protein G sepharose (PGS) columns (GenScript), followed by PBS wash and elution with 100mM glycine (pH 2.8) and immediate neutralization with 1M Tris-HCl (pH 8.0). The eluted IgG was then dialysed in PBS before concentration using Amicon® Ultra Centrifugal Units (10kDa molecular weight cut-off [MWCO], Millipore, Burlington, MA, USA) and filtration via a 0.45µm filter. Antibody concentration was determined by measuring the absorbance at 280nm using Nanodrop Spectrophotometer (Thermo Fisher Scientific).

MAb24 Fab was generated using Pierce™ Fab preparation kit (Thermo Fisher Scientific) according to the manufacturer's instructions. Briefly, the MAb24 IgG was digested in the immobilized papain resin for 3 hours at 37˚C before purification on Protein A column and concentration and buffer exchange into PBS using Amicon® Ultra Centrifugal Units (3kDa MWCO, Millipore). The cleavage of MAb24 IgG into Fab was confirmed using 10% sodium dodecyl sulfate polyacrylamide gel electrophoresis (SDS-PAGE) gels under both reducing and non-reducing conditions followed by visualization with Coomassie staining (detailed in Section 2.7.2). Crystallization trials and structural determination of MAb24 Fab in complex with its epitope peptide (Q^{412}LINTNGSWHVN, GenScript) was performed by Joshua Hardy and Associate Professor Fasséli Coulibaly (Department of Biochemistry and Molecular Biology, Monash University, Clayton, VIC, Australia).

2.5 Polyclonal antibodies

2.5.1 Guinea pig sera

Immune sera were generated and collected from Albino Dunkin Hartley guinea pigs by Dr Patricia Vietheer in collaboration with CSL Ltd (Vietheer *et al.*, 2017). Briefly, groups of 10 guinea pigs were immunized with three doses of 100µg unfractionated WT E2 or D123 proteins with the ISCOMATRIX adjuvant at three-week intervals, alongside 5 control animals immunized with no antigen, before blood was collected. For immunization experiments with fractionated D123 or WT E2 proteins, groups of 8 animals were immunized with three doses of 100µg HMW1, HMW2, dimeric or monomeric forms of D123 or WT E2 with the ISCOMATRIX adjuvant at three- or two-week intervals, alongside 5 control animals as above. Sera were kept at 4˚C for ELISA assays.

2.5.2 Human plasmas

A cohort of IDUs were recruited across metropolitan Melbourne between 2005 and 2007, using a social network approach, as part of the ongoing, longitudinal Network II study, led by Professor Margaret Hellard, at the Centre for Population Health of the Burnet Institute (Aitken *et al.*, 2008). Ethics approval was obtained from the Victorian Department of Health and Human Services Human Research Ethics Committee under the project codes 02/05, 54/06 and 28/13. All participants were interviewed for their social relationships and injecting behaviors, and followed up at 3 to 6-month intervals. Blood specimens were obtained at the time of follow-up with informed written consent, and were screened for the presence of anti-HCV antibodies and HCV RNA by the Victorian Infectious Diseases Reference Laboratory (Melbourne, VIC, Australia) using commercially available tests according to the manufacturer's instructions. HCV seropositivity was determined by a third-generation immunoassay (Abbott Laboratories, Chicago, IL, USA) followed by confirmation using Murex anti-HCV version 4.0 assay (HCV antigens, core, NS3, NS4 and NS5, Murex Biotech Ltd, South Africa). The presence of viral RNA was determined using the COBAS AMPLICOR HCV test version 2.0 (Roche Molecular Systems, Pleasanton, CA, USA). Genotyping was performed using the 5'-UTR-

based, commercially available Versant HCV Genotyping Assay (LiPA) (Bayer, Leverkusen, Germany).

Twenty-two subjects who had become HCV positive for >6 months were selected from the Network II study for further characterization in this study, as shown in Table 2.2. As all of the subjects tested positive for HCV antibody and entered the cohort chronically infected, it is not known how long they have been infected with HCV. The plasma samples were heat-inactivated at 56˚C for 1 hour to inactivate complement activities, prior to testing in neutralization assays. For use in ELISA binding assays, Triton X-100 was added to the plasma samples to a final concentration of 1% to inactivate viruses.

Table 2.2 Human plasma samples used in this study.

Code	*Date of Bleed*	*Genotype*
5009	10/01/2006	1a
5029	22/03/2006	1a
2015	9/03/2006	1a
2030	17/11/2005	1b
2059	16/06/2006	1a
1009	9/12/2005	1a, 3a
1010	21/07/2006	1a
4052	12/10/2005	1a
3077	6/04/2006	1a
5008	18/05/2006	3a
5016	14/10/2005	3a
2032	17/11/2005	3a
1004	14/10/2005	3a
1022	18/10/2006	3a
4005	11/11/2005	3a
4030	16/09/2005	3a
4031	16/09/2005	3a
4070	18/11/2005	3a
3067	20/01/2006	3a
30112	15/02/2006	3a
5032	17/11/2006	6a
5040	20/01/2006	6a

2.6 Construction and expression of E2 epitope mutants

2.6.1 Site-directed mutagenesis of E2

A total of thirty-six E2 epitope mutants (G1a H77c, residues 384-661) were constructed in this study. Twenty-nine amino acid residues on E2 that were implicated in NAb epitopes or E2-CD81 binding were mutated, through a single PCR or overlap extension PCR, using Expand^{TM} High Fidelity PCR system (Sigma-Aldrich) and the primers listed in Table 2.3 and Table 2.4 (GeneWorks Pty Ltd, Thebarton, SA, Australia, or Bioneer Corporation, Daejeon, South Korea).

Nine of the E2 epitope mutants were generated by amplifying the E2 RBD regions of previously described $E2_{661}$myc mutants ($E2_{661}$myc G436A, W437A, L438A, A439P, A439S, G440A, L441A, F442A and Y443A) (Drummer *et al.*, 2006). The C-terminal myc tag was replaced with a 6×HIS tag, and two restriction enzyme sites *Nhe*I and *Xba*I were introduced using the H77c E2 forward and reverse primers shown in Table 2.4. The remaining twenty-eight E2 RBD mutants (Q412A, L413A, N415A, N417A, G418A, W420A, W420F, H421A, N423A, S424A, L427A, N430A, W437F, G523A, P525A, P525G, Y527A, W529A, W529F, G530A, D535A, N540A, W549A, W549F, Y613A, W616A, W616F) were generated using overlap extension PCR of the codon-optimised WT E2 vector pcoE2, which contains *Kpn*I/*Xho*I restriction enzyme sites, as well as the primer pairs listed in Table 2.3 and coE2 forward and reverse primers in Table 2.4. The PCR conditions are listed in Table 2.5.

The PCR products were separated on 0.8 or 1% agarose gels (w/v in Tris-acetate-EDTA or TAE buffer) and DNA fragments of desired lengths were excised from the gels and purified using UltraClean® GelSpin® DNA Extraction kit (Mo Bio Laboratories, Carlsbad, CA, USA) according to the manufacturer's instructions. The DNA fragments were then digested with *Nhe*I/*Xba*I or *Kpn*I/*Xho*I (New England BioLabs Inc., Ipswich, MA, USA), before being cloned in the similarly digested DNA vector using T4 DNA ligase (Invitrogen) and transformed into *Escherichia coli* DH10ß cells using the heat shock methods (42˚C for 45 seconds). Individual clones were selected and amplified, and plasmid DNA was extracted using UltraClean® 6

Minute MiniPrep kit (Mo Bio Laboratories). Clones with correct sequences and mutations were confirmed using Applied Biosystems PRISM BigDye Terminator chemistry (version 3.1, Thermo Fisher Scientific). Large scale DNA preparation was then performed using QIAGEN-tip 100 plasmid kits (Qiagen, Hilden, Germany) followed by phenol-chloroform extraction.

2.6.2 Expression of E2 mutant proteins

The E2 epitope mutant proteins were produced by transfecting HEK293T cell monolayers that were grown to 80% confluence in T175 culture flasks, with 35µg plasmid DNA and 105µg PEI. After 4 hours of transfection, the transfection mix was removed and the cell monolayers were maintained in the Opti-MEM serum reduced media for up to 5 days. Cell culture supernatant containing the secreted E2 mutant proteins was collected daily, before being concentrated with Vivaspin Protein Concentrator Spin Columns (30kDa MWCO, Vivaproducts Inc., Littleton, MA, USA) and kept at 4˚C.

Table 2.3 Oligonucleotides used to introduce single point mutations in the codon-optimised E2 RBD. Mutations introduced are in bold.

Mutant	**Primer 1**	**Primer 2**
Q412A	CCTGGCGCCAAGCAGAACATC**GCC**CCTGATCAACACC AACGGCAGC	GATGTTCTGCT TGGCGCC AGG
L413A	CCTGGCGCCAAGCAGAACATCCAG**GCC**ATCAACACC AACGGCAGCTGG	
N415A	CCTGGCGCCAAGCAGAACATCCAGCTGATC**GCC**ACC AACGGCAGCTGGCACATC	
N417A	AACATCCAGCTGATCAACACC**GCC**GGCAGCTGGCAC ATCAACAGC	GGTGTTGATC AGCTGGATGT T
G418A	AACATCCAGCTGATCAACACCAAC**GCC**AGCTGGCAC ATCAACAGCACC	
W420A	AACATCCAGCTGATCAACACCAACGGCAGC**GCC**CAC ATCAACAGCACCGCCCTG	
W420F	AACATCCAGCTGATCAACACCAACGGCAGC**TTT**CAC ATCAACAGCACCGCCCTG	
H421A	CCAACGGCAGTTGG**GCC**ATCAATAGCACGG	CCAACTGCCG TTGGTGTTG
N423A	ACCAACGGCAGCTGGCACATC**GCC**AGCACCGCCCTG	GATGTGCCAG CTGCCGTTGGT
S424A	ACCAACGGCAGCTGGCACATCAAC**GCC**ACCGCCCTG	
L427A	TGGCACATCAACAGCACCGCC**GCC**AACTGCAACGAG	GGCGGTGCTG TTGATGTGCCA
N430A	TGGCACATCAACAGCACCGCCCTGAACTGC**GCC**GAG AGCCTG	
W437F	AACTGCAACGAGAGCCTGAACACCGGC**TTT**CTGGCC GGC	GCCGGTGTTC AGGCTCTCGTT
G523A	GTGGGCACCACCGACAGAAGC**GCC**GCCCCCACCTAC AGCTGGGGC	GCTTCTGTCGG TGGTGCCCAC
P525A	GTGGGCACCACCGACAGAAGCGGAGCC**GCC**ACCTAC AGCTGGGGCGCCAAC	
P525G	GTGGGCACCACCGACAGAAGCGGAGCC**GGC**ACCTAC AGCTGGGGCGCCAAC	
Y527A	GTGGGCACCACCGACAGAAGCGGAGCCCCCACC**GCC** AGCTGGGGCGCCAACGACACC	
W529A	AGCGGAGCCCCCACCTACAGC**GCC**GGCGCCAACGAC ACCGACGTG	GCTGTAGGTG GGGGC
W529F	AGCGGAGCCCCCACCTACAGC**TTT**GGCGCCAACGAC ACCGACGTG	
G530A	AGCGGAGCCCCCACCTACAGCTGG**GCC**GCCAACGAC ACCGACGTGTTC	
D535A	GCCCCCACCTACAGCTGGGGCGCCAACGACACC**GCC** GTGTTCGTGCTGAACAACACC	

Table 2.3 *continued*. Oligonucleotides used to introduce single point mutations in the codon-optimised E2 RBD.

Mutant	**Primer 1**	**Primer 2**
N540A	GACACCGACGTGTTCGTGCTG**GCC**AACACCAGACC CCCCCTGGGC	CAGCACGAACA CGTCGGTGTC
W549A	ACCAGACCCCCCCTGGGCAAC**GCC**TTCGGCTGCACC TGGATG	GTTGCCCAGGG GGGGTCTGGT
W549F	ACCAGACCCCCCCTGGGCAAC**TTT**TTCGGCTGCACC TGGATG	
Y613A	CGGTGCATGGTGGACTACCCC**GCC**CGGCTGTGGCAC	GGGGTAGTCCA CCATGCACCG
W616A	CGGTGCATGGTGGACTACCCCTACCGGCTG**GCC**CAC TATCCCTGC	
W616F	CGGTGCATGGTGGACTACCCCTACCGGCTG**TTT**CAC TATCCCTGC	

Table 2.4 Oligonucleotides used in the site-directed mutagenesis of the non-codon optimised E2 RBD. Restriction enzyme sites are underlined.

Primer Name		**Sequence**
H77c E2*	Forward	CCAGCTAGCGAAACCCACGTCACCGGGGGAAATGC
	Reverse	CCCTCTAGATTAGTGGTGGTGGTGGTGGTGGCCGCCCTCG GACCTGTCCCTGTC
coE2^	Forward	GGTACCGCTAGCGCCACCATGAACCC
	Reverse	GAGCTCGAGTTATCAGTGGTGATGG

*Oligonucleotides used to convert previously described $E2_{661}$myc mutants into $E2_{661}$HIS mutants, i.e. E2 RBD mutants with the C-terminal 6×HIS tag.

^Oligonucleotides used as universal forward and reverse primers in the overlap extension PCR of the codon-optimised E2 RBD.

Table 2.5 The overlap extension PCR conditions used in the site directed mutagenesis of E2 RBD.

Steps	**Cycles**	**Temperature**	**Time**
Denaturation	1×	94˚C	2 minutes
Amplification	30×	94˚C	15 seconds
		64˚C	30 seconds
		72˚C	45 seconds
Extension	1×	72˚C	7 minutes
		4˚C	hold

2.7 Protein Analyses

2.7.1 Western blot analyses

Tissue culture fluids containing E2 RBD proteins were boiled in 5% ß-mercaptoethanol (v/v) in Laemmli sample buffer for 5 minutes (Laemmli, 1970). Together with the pre-stained SDS-PAGE broad range protein standards (Bio-Rad Laboratories, Hercules, CA, USA), the protein samples were analyzed on 10% SDS-PAGE gels at 100 volts for 2 hours before being transferred to Hybond-C extra nitrocellulose membrane (GE Healthcare, Chicago, IL, USA) at 100 volts for 2 hours at 4˚C. Polyclonal rabbit anti-HIS epitope tag antibody (Rockland Immunochemicals Inc., Limerick, PA, USA) and IRDye® 800CW goat anti-rabbit antibody (LI-COR Biosciences, Lincoln, NE, USA) in 5% skim milk/PBS (w/v) were used to detect E2 proteins. The immunoblots were then imaged and quantitatively analyzed on the Odyssey Imager (LI-COR Biosciences).

2.7.2 Coomassie stain

Purified E2 proteins (WT E2 or D123), IgG or Fab samples were boiled with or without 5% ß-mercaptoethanol (v/v) in Laemmli sample buffer before being separated on 10% SDS-PAGE gels alongside pre-stained SDS-PAGE broad range protein standards. Gels were stained with 0.05% Coomassie Brilliant blue R-250 (w/v) in 5% glacial acetic acid (v/v) and 50% methanol (v/v) for ½ hour at room temperature (RT), and de-stained with 10% acetic acid and 10% methanol overnight. Polyacrylamide gels were imaged on the Odyssey Imager.

2.8 Enzyme linked immunosorbent assay (ELISA)

2.8.1 CD81 binding ELISA

The CD81 binding assays were performed with the bacterially-expressed, column-purified large extracellular loop (LEL) of CD81 (residues 113-201) fused with a maltose-binding protein (MBP), MBP-LEL$^{113\text{-}201}$ or MBP-LEL$^{113\text{-}201}$ F186S mutant, as described previously (Drummer *et al.*, 2002). MaxiSorp^{TM} 96-well, flat-bottom plates (Nunc, Roskilde, Denmark) were coated overnight at 4˚C with 5µg/mL MBP-LEL$^{113\text{-}201}$ or MBP-LEL$^{113\text{-}201}$ F186S in PBS. Excess CD81 proteins were removed with the washing buffer PBSTw (0.05%Tween-20 [Sigma-Aldrich] in PBS

v/v) and any unoccupied sites were blocked at RT for 1 hour with the blocking buffer $BSA_{10}PBS$ (10mg/mL bovine serum albumin [BSA, Sigma-Aldrich] in PBS). Normalized amounts of E2 epitope mutant-containing tissue culture fluids were serially diluted in the diluent buffer BSA_5PBSTw (5mg/mL BSA in PBSTw), and added to the wells for 2 hours at RT. The CD81-bound E2 epitope mutants were detected using polyclonal rabbit anti-HIS antibody followed by horseradish peroxidase (HRP)-labeled goat anti-rabbit antibody (Dako, Agilent Pathology Solutions, Santa Clara, CA, USA). The plates were then developed with 3,3',5,5'-tetramethylbenzidine (TMB) substrate (Sigma-Aldrich) before the reactions were stopped with 1M HCl. The optical density at 450nm (OD_{450}) and the background 620nm (OD_{620}) were measured using FLUOstar OPTIMA microplate reader (BMG Labtech, Offenburg, Germany).

2.8.2 GNA lectin-captured E2 binding ELISA

MaxiSorp™ 96-well, flat-bottom plates were coated with 5µg/mL *Galanthus nivalis* lectin (GNA-lectin, Sigma-Aldrich) in PBS overnight at 4˚C. After blocking with $BSA_{10}PBS$ and washing with PBSTw as above, normalized amount of E2 epitope mutant proteins were added to the wells for 2 hours at RT. Mouse MAb hybridoma supernatants, or polyclonal rabbit anti-HIS antibody, were diluted in BSA_5PBSTw and allowed to bind to the GNA-captured E2 for 1 hour at RT. MAb-E2 binding was detected by HRP-labeled rabbit anti-mouse antibody (Dako), or HRP-labeled goat anti-rabbit antibody. Plates were developed and measured as above.

2.8.3 Direct binding ELISA

MaxiSorp™ 96-well, flat-bottom plates were coated with 5µg/mL synthetic peptide (Table 2.1) or D123 proteins (described in Section 2.3) in 0.1M bicarbonate buffer or PBS overnight at 4˚C, before being blocked and washed as above. Inactivated guinea pig immune sera or human plasmas were serially diluted in BSA_5PBSTw and added to the plates for 2 hours at RT. Antigen reactivity was detected by HRP-labeled rabbit anti-guinea pig antibody (Dako), HRP-labeled rabbit anti-human antibody (Dako), or HRP-conjugated streptavidin (as coating controls for plates coated with biotinylated peptides, Thermo Fisher Scientific). Plates were developed and measured as above.

2.9 HCV pseudotyped particles neutralization assay

The HCV H, H77c and Con1-derived HCVpp were generated as previously described (Drummer *et al.*, 2003). Briefly, in 6-well plates, HEK293T cells were pre-seeded at 5×10^5 cells per well overnight. The HEK293T monolayers were then co-transfected with 1µg pNL4-3.LUC.R-E- plasmid and 1µg pH77cE1E2 or pCon1E1E2 or pHE1E2 or pCDNA3.1 (empty vector control) using FuGENE® 6 transfection reagent (Promega, Madison, WI, USA) or PEI in Opti-MEM reduced serum media with GlutaMAX supplement (Invitrogen). Tissue culture fluids containing HCVpp were harvested and clarified using 0.45µm filters after three days. For HCV H-derived HCVpp (pHE1E2), tissue culture supernatant was additionally centrifuged at 25,000rpm for 2 hours before the pelleted HCVpp viruses were resuspended in DMF10NEA media.

HCVpp neutralization assays were performed in four replicates in 48-well tissue culture plates. Huh7.5 cells were pre-seeded at 3×10^4 cells per well overnight. Human plasma samples or MAb24 were serially diluted in DMF10NEA media and incubated with a constant amount of HCVpp containing H77c-, Con1- or H-derived E1E2 for 1 hour at 37˚C. The plasma/HCVpp mixture was then applied to pre-seeded Huh7.5 cells for 4 hours before PBS wash and replacement with fresh DMF10NEA media. After three days, the luciferase activities in the Huh7.5 cell lysates were measured with *Firefly* Luciferase System (Promega) and detected using FLUOstar OPTIMA reader fitted with luminescence optics. Neutralization curves were plotted using one-site specific binding with Hill slope (Prism v7), and the inhibitory doses, ID_{50}s and ID_{80}s of the plasma samples were determined.

2.10 Cell culture-derived HCV (HCVcc)

2.10.1 Site directed mutagenesis of HCVcc

Single point mutations, N415D or N417S, were introduced into pJC1FLAG2 (p7-NS-GLUC2A) DNA using QuikChange II XL site-directed mutagenesis kit (Agilent Technologies) following the manufacturer's instructions. Primers used in the QuikChange reactions are listed in Table 2.6 and the RT-PCR conditions are listed in Table 2.8. The mutated and amplified constructs were digested with *BSi*WI and *Bgl*II, and cloned into similarly digested pJC1FLAG2 vector. Sequences were confirmed using Applied Biosystems PRISM BigDye Terminator chemistry (version 3.1). The double mutant H386R/N415D was constructed by introducing H386R mutation into pJC1FLAG2 (p7-NS-GLUC2A) construct containing N415D using the same procedure.

2.10.2 The production of HCVcc

HCVcc was generated as previously described (Fraser *et al.*, 2011). Briefly, pJC1FLAG2 (p7-NS-GLUC2A) DNA or the related mutant DNA (N415D, N417S and H386R/N415D) were linearized with *Xba*I and transcribed into RNA *in vitro* using AmpliScribe^{TM} T7 Flash Transcription kit (Epicentre, Madison, WI, USA) before purification using the RNeasy mini kit (Qiagen) according to the manufacturer's instructions. To produce HCVcc, viral RNA was transfected into Huh7.5 cells pre-seeded at $3.5x10^5$ cells per well in 6-well plates using DMRIE-C transfection reagent (Invitrogen) following manufacturer's recommendation. Alternatively, HCVcc was produced by electroporation of the RNA into Huh7.5 cells in T175 tissue culture flasks (Ms Irene Boo, Burnet Institute). Three days after transfection, virus-containing cell culture supernatant was harvested and clarified before storage at -80˚C. To determine the infectivity of HCVcc, media containing HCVcc was added to Huh7.5 cells pre-seeded at $6x10^3$ cells per well and incubated for 4 hours before PBS wash and replacement with fresh media. Cell culture supernatant was lysed after 72 hours and luciferase activity was measured using *Renilla* luciferase assay system (Promega) and a FLUOstar OPTIMA reader fitted with luminescence optics.

2.10.3 HCVcc neutralization assay

HCVcc neutralization assays were performed in triplicate in 96-well plates as previously described (Vietheer *et al.*, 2017). All HCVcc were either diluted or concentrated to yield luciferase counts of between $5x10^5$-$2x10^6$ from each infected well of Huh7.5 cells. Monoclonal antibodies or heat-inactivated human plasmas were serially diluted with DMF10NEA media before incubation with an equal volume of media containing normalized amounts of HCVcc for 1 hour at 37˚C. The mixture was then added onto the Huh7.5 cells pre-seeded at $6x10^3$ cells per well and incubated for 4 hours before PBS wash and replacement with fresh media. Cell culture supernatant was lysed after 72 hours and luciferase activity was measured using *Renilla* luciferase assay system (Promega) and a FLUOstar OPTIMA reader fitted with luminescence optics. Non-linear regression analysis was used to determine the 50% inhibitory concentration (IC_{50}) and 80% inhibitory concentration (IC_{80}) of MAbs.

2.10.4 The generation of MAb24 resistant HCVcc

The starting HCVcc stock was produced by transfecting pJC1FLAG2 (p7-NS-GLUC2A) RNA into Huh7.5 cells as per Section 2.10.2, and the IC_{50}, IC_{70} and IC_{90} of MAb24 against the starting HCVcc stock was determined using HCVcc neutralization assay as per Section 2.10.3 (0.245, 0.98, and 9.8µg/mL respectively). HCVcc was passaged either using a "cell-free" method or a "passaging with infected cells" method. For the "cell free" passaging experiment, at Passage 0, HCVcc was incubated with either 0, 0.245, 0.98, or 9.8µg/mL of MAb24 IgG for 1 hour at 37˚C before addition to a monolayer of naïve Huh7.5 cells, pre-seeded at 4×10^4 cells per well in 24 well plates. After 4 hours, media was replaced with DMF10NEA containing MAb24 at the corresponding concentration. Cell culture supernatant was monitored daily for *Renilla* luciferase activity. This was repeated every four days. In the parallel "passaging with infected cells" experiment, HCVcc was passaged with infected cells at three-day intervals. The virus was neutralized and allowed to replicate in the presence of MAb24 IgG as above. In addition, the infected Huh7.5 cells from the previous passage were trypsinized, and a fraction was added to the naïve Huh7.5 cells. *Renilla* luciferase activity in the cell culture supernatant was monitored daily. MAb24 concentration was increased to 2 times (Passage 4), 5 times (Passage 5), 10 times (Passage 6) and 20 times (Passage 7 and onwards) of the

corresponding starting concentration. The proportion of infected Huh7.5 cells added in each round of passage was reduced from 10% (Passage 1), to 5% (Passage 6) and 4% (Passage 7 and onwards). The extracellular HCVcc and intracellular HCVcc (in infected cells) were collected at the end of each passage and stored at -80˚C.

2.10.5 HCVcc sequencing

Viral RNA was extracted from cell culture fluids containing the extracellular HCVcc using the QIAamp Viral RNA mini kit (Qiagen). The E1E2 or E2 region was amplified using primers in Table 2.7 and SuperScript^{TM} III one step RT-PCR system with Platinum Taq High Fidelity (Invitrogen). The resulting cDNA was cloned into either pGEM®-T or pGEM®-T easy vectors (Promega) and individual clones were sequenced using Applied Biosystems PRISM BigDye Terminator chemistry in 96-well plate format (version 3.1) and primers in Table 2.7. For the next generation sequencing of HCVcc quasispecies, viral sequences of both the extracellular and intracellular HCVcc were determined. The isolation of viral RNA of the extracellular HCVcc was performed as above. For intracellular HCVcc, total RNA was prepared from infected cells from selected passages using RNAeasy mini kit. Next generation sequencing was performed by Dr Abha Chopra and Associate Professor Silvana Gaudieri (Murdoch University, Perth, WA, Australia) and was described previously (Gu *et al.*, 2018).

2.10.6 HCVcc infectivity and immunofluorescence

Huh7.5 cells were pre-seeded in 24-well plates, at a density of $6x10^4$ cells per well on coverslips pre-treated with 0.01% poly-L-lysine (Sigma-Aldrich). HCVcc mutants were diluted and allowed to infect the cells for 4 hours before replacement with fresh media. *Renilla* luciferase activity was measured at 24, 48 and 72-hours post infection. To visualize the level of infectivity, infected cells were washed and fixed with 100% ice-cold methanol before being blocked with 3% fetal bovine serum for 1 hour at RT. Infected cells were detected using the mouse anti-NS5A antibody, 9E10 followed by Alexa Fluor® 488 goat anti-mouse IgG secondary antibody (Invitrogen). Cell nuclei were counter-stained with propidium iodide for 5 minutes in the dark. Coverslips were mounted on slides and examined using an Olympus IX50 inverted microscope.

Table 2.6 Oligonucleotides used in the site-directed mutagenesis of HCVcc (Bioneer). Introduced mutations are in bold.

Primers	**Sequences (5' to 3')**
N415D	CCAGCTCGTT**GAC**ACCAATGGC
	CATTGGT**GTC**AACGAGCTGGATTTTC
N417S	AATCCAGCTCGTTAACACC**AGT**GGCAGCTGGC
	GCCAGCTGCC**ACT**GGTGTTAACGAGCTGGATT
H386R	GCGCGCGCACC**CGT**ACTGTTGGGGG
	CCCCCAACAGT**ACG**GGTGCGCGCGC

Table 2.7 Oligonucleotides used in the sequencing of HCVcc (Bioneer). Introduced mutations are in bold.

Primers	**Sequences (5' to 3')**
JC1E1FwdEcoRI*	GGTTGCTCCTTTTCTATCTTC
JC1E1end-F1321^	TACAAGGACGACGACGACAAGGGC
J6E2XbaIRev*^	GGCTCTAGATTATGCTTCG GCCTGGCCCAA
pUC/M13 Fwd#	GTTTTCCCAGTCACGAC
J6E2for1#	CGCACCCATACTGTTGGG
pUC/M13 Rev#	CAGGAAACAGCTATGAC

*used for the amplification of the E1E2 region of HCVcc
^used for the amplification of the E2 region of HCVcc
#used for sequencing E2 or E1E2 cloned in pGEM®-T or pGEM®-T easy vectors

Table 2.8 The reverse transcription-PCR (RT-PCR) conditions used in the amplification of E1E2 or E2 region of the MAb24-resistant HCVcc quasispecies.

Steps	**Cycles**	**Temperature**	**Time**
cDNA synthesis	1×	47.5˚C	30 minutes
Denaturation	1×	94˚C	4 minutes
Amplification	40×	94˚C	30 seconds
		55˚C	30 seconds
		72˚C	2 minutes
Extension	1×	72˚C	5 minutes
		12˚C	hold

2.11 Phage display library construction and characterization

2.11.1 Phage library construction

A total of 40mL of fresh blood was collected from the IDU subject 5032 with patient's informed written consent by Dr Peter Higgs (Burnet Institute). Peripheral blood mononuclear cells (PBMCs) were isolated from the whole blood using Ficoll-Paque PLUS (GE Healthcare), and washed twice with PBS. Total RNA of the PBMCs were extracted using TRIzol™ LS reagent (Invitrogen) as per manufacturer's instructions. Library cDNA were prepared using SuperScript III First-Strand Synthesis SuperMix (Invitrogen) and random hexamers according to the user's manual.

The phage library cloning and expression construct vector pCES was an optimised version of the pCES vector originally described by de Haard (2002) and was kindly provided by Dr Stewart Nuttall, Dr Greg Coia, and Ms Lesley Pearce (CSIRO, Parkville, VIC, Australia). The exact gene arrangement and restriction enzyme map of pCES vector used for phage library construction is depicted in Figure 2.1. It contains an ampicillin-resistance gene as well as *ApaLI*/*Asc*I sites for the cloning of entire light chain sequences (LC) and *Sfi*I/*BstE*II sites for the cloning of the variable regions of heavy chains (V_H of HC). *E. coli* TG1 cells were used for the amplification of library clones and the generation of phages, and was generously provided by Dr Stewart Nuttall, CSIRO).

All of the library PCR were performed using GoTaq® Green Master Mix (Promega) and the PCR conditions are described in Table 2.11. The entire light chain sequences were amplified from library cDNA with a single PCR, using primer pairs specific to the constant and variable regions of the lambda and kappa light chain genes (Cκ/Cλ and Vκ/Vλ, containing *Asc*I and *ApaL*I respectively, Table 2.9). For heavy chains, the complete heavy chain sequences were first amplified from library cDNA using primers specific to the variable regions (V_H, containing *Sfi*I site, Table 2.10) and the constant regions of IgG or IgM (C_H, Table 2.10). This was followed by a second PCR that further amplifies the variable regions of the heavy chain, using the

V_H primers (containing *Sfi*I site, Table 2.10) and the C_HJ primers (containing *BstE*II site, Table 2.10).

PCR products were analyzed on 1.5% agarose/TAE gels before DNA fragments of desirable sizes were excised and purified using QIAquick gel extraction kit (Qiagen) following the user's manual. The purified light chain PCR products were pooled and digested with *ApaL*I/*Asc*I before being cloned into the similarly digested pCES vectors using T4 ligase (NEB) at RT overnight (LC library). For the heavy chain PCR products, restriction enzyme digestion with *Sfi*I/*BstE*II revealed three cleavage products. One product (~600bp) appeared to be the desired V_H pool and was readily cloned into pCES as described above (V_H I library). The other two (~400bp and ~200bp) appeared to be derived from a single V_H sequence (V_H II library) truncated by the additional *BstE*II site at the frame region-3 (FR3). The V_H II library was reconstituted by cloning the ~400bp and ~200bp products into the pCES vector in a step-wise manner and was confirmed by sequencing using the Applied Biosystems PRISM BigDye Terminator chemistry (version 3.1). Ligation mixtures were precipitated and purified with sodium acetate and 100% ethanol before being transformed into *E. coli* TG1 cells via electroporation and extracted using QIAprep Spin Miniprep Kit (Qiagen). LC library and V_H I or II libraries (Library I and II) were recombined using *Sfi*I/*Not*I complementary digestion, and transformed into *E. coli* TG1 cells before storage in 30% glycerol at -80˚C.

To validate the successful cloning of LC and V_H sequences into the pCES vector, library clones from well-separated single colonies were randomly selected. Plasmid DNA was amplified and prepared using AccuPrep Nano-Plus Plasmid mini extraction kit (Bioneer) before being sequenced in a 96-well plate format using Applied Biosystems PRISM BigDye Terminator chemistry (version 3.1) and the primers listed in Table 2.12.

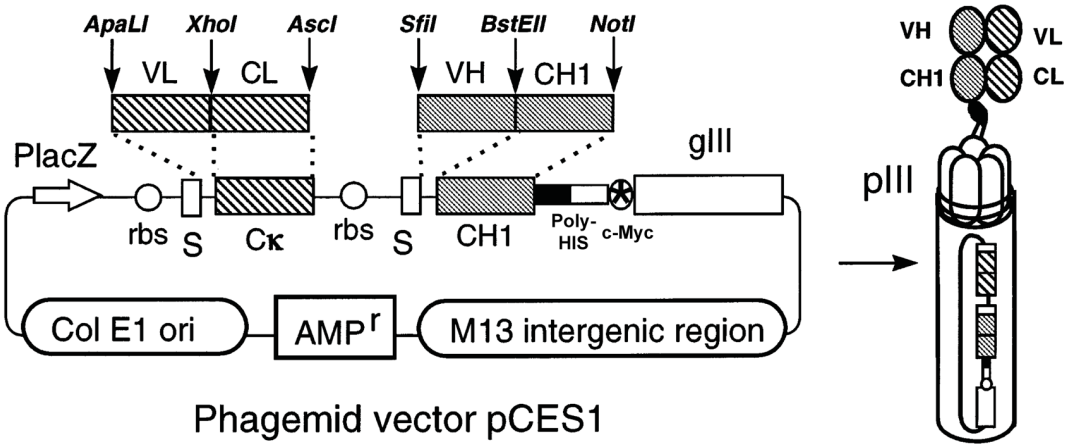

Figure 2.1 Schematic diagram showing key features of the pCES vector. Modified from (Hoogenboom *et al.*, 1998). AMP^r: ampicillin resistance gene.

Table 2.9 Oligonucleotides used to amplify the light chain sequences from the subject 5032 (provided by Dr Stewart Nuttall).

		Sequence (5' to 3')
Cκ	**$C_κ$**	ACCGCCTCCACCGGGCGCGCCTTATTAACACTCTCCCCTGTTGAAG CTCTT
Vκ	**$V_κ$1B**	ACCGCCTCCACCAGTGCACTTGACATCCAGWTGACCCAGTCTCC
	$V_κ$2	ACCGCCTCCACCAGTGCACTTGATGTTGTGATGACTCAGTCTCC
	VK3B	ACCGCCTCCACCAGTGCACTTGAAATTGTGWTGACRCAGTCTCC
	$V_κ$4B	ACCGCCTCCACCAGTGCACTTGATATTGTGATGACCCACACTCC
	$V_κ$5	ACCGCCTCCACCAGTGCACTTGAAACGACACTCACGCAGTCTCC
	$V_κ$6	ACCGCCTCCACCAGTGCACTTGAAATTGTGCTGACTCAGTCTCC
Cλ	**$C_λ$2**	ACCGCCTCCACCGGGCGCGCCTTATTATGAACATTCTGTAGGGGCC ACTG
	$C_λ$7	ACCGCCTCCACCGGGCGCGCCTTATTAAGAGCATTCTGCAGGGGCC ACTG
Vλ	**$V_λ$1A**	ACCGCCTCCACCAGTGCACAGTCTGTGCTGACTCAGCCACC
	$V_λ$1B	ACCGCCTCCACCAGTGCACAGTCTGTGYTGACGCAGCCGCC
	$V_λ$1C	ACCGCCTCCACCAGTGCACAGTCTGTCGTGACGCAGCCGCC
	$V_λ$2	ACCGCCTCCACCAGTGCACARTCTGCCCTGACTCAGCCT
	$V_λ$3A	ACCGCCTCCACCAGTGCACTTTCCTATGWGCTGACTCAGCCACC
	$V_λ$3B	ACCGCCTCCACCAGTGCACTTTCTTCTGAGCTGACTCAGGACCC
	$V_λ$4	ACCGCCTCCACCAGTGCACACGTTATACTGACTCAACCGCC
	$V_λ$5	ACCGCCTCCACCAGTGCACAGGCTGTGCTGACTCAGCCGTC
	$V_λ$6	ACCGCCTCCACCAGTGCACTTAATTTTATGCTGACTCAGCCCCA
	$V_λ$7/8	ACCGCCTCCACCAGTGCACAGRCTGTGGTGACYCAGGAGCC
	$V_λ$9	ACCGCCTCCACCAGTGCACWGCCTGTGCTGACTCAGCCMCC

Degenerate primers: W:A/T; R:A/G; Y:C/T; M:A/C

Introduced cloning sites: AscI; ApaLI

Table 2.10 Oligonucleotides used to amplify the heavy chain sequences from the subject 5032 (provided by Dr Stewart Nuttall).

		Sequence (5' to 3')
C_H	**IgM**	TGGAAGAGGCACGTTCTTTTCTTT
	IgG C_H1	GACCGATGGGCCCTTGGTGGA
C_HJ	**$C_HJ1/2$**	TGAGGAGACGGTGACCAGGGTGCC
	C_HJ3	TGAAGAGACGGTGACCATTGTCCC
	$C_HJ4/5$	TGAGGAGACGGTGACCAGGGTTCC
	C_HJ6	TGAGGAGACGGTGACCGTGGTCCC
	C_HJ-IgG2	CGATGGGCCCTTGGTGGAGGCTGAAGAGACGGTGACCATTGT
V_H	**$V_H1B/7A$**	GTCCTCGCAACTGCGGCCCAGCCGGCCATGGCCCAGRTGCAG CTGGTGCARTCTGG
	V_H1C	GTCCTCGCAACTGCGGCCCAGCCGGCCATGGCCSAGGTCCAG CTGGTRCAGTCTGG
	V_H2B	GTCCTCGCAACTGCGGCCCAGCCGGCCATGGCCCAGRTCACCT TGAAGGAGTCTGG
	V_H3B	GTCCTCGCAACTGCGGCCCAGCCGGCCATGGCCSAGGTGCAG CTGGTGGAGTCTGG
	V_H3C	GTCCTCGCAACTGCGGCCCAGCCGGCCATGGCCGAGGTGCAG CTGGTGGAGWCYGG
	V_H4B	GTCCTCGCAACTGCGGCCCAGCCGGCCATGGCCCAGGTGCAG CTACAGCAGTGGGG
	V_H4C	GTCCTCGCAACTGCGGCCCAGCCGGCCATGGCCCAGSTGCAG CTGCAGGAGTCSGG
	V_H5B	GTCCTCGCAACTGCGGCCCAGCCGGCCATGGCCGARGTGCAG CTGGTGCAGTCTGG
	V_H6A	GTCCTCGCAACTGCGGCCCAGCCGGCCATGGCCCAGGTACAG CTGCAGCAGTCAGG

Degenerate primers: S: C/G; W:A/T; R:A/G; Y:C/T

Introduced cloning sites: SfiI site; BstEII

Table 2.11 The PCR conditions used in the amplification of heavy and light chain sequences from the subject 5032.

Steps	**Cycles**	**Temperature**	**Time**
Denaturation	1×	94˚C	3 minutes
Amplification	35×	94˚C	1 minute
		50˚C	1 minute
		72˚C	2 minutes
Extension	1×	72˚C	10 minutes
		4˚C	hold

Table 2.12 Oligonucleotides used for sequencing phage clones or amplifying Fab inserts in the post-panning library (provided by Dr Stewart Nuttall)

Primers	**Sequences (5' to 3')**
pUC/M13Rev^	TCACACAGGAAACAGCTATGAC
pCESV$_H$Fwd*	CCAATTCTATTTCAAGGAGACAGTC
Fab insert Forward	AAACAGCTATGAC
Fab insert Reverse	GGTAATAAGTTTTAACGCCCTCAGTGCCT

^for sequencing $V_{L.}$ *for sequencing $V_{H.}$

Table 2.13 The PCR conditions used to amplify the Fab inserts from the output libraries.

Steps	**Cycles**	**Temperature**	**Time**
Denaturation	1×	95˚C	2 minutes
Amplification	25×	95˚C	1 minute
		46˚C	1 minute
		72˚C	1.5 minutes
Extension	1×	72˚C	5 minutes
		4˚C	hold

2.11.2 Phage rescue and panning

Preparation of helper phages

E coli TG1 cells were grown in 2×TY media (16g/L tryptone, 10g/L yeast extract, 5g/L sodium chloride, pH7.0) overnight at 37˚C. After reaching log-phase (OD_{600}=0.6), TG1 cells were infected with kanamycin-resistant M13KO7 helper phages (Dr Steward Nuttall, CSIRO) for 15 minutes at 37˚C without shaking. The phage-infected TG1 cells were then allowed to recover and amplify in fresh 2×TY media for 2.5 hours at 37˚C with aerated shaking. Any uninfected cells were inactivated and removed by the addition of 50µg/mL kanamycin, and the helper phage-producing TG1 cells were cultured at 37˚C overnight. The helper phages were collected and purified by first clarifying phage-containing culture supernatant at 5,000g at 4˚C to remove any TG1 cells and cell debris. Helper phages were then pelleted by incubating with 20% polyethylene glycol (PEG)-8000 and 15% sodium chloride for 1 hour on ice, followed by centrifugation at 10,000g for 45 minutes. The pelleted phages were washed and resuspended in PBS before being filter sterilized and stored at 4˚C.

Phage rescue and amplification in E coli TG1 cells

Prior to biopanning, the 5032 library phages were first rescued from glycerol stocks of the two 5032 libraries (library I and library II). The pCES-transformed, ampicillin-resistant *E coli* TG1 cells were thawed from -80˚C and incubated at 37˚C with shaking for 45 minutes, in 2×TY media with increasing concentrations of ampicillin (17µg/mL, 33µg/mL, 37.5µg/mL to the final 50µg/mL). Alternatively, for the amplification of post-panning phages, *E coli* TG1 cells at log-phase growth were infected with the eluted phages (Round 1 and 2 output phages) for ½ hr at 37˚C without shaking. The infected TG1 cells were allowed to recover in fresh 2×TY media with increasing concentrations of ampicillin (17µg/mL, 50µg/mL to the final 62.5µg/mL) for 2.5 hours at 37˚C with aerated shaking.

Kanamycin-resistant M13KO7 helper phage ($7x10^8$ plaque forming units or PFU) was then added to the TG1 culture for ½ hour at 37˚C without shaking. The phage-infected TG1 cells were transferred into fresh 2×TY with 100µg/mL ampicillin for 2 hours with aerated shaking before being cultured overnight at 26-28˚C with

25µg/mL kanamycin. The library phages were prepared and purified using 20% PEG-8000/15% sodium chloride using the same methods for helper phage preparation.

Phage panning

Three rounds of biopanning of the 5032 phage libraries were performed in duplicates in 5mL Maxisorp™ immunotubes (Nunc). Immunotubes were coated overnight at 4˚C, with either 25µg, 10µg or 5µg unfractionated D123 proteins (Round 1, 2 and 3), or 2.5µg D123 HMW1 and 2.5µg D123 HMW2 proteins (Round 3) in PBS. Tubes were then washed with PBS before being blocked with 2% skim milk in PBS. Amplified library phages were diluted in 2% skim milk/PBS before addition to the immunotubes and incubation at RT for 1 hour with rotation and 1 hour without. Non-specific phage-protein interaction was removed by vigorous washing with PBS and PBSTw eight times. Bound phages were then eluted with 0.1M glycine (pH 2.3) followed by immediate neutralization with 1M Tris (pH 8.0). The eluted phages were either immediately allowed to infect log-phase TG1 cells for amplification for next round of panning (Round 1 and 2 output phages) or stored at 4˚C (Round 3 output phages).

2.11.3 Post-panning library analyses

Post-panning phage DNA rescue

Post-panning phages were allowed to infect log-phase TG1 cells for an hour at 37˚C without shaking. The infected TG1 cells were then cultured overnight in TY media containing 100µg/mL ampicillin and 4% glucose, and plasmid DNA of post-panning phages was extracted and purified using QIAprep Spin Miniprep Kit. Amplification of Fab inserts in the post-panning library DNA was performed using GoTaq® Green Master Mix and the primers, Fab insert Forward and Reverse primers, as shown in Table 2.12 and the PCR conditions are described in Table 2.13.

Fab expression in E coli TOP10F' cells

Post-panning library DNA was electroporated into One Shot TOP10F' *E coli* cells (Invitrogen, provided by Dr Stewart Nuttall) to produce Fab proteins. The Fab proteins were expressed into the periplasmic space of TOP10F' cells and contained the poly-HIS tag and c-myc tag for ease of detection and purification. Single, well-

isolated colonies were cultured in 2×TY media with 100µg/mL ampicillin and 4% glucose for 8 hours. This was followed by the addition of 1mM isopropyl ß-D-1-thiogalactopyranoside (IPTG), which induces the expression of Fab clones at 30˚C overnight. Corresponding clones were also patched on TY agar plates containing 100µg/mL ampicillin and 2% glucose for plasmid DNA extraction.

The expressed Fab proteins were harvested from TOP10F' cells using the Minsky methods (Minsky *et al.*, 1986). Briefly, overnight cultures of TOP10F' cells were pelleted and resuspended in ice-cold 1× spheroplast buffer (100mM Tris-HCl, 0.5M sucrose, 0.5mM EDTA, pH 8.0) and 6µg lysozyme for 10 minutes. Osmotic shocks were then introduced to the cells with the addition of ice-cold ½× spheroplast buffer, before the Fab-containing periplasmic fractions were collected.

Direct Fab binding ELISA

MaxiSorp™ 96-well flat-bottom plates were coated with 5µg/mL unfractionated D123 protein, D123 HMW1, or D123 HMW2 in PBS overnight at 4˚C before being blocked with 5% skim milk/PBS for an hour at RT. Fab-containing periplasmic fractions or the positive control MAb24 were added for ½ hour. Fab-D123 binding was detected using mouse anti-myc antibody 9E10 (Sigma-Aldrich) in 2% skim milk/PBS followed by HRP-labeled goat anti-mouse antibody (Dako). The assays were developed in 2,2'-Azino-bis(3-ethylbenothiazoline-6-sulphonic acid) (ABTS, Boehringer, Mannheim, Germany) for 10-15min. Optical density at 405nm (OD_{405}) was measured.

Chapter 3 The role of the hypervariable regions of E2 in antibody recognition and generation

3.1 Introduction

HCV glycoprotein E2 is essential for viral entry and a major target for NAbs. Further knowledge of the CD81 binding motifs and NAb epitopes on E2 will therefore contribute to our understanding of the early events in HCV entry and guide the rational design of an antibody-based prophylactic vaccine for HCV. Structural characterization of two truncated forms of E2 RBD revealed that as a monomeric unit in the absence of E1, E2 displays a compact globular fold (Khan *et al.*, 2014; Kong *et al.*, 2013), as depicted in Figure 3.1. Solution-based studies conducted by Khan and colleagues showed that the N-terminus of E2 (residues 384-463), which includes the two hypervariable regions, HVR1 and HVR2, and two known NAb epitopes, epitope I (residues 412-423) and II (residues 430-451), can be removed enzymatically, suggesting that these regions form independent subdomain(s) and are highly exposed and structurally flexible from the remaining portion of E2 (residues 456-656) (Khan *et al.*, 2014).

Using co-crystallization of E2 with AR3C Fab, a conformational antibody that stabilizes the N-terminus of E2, Kong and colleagues were able to obtain structural data for the amino acid residues at the N-terminus of E2 (residues 421-460) in the context of a monomeric soluble E2 protein (Kong *et al.*, 2013). In combination with previous mutagenesis findings, Kong *et al* proposed that the N-terminal sequence of E2, together with the adjacent flexible loop of epitope III (residues 523-549), is organized into a CD81 binding interface on the E2 core structure that overlaps with the neutralizing face of E2. Although this has provided a structural framework for the distribution of NAb/CD81 binding residues on E2, it is possible that to some extent, the conformation of the neutralizing face/CD81 binding interface at the front layer of the E2 core domain, is induced by AR3C binding. The arrangement of the CD81 binding motif of E2 in its native unliganded state remains unknown.

As key structural features of the E2 RBD, the HVRs form flexible, surface-exposed and disulfide-constrained loops. Whilst no structural information for either HVR1 or HVR2 are provided in the two crystal structures of E2, replacement of all three HVRs, individually or in combination, with GSSG linkers in the E2 RBD proteins of G1a and G1b (residues 384-661) does not substantially alter its ability to interact with CD81 or its recognition by conformation-dependent HMAbs (McCaffrey *et al.*, 2007; McCaffrey *et al.*, 2017). However, deletion of all three HVRs in the G2a E2 RBD resulted in a 10-fold increase in its ability to bind CD81. Additionally, the G1a D123 showed enhanced recognition by a conformation-dependent neutralizing HMAb CBH-5 as well as several murine MAbs, indicating that one or more HVRs may influence the exposure of antibody epitopes on E2 or the global conformation of the E2 RBD core (Alhammad *et al.*, 2015a; McCaffrey *et al.*, 2007). Furthermore, the presence of HVRs on the surface of E2 may potentially shield the conserved core regions of E2. Together, these data indicate that the intact E2 RBD core (WT E2, residues384-661) and E2 RBD lacking all three HVRs (D123) share a similar fold but the variable regions modulate the exposure of the CD81 binding site and underlying NAb epitopes in a strain-specific manner.

Both WT E2 and D123 proteins inherently form heterogeneous mixtures of disulfide-linked E2 glycoforms when expressed in HEK293T and FreeStyle 293F cells (Vietheer *et al.*, 2017). Size exclusion chromatography of affinity-purified WT E2 and D123 proteins suggested that their molecular sizes range from 44kDa to >600kDa. A closer examination of four representative forms of D123 (monomer [46.6kDa], dimer [97.3kDa], HMW2 [239.3kDa] and HMW1 [2402.4kDa]) and their corresponding WT E2 counterparts showed that different forms of WT E2 and D123 have distinctly different antigenic surfaces, as the neutralizing HMAbs such as AR3C-related antibodies and the non-neutralizing HMAbs, CBH-4B and CBH-4D preferentially bind to the monomeric forms (Vietheer *et al.*, 2017). A more dramatic reduction in CBH-4B and AR3C binding was observed in WT E2 HMW1 than the monomeric WT E2. In addition, WT E2 HMW1 displayed reduced binding to MAb36, a monoclonal antibody whose epitope resides in HVR1. These findings suggested that these alternatively folded, antigenically distinct forms of D123 and WT may elicit antibody responses with different specificities.

This chapter aims to further characterize the functional and immunological features of E2 proteins. The overlapping NAb/CD81 binding interface on E2 was examined, and the roles of HVRs and intermolecular disulfide bonding of E2 on the exposure and immunogenicity of NAb epitopes and/or CD81 binding residues on E2 were investigated.

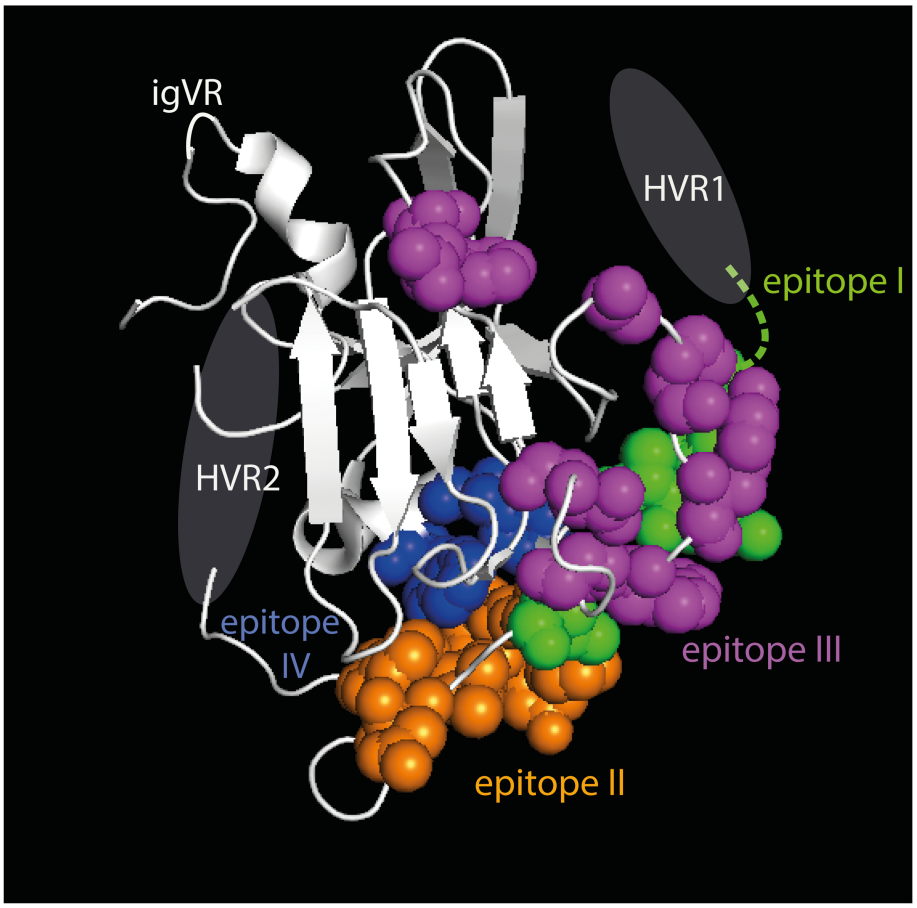

Figure 3.1 The arrangement and distribution of the four NAb epitopes (epitope I-IV, as colored spheres) and the three HVRs on AR3C-bound E2 core structure (Kong *et al.*, 2013). The unsolved N-terminal epitope I is shown here as dotted line and the predicted locations of HVR1 and HVR2 is shown as transparent ovals and not to scale. The electron density of AR3C Fab is removed.

3.2 Characterization of the neutralizing epitopes on E2

A comprehensive review of cross NAb epitopes reported to date revealed 29 amino acid residues that can be mapped into four distinct regions (highlighted in red in Figure 3.2A and labeled with a red X above in Figure 3.2B), with 19 of them critical for E1E2-CD81 interaction (highlighted in blue in Figure 3.2B). In prototypic strains of HCV from 7 genotypes, all of the NAb residues, except for residues S424, G440 and the glycan N540, are either entirely conserved or contain conservative changes (Figure 3.2B). The high-resolution structure of the E2 core published by Kong *et al* (2013) suggests that the N-terminal residues (Q412, L413, N415, N417, G418 and W420) of epitope I are disordered and absent. Structural details for residues at the C-terminus of epitope I (Figure 3.2C epitope I, H421, N423, S424 and L427) are available and showed a direct contact between the C-terminal epitope I residues and those within the epitope III loop (Figure 3.2C epitope III, G523, P525, Y527, W529 and G530). Located at the distal end of the epitope III loop, the C-terminal residues of epitope III, N540 and W549, are found at the interface between the inner and outer sheets of the ß sandwich, and therefore likely to play a role in maintaining the global conformation of E2. At the front layer of E2, the residues of the G^{436}WLAGLFY motif (Figure 3.2C, epitope II) adopt an α-helical conformation (α1) whilst forming a compact cluster with the adjacent glycan at residue N430. Packed against epitope II is the α2-helix from the back layer (Y^{613}RLWHYPCTINY). Whilst most of the amino acids are buried in the AR3C-bound E2, the α2-helix contains Y613 and W616 (Figure 3.2C, epitope IV), which form contacts with W437, G440 and L441 from epitope II (based on the PyMOL contact calculation of the α1 and α2 helices within the AR3C-bound E2 core structure published by Kong *et al*, with a distance cut-off of 4Å)

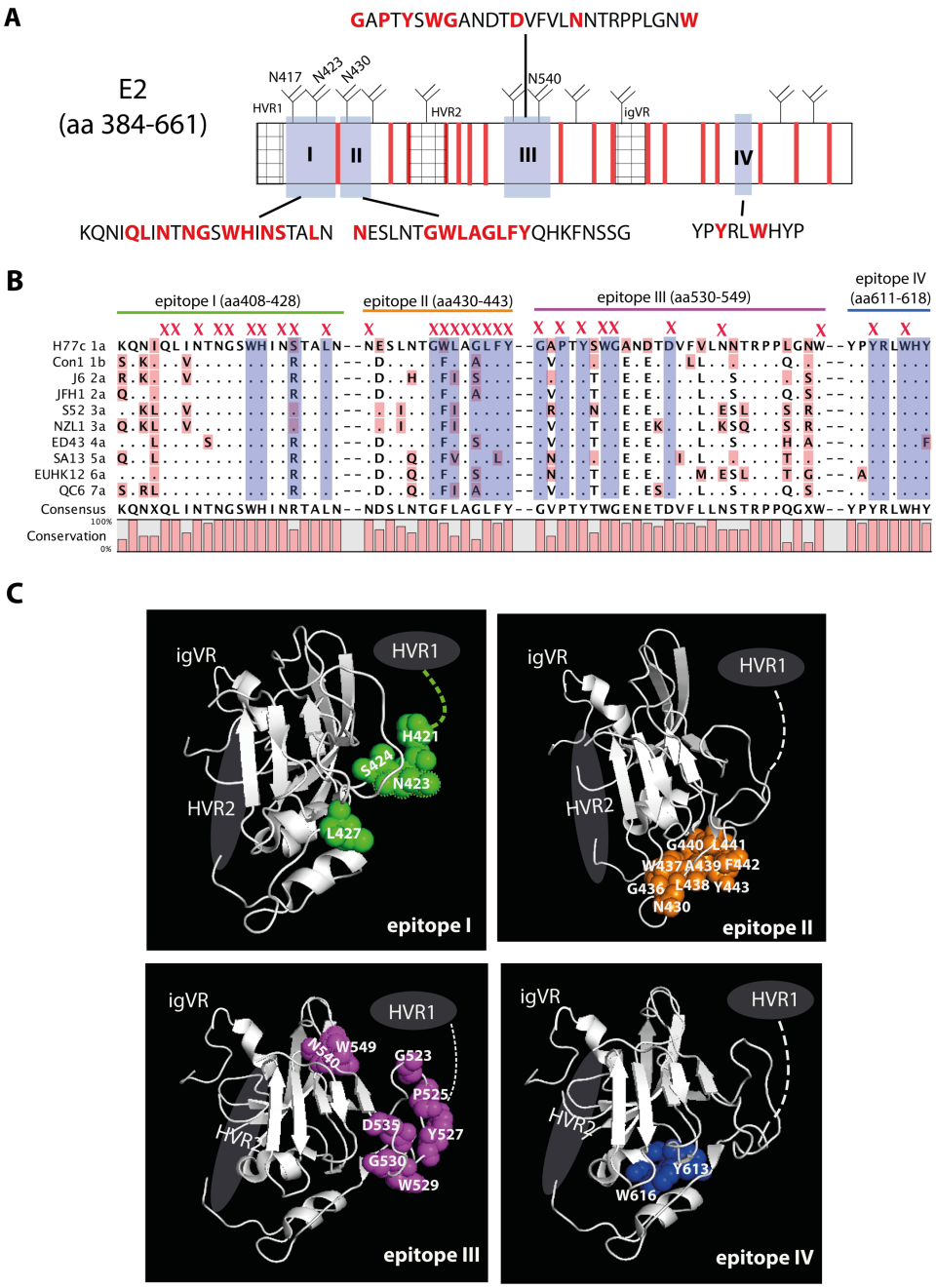

Figure 3.2 Amino acid residues involved in the formation of NAb epitopes on E2. (A) Schematic diagram showing the organization of the E2 RBD (residues 384-661) which contains three HVRs (HVR1, HVR2 and igVR, grid boxes) and four NAb epitope regions (epitope I-IV, residues numbering according to the G1a H77c strain). NAb epitope residues are highlighted in red. Trees and red lines represent positions of N-linked glycans and cysteines within the E2 RBD respectively. (B) Sequence conservation of epitope I-IV amongst prototypic strains of HCV. Alignment was performed using CLC workbench v7. NAb epitope residues are labeled with a red X and CD81 binding residues are highlighted in blue. Matching residues are represented as dots. (C) The structures of NAb epitope regions (epitope I-IV) on the E2 core (Kong *et al.*, 2013). NAb residues are labeled and shown as colored spheres. The predicted location of HVR1 and HVR2 is shown as white ovals and not to scale.

To further define amino acid residues involved in the formation of NAb epitopes on E2, single point alanine substitutions were introduced into all of the NAb residues discussed above. The exception was A439, which was mutated to a Pro or a Ser. Additionally, for NAb residues with a Trp (W420, W437, W529, W549 and W616) or Pro (P525), a Phe or Gly replacement was included respectively, in order to minimize the disruption to the overall fold of E2. Using site-directed mutagenesis, a total of thirty-six E2 epitope mutants were generated in the context of a recombinant E2 RBD protein (H77c strain, residues384-661). Their expression and ability to bind to CD81 were characterized.

3.2.1 The expression of E2 epitope mutants

To determine whether mutations at E2 NAb epitope residues affect overall folding and secretion of the E2 RBD, the expression of E2 epitope mutants in HEK293T cells was examined. Cell culture supernatant containing the secreted WT E2 and E2 mutants were analyzed on reducing SDS-PAGE gels, and E2 was visualized by an antibody directed to the C-terminal HIS tag. As shown in Figure 3.3A, all of the E2 mutants were expressed at similar levels to the WT E2. Consistent with its expression as heterogeneous glycoforms, E2 migrated as a diffuse band under reducing conditions on SDS-PAGE, with molecular sizes ranging from 47 to 73kDa. In addition, mutations of E2 at Asn residues within N-linked glycosylation sites located at N417 and N430 resulted in modest increases in the migration of E2, indicative of a reduction in molecular weight, presumably due to the loss of an N-linked glycan at these sites. By contrast, the effects of glycan removal at positions N423 and N540 on the migration of E2 appeared to be less pronounced on SDS-PAGE gels (Figure 3.3A).

3.2.2 The ability of E2 epitope mutants to bind to CD81

The ability of E2 epitope mutants to bind to the host receptor CD81 was determined using a recombinant CD81-LEL dimer fused with the mannose-binding protein, or MBP-LEL$^{113-201}$ (Drummer *et al.*, 2002). Each E2 mutant was expressed in HEK293T cells, and secreted proteins were analyzed on reducing SDS-PAGE followed by Western blotting using anti-HIS antibody (Figure 3.3A). Densitometry was performed to determine the relative amount of E2 expressed for each mutant. A normalized amount of E2 protein was then applied to GNA-lectin coated ELISA

plates and bound E2 was detected with anti-HIS antibody. The results showed that similar amounts of E2 proteins were obtained and used in ELISA assays (Figure 3.3B, insert). To determine the ability of E2 mutants to interact with CD81, ELISA plates were coated with the dimeric MBP-LEL$^{113-201}$ followed by serial dilutions of E2 proteins. As expected, none of the E2 proteins showed binding to a CD81-LEL mutant, MBP-LEL$^{113-201}$ F186S, previously shown to abrogate interaction with E2 (Drummer *et al.*, 2002).

Mutations at the N-terminal end of epitope I (Q412A, L413A, N415A, N417A and G418A) did not affect E2-CD81 interaction, as shown in Figure 3.3B. The N430A mutation completely abrogated CD81 binding, suggesting the presence of an N-linked glycan at residue 430 is essential in maintaining the ability of E2 to bind CD81. By contrast, the N423A mutation that abrogates the glycan at position N423 increased CD81 binding by 28%, indicating that this glycan may shield the CD81 binding interface. While alanine replacement of W420 and W529 drastically reduced E2-CD81 binding, conservative substitutions of W420 and W529 with a Phe restored their ability to bind to CD81 to levels similar to WT E2. Interestingly, the mutation W437F, a common variant found amongst HCV strains of all genotypes except for G1a (shown in Figure 3.2B), demonstrated significantly reduced binding of E2 to CD81. This is likely to reflect the previously reported differences in the CD81 binding conformation between recombinant E2 RBD and virion-incorporated E1E2, as mutagenesis studies on HCVpp containing E1E2 showed that W437F does not affect E2 binding to CD81 (Drummer *et al.*, 2006).

In summary, characterization of E2 epitope mutants suggests that most NAb residues are also involved in E2-CD81 interactions although further structural studies are needed to determine the exact contact residues and CD81 binding conformation of E2. Furthermore, the successful construction of this library of E2 epitope mutants provides a useful tool for the rapid identification of epitope residues of novel HCV E2-specific MAbs.

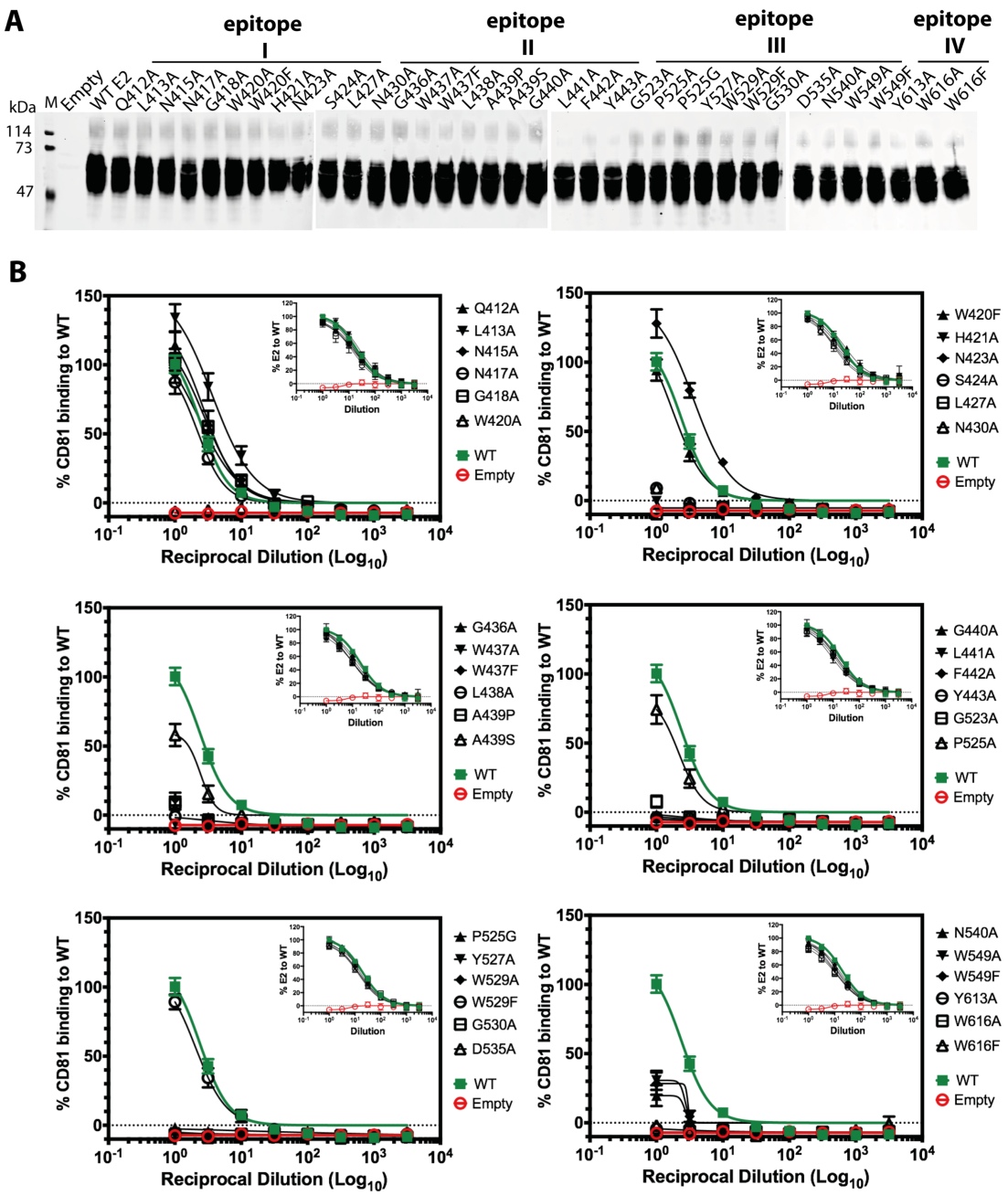

Figure 3.3 The expression and CD81 binding capacity of E2 epitope mutants. (A) Western blot analyses of E2 mutant proteins using reducing SDS-PAGE and followed by visualization with anti-HIS antibodies. (B) The ability of E2 mutants to bind to dimeric MBP-LEL$^{113\text{-}201}$. A normalized amount of E2 protein was applied to MBP-LEL$^{113\text{-}201}$ coated plates, as shown in the GNA lectin loading controls (inserts). Background levels of binding is represented by the OD levels of binding to MBP-LEL$^{113\text{-}201}$ F186S mutant that fails to bind E2, indicated by the dotted lines (n=2). % CD81 binding relative to WT E2 is calculated by (the OD binding of E2 mutant to CD81/ the maximal OD binding of WT E2 to CD81)×100%. The CD81 binding curves were fitted using nonlinear regression, one-site specific binding with Hill slope (Prism 7.0a). Data shown are the mean and standard errors of three independent experiments.

3.3 The antigenic domains on WT E2 and D123 proteins

3.3.1 Characteristics of mouse monoclonal antibodies raised to WT E2 and D123

Previously, Drs Patricia Vietheer and Yousef Alhammad isolated and partially characterized 18 murine MAbs raised to either WT E2 or D123 proteins in collaboration with CSL Ltd (Alhammad *et al.*, 2015a). This section will discuss key information on the main characteristics of the 18 MAbs and provide background for the interpretation of results in the subsequent sections of this chapter (characterization performed by Dr Yousef Alhammad and summarized in Table 3.1). All of the 18 MAbs recognize E2 in the forms of intracellularly expressed E1E2 heterodimers (Table 3.1). Using an overlapping 18-mer peptide library which spans the E2 RBD sequences (G1a, H77c, residues384-662) as well as a synthetic peptide representative of an extended HVR1 region (G1a, H, residues384-410), Alhammad *et al* identified several continuous regions on E2 that are recognized by a subset of MAbs. In addition, the reactivity of the 18 MAbs to denatured E2 proteins, E2 RBD with HVR deletion(s) as well as heterologous E2 proteins were determined, and their capacity to inhibit E2-CD81 binding and prevent HCVpp and HCVcc infections *in vitro* were characterized. Based on these features, the 18 MAbs can be loosely categorized into six different groups (summarized in Table 3.1, Group I to III, raised to D123; Group IV to VI, raised to WT E2).

Group I (MAb1, MAb7, MAb10, MAb12, MAb16 and MAb20)

Isolated from D123 immunization, Group I MAbs include MAb1, MAb7, MAb10, MAb12, MAb16 and MAb20, all of which appear to recognize their epitopes in the context of structurally and conformationally intact regions on WT E2 that are occluded in intact HCV virions as none of them can bind to denatured WT E2 or VLPs. Although these MAbs do not recognize any of the continuous regions on E2 that are 18 amino acids in length and their exact epitopes are not known, they preferentially bind to D123 over WT E2, with deletion of any HVR(s) resulting in a 2 to 3-fold increase in their apparent affinity to E2. This indicates that the presence of

HVRs modulate the exposure of Group I MAb epitopes, which may also explain the limited cross-reactivity towards heterologous E2 proteins observed amongst Group I MAbs. Whilst all of the Group I MAbs can inhibit E2-CD81 binding, HVR deletions resulted in 3.5 to 16-fold increase in their capacity to inhibit E2-CD81 binding. MAb7 in particular, fails to achieve 50% inhibition of WT E2-CD81 binding at 20µg/mL but is able to inhibit D123-CD81 binding to 50% at 2µg/mL. However, despite their capacity to inhibit E2-CD81 interactions, only MAb10 was able to weakly neutralize homologous strain of HCVpp with an IC_{50} of 34µg/mL (Alhammad *et al.*, 2015a). These results suggest that Group I MAbs recognize E2 regions that are closely associated with the CD81 binding interface on E2 and heavily modulated by HVRs.

Group II (MAb24)

Distinct from the other 17 MAbs, the Group II MAb MAb24 is a broadly neutralizing antibody that cross reacts with E2 proteins from all of the seven genotypes examined (G1a to G7a). It is able to neutralize the infections of HCVpp or HCVcc carrying E1E2 from G1a, 2a, 3a, 4a, 5a, 6a and 7a *in vitro* by >50%, with IC_{50}s ranging from 6µg/mL to 60µg/mL, and at <100µg/mL, it can inhibit infection of G1a, G2a, G4a and G5a viruses by 90% (Alhammad *et al.*, 2015a). Epitope mapping of MAb24 indicates that it recognizes the 407-424 peptide, a continuous sequence immediately downstream of HVR1 which is also highly accessible on both denatured E2 and intact HCV virions. Using an alanine scan of peptide 411-428, Alhammad *et al* further revealed that the binding to MAb24 to the peptide involves 7 residues, L413, I414, N415, T416, G418, W420 and H421, two of which are known CD81 binding residues, W420 and H421 (Boo *et al.*, 2012; Kong *et al.*, 2013; Owsianka *et al.*, 2006) (also in Section 3.2.2). MAb24 is able to inhibit E2-CD81 interactions, and although its binding to E2 is not greatly affected by HVR deletion(s), a 12-fold decrease in the IC_{50} of E2-CD81 inhibition was observed when all three HVRs were deleted.

Group III (MAb6, MAb13, MAb14, MAb22, MAb23)

Also raised to D123, the Group III MAbs include MAb6, MAb13, MAb14, MAb22 and MAb23. Similar to Group II MAb24, Group III MAbs also display pan-genotypic cross-reactivity towards heterologous E2 proteins and their binding to E2 is

not affected by HVRs. However, none of them inhibit E2-CD81 binding or neutralize homologous HCVpp *in vitro*, and they all appear to bind to discontinuous E2 regions that are surface exposed on denatured E2 and VLPs. While MAb6, MAb13, and MAb22 showed strong binding to denatured E2, MAb14 and MAb23 react weakly with E2 on Western blot, suggesting that there are epitope differences amongst Group III MAbs.

Group IV (MAb25, MAb39, MAb44)

Group IV MAbs were raised against WT E2 immunization and include MAb25, MAb39 and MAb44, all of which recognize the 512-529 peptide. Despite sharing the common epitope, epitope III, the Group IV MAbs differ in their reactivity towards denatured E2 and VLPs as well as their inhibition of E2-CD81 binding. As the most cross-reactive MAb in the group (G1a, 1b, 2a, 3a, 4a), MAb25 binds strongly to the 512-529 region on VLPs but fails to inhibit E2-CD81 binding by 50% at 20µg/mL. By contrast, MAb39 and MAb44, whose reactivity to E2 is limited to G1a, were able to inhibit E2-CD81 interaction by 50% at 3µg/mL. Furthermore, MAb44 is able to neutralize homologous HCVpp with an IC_{50} of 8µg/mL (Alhammad *et al.*, 2015a). These findings indicate that the epitope conformation or the exact epitope residues of Group IV MAbs, or epitope III-specific MAbs may differ, which contributes to the observed differences in their ability to inhibit of E2-CD81 and to neutralize the virus.

Group V (MAb26)

As a cross-reactive MAb isolated from WT E2 immunization (all E2 except G4a and G6a), the Group V MAb26 recognizes a continuous region at the C-terminus of E2, the 645-662 peptide. Consistent with the findings that the C-terminal sequences of E2 are not involved in CD81 binding, MAb26 cannot inhibit E2-CD81 or neutralize homologous HCVpp. Nevertheless, based on the reactivity of MAb26 to denatured E2, VLPs and HVR(s)-deleted E2 proteins, the MAb26 epitope which includes the 645-662 region appears to be exposed on the virion surface and is not affected by HVRs.

Group VI (MAb33 and MAb36)

Generated from WT E2 immunization, the two Group VI MAbs, MAb33 and MAb36 are sensitive to HVR deletion(s). HVR1 delection alone (D1) or in combination with HVR2 and/or igVR (D12, D13 or D123) resulted in a complete loss of their binding to E2, suggesting that the epitopes of both MAbs contains residues from the HVR1. Consistent with this, MAb36 recognizes an extended version of HVR1 (peptide 384-410, G1a, H strain). Whilst HVR2 deletion (D2) did not greatly affect the binding of E2 by the two MAbs, the removal of igVR (D3) from E2 significantly reduced the binding of MAb36 to E2 and completely abolished MAb33-E2 interaction. The ability of MAb36 to bind to E2 was mildly restored when both igVR and HVR2 were removed (D23). In contrast to MAb36 which is a type-specific, weakly neutralizing MAb (HCVpp G1a H77c IC_{50}: 53µg/mL), MAb33 is able to neutralize homologous HCVpp to 50% at 0.1µg/mL and weakly cross neutralize G4a, G6a and G7a viruses (Alhammad *et al.*, 2015a). Furthermore, the MAb33 epitope is more exposed on virions than that of MAb36, suggesting that MAb33 may have additional epitope residues that are outside HVR1.

Table 3.1 The key features of the 18 mouse MAbs isolated to WT E2 or D123 (Alhammad *et al.*, 2015a).

Group	MAbs[1]	Peptide Reactivity	Binding to denatured WT E2	Cross-Reactivity to heterologous E2							VLPs binding	Fold changes in apparent affinity to HVR(s)-deleted E2 relative to WT E2[2]								E2-CD81 inhibition (μg/mL)	
				1a	1b	2a	3a	4a	5a	6a		WT	D1	D2	D3	D12	D13	D23	D123	WT	D123
I	MAb1	– [3]	-	+	-	-	-	-	-	-	-	1	2.08	2.63	2.70	2.17	2.38	3.33	2.04	9	2.5
	MAb7		-	+	-	-	-	+	-	-	-	1	2.04	2.63	2.78	2.08	2.44	3.57	2.22		2
	MAb10		-	+	-	-	+	-	+	-	-	1	1.30	1.54	1.67	1.37	1.85	1.79	1.09	3	5
	MAb12		-	+	-	-	-	-	-	-	-	1	1.91	2.41	2.73	2.07	2.76	3.35	2.00	12	2
	MAb16		-	+	-	-	-	-	-	-	-	1	1.89	2.29	2.43	1.95	2.00	2.95	1.97	2.5	0.7
	MAb20		-	+	-	-	-	-	-	-	-	1	2.58	2.93	3.62	2.85	3.18	2.75	2.55	8	0.5
II	MAb24	407-424	+++	+	+	+	+	+	+	+	+++	1	1.14	0.78	1.14	1.00	1.40	0.75	0.94	18	1.5
III	MAb6	-	+++	+	+	+	+	+	+	+	++	1	0.99	1.00	0.99	0.98	0.99	0.82	0.78	-	-
	MAb13		+++	+	+	+	+	+	+	+	++	1	1.02	0.89	0.95	0.85	0.92	0.69	0.71	-	-
	MAb14		+	+	+	+	+	+	+	+	++	1	1.27	1.20	1.20	1.12	1.05	1.30	0.93	-	-
	MAb22		+++	+	+	+	+	+	+	+	++	1	1.35	1.16	1.17	1.09	1.06	0.61	0.72	-	-
	MAb23		+	+	+	+	+	+	+	+	+	1	1.02	0.81	0.69	1.15	1.48	0.79	0.81	-	-
IV	MAb25	512-529	+	+	+	+	+	+	-	-	+++	1	0.98	1.01	0.99	0.98	0.91	0.84	0.87	-	-
	MAb39	512-529	+++	+	-	-	-	-	-	-	+++	1	0.96	1.08	1.06	0.96	0.92	1.01	1.01	3	3
	MAb44	512-529	+	+	-	-	-	-	-	-	+	1	1.01	1.01	1.01	0.93	0.91	1.00	1.02	3.1	1.9
V	MAb26	645-662	+++	+	+	+	+	-	+	-	+++	1	1.12	1.07	1.00	0.90	0.86	0.58	0.67	-	-
VI	MAb33	-	+++	+	-	-	-	+	-	+	+++	1	-	0.54	-	-	-	0.06	-	16	-
	MAb36	384-410	+++	+	-	-	-	-	-	-	+	1	-	1.13	0.14	-	-	0.42	-	-	-

[1]highlighted in blue are MAbs that can neutralize homologous HCVpp (G1a, H77c) entry to 50% at concentrations <60μg/mL: MAb10 (IC_{50} 34μg/mL), MAb24 (IC_{50} 6μg/mL), MAb44 (IC_{50} 8μg/mL), MAb33 (IC_{50} 0.1μg/mL) and MAb36 (IC_{50} 53μg/mL) ; [2]green, enhanced binding affinity or inhibitory capability compared to WT; orange, reduced binding affinity compared to WT; [3]Grey, low or no activities.

3.3.2 Identification of E2 residues involved in monoclonal antibody recognition

The 18 MAbs discussed in Section 3.3.1 appear to recognize distinct antigenic domains on E2 region(s) and have different structural requirements for binding to their epitopes. While peptide mapping of the 6 MAbs (MAb24, MAb25, MAb33, MAb36, MAb39 and MAb44) revealed four continuous antigenic domains on E2, the remaining 12 MAbs appear to recognize discontinuous regions that require the tertiary organization and/or post-translational modification, such as glycosylation of the intact E2 protein. In Section 3.2, a library of thirty-six E2 proteins with single point mutations at known NAb epitope residues was constructed and the ability of each mutant to interact with CD81-LEL was defined. Here, to identify the exact epitope residues of each MAb on E2, the ability of the 18 MAbs to bind to these epitope mutants was examined. Each epitope mutant protein was expressed in HEK293T cells before concentration from the cell culture supernatant. The amount of E2 proteins captured on solid-phase GNA lectin was then normalized using ELISA and detected with anti-HIS antibody as indicated by the anti-His antibody control in Figure 3.4. The level of MAb binding to E2 epitope mutants was quantitatively determined and expressed as the percentage binding relative to the maximum binding observed for WT E2, shown in Figure 3.4.

The overall conformation of E2 appeared to be intact in all E2 mutants as conformational antibodies H53 and CBH-7 were able to recognize all of the mutants, at levels similar to WT E2 (Figure 3.4). Exceptions were W549 and N540 mutants which have previously been shown to affect the ability of H53 and CBH-7 to bind E1E2 (Owsianka *et al.*, 2006; Owsianka *et al.*, 2008). Group II MAb24 showed significantly reduced binding to E2 epitope mutants within the epitope I region (residues 412-423). Consistent with the previous peptide mapping results, mutations at residues L413, N415, G418 and W420 in E2 reduced the level of MAb24-E2 binding to <10% while alanine replacement of residue H421 reduced MAb24-E2 binding by 50%. Although not involved in MAb24 recognition of the 411-428 peptide, the Q412A mutation reduced MAb24 binding to E2 by 50%, suggesting that there may be some conformational differences in epitope I between the 411-428

peptide and the recombinant glycosylated form of E2. Binding of MAb24 to N417A and N423A (80% and 112% relative to WT E2 respectively) also confirms that the N-linked glycans at residue 417 and 423 are not required for MAb24 recognition of E2. In summary, MAb24 showed extensive interactions with residues from the epitope I region, including Q412, L413, N415, G418, W420 and H421, while I414 and T416 appear to make smaller contributions to MAb24 binding. However, structural studies are needed to determine the exact contact residues of MAb24 on epitope I and will be discussed further in Chapter 4.

Binding of Group VI MAb33 and MAb36 to E2 mutants also identified the epitope differences between the two MAbs. MAb36 was HVR1-specific and its binding to E2 is not significantly affected by any mutations within the four epitope regions (>50% relative to WT E2). By contrast, MAb33 binding to E2 requires the presence of HVR1 as well as an additional residue L413 whose mutation resulted in a 75% decrease in MAb33-E2 binding. Found in epitope I adjacent to the two CD81 binding residues W420 and H421, L413 is 100% conserved in prototypic strains of HCV (Figure 3.2B). The requirement of L413 places the epitope of MAb33 more proximal to the CD81 binding site than MAb36. As a result, the footprint of MAb33 interacting with E2 is likely to at least partially occlude E2-CD81 interactions, accounting for the moderate level of cross-reactivity and E2-CD81 inhibition potentials observed for MAb33. Further structural studies are needed to fully determine the exact interaction between MAb33 and its epitope on E2.

Consistent with their ability to bind to peptide 512-529, the binding of Group IV MAb25, MAb39 and MAb44 was affected by mutations within the epitope III region (residues 523-549, Y527, W529, G530 and D535 for MAb25; G523 and P525 for MAb39 and MAb44) of E2. In addition, Group III MAb6, MAb13, MAb14, MAb22 and MAb23 were also affected by mutations within epitope III (Figure 3.4). Based on their residue specificities, the epitope III-specific MAbs (Group III and Group IV MAbs) can be organized into three subsets. The first subset of MAbs include all of the Group III MAbs as well as the Group IV MAb25, which recognizes residues Y527, W529 and G530. In the case of MAb6, MAb14 and MAb25, P525 or D535 is additionally required for binding. MAbs in this subset exhibit high levels of

cross-reactivity but do not inhibit E2-CD81 binding. The second MAb subset includes Group IV MAb39 that recognizes residues G523 and P525 and can inhibit E2-CD81 interaction. The third subset includes the strain-specific neutralizing MAb44 whose epitope comprises or is affected by mutations at residues G523, P525, N540, W549 and Y613.

None of the mutations at the NAb epitope residues significantly impacted the ability of Group V MAb26 to bind E2, except for H421A, G436A and L438A which reduced MAb26-E2 binding to <55%. This suggests that there may be some structural linkage between the front layer of E2 (epitope I and II) and the MAb26 epitope which is located within the 645-662 region and absent from the crystal structure of the E2 core. Lastly, the epitope of the Group I MAbs MAb1, MAb7, MAb10, MAb12, MAb16 and MAb20 cannot be determined as none of them displayed significant reactivity towards GNA lectin-captured WT E2 proteins, despite a 4-fold increase in the amount of E2 loaded (data not shown). This is possibly due to the low affinity of Group I MAbs to WT E2. Affinity-purified E2 mutant proteins may be required to perform the epitope mapping of Group I MAbs. Alternatively, given that Group I MAbs were raised to D123 protein and have displayed high affinity to D123 (Table 3.1), future alanine mutagenesis of D123 can be used to determine the specific amino acid residues that are involved in the E2 recognition by these MAbs.

Figure 3.4 The ability of MAbs to bind E2 epitope mutants^.

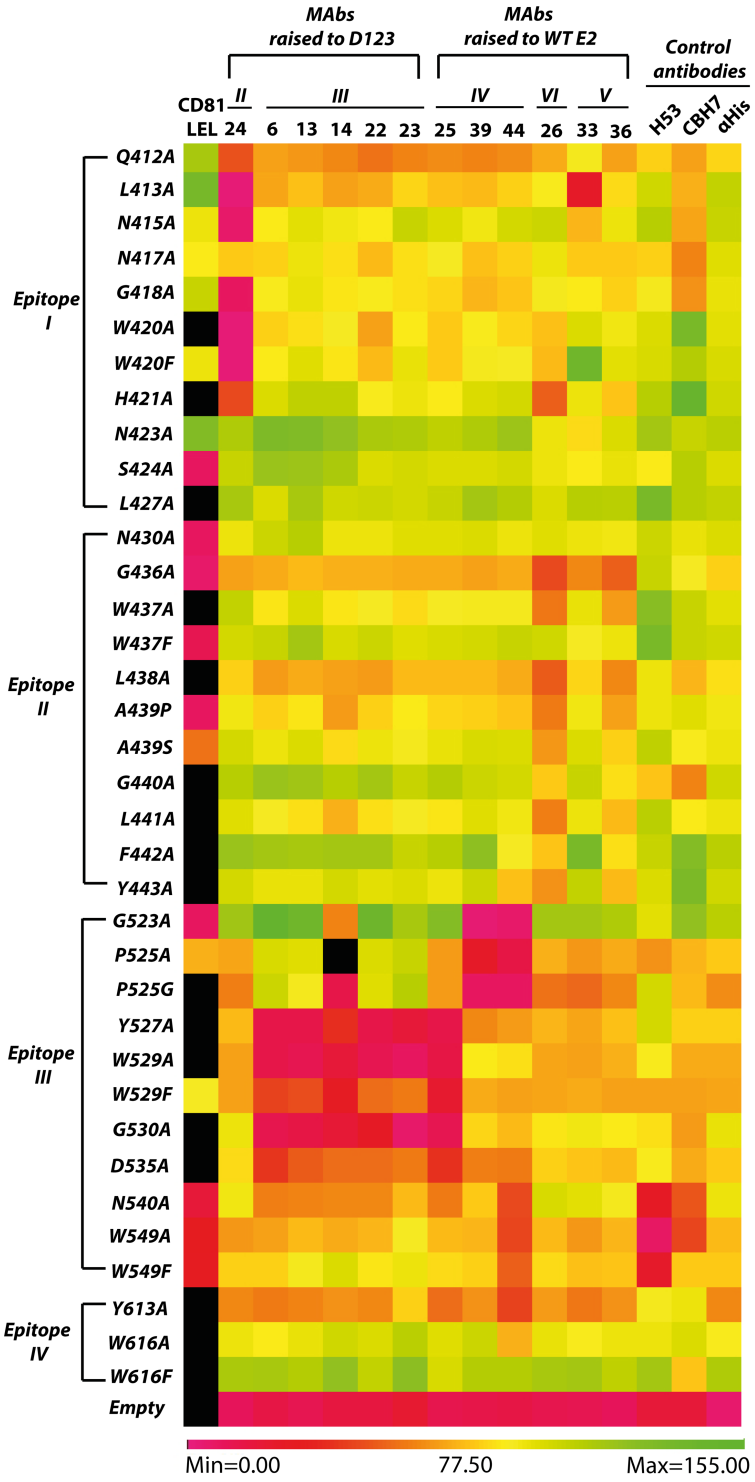

^The levels of MAbs binding to E2 epitope mutants are calculated by (the OD of MAb binding to E2 mutant/the OD of MAb binding to WT E2)x100. The average percentage of MAb-E2 mutant binding relative to WT E2 (n=2) is shown on the map. Map was generated using PermutMaxtrix software (Caraux & Pinloche, 2005). The CD81-LEL binding capacity of each epitope mutant (Figure 3.3B) is also included here. Black indicates 0% binding relative to WT.

3.4 Polyclonal antibody response to intact E2 and D123 proteins in guinea pigs

While the epitopes of the 18 MAbs can be partially defined with E2 mutagenesis and reveal antigenic similarities and differences between WT E2 and D123, the selection and isolation of these MAbs is a random process. A limited number of B cells fuse with the myeloma cell line, proliferate and make stable hybridoma clones, and only a small subset is selected for characterization. In vaccine settings, the B cell response is polyclonal and heterogeneous amongst subjects. Therefore, the full spectrum of antibody specificities generated by WT E2 or D123 vaccination cannot be recapitulated through the characterization of MAbs alone. Furthermore, both WT E2 and D123 spontaneously generate complex heterogeneous mixtures with varying oligomeric valences, and the antigenicity and immunogenicity of these varied oligomeric forms of E2 had not previously been investigated.

To compare the immunogenicity of WT E2 and D123 proteins and their oligomers, Vietheer *et al* (2017) conducted an immunization study in outbred guinea pigs. The potency and breadth of antibody response generated by each E2 immunogen was assessed using E2-CD81 inhibition assay (homologous G1a, H77c and heterologous G2a, JFH-1 E2 proteins) and *in vitro* neutralization assays (homologous HCVpp G1a, H77c and heterologous HCVcc G2a, J6). In addition, the immunogenicity of both neutralizing and non-neutralizing epitopes on HMW1 and monomeric forms of WT E2 and D123 was indirectly measured using competition ELISA with neutralizing HMAbs (HCV1, AR3C and HC84.27) and non-neutralizing HMAb (CBH-4B). Here, to further characterize the antibody specificity elicited by various forms of WT E2 and D123, the ability of immune sera to recognize the three known neutralizing epitopes 408-428, 430-451 and 523-549 were quantitatively determined using peptide sequences from homologous (G1a, H77c) and heterologous (G2a, J6) strains.

3.4.1 Antibody specificities elicited by unfractionated WT E2 or D123 proteins

Vietheer *et al* (2017) found that unfractionated WT E2 and D123 were equally immunogenic and elicited similar titres of type-specific neutralizing antibodies. However, D123 elicited significantly higher titres of antibodies that inhibited the binding of a heterologous G2a E2 to CD81 and higher titres of cross neutralizing antibodies against G2a HCV than WT E2. As expected, high titres of HVR1-specific antibodies were found in animals that received WT E2 but were not observed in D123-vaccinated animals. Together, these findings indicate that the deletion of all three HVRs may direct antibody responses towards conserved NAb epitope regions.

To investigate whether the HVRs alter the specificity of the antibody response to E2, the immune sera from guinea pigs vaccinated with unfractionated WT E2 or D123 were examined for their ability to bind homologous (G1a) and heterologous (G2a) peptides that overlap NAb/CD81 binding region: 408-428, 430-451 and 523-549. As shown in Figure 3.5, the binding titres of sera generated to D123 was significantly higher towards regions 408-428 and 523-549 than WT E2 immune sera. Antibody titres towards the 408-428 region in particular, were consistently high in D123-immunized animals whereas mixed responses were observed in animals vaccinated with WT E2 (10-fold difference in geometric means, $p<0.0001$). This highlights the differences in the structure and immunogenicity of the 408-428 region between WT E2 and D123, and may be a result of the deletion of all three HVRs, particularly the adjacent HVR1 region.

The modulation of antibody response by HVRs was further demonstrated in the differences in the cross-reactivity of immune sera towards heterologous peptides. While the immune sera of D123-vaccinated animals had high titres of antibodies to heterologous peptides 408-428 and 523-549, significantly lower titres were generated in WT E2-immunized animals, and 3 out of 10 animals failed to generate any cross-reactive antibodies to these regions. No cross-reactive antibodies were detected against the 430-451 peptide in either groups, except for one animal from the WT group. In summary, D123 elicited high titres of cross-reactive antibodies to at least two of the known neutralizing epitopes 408-428 and 523-529. By contrast, the

antibody responses generated by WT E2 were HVR1-specific and had limited cross-reactivity to known neutralizing epitopes.

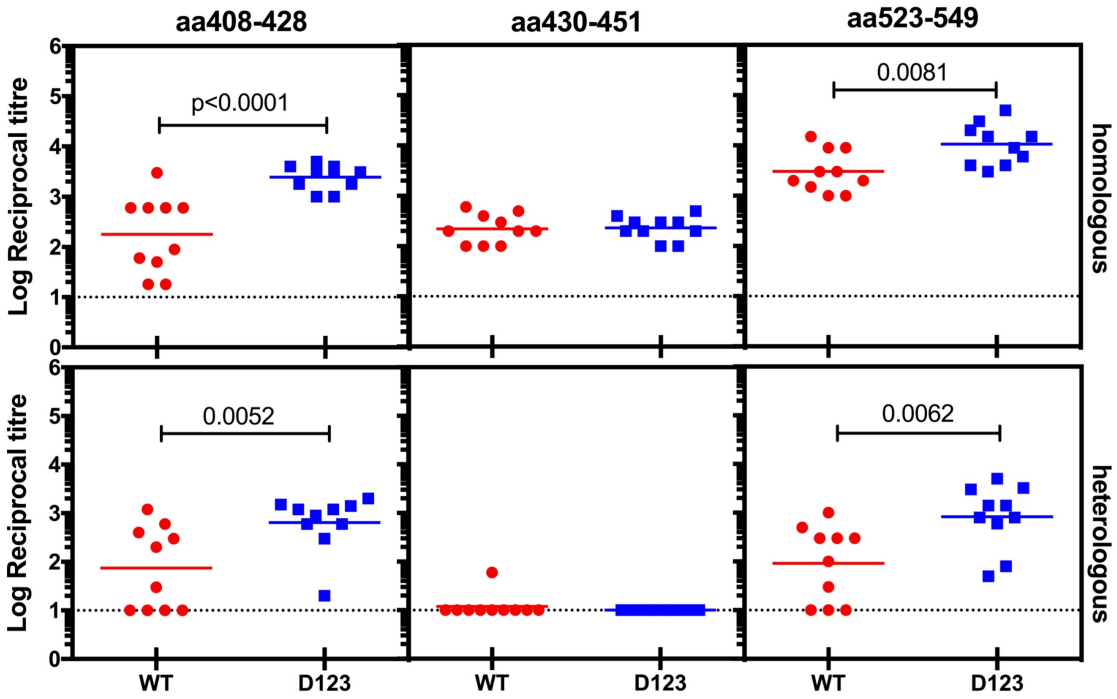

Figure 3.5 The immunoreactivity of sera from WT E2 and D123-vaccinated guinea pigs towards homologous (G1a, H77c) and heterologous (G2a, J6) peptides. The mean background peptide binding of the no immunogen control group is represented as dotted line. Mann-Whitney test was used to determine the *p* values (Prism 7.0a).

3.4.2 Antibody specificities elicited by oligomeric forms of WT E2

Based on the findings published by Vietheer (2017), different oligomeric forms of WT E2 exhibit distinctly different antigenic and immunogenic properties, as summarized in Table 3.2. For instance, despite an occluded HVR1 structure, WT HMW1 elicits an antibody response that is predominantly HVR1-specific and do not inhibit E2-CD81 binding. Amongst the four WT E2 immunogens examined, WT HMW2 appears to be the only one that generates significant levels of cross-reactive antibodies that block E2-CD81 interactions. Correlated with their HVR1 specificity and/or E2-CD81 inhibition potential, HMW1 and HMW2-immune sera contains both neutralizing and cross-neutralizing antibodies, at levels significantly higher than monomeric WT E2 (~10-fold, $p<0.05$). Whilst monomeric WT E2 appears to have an immunogenic non-NAb region that generates CBH-4B-competing antibodies, no CBH-4B-competing antibodies were found in HMW1-immunized animals (Table 3.3). Instead, high titres of antibodies that compete with the broadly neutralizing HMAb HCV1 for binding to WT E2 were observed in the WT HMW1 group. Overall, these results indicate that as an immunogen, WT E2 has limited capacity in eliciting cross neutralizing antibodies and different forms of WT E2 elicit distinct antibody specificities.

To examine how the oligomeric status of WT E2 alters the immunogenicity of the NAb epitopes on E2, the ability of WT oligomer-immune sera to recognize homologous and heterologous NAb epitope regions 408-428, 430-451 and 523-549 was investigated. Compared to the monomeric WT E2 group, animals that received HMW forms of WT E2 have significantly higher titres of antibodies to homologous 408-428 and 523-549, as shown in Figure 3.6. Despite this, the antibody titres to the 408-428 region in the WT E2 HMW1 and HMW2 groups were observed at considerably low levels. Thus, the high levels of HCV1-competing antibodies observed in WT E2 HMW1 group is more likely to be associated with the presence of interfering HVR1-specific antibodies (Table 3.2) than those targeting epitope I in WT HMW1 immune sera. Irrespective of the oligomeric form of WT E2 proteins, the antibody titres to heterologous NAb epitopes were low across all groups, with no cross-reactive antibodies to the 430-451 region detected in any animals. Compared to

other groups, HMW2 elicited higher titres of cross-reactive antibodies to the 408-428 and 523-549 region as shown in Figure 3.6, correlated with the higher titres of cross-neutralizing antibodies observed within the group. Overall, these results suggest that HMW forms of WT E2 enhances the immunogenicity of the neutralizing face of E2 with a less exposed non-neutralizing surface than monomeric WT E2. In order to generate cross-reactive antibodies, albeit at low titres, more than two subunits of WT E2 monomers is required within the oligomer.

3.4.3 Antibody specificities elicited by oligomeric forms of D123

Similar to WT E2, the antigenic properties differed significantly amongst D123 oligomers (Table 3.2) (Vietheer *et al.*, 2017). In contrast to WT E2 oligomers, which had limited ability to generate cross reactive antibodies, all of the four D123 oligomers were able to elicit antibodies that inhibited heterologous G2a E2 binding to CD81 in guinea pigs. The D123 HMW2 group in particular, showed significantly higher titres of such antibodies than immune sera generated to monomeric D123. Immune sera from animals receiving HMW forms of D123 displayed pan-genotypic neutralization capacity across all 7 genotypes of HCV by >80% (Vietheer *et al.*, 2017). Antibody competition analyses revealed that the antibody specificities elicited by D123 HMW1 and D123 monomer are remarkably different (Table 3.3). Whilst high titres of antibodies that compete with the non-neutralizing HMAb CBH-4B were found in the D123 monomer-immunized animals, the antibody response generated by D123 HMW1 appeared to target the neutralizing face of E2, with antibody specificities competing with broadly neutralizing HMAbs HCV1 and AR3C.

To investigate how the oligomerization of HVRs-deleted E2 (D123) alters the specificity of antibody response, the antibody binding titres to homologous and heterologous 408-428, 430-451 and 523-549 peptides of D123 oligomer-immunized animals were determined. Compared to the D123 monomer, the HMWs elicited significantly higher titres of antibodies to all of the three homologous peptide analogs (Figure 3.7). In contrast to WT E2, that generated low titres of cross-reactive antibodies towards heterologous peptides, the HMW1 D123 and HMW2 D123 elicited significantly higher levels of cross-reactive antibodies to regions 408-428 and 523-549. Only trace levels of antibodies to the 430-451 region was detected in D123 oligomer-immunized animals, particularly the HMW2 group. These results indicate that when all three HVRs are deleted a higher order arrangement of E2 is associated with increased titres of brNAbs with a concomitant increase in 408-428 and 523-549 specific antibodies, and decreased titres of non-NAbs.

Table 3.2 Characteristics of immune sera from guinea pigs immunized with oligomeric forms of WT E2 or D123 (Viethеer *et al.*, 2017).

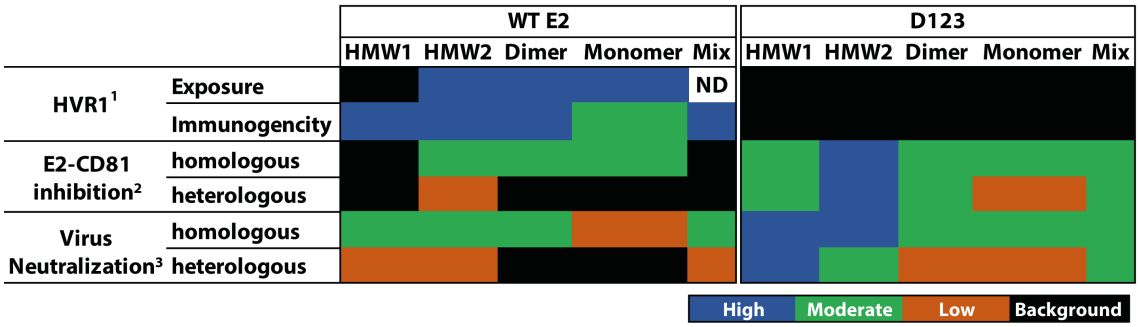

[1]HVR1 exposure was determined by the binding of the HVR1-specific MAb36 to each form of WT E2. The binding of MAb36 to unfractionated (mix) WT E2 was not investigated (ND). The immunogenicity of HVR1 amongst WT E2 oligomers was indicated by the titres of HVR1 peptide (residues 384-410)-specific antibodies in the immune sera.

[2]Antibody titres that inhibit homologous (G1a, H77c) or heterologous (G2a, JFH-1) E2-CD81 binding to 50%

[3]Antibody titres that neutralize homologous (G1a, H77c) HCVpp or heterologous HCVcc (G2a, J6) to 50%.

Table 3.3 Antibody specificities of immune sera from guinea pigs vaccinated with HMW1 and monomeric form of WT E2 and D123 (Viethеer *et al.*, 2017).

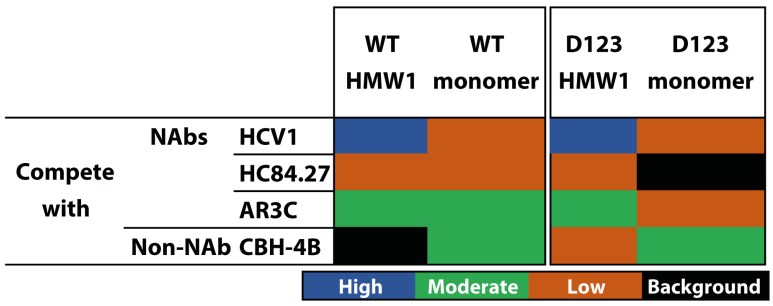

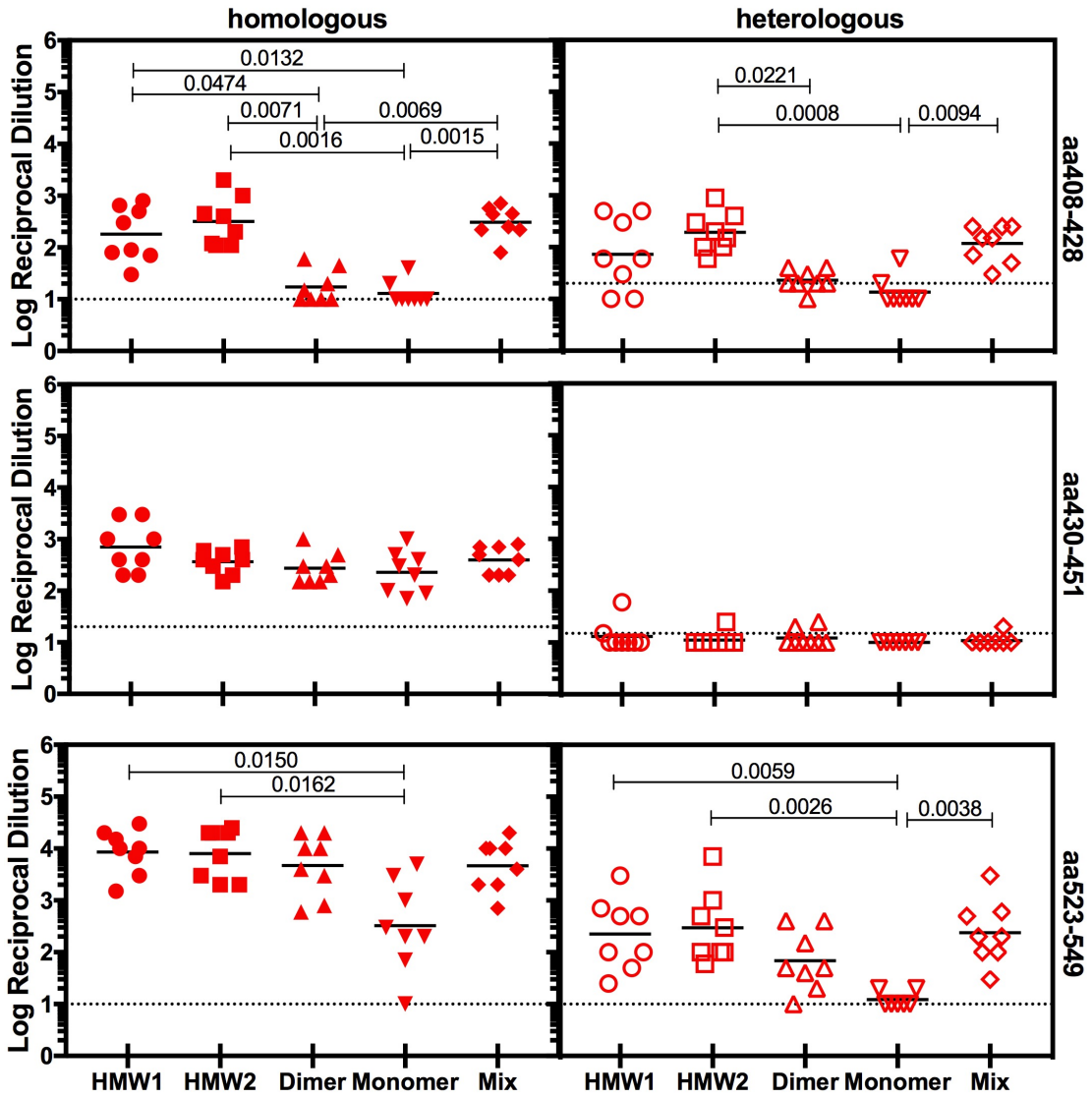

Figure 3.6 Immunoreactivity of immune sera from guinea pigs vaccinated with different oligomeric forms of WT E2 against homologous (G1a, H77c) and heterologous (G2a, J6) peptides. The mean background peptide binding of the no immunogen control group is represented as dotted line. *P* values were determined using Kruskal-Wallis test with Dunn's post-test correction for multiple comparisons (Prism 7.0a).

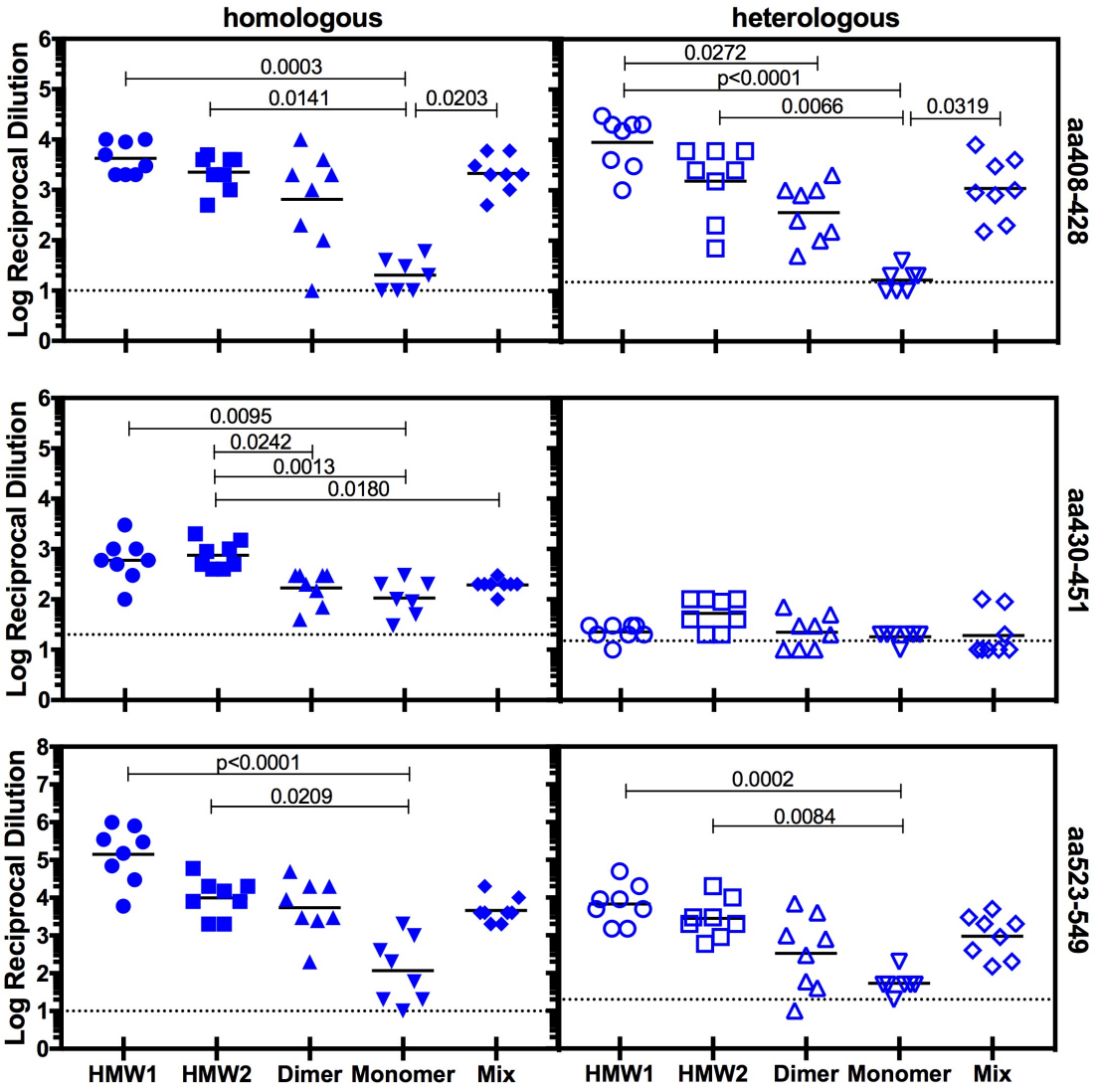

Figure 3.7 Immunoreactivity of immune sera from guinea pigs vaccinated with different oligomeric forms of D123 against homologous (G1a, H77c) and heterologous (G2a, J6) peptides. The mean background peptide binding of the no immunogen control group is represented as dotted line. *P* values were determined using Kruskal-Wallis test with Dunn's post-test correction for multiple comparisons (Prism 7.0a).

3.5 Discussion

The interaction between HCV glycoprotein E2 and its host receptor CD81 is essential for HCV infection and the CD81 binding interface on E2 is a key target for neutralizing antibodies that inhibit HCV entry. However, the interaction between E2 and CD81 is yet to be fully characterized. Structural studies combined with site-directed mutagenesis findings showed that the head subdomain of CD81-LEL, including residues L162, I182, N184 and F186, are involved in E2 binding (Bertaux & Dragic, 2006; Cunha *et al.*, 2017; Drummer *et al.*, 2002; Higginbottom *et al.*, 2000; Kitadokoro *et al.*, 2001). Based on the current knowledge of the E2 structure and site-directed mutagenesis of E1E2 heterodimers or HCVpp, E2 residues involved in CD81-LEL binding are found in four highly conserved, discontinuous regions including W^{420}H-S^{424}-L^{427}N (partly epitope I), G^{436}WL-G^{440}LFY (epitope II), G^{523}-P^{525}-Y^{527}-W^{529}G-D^{535} (epitope III), and Y^{613}R-W^{616}HY (epitope IV) (Boo *et al.*, 2012; Drummer *et al.*, 2006; Kong *et al.*, 2013; Owsianka *et al.*, 2006; Roccasecca *et al.*, 2003; Rothwangl *et al.*, 2008). It is noteworthy to point out that all of the CD81 binding regions characterized to date were based on E2 binding to recombinant CD81-LEL protein, and the full extent of virion-associated E2 and cellular CD81 interaction during HCV entry may differ from that of E2 RBD and CD81-LEL. Nevertheless, there is no co-crystal structure of the E2-CD81 complex, which is essential for refinement of the binding interface between this receptor-ligand interaction.

Given the overlap between the proposed CD81 binding region and known NAb epitopes, it is likely that residues recognized by some NAbs overlap with residues involved with E2-CD81 binding. In this study, amino acid changes were introduced into residues within the known NAb epitopes on E2 in the context of a minimal CD81 binding subdomain of E2 comprising amino acid residues 384-661. Overall, the findings here support and complement the CD81 binding interface previously proposed on E2 (Boo *et al.*, 2012; Drummer *et al.*, 2006; Kong *et al.*, 2013; Owsianka *et al.*, 2006). For instance, the steric hindrance introduced by a Pro at position 439 (A439P) is likely to disrupt the helical structure of epitope II and therefore significantly affected the ability of E2 to bind to CD81 whereas the E2-CD81 interaction was less affected by the A439S mutation. Also consistent with

Kong's observation is that a P525A mutation does not disrupt E2-CD81 interaction while a P525G mutation abolished E2 binding to CD81. Furthermore, in addition to the residues identified in the CD81 binding interface of the E2 core, it was found that mutations at N540, W549, W616 and Y613 reduced the levels of E2 binding to CD81 by at least 80%. Given the distance of these residues from the described CD81 interface on the E2 core, it is likely that they are indirectly involved in the E2-CD81 interaction, possibly via the conformational modification of the CD81 binding site, either allosterically (N540 and W549) or at a local level (Y613 and W616).

Also, the CD81-LEL binding capacity of E2 mutants corroborates previous findings that were achieved using HCVpp and E1E2 heterodimers, as shown in Table 3.4 (Boo *et al.*, 2012; Drummer *et al.*, 2006; Kong *et al.*, 2013; Owsianka *et al.*, 2006; Rothwangl *et al.*, 2008). Exceptions were the modification of glycosylation sites (N417A and N423A), which had different effects on the CD81 binding capacity of E2 RBD and intracellularly expressed E1E2. For instance, the N423A mutation enhances the CD81 binding capacity of E2 RBD (128% relative to WT E2, Figure 3.3B) whereas in intracellularly expressed E1E2, the same N423A mutation reduced CD81 binding level to <70% (Owsianka *et al.*, 2006). This highlights the differences in the glycan surface and/or conformation between different forms of E2. In addition, non-conservative mutations at any of the residues from the epitope II region (residues 436-443) completely abrogated E2 binding to CD81, whereas the same amino acid substitutions are more tolerated in intracellularly-expressed E1E2 heterodimers and HCVpp (Drummer *et al.*, 2006). Together, these findings underscore the structural differences in the CD81 binding interface within different forms of E2.

Consistent with Kong's findings, the N-terminus of epitope I (residues 412-419) is not required for E2-CD81 binding, whilst mutations in most of the other NAb epitope residues affect the ability of E2 to bind to CD81. The mapping of these residues onto the E2 crystal structure published by Kong *et al* (2013) revealed an extensive interface on E2 that is involved in E2-CD81 binding, including the front layer of the E2 protein (residues 420-443, epitope I and II) as well as the CD81 binding loop (residues 523-535, epitope III) from the central sandwich, shown in Figure 3.8. As suggested by hydrogen-deuterium exchange analyses of monomeric

E2, the CD81 binding interface exhibits a high degree of structural flexibility (Khan *et al.*, 2014; Kong *et al.*, 2016). Thus, to fully determine the CD81 contact residues on E2, crystallographic studies of CD81-bound E2 are needed. In HIV studies, MAbs such as VRC01 can directly bind to the CD4 binding site on gp120 and mediate neutralization. Co-crystallization of HCV E2 with CD81 binding site-specific brNAbs such as HC84.1 and HC84.27 may therefore further help to delineate features of the CD81 binding interface on E2 as well as elucidate the neutralization mechanisms of these potent antibodies.

The proposed CD81 binding loop located within the 523-549 region, also referred to as epitope III, appears to be quite immunogenic in mice, with 8 out of the 18 mouse MAbs isolated to WT E2 or D123 recognizing this region. Comparative analyses of the epitope residues of these 8 MAbs revealed three micro-domains within epitope III, represented by the target sites of MAb25, MAb39 and MAb44. Using the AR3C-bound E2 core structure as the template, the distribution and organization of the three micro-domains are determined, shown in Figure 3.9. In contrast to non-neutralizing MAb25 and MAb39 whose epitopes comprise residues on the proposed CD81 binding loop (P525, Y527, W529, G530 and D535; or G523 and P525), the neutralizing MAb44 appears to interact with the N-terminal components of the CD81 binding loop (G523 and P525) as well as residues from the adjacent central sandwich (N540, W549 and Y613). Therefore, MAb44 is expected to have a larger footprint of E2 interaction than MAb25 and MAb39, and this may contribute to its ability to neutralize HCV. However, comparative structural analyses of the E2-CD81 binding interface and the MAb binding sites on E2 are required to confirm this. Another neutralizing epitope on E2 found immunogenic in mice is the epitope I region (residues 408-428). In contrast to epitope III-specific MAbs which differ in their cross-reactivity and neutralization potentials, almost all of the MAbs specific to epitope I isolated to date appears to be broadly neutralizing, including HMAbs HCV1, HC33.1-related MAbs, rat MAb 3-11 and mouse MAbs AP33 and MAb24 (Alhammad *et al.*, 2015a; Broering *et al.*, 2009; Flint *et al.*, 1999a; Keck *et al.*, 2013; Owsianka *et al.*, 2005). This is possibly associated with the high degree of sequence conservation of epitope I, which in turn makes it a desirable specificity for HCV vaccines to generate.

In addition to identifying the immunogenic domains on E2, the characterization of the 18 mouse MAbs also revealed that the antigenic surface of E2 is heavily modulated by the presence of HVRs. In Group I MAbs, which were raised to D123, the presence of HVRs greatly reduced their ability to bind to E2 and inhibit E2-CD81 binding. A >10-fold reduction in E2-CD81 inhibition was also observed in the broadly neutralizing MAb24 (Table 3.1) (Alhammad *et al.*, 2015a). These results indicate that the HVRs play an important role in the modification of antibody epitope exposure and the CD81 binding interface on E2. In the case of the two HVR1-specific MAbs, MAb33 and MAb36, their binding to E2 is influenced by the presence of HVR1 as well as HVR2 and igVR, suggesting a structural link amongst the HVRs, via intermolecular or intramolecular interactions (Table 3.1) (Alhammad *et al.*, 2015a). This corroborates a recent report that an intramolecular interaction amongst the HVRs modulates the binding of E2 monomer to CD81 dimer (McCaffrey *et al.*, 2017). Together, these findings indicate that sequence variations and structural flexibility of the HVRs are major contributing factors in the antigenic heterogeneity of E2.

Table 3.4 Comparison of E2 residues involved in the CD81-LEL binding of E2 with those identified in intracellularly expressed E1E2 or HCVpp (Boo *et al.*, 2012; Drummer *et al.*, 2006; Kong *et al.*, 2013; Owsianka *et al.*, 2006; Rothwangl *et al.*, 2008).

Epitope I	E2 RBD	HCVpp	intracellular E1E2
Q412A	114		
L413A	134		
N415A	93		
N417A	87		
G418A	105		
W420A	0		
W420F	94		
H421A	0		
N423A	128		
S424A	9		
L427A	0		
N430A	9		

Epitope II	E2 RBD	HCVpp	intracellular E1E2
G436A	6		
W437A	0		
W437F	11		
L438A	0		
A439P	8		
A439S	57		
G440A	0		
L441A	0	*	*
F442A	0		
Y443A	0		

Epitope III	E2 RBD	HCVpp	intracellular E1E2
G523A	7		
P525A	74		
P525G	0		
Y527A	0		
W529A	0		
W529F	90		
G530A	0		
D535A	0		
N540A	19		
W549A	30		
W549F	28		

Epitope IV	E2 RBD	HCVpp	intracellular E1E2
Y613A	0		
W616A	0		
W616F	3		

% CD81 binding relative to WT
Not determinded
<25%
25-50%
50-75%
75-100%
>100

* Based on the observation of L441M/V/F mutations

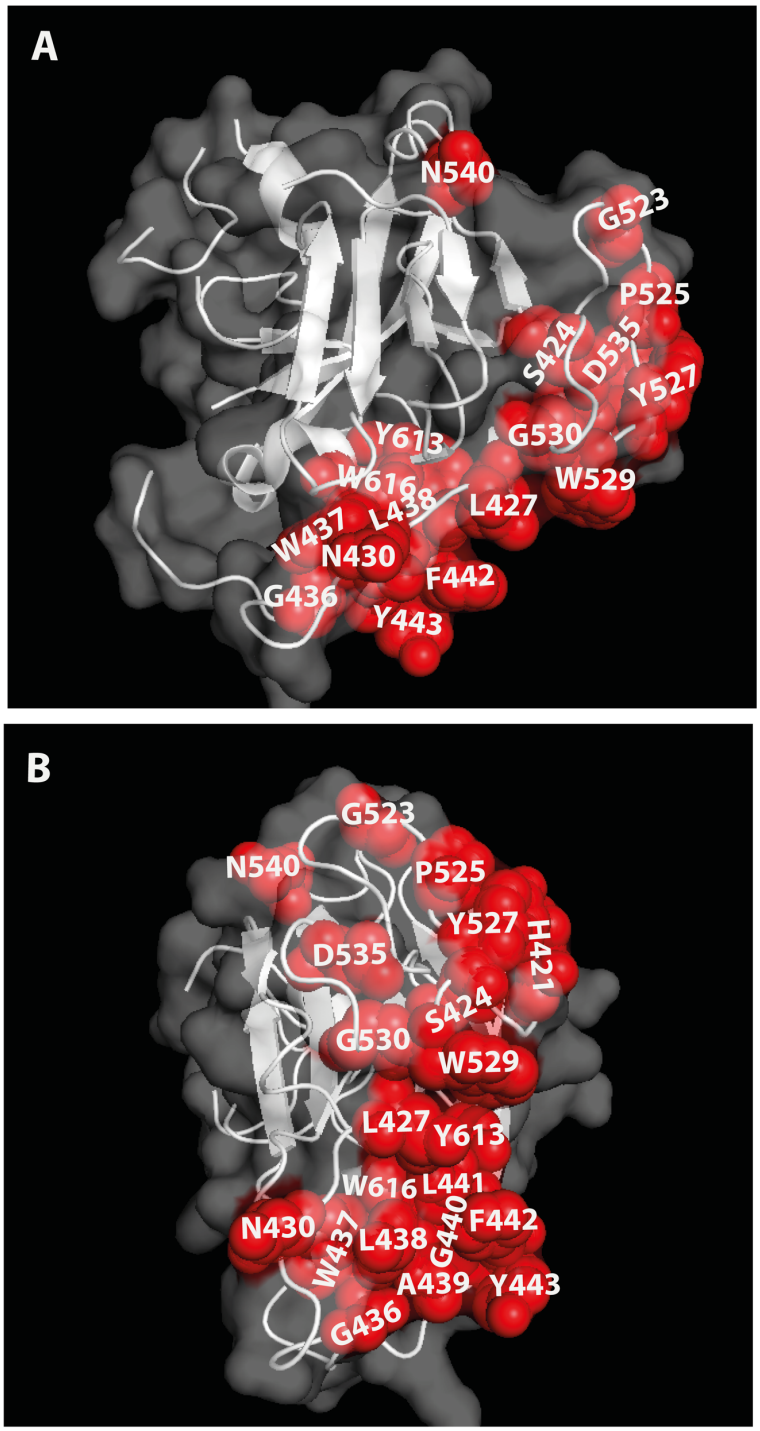

Figure 3.8 The distribution of E2 residues implicated in the binding of E2 RBD protein to the CD81-LEL dimer (Kong *et al.*, 2013). The electron density of AR3C Fab was removed and the CD81 binding residues are depicted as red spheres and shown from different angles (A and B). The CD81 binding residue W420 and the HVR structures are not shown.

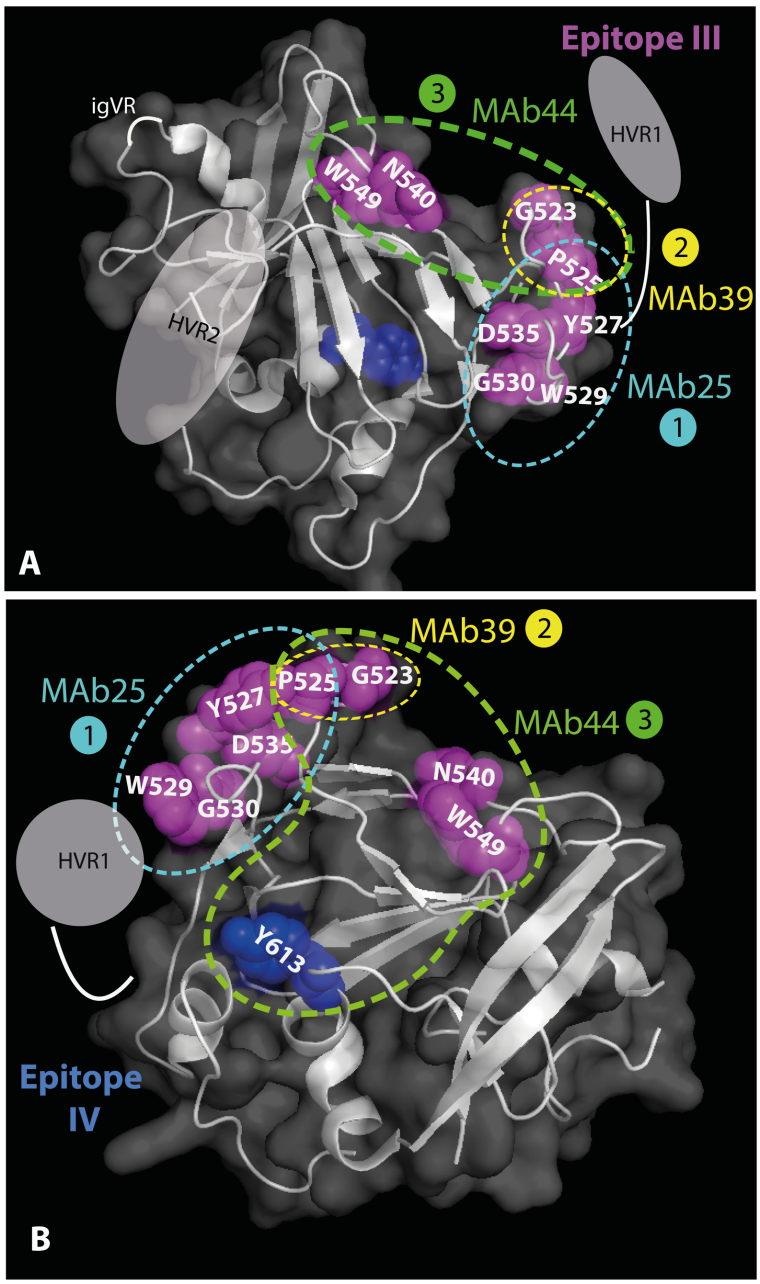

Figure 3.9 Three micro-domains within epitope III. Images were created using the AR3C-bound E2 core structure (Kong *et al.*, 2013). The electron density of AR3C is removed and the surface and cartoon structure of the E2 core protein is shown at two different angles, the neutralizing face (A) and the non-neutrlaizing face (B). Micro-domain 1 involves residues P525, Y527, W529, G530 and D535 which are found in the CD81 binding loop. Micro-domain 2 includes residues G525 and P525 that are located at the N-terminal end of the CD81 binding loop. Micro-domain 3 involves residues G523 and P525 found on the CD81 binding loop as well as residues N540, W549 and Y613 on the central sandwich. The predicted location of HVR1 is shown and not to scale.

To further explore the hypothesis that the presence of three HVRs modulate the antigenic surface and may therefore be involved in the masking of the underlying neutralizing epitopes on E2, immunizations were performed in guinea pigs with nickel-affinity purified forms of WT E2 and D123 in the presence of ISCOMATRIX adjuvant. These affinity-purified forms of E2 contains a complex mixture of different glycoforms, monomeric and oligomeric forms of WT E2 and D123 proteins. The deletion of HVRs greatly enhanced the immunogenicity of at least two continuous brNAb regions (aa408-428 and 530-549) within E2. This is also evident in antibody responses to the 408-428 region elicited by WT E2 HMW1 and D123 HMW1. Whilst both HMW1 forms elicited similar titres of antibodies that compete with HMAb HCV1 (epitope: 408-428) for E2 binding, there is ~20-fold difference in the antibody titres to the 408-428 region between WT E2 HMW1 (geometric mean 200) and D123 HMW1 immune sera (geometric mean 4000). These data indicate that the inhibition of HCV1 by D123 HMW1 sera is driven by antibodies directed to the 408-428 region whereas HCV1 inhibition by WT E2 HMW1 sera is possibly associated with the presence of HVR1-specific antibodies, which has been shown to interfere with epitope I specific antibody binding to E2 (Keck *et al.*, 2016).

The NAb epitope region 430-451 displays relatively high sequence variability (68% identity and 77% conservation between G1a, H77c and G2a, J6), compared to the 408-428 (81% identity and 90% conservation) and 523-549 sequences (78% identity and 89% conservation), and this may contribute to the observed low levels of cross-reactive antibodies to this region in all of the immune groups examined in this study. Alternatively, it is also possible that in immunized animals, cross reactive antibodies generated to this region are mostly conformation-dependent, like HMAb HC84.20 from the HC84 series, and cannot therefore be detected by the peptide assays used in this study. Corroborating the low titres of peptide 430-451-specific antibodies observed across all immune groups, HMAb competition assays performed by Vietheer *et al* showed that antibodies that are able to compete with HC84.27 (epitope II 430-451) are infrequently elicited, or elicited at low levels in animals receiving WT E2 HMW1, WT E2 monomer, D123 HMW1 or D123 monomer (Table 3.3), although one animal from the D123 HMW1 group appeared to have moderate level of such antibodies (Vietheer *et al.*, 2017). These findings indicate that

vaccination with E2 RBD-based immunogens may generate low titres of antibodies towards the 430-451 region.

The oligomerization status of both WT E2 and D123 markedly influences the specificity of the antibody response. Whilst monomeric E2 has long been considered as the functional subunit that mediates HCV-CD81 interaction during entry, given its high affinity to CD81, the HMWs are thought to be non-functional aggregates (Michalak *et al.*, 1997; Roccasecca *et al.*, 2003). Vietheer *et al* (2017) found that in WT E2 and D123 HMWs, the epitopes of several NAbs, such as the AR3C-related HMAbs, are occluded, and that the structures of the 424-428 and 630-635 regions have distinct conformations in different WT E2 and D123 oligomers. Immunogenicity studies showed that despite an occluded NAb face and reduced affinity for CD81, HMW forms of WT E2 and D123 elicit more favourable antibody specificities than their monomeric counterparts. In the case of D123, high titres of antibodies to all three NAb epitopes 408-428, 430-451 and 523-549 were observed in the HMW groups, correlating with the ability of immune sera to neutralize homologous (430-451, $r=0.7898$, $p<0.0001$) or heterologous viruses *in vitro* (408-428, $r=0.6956$, $p<0.0001$; 523-549, $r=0.6570$, $p<0.0001$) (Vietheer *et al.*, 2017). Consistent with this, higher titres of antibodies that compete with the neutralizing HMAbs HCV1 and AR3C were found in D123 HMW1 immune sera compared to immune sera generated by vaccination with monomeric D123. By contrast, the antibody responses generated by E2 monomers predominantly target the non-neutralizing 630-635 region. Together, these results showed that the intermolecular disulfide bonding between E2 monomers alters the exposure of NAb and non-NAb epitopes on E2 and thereby alters the specificity of the immune response generated through vaccination.

Whilst the exact antigenic structures of E2 HMWs remains unclear, it is well established that monomeric E2 exhibits substantial structural flexibilities. Except for the central ß sandwich (residues 492-566) and the large ß sheet (residues 621-643) at the back layer, most of the regions on the E2 monomer (~62% of E2 residues) do not have regular secondary structures (Khan *et al.*, 2014; Kong *et al.*, 2013). The front neutralizing/CD81 binding face in particular, is the most flexible region in the E2

structure with a deuterium exchange rate of >90% at 10s (Kong *et al.*, 2016). In addition, the NAb epitope region 408-428, adopts at least three different conformations upon antibody recognition (Kong *et al.*, 2012b; Li *et al.*, 2015a; Meola *et al.*, 2015; Potter *et al.*, 2012). This structural flexibility of the neutralizing face of E2 may therefore limit the immunogenicity of NAb epitopes on monomeric E2, and antibody responses are more likely to be generated towards the structurally stable but non-neutralizing components on monomeric E2, such as the 621-643 region at the back layer. This may contribute to the high titres of CBH-4B (epitope residues 630-635)-competing antibodies observed in animals immunized with E2 monomers (Vietheer *et al.*, 2017). Compared to E2 monomers, the neutralizing face of E2 HMW species is likely to be more stable due to structural constraints within the oligomers, and this may be associated with the enhanced productions of NAb specificity. Whilst the stabilization of the neutralizing face does not drastically change NAb epitope conformation, limited structural flexibility at the overlapping CD81 binding sites may prevent the full engagement of E2 from its high-affinity interaction with CD81. This may explain the lower levels of binding to CD81 observed with increasing E2 valency.

In conclusion, the ability of D123 HMWs to elicit a strong cross-reactive antibody response towards multiple NAb regions on E2 is unprecedented. Correlated with the induction of a poly-specific antibody response, antibodies generated by D123 HMWs are capable of potently neutralizing all 7 genotypes of HCV *in vitro*. Whilst the poly-specific NAb response generated by D123 HMW species can greatly minimize the possibility of viral escape in quasispecies challenges, the lack of interfering HVR1 specific antibodies in D123 HMWs immunization may further augment their efficacy *in vivo*. Together, these results show that D123 HMW species are promising candidates for a universal HCV vaccine, and have provided a new direction for the development of E2-based immunogens. Further structural studies on the oligomers and glycoforms of E2 will improve our understanding in the antigenicity of E2 NAb epitopes and greatly benefit the design of E2-based vaccines.

Chapter 4 The escape of HCV from the broadly neutralizing antibody MAb24

4.1 Introduction

A major broadly neutralizing epitope on E2 is the 412-423 region (also known as epitope I or domain E). It contains two conserved CD81 binding residues, W420 and H421, and is essential for HCVcc and HCVpp entry (Boo *et al.*, 2012; Meola *et al.*, 2015; Owsianka *et al.*, 2006). A number of MAbs specific to this region have been isolated from immunized animals including mouse AP33 (Owsianka *et al.*, 2001; Patel *et al.*, 2000; Patel *et al.*, 1999), rat 3/11 (Flint *et al.*, 1999a; Owsianka *et al.*, 2001), human HCV1 (from transgenic mouse with human antibody genes) (Broering *et al.*, 2009), mouse MAb24 (Alhammad *et al.*, 2015a), as well as from HCV-infected individuals such as HMAbs HC33.1, HC33.4 and HC33.8 (Keck *et al.*, 2013). Common to all these MAbs is their ability to inhibit E2-CD81 binding and cross-neutralize diverse strains of HCVcc and HCVpp.

Structural studies of truncated E2 proteins suggested that the 412-423 region exhibits extreme structural flexibility and possibly forms one or more subdomains independent from the remaining portion of the E2 fold (Khan *et al.*, 2014; Kong *et al.*, 2013; Meola *et al.*, 2015). In the AR3C-bound E2 structure, the N-terminal residues 412-419, as well as the two glycans N417 and N423, are completely disordered and are predicted to be located proximal to the neutralizing face of E2 and adjacent to HVR1, which is also absent from the structure (Kong *et al.*, 2013). When complexed with Fabs to this region, the 412-423 peptide adopts at least three distinct conformations: an antiparallel β hairpin (AP33 and HCV1), an extended structure (3/11), and an intermediate between the hairpin and extended structure (HC33.1) (Kong *et al.*, 2012a; Kong *et al.*, 2012b; Li *et al.*, 2015a; Meola *et al.*, 2015; Potter *et al.*, 2012). This structural flexibility has been proposed as an immune evasion strategy by limiting the engagement of B cell receptors, and may contribute to the low immunogenicity of 412-423 region, which has an estimated seroprevalence rate of 2.5-15% in chronic HCV (Keck *et al.*, 2013; Tarr *et al.*, 2007).

In D123-immunized guinea pigs, the 412-428 region is one of the major antibody specificities elicited and positively correlates with the ability of the immune sera to cross neutralize diverse strains of HCVcc *in vitro* (Chapter 3) (Vietheer *et al.*, 2017). However, the exact role of such antibodies towards the control and clearance of HCV quasispecies is not known. Isolated from D123-immunized mice, MAb24 is able to inhibit E2-CD81 binding and is capable of neutralizing HCVpp (G1a) and HCVcc (G2a, G3a, G4a, G5a, G6a and G7a) by >50% *in vitro*, with IC_{50}s between 6µg/mL and 60µg/mL (Alhammad *et al.*, 2015a). Epitope mapping suggested that MAb24 recognizes its epitope within the 412-423 region of E2, with residues L413, N415, G418, W420 and H421 particularly critical for binding (Chapter 3).

This chapter examined the effects of MAb24 on the evolution of HCV quasispecies. HCVcc JC1FLAG2 (G2a, J6/JFH-1) encoding the structural region of the G2a J6 strain, was cultured *in vitro* under the selective pressure of MAb24 IgG. Adaptive mutations associated with MAb24 escape were identified and quantitated using next generation sequencing. In addition, the effect of mutations conferring MAb24 resistance on the overall viral fitness and susceptibility towards neutralization by a panel of well characterized human brNAbs was examined. Lastly, the structural basis of MAb24 engagement with its epitope, the mechanism of neutralization, and escape from neutralization was investigated.

4.2 The dynamic evolution of HCV under the selective pressure of MAb24

4.2.1 The *in vitro* passaging of extracellular HCVcc in the presence of MAb24

To select for MAb24-resistant HCV *in vitro*, extracellular HCVcc was incubated with either 0, 0.245, 0.98 or 9.8μg/mL of MAb24 IgG, which neutralizes 0%, 50%, 70%, and 90% of the starting HCVcc stock, respectively. Mixture of virus and MAb24 were used to infect naïve Huh7.5 monolayers for four hours before removal of the inoculum and replacement with media containing the corresponding MAb24 concentrations. To enable replication of escape mutants, cultures were maintained for four days before the media (containing cell-free HCVcc if present) was passaged onto naïve cells, again in the presence of MAb24. As shown in Figure 4.1A, at Passage 3, only background levels of replication were observed in cultures passaged in the presence of MAb24, with replication levels similar to HCVcc containing the GND mutation in NS5B that renders viral replication incompetent (GND). By contrast, high levels of viral replication were observed in cultures passaged in the absence of MAb24. Viral replication in the presence of MAb24 remained at background levels in all subsequent passages and until the end of the experiment (Passage 7), suggesting that MAb24-resistant HCVcc was not selected by passaging cell free virus in the presence of MAb24.

4.2.2 *In vitro* passaging of extracellular and intracellular HCVcc in the presence of MAb24

To maximize the chance of selecting resistant mutants, both the extracellular and intracellular HCVcc were passaged in the above MAb24 concentrations in a parallel experiment. Both extracellular HCVcc subjected to MAb24 neutralization and intracellular HCVcc-containing infected Huh7.5 cells from the previous passage were added to the naïve Huh7.5 monolayer. This was repeated at 3-day intervals. The HCVcc-producing infected cells were included here to ensure a continued supply of a viable and diverse HCV quasispecies pool, which was hypothesised to help

facilitate the selection of MAb24-resistant variants. In addition, the concentration of MAb24 was increased from Passage 4 onwards to increase the selective pressure.

During the first 12 days of culture, progressively increasing level of viral replication was observed in cultures passaged in the absence of MAb24 and in the presence of low concentrations of MAb24 (0.245 and 0.98μg/mL MAb24). By contrast, only very low levels of replication were detectable during the first 12 days (four passages) of culture in the presence of 9.8μg/mL MAb24, as shown in Figure 4.1B. Significant levels of viral replication in cultures containing 0.245 and 0.98μg/mL MAb24 were maintained throughout the experiment, in spite of a gradual increase in the MAb24 concentration from 2-fold (Passage 4), 5-fold (Passage 5), 10-fold (Passage 6) to 20-fold (Passage 7 and onwards) of the original MAb24 concentration and a decrease in the amount of intracellular HCVcc input from 10% (Passage 0 to Passage 5), to 5% (Passage 6) to 4% (Passage 7 and onwards). In cultures containing a starting concentration of 9.8μg/mL MAb24, viral replication steadily increased between Passage 4 and 9 despite gradually increasing MAb24 concentration to 196μg/mL, 20-fold the IC_{90} used at Passage 0. Neutralization assays performed on Passage 9 media containing the extracellular viral quasispecies confirmed resistance to MAb24 at 10μg/mL whereas the control viruses (cultured without MAb24) remained sensitive to MAb24 neutralization (Figure 4.2A). Entry assays also showed that both quasispecies were able to infect naïve Huh7.5 cells and replicate in the absence of MAb24 (Figure 4.2B). In summary, these results indicate that HCV is able to acquire neutralization resistance in the presence of high concentrations of MAb24 when both infected cells and media containing extracellular virions are passaged providing a large pool of viral quasispecies.

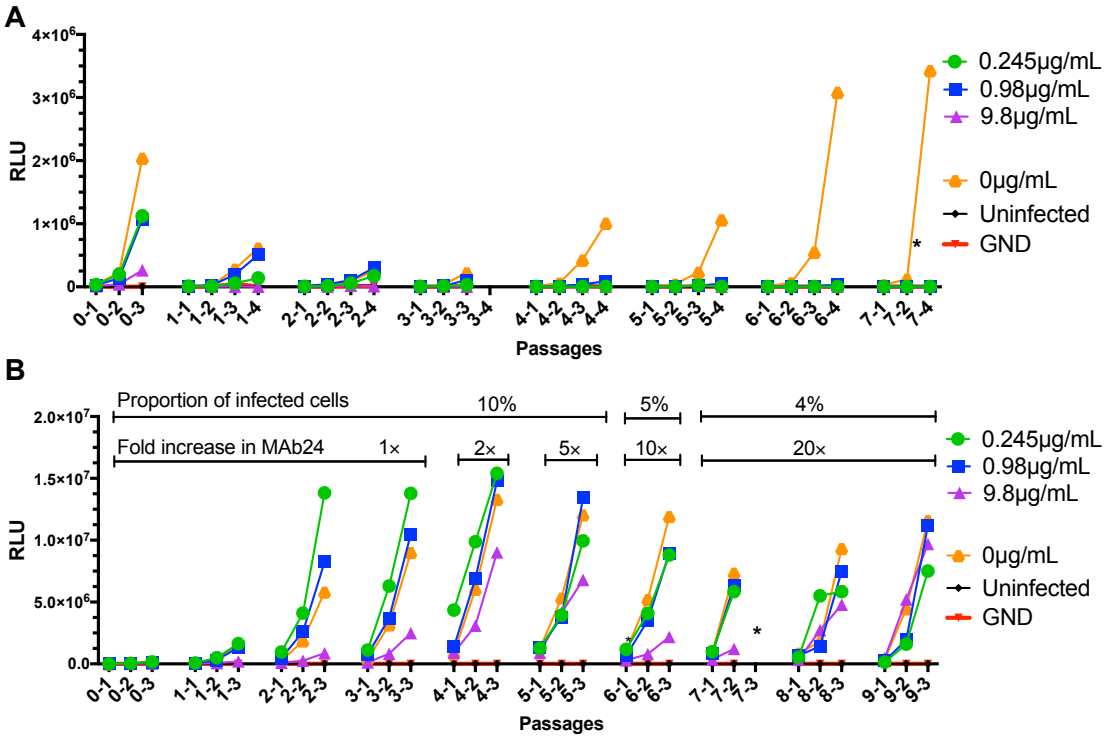

Figure 4.1 The replication of HCV with or without MAb24 *in vitro*. (A) The passaging of extracellular HCVcc under various concentrations of MAb24. HCVcc viruses, harvested from JC1FLAG2 RNA-transfected Huh7.5 cells were incubated with either 0, 0.245, 0.98 or 9.8µg/mL MAb24 IgG before addition to a monolayer of naïve Huh7.5 cells with the corresponding concentration of MAb24 IgG. This was repeated every four days. HCVcc replication was monitored daily by measuring luciferase activity (relative light unit, RLU) with the exception of Passage 7 Day 3 (7-3). (B) The passaging of extracellular and intracellular HCVcc in the presence of MAb24. Each passage contained a fraction of infected cells and culture media containing infectious virus from the previous passage. This was repeated every three days, and viral replication was monitored daily except for Passage 7 Day 3 (7-3). As shown, the MAb24 IgG concentration was gradually increased to 20-fold (Passage 7 and onwards) of the starting concentration. The proportion of infected cells added from the previous passage was reduced from 10% to 4%. The background is provided by the NS5B GND mutation, which renders the virus replication incompetent.

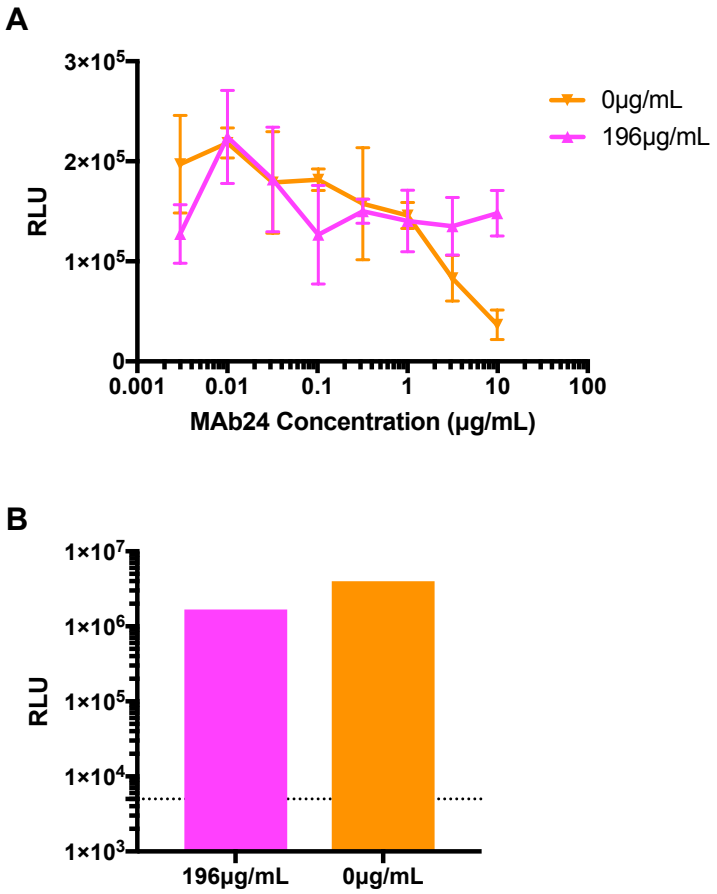

Figure 4.2 Resistance of HCV quasispecies after 30 days of *in vitro* culture in the presence or absence of MAb24. Passage 9 viruses generated using a starting MAb24 concentration of 9.8µg/mL (final concentration 196µg/mL) or 0µg/mL were collected from Figure 4.1B Passage 9 Day 3. (A) The ability of MAb24 to neutralize the Passage 9 viruses. (B) The ability of Passage 9 viruses to infect naïve Huh7.5 cells in the absence of MAb24. Normalized amount of HCVcc was added to the naïve Huh7.5 cell monolayer and infectivity was measured 72 hours later. The background level of viral replication (the GND control) is indicated here as dotted line.

4.3 Characterization of MAb24-resistant HCV quasispecies

To further investigate the evolution of HCV quasispecies under the selective pressure of MAb24 and identify adaptive mutations associated with MAb24 resistance, the HCVcc quasispecies replicated under the highest concentration of MAb24 (9.8-196μg/mL) was selected for further characterization, using both conventional Sanger sequencing and Illumina high throughput sequencing.

4.3.1 Identification of MAb24 resistant mutations

To identify mutations within the E1E2 region of the extracellular HCVcc viruses collected at Passage 4 and Passage 9, RNA was extracted, reverse transcribed into cDNA and cloned. The E1 (residues 191-354, numbering relative to the G1a, H77c strain from here onwards) and the E2 region (residues 419-760) of each clone was sequenced using the Sanger chain termination method and compared with those from the control quasispecies that was cultured without MAb24.

At Passage 4, few adaptive mutations had accumulated in the E1E2 region of cDNA prepared from viruses obtained in the presence or absence of MAb24. Random mutations such as T480A, T435A or N196S/S707T were found in HCVcc replicated with MAb24 whilst variants such as V536A or P250L were observed in the HCVcc passaged without MAb24 (data not shown). However, none of these mutants was identified in more than one clone. By contrast, at Passage 9, two major variants, N415D (~71%) and N417S (~29%), were identified in the MAb24-resistant quasispecies. Neither of these mutations was found in cDNA obtained from virus cultured in the absence of MAb24. No adaptive mutations were found outside the 412-423 region, except for mutations M290T or R521G in resistant quasispecies and T207A or T480S in the control virus (data not shown).

To confirm that the N415D and N417S were genuine stable variants associated with MAb24 resistance, the Passage 9 virus were amplified in naïve Huh7.5 cells and MAb24-free media. The E2 region (residues 384-750) of the resulting quasispecies was sequenced. As shown in Figure 4.3, ~72% of the cDNA

clones carried the N415D mutation whilst ~22% contained N417S. About 30% of the N415D variants also had an additional mutation within the HVR1 region, H386R (referred to as H386R/N415D, occurred in ~22% of total available sequences). None of these mutations was observed in the sequence of viruses passaged in the absence of MAb24. Together, these findings indicated that MAb24 resistance is associated with mutations in its epitope, the 412-423 region, particularly at residues N415 and N417 as well within HVR1 at H386.

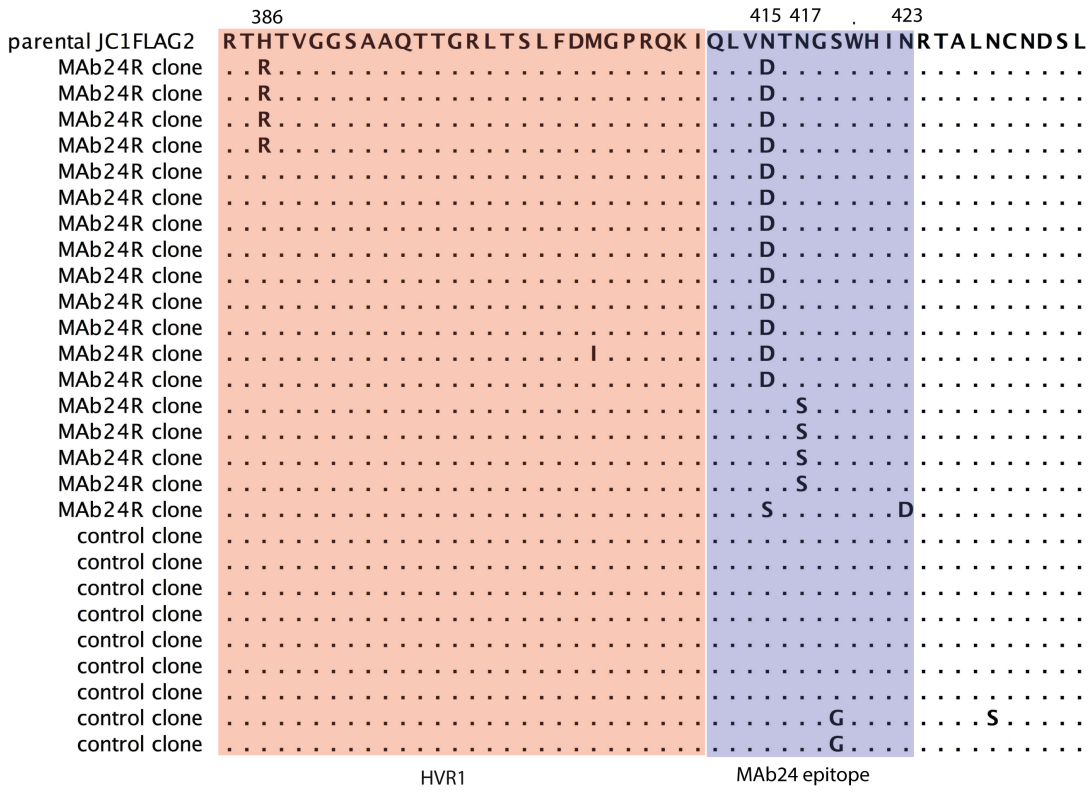

Figure 4.3 Sequencing of cDNA clones obtained from Passage 9 viruses following amplification. Adaptive mutations accumulated in the 384-430 region of the extracellular HCVcc quasispecies are shown here. The parental JC1FLAG2 (G2a, J6) sequence is shown at the top. Clones were isolated from cultures grown in the presence (MAb24R clones) and absence of MAb24 (control clones). Identical amino acids are indicated as dots. Sequences were aligned using CLC Main Workbench v8.

4.3.2 High throughput sequencing analysis of MAb24-resistant quasispecies

To quantitatively determine the frequency of mutations in the 412-423 region, both extracellular and intracellular HCVcc at various time points were analysed using Illumina high throughput sequencing. Viral RNA was isolated from the extracellular HCVcc-containing culture supernatant whilst total RNA was extracted from the cell lysates of infected cells containing intracellular HCVcc. The HCV E2 region (residues 398-548) was then transcribed with barcoded primers and further amplified into cDNA libraries via nested PCR. Transcribed with barcoded primers which contain 8-nucleotide index sequences, each cDNA clone is labeled with a unique barcode tag or Primer ID (PID) (Barnard *et al.*, 2016; Jabara *et al.*, 2011). The total number of unique PID indicates the number of cDNA clones present in each sample prior to cDNA library amplification. This eliminates PCR bias that is associated with over-coverage or resampling of the DNA templates during the amplification process, and therefore accurately determines the diversity of the species in the sample pool. Sequence reads were then generated by Illumina MiSeq sequencer and aligned to their corresponding PIDs and the J6 E2 reference sequence.

At P0, no mutations were detected within the viral population sequenced. However, at P0, due to the low viral load, relatively low coverage was obtained therefore the possibility that very low levels of mutations were present within the viral population cannot be excluded. During the subsequent 30 days of culture, five residue changes (V414, N415, N417, G418 and I422) were observed in the 412-423 region of the extracellular HCV quasispecies cultured with MAb24 over 30 days of culture, as shown in Table 4.1. Whilst mutations at V414, G418 and I422 occurred at very low frequencies (V414A, G418A and I422V, <1%), the population of viruses containing mutations at N415 and N417 increased dramatically over the course of the experiment. Within 6 days (Passage 7 to Passage 9), the percentage of N415 variants in the quasispecies (N415D, N415S, N415T and N415G) increased >1.5 fold. The occurrence of the mutation encoding N415D in particular, increased in frequency from 27.78% at Passage 7 to 79.89% at Passage 9. At position N417, mutations encoding serine were observed at a frequency of 0.33% at Passage 4 which increased to 12.61% at Passage 9. All of the residue changes at V414, N415, N417, G418 and

I422 appeared to be specifically associated with MAb24 resistance, as they were either not modified (V414, G418 and I422) or transiently mutated (N415, N417, occurred <1%, and reverted to WT residue at Passage 9) in virus cultured in the absence of MAb24. Furthermore, the sequencing of intracellular HCVcc at Passage 0 and 3 did not find any traces of N415D and N417S, suggesting that the two major variants emerged at later stages of culture, when MAb24 concentrations were increased 2 to 20-fold. Whilst mutations were identified in the 423-548 region, all either reverted to the WT residue by Passage 9 and/or occurred at extremely low frequency (<0.99%). The exception was L540 (residue numbering relative to H77c, H77c equivalent V538), where a single nucleotide polymorphism (L540P/V/I) was observed in all extracellular and intracellular HCVcc quasispecies collected at Passage 4, 7 and 9, with a frequency of ≤1%. In summary, high throughput sequencing analyses of HCVcc quasispecies showed that MAb24 resistance is associated with the acquisition of N415D and N417S mutations in the MAb24 epitope region.

Table 4.1 Frequency of adaptive mutations in the 412-423 region of the extracellular and intracellular HCV quasispecies replicated with or without MAb24 at selected passages.

		Frequency of mutations within the 412-423 region[1]					Total Unique PID
		V414	N415	N417	G418	I422	
Extracellular HCVcc (MAb24)	P0	V(100%)	N (100%)	N (100%)	G (100%)	I (100%)	26
	P4	V(100%)	N (100%)	N (99.67%), **S (0.33%)**	G (100%)	I (100%)	605
	P7	V(99.16%), **A(0.84%)**	N (70.96%), **D (27.78%), S (1%), T (0.17%), G (0.08%)**	N (98.33%), **S (1.67%)**	G (99.33%), **A (0.59%)**	I (100%)	1195
	P9	V(99.61%), **A(0.39%)**	**D (79.89%),** N (16.43%), **S (3.29%), T (0.26%), G (0.13%)**	N (87.39%), **S (12.61%)**	G (99.61%), **A (0.39%)**	I (99.74%), **V (0.26%)**	761
Extracellular HCVcc (no MAb24)	P0	V(100%)	N (100%)	N (100%)	G (100%)	I (100%)	74
	P4		N (100%)	N (99.53%), **S (0.47%)**			644
	P7		N (99.56%), **T (0.22%), D (0.22%)**	N (99.35%), **S (0.65%)**			1379
	P9		N (100%)	N (100%)			1932
Intracellular HCVcc (MAb24)	P0	V(100%)	N (100%)	N (100%)	G (100%)	I (100%)	470
	P3		N (100%)				1126
Intracellular HCVcc (no MAb24)	P0		N (100%)				92
	P3		N (99.59%), **S (0.41%)**				1696

[1]Pairwise alignment and single nucleotide polymorphism (SNP) report was generated by Dr Abha Chopra and Associate Professor Silvana Gaudieri (Murdoch University, Perth, WA, Australia) using VGAS software. The sequence reads are trimmed here to the region of interest, residues 412-423.

Grey: no change; Residue changes are in bold.

The medium number of PID is 331.

4.4 Characterization of HCVcc viruses with MAb24 resistant mutations

4.4.1 The infectivity of MAb24-resistant HCVcc mutants

To examine the effects of MAb24 escape on viral fitness, the three main resistant mutations identified in the previous sections, N415D, N417S and H386R/N415D, were introduced into the parental WT virus (HCVcc G2a J6). The replication kinetics and infectivity of each mutant were compared with the WT virus. In naïve Huh7.5 cells transfected with viral RNA, the three mutant viruses exhibited similar replication kinetics at 24, 48 and 72 hours post-transfection, all at levels identical to the WT virus (Figure 4.4A). When cell-free virions produced from transfection of RNA were normalized with luciferase activities and inoculated onto naïve Huh7.5 cells, modest differences in viral replication patterns were observed (Figure 4.4B). Whilst the H386R/N415D virus replicated at similar levels to the WT virus, viruses encoding N415D showed lower levels of replication at both 48 and 72 hours post-infection. This suggests that the N415D mutation may be associated with a reduction in viral fitness and the acquisition of an additional H386R mutation restores the infectivity of the N415D virus to WT levels. By contrast, the N417S mutant appeared to have slightly increased levels of replication compared to the WT virus, 48-72 hours post-infection.

The differences in infectivity of the N415D and N417S mutants were further characterized using a focus forming assay. Naïve Huh7.5 cells were infected with each virus and after 24, 48 and 72 hours, cell monolayers were fixed and stained to visualize foci of infection using immunofluorescence. The total number of NS5A-positive foci and the size of each infection focus were counted. As shown in Figure 4.4C, all three viruses produced <20 foci of infection after 24 hours of infection. At 48 and 72 hours post-infection, the WT and N415D viruses resulted in a similar number of foci whereas the total number of foci formed by the N417S mutant was significantly higher. At 72 hours post-infection, the total number of positive foci in N417S was ~3-fold higher than that of WT and N415D and more foci with a greater number of nuclei (>2-nuclei per foci) were observed in cultures infected with the

N417S virus. Consistent results were obtained in two independent foci forming assays, which correlates with the viral replication kinetics discussed above (Figure 4.4B). In summary, these findings showed that the acquisition of MAb24 resistance mutations, N415D, H386R/N415D and N417S, does not compromise viral fitness, and in the case of N417S, it may modestly enhance viral fitness.

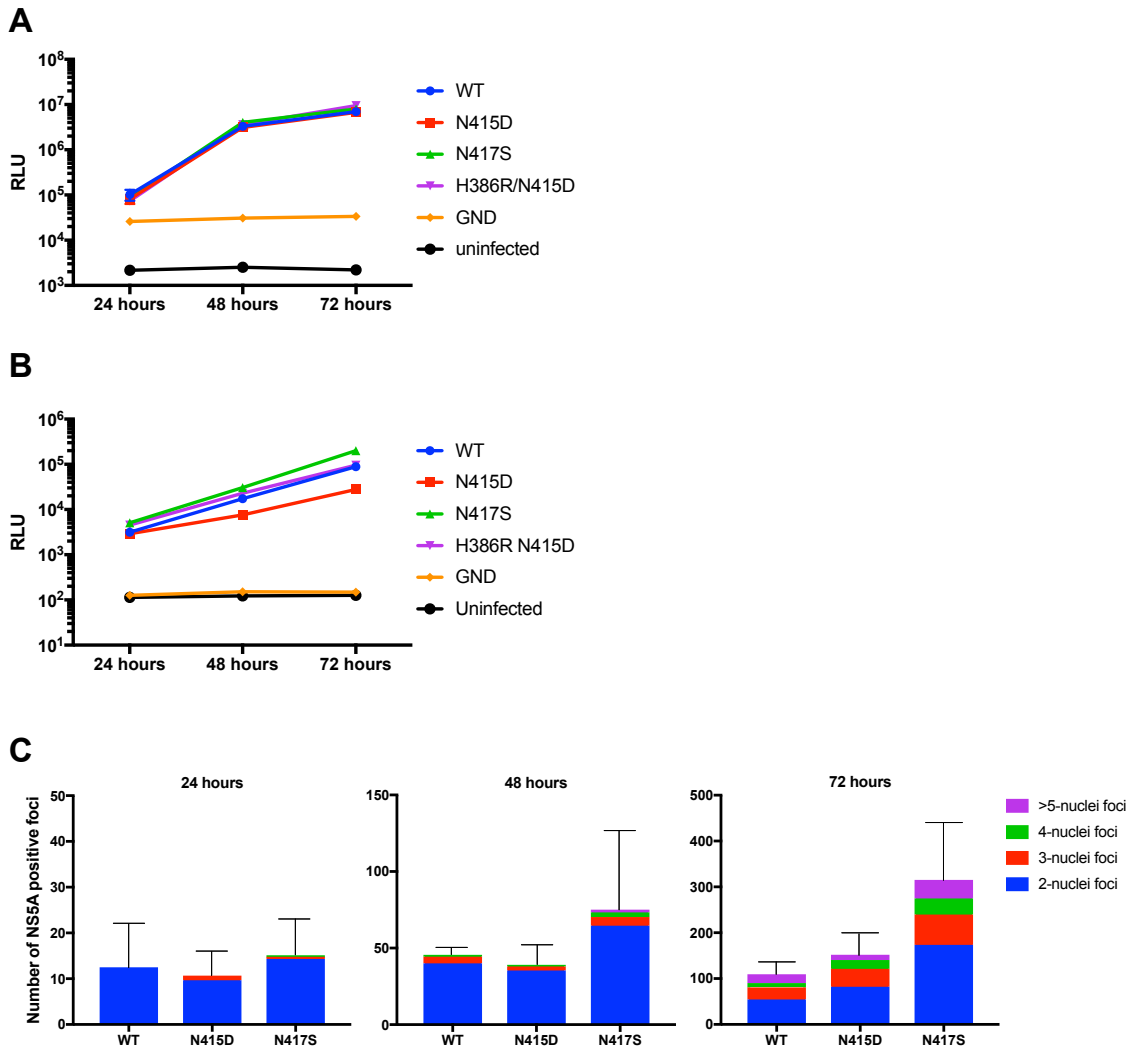

Figure 4.4 Characterization of HCVcc with N415D, N417S or H386R/N415D mutations. (A) The replication kinetics of HCVcc mutants in naïve Huh7.5 cells transfected with viral RNA. *Renilla* luciferase activity (RLU) in the cell culture supernatant was measured at 24, 48 and 72 hours post-transfection. Assays were performed in triplicate and the data shown here is representative of three independent experiments. (B) The infectivity and replication kinetics of HCVcc mutants in naïve Huh7.5 cells. Normalized quantities of virions were added to naïve Huh7.5 cells for 4 hours before replacement with fresh culture media. Viral replication was monitored at 24, 48 and 72 hours post-infection as RLU in the cell culture supernatant. Assay was performed in triplicate and results are representative of three independent assays. (C) The formation of foci by HCVcc mutants. Normalized quantities of each virus was added to naïve Huh7.5 cells for 4 hours before replacement with fresh culture media. After 24, 48 and 72 hours of infection, the number of foci and the number of nuclei in each focus was detected and measured using an anti-NS5A antibody followed by immunofluorescence. Error bars represent the SD of the total number of NS5A-positive foci. Assays were performed in triplicate and results are representative of two independent assays.

4.4.2 The sensitivity of MAb24-resistant mutants towards broadly neutralizing antibodies

To determine the effect of each MAb24-associated resistance mutation on viral susceptibility to neutralizing antibodies, JC1FLAG2 viruses containing either N415D, N417S or H386R/N415D viruses were subjected to neutralization using a series of well-characterized brNAbs, as shown in Table 4.2. As expected, all three mutant viruses were resistant to neutralization by MAb24 with an IC_{50} >100μg/mL whereas the WT virus remained sensitive to MAb24 neutralization (IC_{50}: 9.77μg/mL). A similar pattern of resistance was also observed using human brNAb HCV1 targeting the same 412-423 region. By contrast, the acquisition of MAb24-resistance mutations appeared to render the virus 2 to 5-fold more sensitive to neutralization by HC33.1, a human brNAb specific to the same region that recognizes its epitope in a different conformation to that of HCV1 (Kong *et al.*, 2012b; Li *et al.*, 2015a). These results suggest that the N415D, N417S and H386R/N415D mutations are associated with increased resistance to brNAbs to the 412-423 region, MAb24 and HCV1, but not HC33.1.

The effect of the MAb24-associated resistance mutations on neutralization by NAbs targeting other regions within E2 or the E1E2 heterodimer was also investigated. As shown in Table 4.2, compared to the WT virus, the three mutants exhibited significantly increased sensitivity, to almost all human brNAbs tested, except for N417S to CBH-7 and N415D to AR5A. A >5-fold reduction in IC_{50} was observed in human brNAbs targeting the neutralizing face of E2, including AR3C, HC84.1 and HC84.27. Together, these findings suggest that MAb24-associated resistance mutations, N415D, N417S and H386R/N415D result in increased viral sensitivity to brNAbs targeting other regions of E2 and E1E2.

Table 4.2 The sensitivity of HCVcc mutants, N415D, N417S and H386R/N415D to known human broadly neutralizing antibodies (Gu *et al.*, 2018).

			WT IC_{50} (μg/mL)	Fold change in IC_{50} relative to WT IC_{50}		
				N415D	**N417S**	**H386R/ N415D**
E2	**epitope I (412-423)**	**MAb24**	9.77	>10 ***	>10***	>10***
		HCV1	1.38	>15 ***	>15***	>15***
		HC33.1	1.86	0.19***	0.31***	0.49***
	Domain D (434-446)	**HC84.1**	0.04	0.10***	0.07***	0.09***
		HC84.27	0.12	0.07***	0.10***	0.04***
	AR3	**AR3C**	0.003	0.15***	0.14***	0.17***
	Domain B	**CBH-2**	0.03	0.16***	0.20***	0.16***
		CBH-5	0.04	0.13***	0.20***	0.10***
	Domain C	**CBH-7**	14.79	0.39**	0.56NS	0.39***
	E1E2 heterodimer	**AR4A**	0.14	0.45***	0.45***	0.71**
		AR5A	0.30	0.69NS	0.44**	0.26***

Neutralization curves and IC_{50}s were generated and calculated by Ms Irene Boo and A/P Heidi Drummer from the mean of at least three experiments using the log inhibitor versus normalized response curve in Prism v7.0 (*** $p<0.001$, ** $p<0.01$, NS $p>0.05$).

4.5 The crystal structure of MAb24 in complex with the 412-423 peptide

To elucidate the mechanism of MAb24 neutralization and resistance at molecular levels, the antigen-binding fragment of MAb24 (MAb24) was cleaved from the immunoglobulin using immobilized papain and the structure of MAb24 and the 412-423 peptide complex was solved at 1.4Å resolution (Gu *et al.*, 2018). As shown in Figure 4.5A and B, the 412-423 peptide (Q^{412}LINTNGSWHVN^{442}) adopts a compact anti-parallel β hairpin conformation and sits in the paratope surface of MAb24, in parallel with the interface between the heavy and light chain complementarity determining regions (CDRs).

The electron density of all peptide residues except for the two terminal residues Q412 and N423 were solved. A total of 8 pairs of intramolecular hydrogen bonds were found within the MAb24-bound peptide, providing structural stability to the β hairpin (PDB: 5VXR, Figure 4.6A and Table 4.3). While the 2 hydrogen bonds between I414 and H421 are responsible for stapling the two strands together, the hydrogen bond pairs, T416-S419 (3 hydrogen bonds) and N415-G418 (1 hydrogen bond), further stabilize the peptide conformation at the base of the β turn. Peptide residues, L413, N415, G418 and W420 form strong hydrogen bonds (6 pairs, bond distance of ≤2.0 Å) with the MAb24 paratope (CDR-H1, H2, H3 or L1), and extensive van der Waals interaction can be observed between all peptide residues except for T416 and N417, and MAb24 CDRs (L1, L3, H2 and H3) (Figure 4.6B and Table 4.4).

The β hairpin structure adopted by the MAb24-bound peptide showed almost identical conformation to those complexed with the Fab of AP33 (PDB: 4GAG) and HCV1 (PDB: 4DGY, C2 form), with the all-atom root mean square deviations (rmsd) of 1.26Å and 1.45Å respectively (Figure 4.7A) (Kong *et al.*, 2012a; Potter *et al.*, 2012). All three hairpin structures appeared to have two common intramolecular hydrogen bond pairings, I414-H421 and N415-G418, highlighting the importance of the four residues in the formation and/or stabilization of the hairpin structure of the 412-423 region formed with MAb24 (Table 4.3). By contrast, the conformation of the

412-423 region bound to MAb24 is distinctively different from the extended structures formed by peptides spanning the same region in complex with MAb 3/11 (PDB: 4WHY) and HC33.1 (PDB: 4XVJ) (Figure 4.7B and C) (Li *et al.*, 2015a; Meola *et al.*, 2015). No common overlaying residues were observed between 3/11 and MAb24-bound peptide structures whilst the epitope structures in MAb24 and HC33.1 share a similar β turn-like micro-motif (T^{416}NGSW).

Despite similar conformation of the MAb-bound peptide structure observed for MAb24, AP33 and HCV1, the angles of approach of these three MAbs differ (Figure 4.8). In MAb24 and AP33 paratope surfaces, the peptides are found in alignment with the interface between the heavy and light chain CDRs, whereas the peptide in HCV1 structure spans across the paratope interface. Compared to HCV1 which primarily forms intermolecular hydrogen bonds with the peptide via its CDR-H2 and CDR-L3, AP33 and MAb24 utilise all three CDR-Hs as well as CDR-L3 to interact with the peptide, although the same peptide residues (L413, N415, G418 and W420) are involved in the Fab-peptide interaction in all three structures (Table 4.4). Together, these results show that MAb24 is structurally most similar to AP33, in epitope conformation, paratope surface as well as angle of approach.

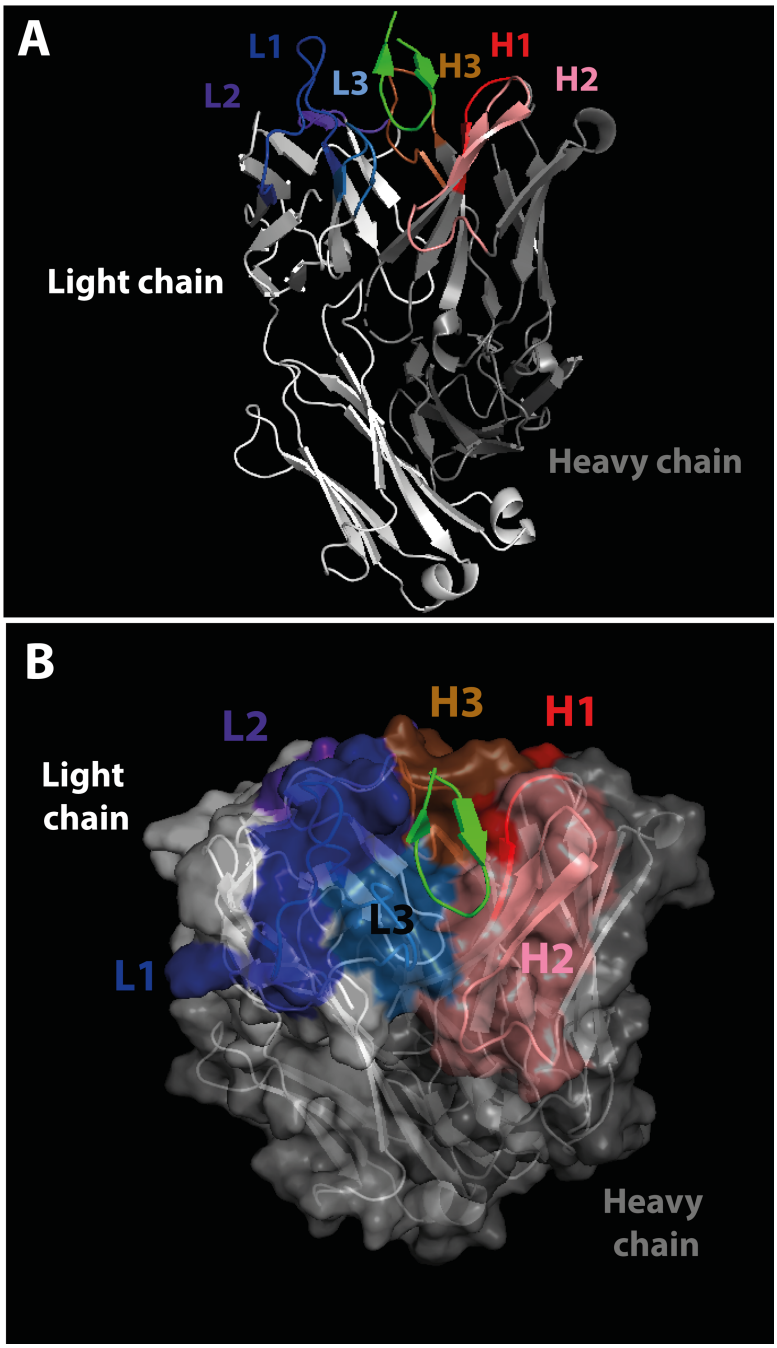

Figure 4.5 Crystal structure of MAb24 in complex with the 412-423 peptide (PDB: 5VXR). (A) Cartoon representation of MAb24 complexed with the 412-423 peptide. The 412-423 peptide is highlighted in green. The light and heavy chains of MAb24 are highlighted in white and dark grey, respectively. The CDR-H1, H2, H3 and L1, L2, L3 of MAb24 are shown as red, pink, orange, dark blue, purple and light blue respectively. The same colour schemes are used throughout. (B) Paratope surface of MAb24 when bound to the 412-423 peptide.

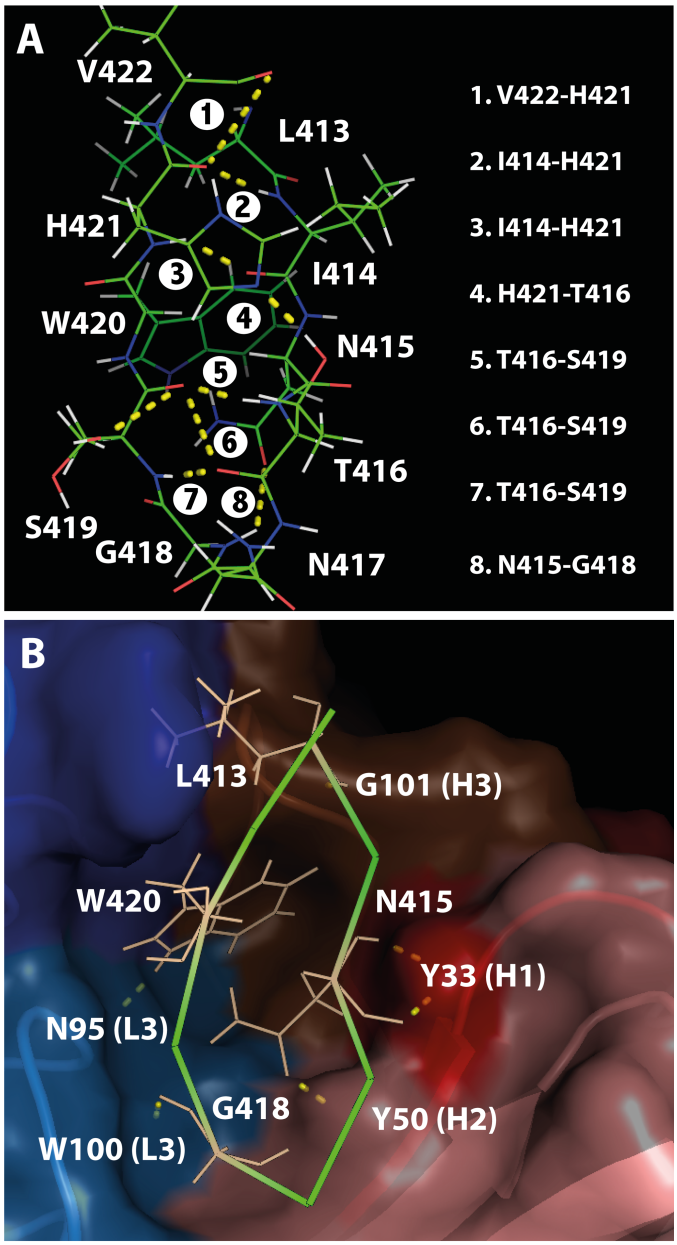

Figure 4.6 Hydrogen bond pairing in the MAb24-peptide complex. (A) The intramolecular hydrogen bonding in the 412-423 peptide when complexed with MAb24. A total of 8 hydrogen pairs are identified by PyMOL and indicated here as yellow dotted lines. The strength or distance of each hydrogen pair is shown on the right. A 9th hydrogen bond was also identified within the Ser419 residue and is shown but not numbered here. (B) The intermolecular hydrogen bonding between the 412-423 peptide and MAb24. The 412-423 peptide is shown as green ribbon. Residues L413, N415, G418 and W420 (as line representation in wheat colour) are involved in the formation of hydrogen bonds with residues from the CDR-H1 (H1), CDR-H2 (H2), CDR-H3 (H3) and CDR-L3 (L3) of the MAb24. A total of 6 hydrogen pairs (distance ≤2.0 Å) were identified using PyMOL and indicated as yellow dotted lines.

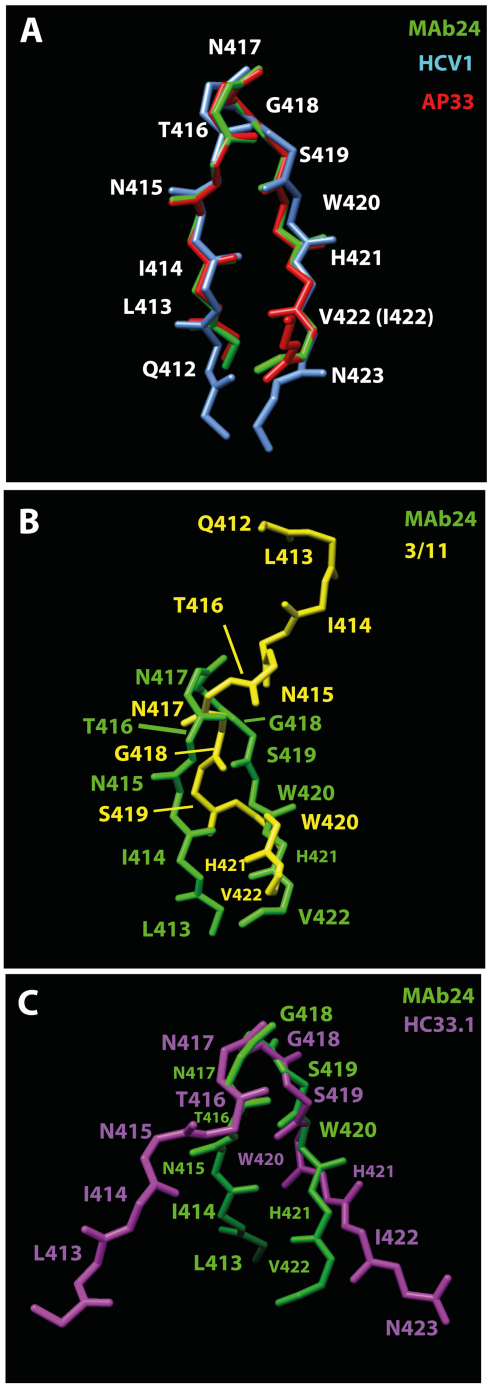

Figure 4.7 The structural flexibility of the 412-423 region. (A) Overlay of the 412-423 conformations when complexed with MAb24 (green, PDB: 5VXR), AP33 (red, PDB: 4GAG) and HCV1 (cyan, PDB: 4DGY, C2 form). (B) Overlay of the 412-423 structures when bound to MAb24 and 3/11 (yellow, PDB: 4WHY). (C) Overlay of the 412-423 structures when complexed with MAb24 and HC33.1 (magenta, PDB: 4XVJ). Structural overlay is generated using UCSF Chimera software (www.rbvi.ucsf.edu/chimera) with Needleman-Wunsch algorithm and MAb24 as the reference structure. Only the peptide backbone is shown here and the electrodensity of the Fab or scFv of each antibody has been removed. In the HCV1 and HC33.1-bound peptide, I422 replaces V422.

Table 4.3 The intramolecular hydrogen bond pairs in the 412-423 peptide when complexed with MAb24, AP33 or HCV1[1].

MAb24	AP33	HCV1
V422-H421 (3.4Å)		
I414-H421 (2.0Å)	I414-H421 (2.8Å)	I414-H421 (2.7Å)
I414-H421 (2.0Å)	I414-H421 (2.9Å)	I414-H421 (2.9Å)
H421-T416 (1.9Å)	H421-S419 (2.8Å)	
T416-S419 (1.9Å)	T416-S419 (1.9Å)	T416-H421 (2.9Å)
T416-S419 (3.3Å)	T416-S419 (1.9Å)	T416-H421 (2.9Å)
T416-S419 (2.1Å)	T416-S419 (1.9Å)	T416-H421 (2.9Å)
N415-G418 (2.4Å)	N415-G418 (3.1Å)	N415-G418 (3Å)

[1]The intramolecular hydrogen bonds and their distance (Å) were determined using PyMOL. Intra-residue hydrogen bonds are not shown. Hydrogen bond pairs common to all three Fabs are highlighted in orange. Hydrogen bond pairs common between MAb24 and AP33 are highlighted in blue. The C2 crystal form of HCV1-petide complex (PDB: 4DGY) was used for hydrogen bond calculation.

Table 4.4 The intermolecular hydrogen bond pairs between the 412-423 peptide and MAb24 or AP33 or HCV1[1].

Residue	MAb24	AP33	HCV1
Q412			
L413	G101 (H3)	Y99 (H3)	N56 (H2) Y58 (H2)
I414			
N415	Y33 (H1) Y50 (H2)	Y33 (H1) Y50 (H2)	Y58 (H2)
T416			
N417			
G418	W100 (L3)	W96 (L3)	W95 (L3)
S419			
W420	N95 (L3)	N91 (L3) N92 (L3)	W95 (L3)
H421			
I/V422		Y28 (L1)	
N423			

[1]Hydrogen bonding pairs were determined using PyMOL. The C2 crystal form of HCV1-petide complex (PDB: 4DGY) was used for hydrogen bond calculation.

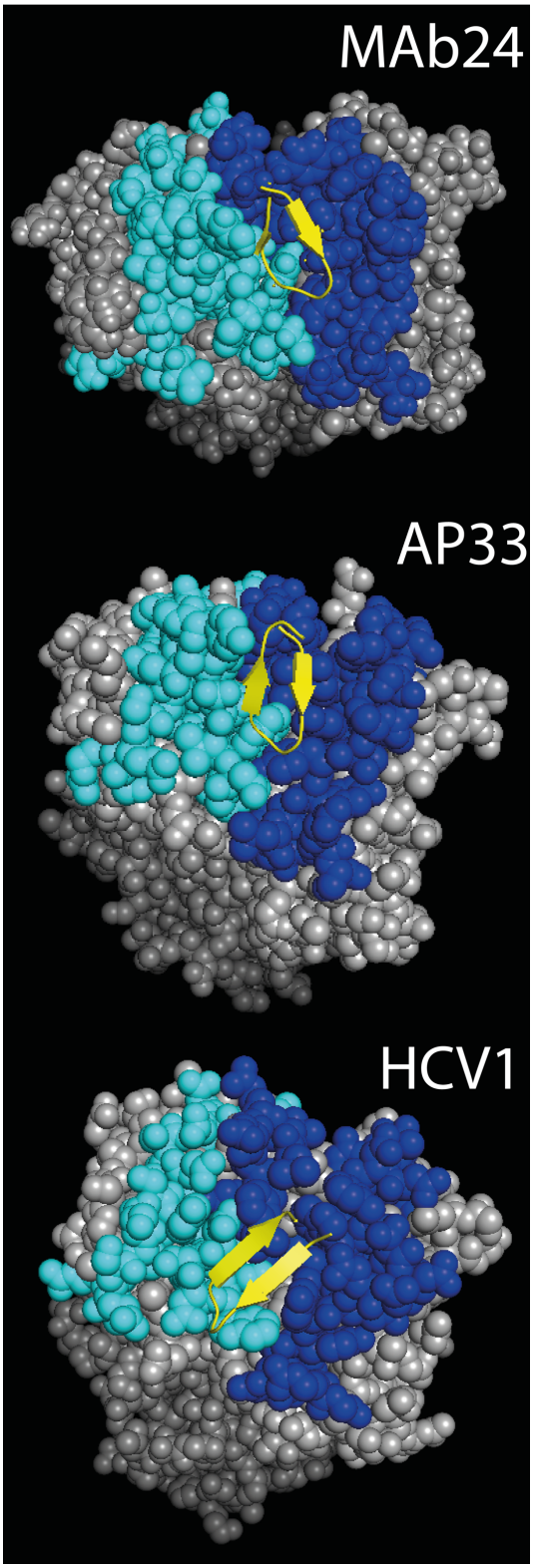

Figure 4.8 The paratope orientation of the 412-423 peptide when bound to MAb24, AP33 and HCV1. The peptide is shown as yellow stick. The CDRs of the heavy and light chains were highlighted in dark blue and light blue, respectively. Images were generated using PyMOL.

4.6 The structural basis of MAb24 neutralization and resistance

One of the major features of the 412-423 region is the presence of two CD81 binding residues, W420 and H421 at its C-terminus. In the MAb24-peptide complex, W420 forms a hydrogen bond with MAb24 residue N95 (CDR-L3, Figure 4.6B and Table 4.4), with its hydrophobic side chain entirely buried in the paratope (Figure 4.9B and C), while H421 is involved in the intramolecular hydrogen bonding with the N-terminal peptide residue I414 and T416, stabilizing the peptide hairpin (Table 4.3). Therefore, when bound to MAb24, W420 and H421 are inaccessible and/or unfavorable for the interaction with host cell coreceptor CD81, creating the site of neutralization.

Resistance to MAb24 is found to be associated with two key mutations, N415D and N417S (Section 4.3 and 4.4). As an integral part of the MAb24-peptide complex, N415 is buried deep in the paratope and forms both intramolecular and intermolecular hydrogen bonds within the complex (intramolecular: 1 hydrogen bond with G418; intermolecular: 3 hydrogen bonds with CDR-H1 and CDRH2, as shown in Table 4.3, Table 4.4, and Figure 4.6). A change from an Asn which contains a polar uncharged side chain to an Asp residue which contains a negatively charged side chain at position 415 (N415D) would therefore disrupt one or more of these hydrogen bonds and also create electrostatic repulsion between the peptide and the largely electronegative paratope surface (Figure 4.9B). The mutation N417S abolishes the glycosylation site at position 417, and creates a glycosylation site at position 415, resulting in a glycan shift from N417 to N415. The addition of a glycan at 415, results in steric hindrance between the peptide and paratope thereby blocking the ability of MAb24 to interact with its epitope.

In comparison, the N415-paratope interaction in HC33.1 is drastically different. The N415 residue does not play a major part in the interaction between HC33.1 and its epitope, forming only one hydrogen bond with other atoms in the structure: with the adjacent peptide residue N417 (Li *et al.*, 2015a). In addition, in the HC33.1-bound peptide, N415 is distant from the two CD81 binding residues W420 and H421

or the site of neutralization. While the C-terminus of the peptide including W420 and H421 is buried in the electropositive pocket of the heavy chain, the N-terminal strand of the peptide including N415 is found on the groove between the light and heavy chain of HC33.1, which is mostly electronegative (Figure 4.9). Thus, modification of residue N415 does not have the same effect on the HC33.1-peptide interaction as observed with MAb24. In the case of N417S, the glycan shift to N415 appeared to re-locate the bulky oligosaccharide such that it is positioned further away from the site of neutralization located at W420 and H421. Together, the drastic difference in the mechanism of neutralization employed by HC33.1 and MAb24 via N415-paratope interaction explains the observed sensitivity of MAb24-resistant viruses containing the N415D and N417S mutations to HC33.1 neutralization.

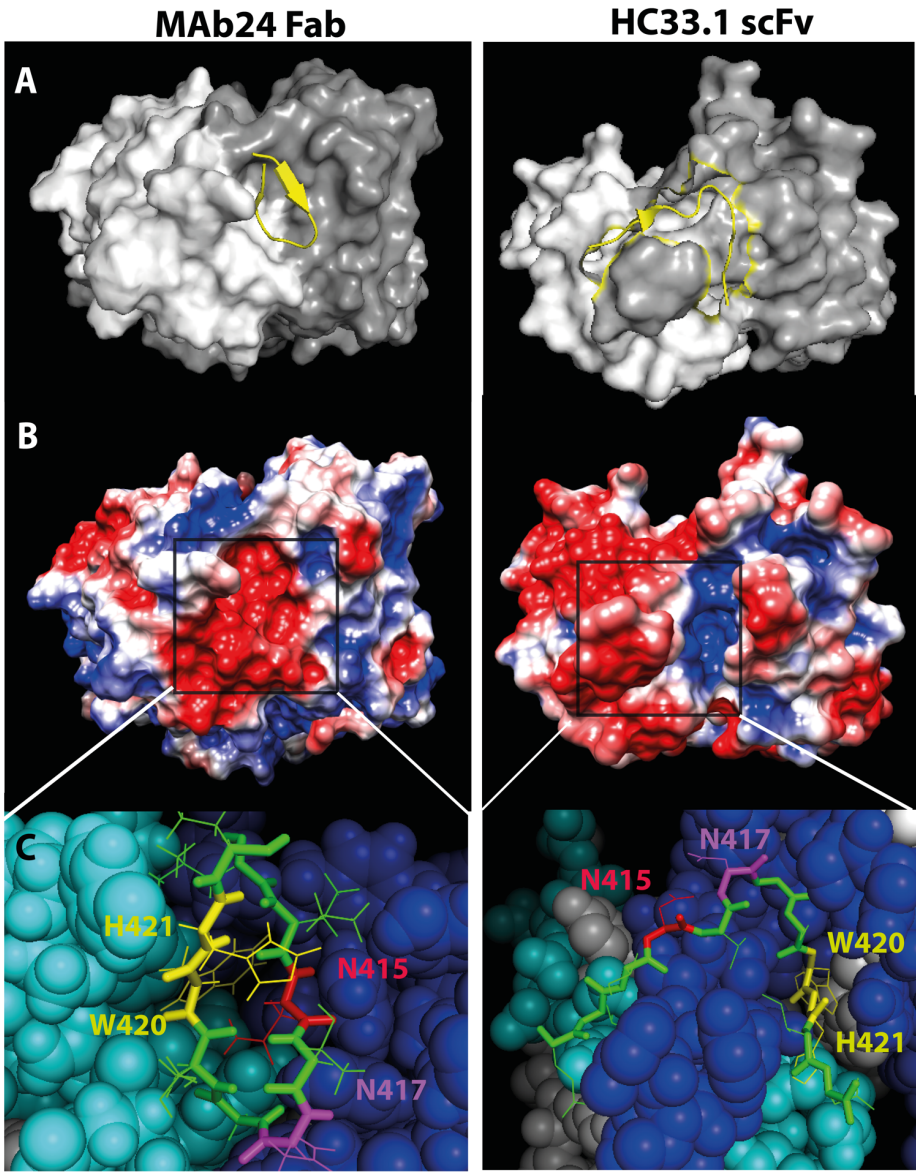

Figure 4.9 The paratope surfaces of MAb24 (left) and HC33.1 (right, PDB: 4XVJ). (A) The surface representation of MAb24 and HC33.1 scFv in complexed with the 412-423 peptide (yellow cartoon). Heavy and light chains are colored in dark grey and white, respectively. Images were generated using PyMOL. (B) The electrostatic surface potential of MAb24 and HC33.1 scFv. Adaptive Poisson-Boltzmann Solver (APBS) and PDB2PQR server (http://nbcr-222.ucsd.edu/pdb2pqr_2.1.1/) were used to calculate the electrostatic potential. Surface structures are colored with surface potential gradient [red (-2kT), white (0kT) and blue (+2kT)] using UCSF Chimera software and are in the same orientation as (A). Boxed areas are the paratope site. (C) Detailed views of the peptide and paratope interaction in MAb24 and HC33.1 scFv. The peptide backbone is shown here as sticks with side chains depicted as lines. The heavy and light chain CDRs of MAb24 are colored in cyan and dark blue respectively. Peptide residues N415 and N417 are highlighted in red and magenta respectively. Peptide residues W420 and H421 are shown in yellow. Images were generated using PyMOL.

4.7 Discussion

The 412-423 region on HCV E2 elicits brNAbs in immunized animals as well as humans, albeit infrequently in natural infection, and is one of the major antibody specificities elicited by D123. It is therefore important to understand the neutralization mechanisms of brNAbs to this region and the escape pathways of HCV against these brNAbs. Raised to D123 immunization, mouse MAb24 recognizes the 412-423 region, and is capable of neutralizing prototypic strains of HCV from G1a to G7a (Alhammad *et al.*, 2015a). Previous biochemical analyses showed that MAb24 inhibits E2-CD81 binding and alanine substitutions at residues L413, N415, G418, W420 and H421 abrogated or greatly reduced MAb24 binding to the 412-423 peptide and E2 RBD (Chapter 3). Given that W420 and H421 are involved in E2-CD81 binding, it was therefore highly likely that MAb24 neutralization was mediated by the engagement of the two CD81 binding residues, W420 and H421(Boo *et al.*, 2012; Owsianka *et al.*, 2006).

In this study, the interaction between MAb24 and the 412-423 region was examined further at the molecular level using X-ray crystallography. The crystal structure of MAb24 complexed with the 412-423 peptide revealed that when bound to MAb24, the peptide adopts a β hairpin conformation, and residues L413, N415, G418, W420, H421 are key components in the stabilization of the peptide hairpin-MAb24 complex. Simulation of these mutations is predicted to disrupt the intramolecular and/intermolecular hydrogen bonding network in the peptide/Fab complex and destabilize peptide-MAb24 interaction, and is consistent with the above epitope mapping findings. Residue N415 in particular, is a central component of MAb24 recognition of the 412-423 peptide, as it forms extensive contacts with the paratope surface as well as intra- and inter-molecular hydrogen bonds in the peptide-MAb24 complex. Based on the crystal structure, MAb24 neutralization mainly involves the burial of W420 and H421 in the paratope, and this possibly modifies the CD81 interface on E2, and inhibits E2-CD81 binding and viral entry.

The broad neutralization mediated by antibodies to the 412-423 region is mainly associated with the high degree of sequence conservation observed in this region amongst HCV isolates (Dhillon *et al.*, 2010; Kong *et al.*, 2012b). To investigate the

functional importance of the 412-423 region in viral replication cycle, *in vitro* outgrowth experiments were performed in this study to determine whether HCV is able to escape MAb24 neutralization. Forced evolution of HCVcc (G2a, J6 E1E2) in the presence of MAb24 *in vitro* showed that mutations can be selected that confer resistance and allow the replication of virus in the presence of MAb24. Sequencing and reverse genetics confirmed that MAb24 resistance is associated with three major mutations, N415D, N417S and H386R/N415D. All of the three mutations involve the modification of residue N415: via a direction mutation (N415D and H386R/N415D) or a glycan shift (N417S). Whilst N415D is associated with a modest reduction in viral fitness, an additional mutation within HVR1, H386R was found to restore viral replication and infectivity to at least WT levels. By contrast, viruses containing N417S had modestly increased infectivity. High throughput next generation sequencing results revealed additional low-frequency polymorphisms at N415, with variants such as N415D, N415S, N415T and N415G. Together, these results showed that HCV escape from MAb24 is associated with changes at N415, and this further highlighted the importance of N415 in MAb24 recognition and function.

Similar resistant variants were observed *in vitro* and *in vivo* with two other brNAbs to the 412-423 regions, AP33 and HCV1. *In vitro* passaging of JC1 virus (G2a, J6) or HJ3-5 virus (G1a H77c/JFH-1 chimera) under AP33 generated resistant variants, N415D and N417S, and N415Y respectively (Gal-Tanamy *et al.*, 2008; Pantua *et al.*, 2013). In chimpanzees and liver transplant patients, N415D, N415K, N415S and N417S mutations were associated with the recurrence of G1a HCV following HCV1 monotherapy (Babcock *et al.*, 2014; Chung *et al.*, 2013; Morin *et al.*, 2012). The emergence of similar N415 variants in AP33 and HCV1 *in vitro* and *in vivo* is not surprising, given that HCV1, AP33 and MAb24 all recognize the 412-423 region, and induce a similar hairpin conformation. Unexpectedly, neutralization assays performed on HCVcc containing N415D, N417S and H386R/N415D showed that acquisition of MAb24/HCV1/AP33-resistant mutations increased the sensitivity of the virus to another brNAb to the same region, HC33.1, consistent with previous reports (Keck *et al.*, 2014). In contrast to MAb24-like antibodies, HC33.1 induces an extended conformation of the 412-423 peptide and has a N415-paratope footprint

distinct from MAb24. Thus, the modification of N415 changes the local epitope environment of the 412-423 region such that it disrupts the recognition of this region by MAb24-like antibodies but favours neutralization by HC33.1.

Neutralization profiles of N415D, N417S and H386R/N415D viruses also suggested that changes at N415 may have a global effect on viral susceptibility to neutralization, at least in the context of HCVcc virions, as the three MAb24-resistant viruses are more sensitive to neutralization by a majority of brNAbs specific to E2 or the E1E2 complex such as HC84.27, AR3C and AR4A. Changes at N415 within the 412-423 region may re-position the adjacent HVR1, potentially via favouring the extended conformation of the 412-423 region, such that the flap-like HVR1 structure is away from the NAb face of E2. A more exposed NAb face in E2 and/or a favoured extended conformation of the 412-423 region in viruses with N415D or N417S mutations may explain the increased viral sensitivity observed with HMAbs such as HC84.27, AR3C and HC33.1. Alternatively, there may be a structural and/or functional link between the 412-423 region and the neutralizing face of E2/E1E2 heterodimer that is not present on the current E2 core models. Or, the 412-423 region is located closer to the NAb face of E2 than previously predicted. Structural studies of the 412-423 region in the context of E2 core protein or E1E2 heterodimer are required to resolve this question.

Recent analyses of 1,749 full sequences of HCV isolates (G1a, 2b and 3a) deposited in the Los Alamos HCV database showed that the probability of variation at residue N415 is limited, with a Shannon entropy of 0.22 (Rodrigo *et al.*, 2017). Given the low immunogenicity of the 412-423 region observed in natural infection, the conservation of N415 in circulating HCV isolates is in part due to the lack of selection pressure on the 412-423 region (Keck *et al.*, 2013; Tarr *et al.*, 2007). This study showed that by imposing MAb24 pressure, HCV generates escape mutants which contained direct changes in the 412-423 region. However, the acquisition of MAb24-associated resistance mutations is associated with reduced immunological fitness. It may additionally explain the low frequencies of naturally occurring N415 variants observed in circulating HCV. In conclusion, the 412-423 region remains a desirable component in HCV vaccine design. An ideal immunogen should be able to elicit a

multi-specific NAb response that consists of MAb24-like antibodies, HC33.1-like antibodies as well as other brNAbs to ensure pan-genotypic efficacy that reduces the possibility of viral escape.

Chapter 5 Characterization of the B cell response in chronic HCV

5.1 Introduction

The NAb response in natural HCV infection is characterized by an initial delayed response that is strain-specific, mainly driven by HVR1-specific NAbs, that primarily neutralize homologous viruses (Dowd *et al.*, 2009; Lavillette *et al.*, 2005a; Pestka *et al.*, 2007). This is followed by an increase in NAb breadth, mostly observed in the plasmas from individuals at >6 months of infections that have the ability to cross neutralize heterologous strains of HCV infection *in vitro* (Logvinoff *et al.*, 2004; Meunier *et al.*, 2005; von Hahn *et al.*, 2007). The exact breadth and specificity of these cross-reactive NAbs is yet to be fully characterized. To date, limited panels of brNAbs have been isolated and/or extensively characterized from HCV-infected humans, and these include the CBH-, HC84- and AR-related antibodies (Giang *et al.*, 2012; Hadlock *et al.*, 2000; Keck *et al.*, 2012; Law *et al.*, 2008).

Phage display technique involves the genetic engineering of a large library of DNA into filamentous bacteriophages so that the library DNA-encoded proteins or peptides of interest are expressed on the phage surface and screened for binding partners (Smith, 1985). Since its development in 1985, the phage library technique has been a powerful tool in the characterization of protein-protein/DNA interactions, especially in the isolation and characterization of MAbs against infectious agents such as HIV, influenza virus and HCV (McCafferty *et al.*, 1990). The preparation of an antibody display library involves the amplification and cloning of host-derived antibody genes into filamentous bacteriophages such as M13. Fused to the phage coat proteins such as pIII, the antibody components, Fab or scFv are displayed on the phage surface. This enables the high throughput analyses of the diverse range of antibody specificities generated within the host, via a process called biopanning, where antigen-specific antibody fragments are selected, enriched and isolated.

To expand our knowledge on the NAb specificities elicited in chronic HCV, this chapter investigated the NAb response in a cohort of IDUs who have chronic

HCV. The ability of their antibodies to cross-neutralize heterologous HCVpp and HCVcc strains *in vitro* was examined. Furthermore, to dissect the antibody response in chronic HCV, a phage display library of a chronically infected individual with high titres of NAbs was constructed and characterized.

5.2 Characterization of the neutralizing antibody response in chronic HCV

As part of the ongoing, longitudinal Network II Study being conducted at the Burnet Institute, plasma samples were obtained from a cohort of IDUs who were recruited, interviewed, and followed up for their social and injecting behaviors (Aitken *et al.*, 2004; Bharadwaj *et al.*, 2009). Their HCV infection history including HCV genotype(s) was also documented. Here, the plasmas of 22 IDUs who developed chronic HCV (> 6 months of infection) were selected for the characterization of NAb response of chronic HCV. They were infected with either G1a (1010, 2015, 4052, 5009, 5029, 2059, 3077), or G1b (2030), or G3a (5008, 4070, 4005, 4030, 2032, 30112, 3067, 4031, 1022, 5016, 1004), or G6a (5032 and 5040), or coinfected with G1a and G3a (1009), which are the representative genotypes affecting individuals in Australia.

Table 5.1 Percent Identity Matrix comparing the E1E2 sequences (residues 191-746) of prototypic strains across HCV genotypes (% identity calculated by Clustal2.1).

	G1a, H	G1a, H77c	G1b, Con1	G2a, J6	G2a, JFH-1	G3a, S52	G4a, ED43	G5a, SA13	G6a, EUHK2	G7a, QC69
G1a, H	100	98.74	80	67.03	67.39	70.99	73.29	74.41	69.86	69.19
G1a, H77c		100	81.08	67.93	68.29	72.25	74.37	75.68	70.94	70.09
G1b, Con1			100	66.31	67.75	72.61	71.84	74.23	68.95	70.99
G2a, J6				100	87.66	64.16	63.6	65.47	61.87	68.64
G2a, JFH-1					100	63.98	65.23	66.19	62.95	69.89
G3a, S52						100	70.27	69.24	67.62	67.44
G4a, ED43							100	70.09	69.86	65.77
G5a, SA13								100	69.37	69.24
G6a, EUHK2									100	65.35
G7a, QC69										100

5.2.1 Neutralizing antibody response against HCVcc

To determine the breadth of NAb responses in individuals with chronic HCV and identify individuals that developed high titres of cross-NAbs, the ability of plasmas obtained during chronic HCV infection to neutralize the G2a HCVcc JC1FLAG2 was examined. The JC1FLAG2 was used to prepare HCVcc since it allows high throughput screening of plasma or serum samples with ease of sampling from the tissue culture fluid to measure luciferase activity. In addition, whilst the E1E2 sequences of the HCV isolates in each individual are not known, comparative analyses of amino acid sequence of G2a E1E2 with those from the prototypic strains of G1, G3a and G6a indicate that the amino acid sequence of the structural components of JC1FLAG2 differ by 32.07-38.13% from those of G1, G3a and G6a (Table 5.1). Therefore, the JC1FLAG2 virus is an ideal *in vitro* model for high-throughput screening for the presence of cross-NAbs in plasma obtained from the chronically infected individuals in this study.

Heat-inactivated plasma samples were serially diluted and incubated with the JC1FLAG2 virus before addition to microtiter plates pre-seeded with the hepatoma cell line Huh7.5. The level of viral entry was measured by quantitating luciferase activity in the tissue culture fluid at 72 hours post infection, and the reciprocal dilution of plasma required to reduce JC1FLAG2 entry to 50 or 20% (inhibitory dose, ID_{50} or ID_{80}) was determined (Table 5.2). Of the 22 plasma samples tested, five failed to achieve ID_{80} (1010, 4005, 4030, 3067 and 5016). Both 3067 and 5016 were able to achieve an ID_{50}, however, 1010, 4005 and 4030 plasmas appeared to contain components that greatly enhanced the infection of the JC1FLAG2 virus *in vitro*. Whilst most of chronic plasmas (2015, 4052, 5009, 1009, 5008, 4070, 2032, 30112, 4031, 1022, 5016, and 1004) weakly neutralized JC1FLAG2 virus (IC_{80} <300), 6 of the 22 chronic plasmas (5029, 2059, 3077, 2030, 5032 and 5040) greatly neutralized HCVcc ($ID_{80} \geq 500$). Two plasmas, 5032 and 5040, recorded the highest ID_{80}s, both from subjects with G6a infection. Thus, there is a wide range of cross neutralizing activity of the antibody response in people with chronic HCV with limited numbers of individuals possessing high titres of cross-NAbs that neutralize G2a virus.

Table 5.2 The ability of chronic HCV plasmas to inhibit the infection of HCVcc JC1FLAG2 virus (G2a, J6 E1E2) to 50% (ID_{50}) and 20% (ID_{80}) *in vitro*[1].

		G2a, J6	
		ID_{50}	ID_{80}
G1a	1010	<40	<40
	2015	301	46
	4052	211	46
	5009	275	83
	5029	4600	500
	2059	12500	1550
	3077	5150	1020
G1b	2030	8000	1085
G1a, 3a	1009	2350	150
G3a	5008	8450	90
	4070	2350	225
	4005	<40	<40
	4030	<40	<40
	2032	225	90
	30112	275	50
	3067	145	<40
	4031	625	86
	1022	245	110
	5016	125	<40
	1004	565	85
G6a	5032	19200	2375
	5040	28000	2600
	MAb24	2500	200
	HCV (-)	<40	<40

[1]The mean ID_{50}s and ID_{80}s of two independent assays is shown. MAb24 and HCV naïve plasma, HCV (-), were used as a positive and negative controls, respectively.

5.2.2 Neutralizing antibody response against HCVpp

To further characterize the breadth of NAb response in those individuals that possessed highly potent cross-NAbs in Section 5.2.1, HCVpp was generated by pseudotyping HCV envelope proteins from HCV G1a and 1b into HIV-1 retroviral particles, and was used to assess the cross-neutralization capacity of the plasmas obtained from IDUs with chronic HCV. Envelope glycoproteins E1E2 derived from G1a H, G1a H77c and G1b Con1 differ by >32% in amino acid sequences from that of the G2a J6 glycoproteins incorporated into HCVcc of JC1FLAG2. In addition, all three envelope proteins reproducibly generate highly infectious HCVpp and are able to mediate high levels of entry in hepatoma cell line Huh7.5, at least 5 times that observed with empty retroviral particles (Drummer *et al.*, 2003).

Plasma samples from the 7 chronically infected IDUs that possessed high levels of cross-NAbs (5029, 2059, 3077, 2030, 4070, 5032 and 5040) were serially diluted and incubated with HCVpp viruses before addition to Huh7.5 cells. The level of HCVpp entry was measured at 72 hours and the reciprocal dilution of plasma that inhibited HCVpp entry to 50% (ID_{50}) and 20% of that observed in the absence of serum (ID_{80}) was determined (Table 5.3). Based on the neutralization patterns of the plasmas tested, the three different strains of E1E2 used to prepare the HCVpp displayed different levels of sensitivity to neutralization. The HCVpp containing the E1E2 of the H strain appeared to be most sensitive to neutralization by plasmas obtained from the chronic phase of infection, followed by the H77c and Con1 strains. Isolated from the same individual, the H and H77c strain only differ by 7 amino acids in the entire E1E2 region, none of which are implicated in previously described neutralizing antibody epitopes (E1: I212V, R297N, D321N and A360K; E2: S391N, H589Y and W602R). Yet, the ID_{50}s against the H-derived HCVpp were on average10-fold higher than those of the H77c-derived HCVpp. The most neutralization resistant strain was Con1-derived HCVpp; only 3077 weakly inhibited its entry (ID_{50}=45). As expected, the plasma samples obtained from G1a infection (5029, 2059 and 3077) had highly potent NAbs towards G1a HCVpp compared to plasmas from G1b, G3a or G6a-infected subjects.

Table 5.3 The ability of chronic HCV plasmas to inhibit the infection of G1-derived HCVpp to 50% (ID_{50}) and 20% (ID_{80})[1].

		G1a, H		*G1a, H77c*		*G1b, Con1*
		ID_{50}	ID_{80}	ID_{50}	ID_{80}	ID_{50}
G1a	5029	2400	46	51	<40	<40
G1a	2059	10350	145	95	<40	<40
G1a	3077	75750	1540	1500	275	45
G1b	2030	275	101	150	<40	<40
G3a	4070	195	<40	150	<40	<40
G6a	5032	1400	60	95	<40	<40
G6a	5040	600	<40	55	<40	<40
	MAb24	3150	55	115	40	45
	HCV (-)	<40	<40	<40	<40	<40

[1]The mean ID_{50}s and ID_{80}s or of two independent assays is shown. MAb24 and HCV naïve plasma, HCV (-), were used as a positive and negative control respectively.

5.2.3 Neutralizing antibody specificities elicited in chronic HCV

The epitopes for a subset of NAbs have been mapped to defined regions on E2, located within residues 408-428, 430-451, and 523-549. To determine whether the cross-neutralizing activities of the plasmas of chronically infected individuals correlates with the presence of such antibody specificities, solid-phase ELISA binding assays were performed using G1a H/H77c and G2a J6 peptide analogs corresponding to these three regions on E2.

As shown in Table 5.4, most of the plasmas showed low reactivity towards both G1a and G2a forms of NAb epitopes, except for two plasmas, 3077 and 5032 which appeared to have relatively high titres of IgG that recognize both J6 and H/H77c forms of NAb epitope 408-428. The neutralization capacity of the plasmas from chronically infected individuals towards G1a H-derived HCVpp (ID_{50}) correlated with their ability to recognize epitopes located with the peptides 408-428 ($r=0.8108$, $p=0.0381$) and 523-549 ($r=0.8895$, $p=0.0143$) (nonparametric Spearman correlation determined using Prism version 7.0c). There was no correlation between the cross-neutralization activity of the plasmas towards HCVcc JC1FLAG2 (J6) and ability to bind G2a derived peptides spanning 408-428, 430-451, and 523-549. This indicates that the antibody specificities in chronic, cross-neutralizing plasmas are directed towards regions that are not represented by the peptide analogues of the three known linear NAb epitopes, and alternative cross-NAb epitopes, linear and/or conformational, may contribute to the cross-neutralization capacity observed in this subject.

Table 5.4 The reactivity of HCV chronic plasmas to the peptide analogues of three continuous NAb epitopes (408-428, 430-451, and 523-549) found on the HCVcc and HCVpp used in this study (G2a J6 and G1a H/H77c)[1].

		H/H77c Peptide			J6 Peptide		
		408-428	430-451	523-549	408-428	430-451	523-549
G1a	5029	20	20	20	<10	<10	<10
	2059	40	10	15	<10	<10	10
	3077	160	20	90	50	<10	60
G1b	2030	15	10	10	<10	<10	<10
G3a	4070	15	<10	<10	<10	<10	<10
G6a	5032	140	<10	15	50	<10	15
	5040	30	20	15	10	<10	<10

[1]The endpoint titres of binding are shown here. The reactivity of chronic plasmas that showed background OD at the lowest dilution (1/10) are denoted as <10.

5.3 Characterization of the antibody repertoire of a subject with chronic HCV

As a participant in the Network II Study, 5032 is an IDU with an injection history of >20 years, and was first enrolled in the study in December 2005 when tested positive for HCV G6a by the 5'UTR-based LiPA assay (Versant HCV genotyping assay). Since then, the subject has been frequently followed up, providing a well-documented HCV infection history (Figure 5.1) and blood samples under informed consent. *In vitro* neutralization assays and peptide binding assays performed on a plasma sample collected in November 2006 (discussed as 5032 in the previous sections in this chapter, described as 5032 2006 from here onwards) indicated, that after being HCV PCR positive for ≥11 months, 5032 developed highly potent cross neutralizing antibodies. Here, to further examine the antibody specificities elicited in this subject, an antibody phage display library was prepared.

5.3.1 The construction of an antibody library of 5032

To construct the antibody library of 5032, peripheral blood mononuclear cells (PBMCs) containing peripheral B cells were used as the source for the extraction and amplification of antibody-related genes. To ensure optimal B cell viability and ideal RNA quality for library construction, fresh blood was collected from 5032 in November 2012 (Figure 5.1). Prior to the blood collection, 5032 had become PCR negative for HCV, as a result of the IFN treatment undertaken between August 2011 and June 2012. Despite achieving clearance of HCV, 5032 appeared to have maintained high levels of E2-specific IgG antibodies, as plasmas from 2012 (5032 2012) were able to recognize the recombinant E2 RBD core proteins (D123) in direct binding ELISA assays at levels almost identical to that of 2006 (5032 2006) (Figure 5.2).

Total RNA was extracted from PBMCs isolated from 5032 and reverse transcribed into library cDNA using random hexamers, followed by the amplification of the variable regions of the heavy chain (HC) sequences (V_H subgroups 1 to 7) and the entire kappa and lambda light chain (LC) gene fragments (Vk subgroups 1 to 6; Vλ subgroups 1 to 7), using degenerate primers described by de Haard (2002) (also

described in Chapter 2 Table 2.9 and Table 2.10). The amplified V_H and LC fragments were each subcloned into library vector pCES to generate HC and LC libraries, respectively, which were then recombined through complementary digestion and cloning to generate combinatorial libraries of 5032.

The majority of the V_H fragments amplified from 5032 were readily digested into the expected ~600bp fragment with the restriction endonucleases *Sfi*I and *BstE*II for cloning into the library vector. However, a proportion of 5032-derived V_H sequences was unexpectedly cleaved into two smaller fragments of ~400bp and ~200bp by the same restriction enzyme digestion. Sequence analysis of the *Sfi*I/*BstE*II-truncated V_H sequences revealed that they consisted of one identical sequence (also shown as VH-25 in Figure 5.5). In addition to the *Sfi*I and *BstE*II restriction enzyme sites at the 5' and 3' ends respectively, this unique V_H sequence (VH-25) contained an additional *BstE*II cleavage site within its framework region-3, or FR3. This resulted in the observed restriction enzyme fragment pattern. Given its level in amplified V_H pools and potential role in HCV-specific antibody response, VH-25 was reconstituted and cloned in the pCES vector through a multi-step cloning strategy. As a result, two different Fab libraries were generated from 5032; library I containing a diverse range of V_H and LC ($1.76x10^6$ clones) and library II containing various LC and a single V_H, VH-25 ($2x10^4$ clones).

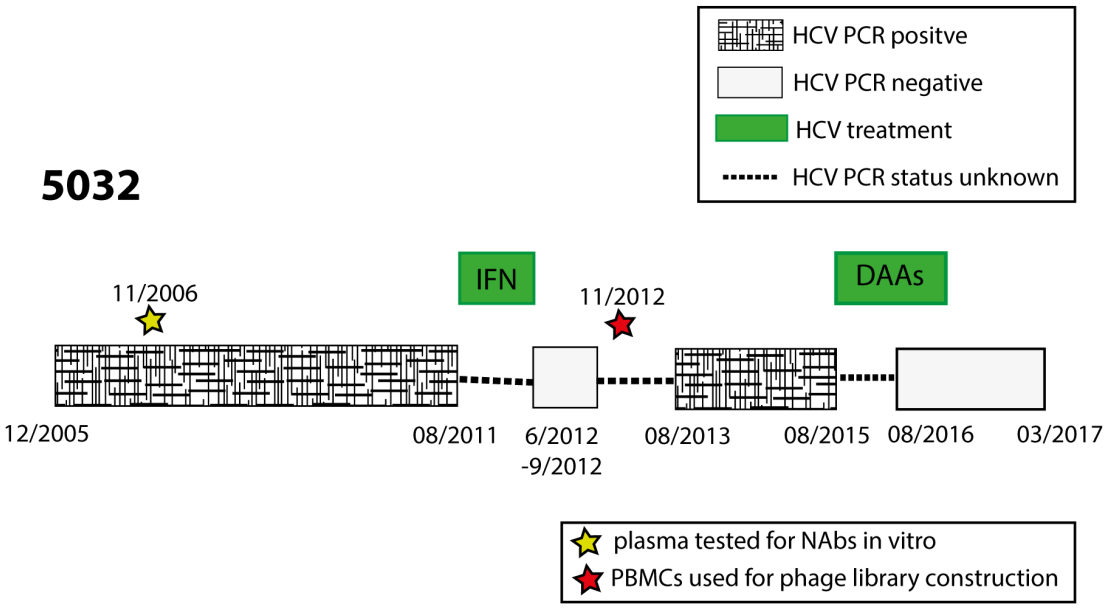

Figure 5.1 The clinical history of the phage library candidate 5032 (Dr Peter Higgs, personal communication). The subject was tested for HCV RNA at least once every six months. The HCV-positive period indicated here is defined as having HCV PCR positive results between tests with no negative results. Between December 2005 and August 2011, the subject was infected with HCV G6a. Between August 2013 and August 2015, the subject was re-infected, although the HCV genotype(s) was not known. The HCV antiviral treatment period (IFN: interferon treatment and DAAs: direct-acting antivirals) is the estimate period based on the subject's self-report.

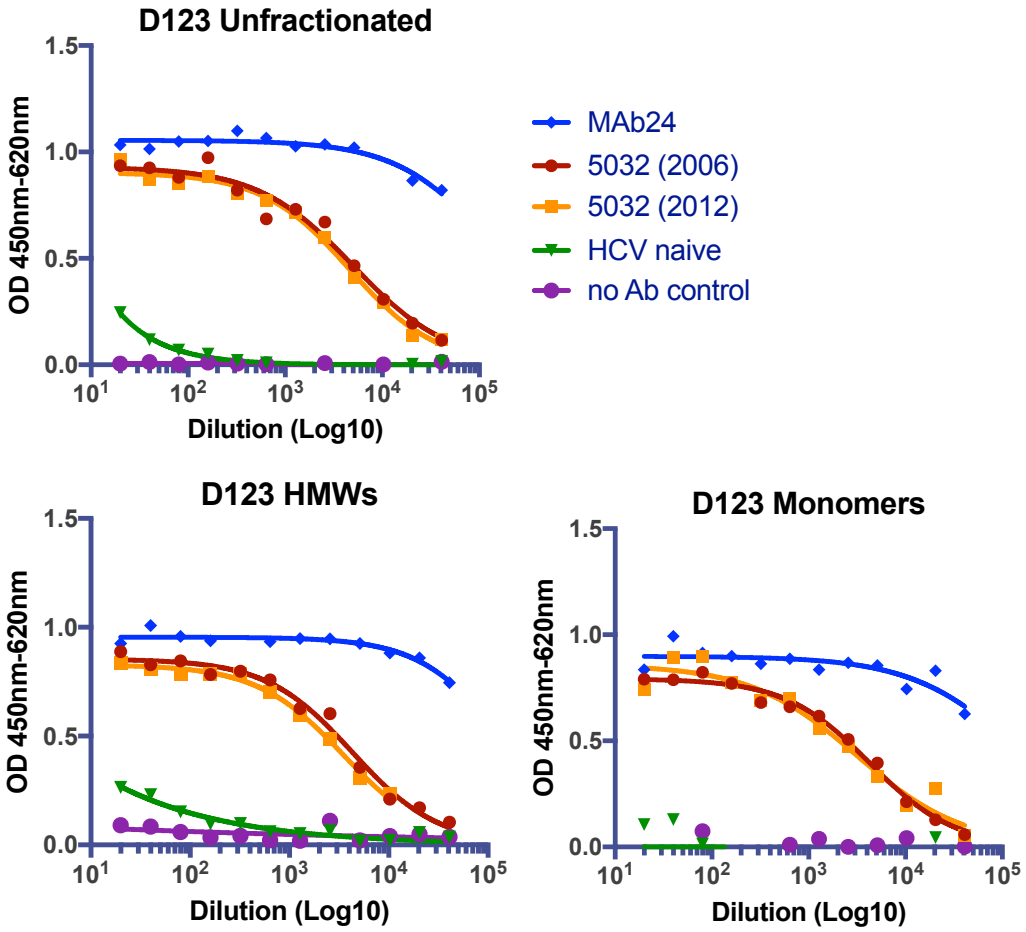

Figure 5.2 The immunoreactivity of 5032 plasma samples in 2006 and 2012 towards different oligomeric forms of D123, including unfractionated, high molecular weight (HMWs) and monomeric forms of D123. Mini-PERM preparation of MAb24 was used as positive control. Background levels of D123 binding is indicated by the negative controls, a HCV naïve plasma and a no antibody control.

5.3.2 The Fab repertoire of the chronic neutralizer 5032

The specificity of a B cell receptor (BCR), or an antibody is predominately determined by its antigen-binding fragments (Fab), mainly the variable regions of the heavy and light chains (V_L and V_H). V_L and V_H consist of four framework regions (FRs: FR1, FR2, FR3 and FR4) that serve as the structural scaffold for the immunoglobulin, as well as three complementarity-determining regions (CDRs: CDR1, CDR2 and CDR3) that play a major role in antigen interaction. The antibody repertoire of an individual is diversified via two major events. During the development of naïve B cells, the heavy and light chain sequences are generated by joining germline-encoded genes, V, D and J genes for the heavy chains (IGHV, IGHD and IGHJ) and V and J genes for the light chains (k: IGKV, IGKJ and λ: IGLV and IGLJ). This so-called combinatorial event involves the recombination of various allelic forms of V(D)J genes as well as the deletion and/or addition of non-templated (N) region and palindromic (P)-nucleotides at the joining junctions, creating theoretically unlimited diversity in V_L and V_H genes, particularly at the CDR3 region. Following an immune stimulus, antigen-specific B cells undergo somatic hypermutation in the germinal centers, driven mainly by follicular T helper cells. This results in the accumulation of mutations in V_L and V_H sequences, in both FRs and CDRs, and is associated with the proliferation of B cell clones that produce high-affinity antibodies.

To examine the antibody repertoire of 5032 with >6 years of HCV and confirm that functional LC and V_H sequences were correctly incorporated into the phage library, Fab clones of the two phage libraries were sequenced (library I: VH/VL 1-24 and library II: VH/VL 25-48), and the V_L and V_H sequences were analyzed using IMGT/V-QUEST (http://www.imgt.org/) (Brochet *et al.*, 2008; Giudicelli *et al.*, 2011). Whilst some Fab clones contained partial V_L and V_H sequences with one or more genuine stop codons, most of the V_L and V_H gene fragments amplified from 5032 encoded full-length functional V_L and V_H sequences, as shown in Figure 5.3 to Figure 5.5. Alignment of the amino acid sequences of V_L and V_H showed that except for V_H sequences in library II (VH-25 to VH-48, only VH-25 shown here), no identical V_L or V_H were found in the Fab clones sequenced. A diverse range of V- and J-gene subgroups and alleles from both kappa and lambda LCs (IGKV/J and IGLV/J)

can be found amongst the V_L sequences (Figure 5.3 and Figure 5.4). Similarly, the V_H sequences were derived from various allelic forms of IGHV, IGHD, IGHJ subgroups, and the lengths of the CDR-H3 ranges from 9 to 19 amino acid residues (Figure 5.5). Together, these results demonstrated that the libraries contain functional V_L and V_H sequences and are of reasonable diversity.

A closer examination of the CDRs of V_H revealed two V_H sequences that have identical CDR-H1 and CDR-H2, VH-10 and VH-11 (Figure 5.5A). Based on the IMGT/V-QUEST analyses, both VH-10 and VH-11 appeared to originate from the germline IGHV1-69 genes, the same germline V-gene used by human brNAbs HC84.1 and AR3C, as shown in Figure 5.6. Despite the same V-gene usage, the CDR-H3 region differ completely amongst the four V_H sequences, as different DJ-genes were joined to the V1-69 gene, suggesting different B cell lineage clones. In addition, in contrast to HC84.1 and AR3C both of which have significantly higher levels of amino acid substitutions compared to the germline, particularly in the CDR-H1 and CDR-H2, VH-10 and VH-11 sequences were almost identical to the germline V1-69.

Extensive somatic hypermutation within the V-regions of V_H and V_L, particularly at the CDRs, often indicates a strong antigenic selection process and is associated with increased antibody affinity and function. To examine whether the available V_H and V_L sequences were under any selection pressure, possibly as a result of chronic HCV infection (≥6 years), the percentage amino acid substitution of the V-regions of the available V_H and V_L sequences was determined, and the selection values ($\sum$s) of each sequence was calculated using BASELINe, a statistical algorithm which provides Bayesian estimation of antigen-driven selection in immunoglobulin sequences based on the ratios of Replacement (R) and Silent (S) mutations (Uduman *et al.*, 2011; Yaari *et al.*, 2012). As shown in Figure 5.7A, all of the V_H and V_L sequences contained no or low levels of amino acid substitutions (0-20%), except for VH-9 (36%). In addition, most of the nonsynonymous mutations were found in the FRs and this was possibly associated with the observed positive antigenic selection in the FRs of some V_Ls and V_Hs ($\sum s>0$, Figure 5.7B). By contrast, the CDRs of the V_L and V_H sequences appeared to be mostly under negative selection ($\sum<0$), except for

VH-14 whose CDRs were positively selected ($\sum$=1.28) and some V_Ls (VL-4, VL-29, VL-41, VL-47) which remained as non-mutated germline sequences. Together, these findings suggested that the V_Ls and V_Hs that underwent extensive somatic hypermutation and contained positively-selected CDRs may occur at low frequencies in the constructed libraries. Overall, the antibody repertoire of 5032 prepared for the phage libraries consists of a diverse range of V_H and V_L sequences, most of which contain no or low levels of somatic hypermutation.

A

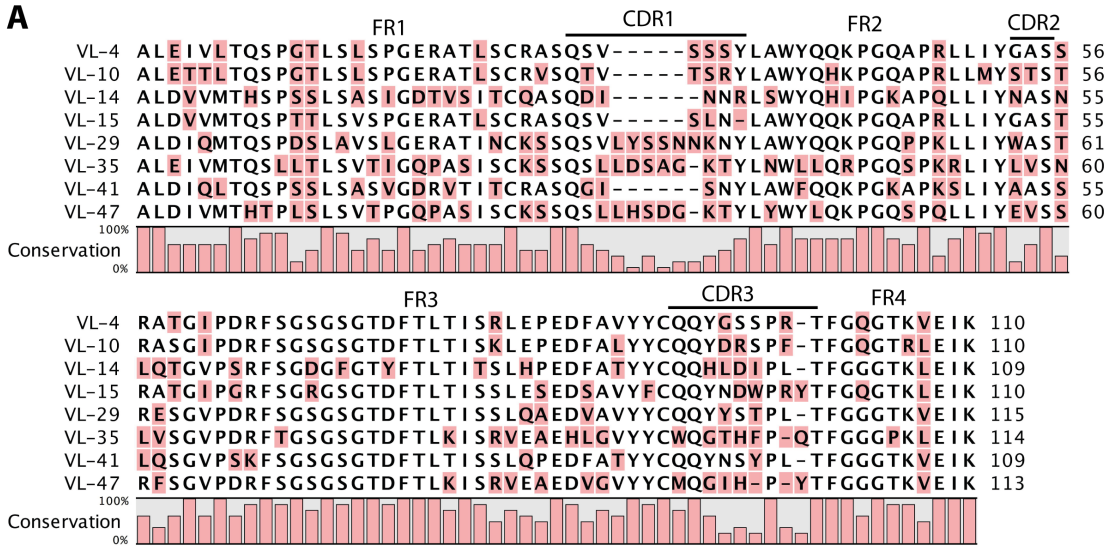

B

Library Clone	V-GENE and allele (% identity)	J-GENE and allele (% identity)	CDR-IMGT lengths
VL-4	IGKV3-20*01 F (100%)	IGKJ1*01 F (100.0%)	7.3.9
VL-10	IGKV3-20*01 F (91.84%)	IGKJ5*01 F (97.3%)	7.3.9
VL-14	IGKV1-33*01 F, or IGKV1D-33*01 (83.87%)	IGKJ4*01 F, or IGKJ4*02 F (91.89%)	6.3.9
VL-15	IGKV3-15*01 F (93.91%)	IGKJ2*01 F (97.37%)	6.3.10
VL-29	IGKV4-1*01 F (99.33%)	IGKJ4*01 F (100.0%)	12.3.9
VL-35	IGKV2-29*01 P, or IGKV2-29*03 F or IGKV2D-29*01 F or IGKV2D-29*02 F(64.29%)	IGKJ2*01 F, or IGKJ4*01 F or IGKJ4*02 F (67.57%)	11.3.9
VL-41	IGKV1-16*02 F (99.64%)	IGKJ4*01 F (100.0%)	6.3.9
VL-47	IGKV2-29*02 F (99.66%)	IGKJ4*01 F (89.19%)	11.3.8

Figure 5.3 The variable regions of the 5032-derived kappa light chain (V_L k). (A) The amino acid sequences of the available V_L k clones. Sequences were aligned using CLC Main Workbench v7. Differences in amino acid residues were highlighted in red. The FRs and CDRs of the V_L k were assigned using IMGT/V-QUEST (ver 3.4.6, reference directory release 20175-4) based on the IMGT-ONTOLOGY identification. (B) The germline V- and J-gene used in each V_L k clone assigned by IMGT/V-QUEST (F: functional germline sequences that are open reading frame without stop codon; P: pseudogene: germline stop codon/frameshift mutations). The % nucleotide identity of each clone to the assigned germline gene is shown in parentheses. The lengths of CDR1, CDR2 and CDR3 of each clone are indicated here as the number of residues within each region, [CDR1.CDR2.CDR3]

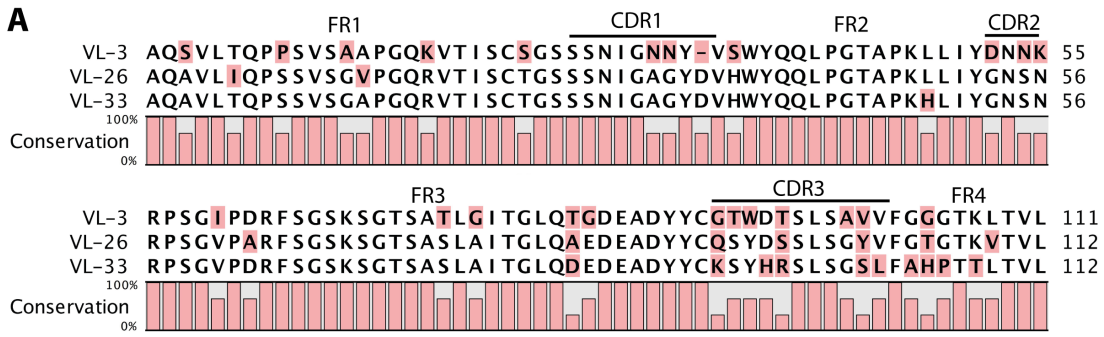

B

Library Clone	V-GENE and allele (% identity)	J-GENE and allele (% identity)	CDR-IMGT lengths
VL-3	IGLV1-51*01 F (99.30%)	IGLJ2*01 F, or IGLJ3*01 F (100.0%)	8.3.11
VL-26	IGLV1-40*01 F (97.22%)	IGLJ1*01 F (100.0%)	9.3.11
VL-33	IGLV1-40*01 F (96.53%)	IGLJ2*01 F, or IGLJ3*01 F or IGLJ3*02 F (67.65%)	9.3.11

Figure 5.4 The variable regions of the 5032-derived lambda light chain (V_L λ). (A) The amino acid sequences of the available V_L λ clones. Sequences were aligned using CLC Main Workbench v7. Differences in amino acid residues were highlighted in red. The FRs and CDRs of the V_L λ were assigned using IMGT/V-QUEST (v3.4.6, reference directory release 20175-4) based on the IMGT-ONTOLOGY identification. (B) The germline V- and J-gene used in each V_L λ clone assigned by IMGT/V-QUEST (F: functional germline sequences that are open reading frame without stop codon). The % nucleotide identity of each clone to the assigned germline gene is shown in parentheses. The lengths of CDR1, CDR2 and CDR3 of each clone are indicated here as the number of residues within each region, [CDR1.CDR2.CDR3].

A

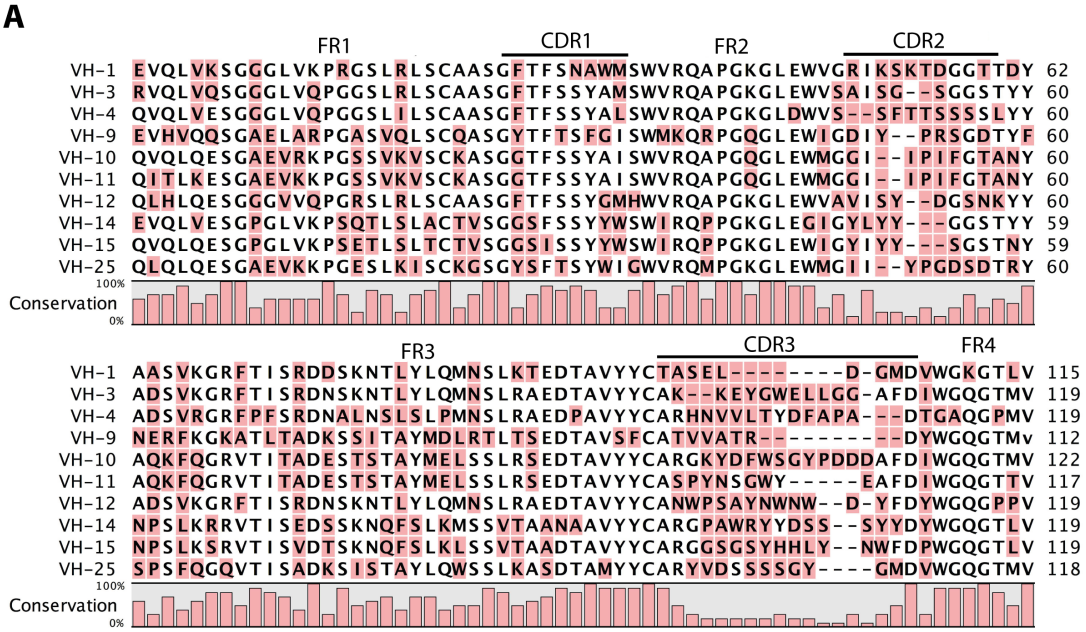

B

Library Clone	V-GENE and allele (% identity)	D-GENE and allele	J-GENE and allele (% identity)	CDR-IMGT lengths
VH-1	IGHV3-15*01 F (97.62%)	IGHD6-13*01 F	IGHJ4*01 F (74.29%)	8.10.10
VH-3	IGHV3-23*04 F (98.61%)	IGHD2-15*01 F	IGHJ3*02 F (94.59%)	8.8.16
VH-4	IGHV3-21*01 F, or IGHV3-48*04 F (89.24%)	IGHD2-21*02 F	IGHJ5*02 F (60.53%)	8.8.16
VH-9	IGHV1-18*01 F (58.33%)	IGHD2-15*01 F	IGHJ4*02 F (68.57%)	8.8.9
VH-10	IGHV1-69*01 F, or IGHV1-69D*01 F (98.26%)	IGHD3-3*01 F	IGHJ3*02 F (97.3%)	8.8.19
VH-11	IGHV1-69*12 F (97.22%)	IGHD6-19*01 F	IGHJ3*02 F (91.89%)	8.8.14
VH-12	IGHV3-30*03 F, or IGHV3-30*18 F, or IGHV3-30-5*01 F (98.26%)	IGHD1-7*01 F	IGHJ4*02 F (91.43%)	8.8.16
VH-14	IGHV4-30-4*01 F (94.16%)	IGHD3-22*01 F	IGHJ4*02 F (85.71%)	10.7.17
VH-15	IGHV4-59*01 F (99.65%)	IGHD3-10*01 F	IGHJ5*02 F (97.37%)	8.7.17
VH-25	IGHV5-51*03 F (97.57%)	IGHD6-6*01 F	IGHJ3*01 F (81.08%)	8.8.15

Figure 5.5 The variable regions of the 5032-derived heavy chain (VH). (A) The amino acid sequences of the available VH clones. Sequences were aligned using CLC Main Workbench v7. Differences in amino acid residues were highlighted in red. The FRs and CDRs of the VH were assigned using IMGT/V-QUEST (ver 3.4.6, reference directory release 20175-4) based on the IMGT-ONTOLOGY identification. (B) The germline V-, D- and J-gene used in each VH clone assigned by IMGT/V-QUEST (F: functional germline sequences that are open reading frame without stop). The % nucleotide identity of each clone to the assigned germline gene is shown in parentheses. The lengths of CDR1, CDR2 and CDR3 of each clone are indicated here as the number of residues within each region, [CDR1.CDR2.CDR3].

A

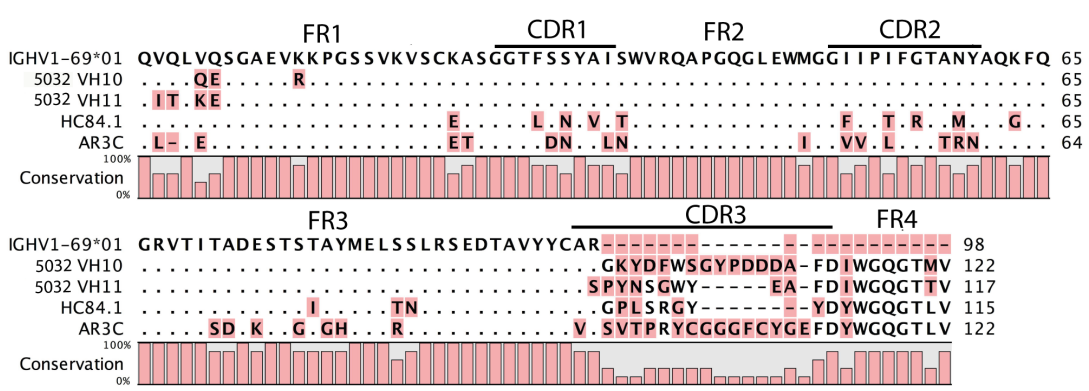

B

VH sequence	Heavy chain		
	V-gene	D-gene	J-gene
HMAb HC84.1	IGHV1-69*01	IGHD3-22*01	IGHJ4*02
HMAb AR3C	IGHV1-69*06	IGHD2-21*01	IGHJ4*02
5032 VH-10	IGHV1-69*01	IGHD3-3*01	IGHJ3*02
5032 VH-11	IGHV1-69*12	IGHD6-19*01	IGHJ3*02

Figure 5.6 IGHV1-69-derived VH sequences. (A) The variable regions of 5032 VH-10 and VH-11 were aligned with human brNAb HC84.1 and AR3C, using CLC Main Workbench v7. Differences in amino acid residues were highlighted in red and matching residues were shown as dots. The FRs and CDRs of the four VH sequences were assigned using IMGT/V-QUEST (ver 3.4.6, reference directory release 20175-4) based on the IMGT-ONTOLOGY identification. (B) VDJ gene usage in 5032 VH-10, VH-11 and HC84.1 and AR3C. Germline VDJ genes of 5032 VH-10 and VH-11 were predicted using IMGT/V-QUEST and those of HC84.1 and AR3C were as published previously (Kong et al., 2013; Krey et al., 2013).

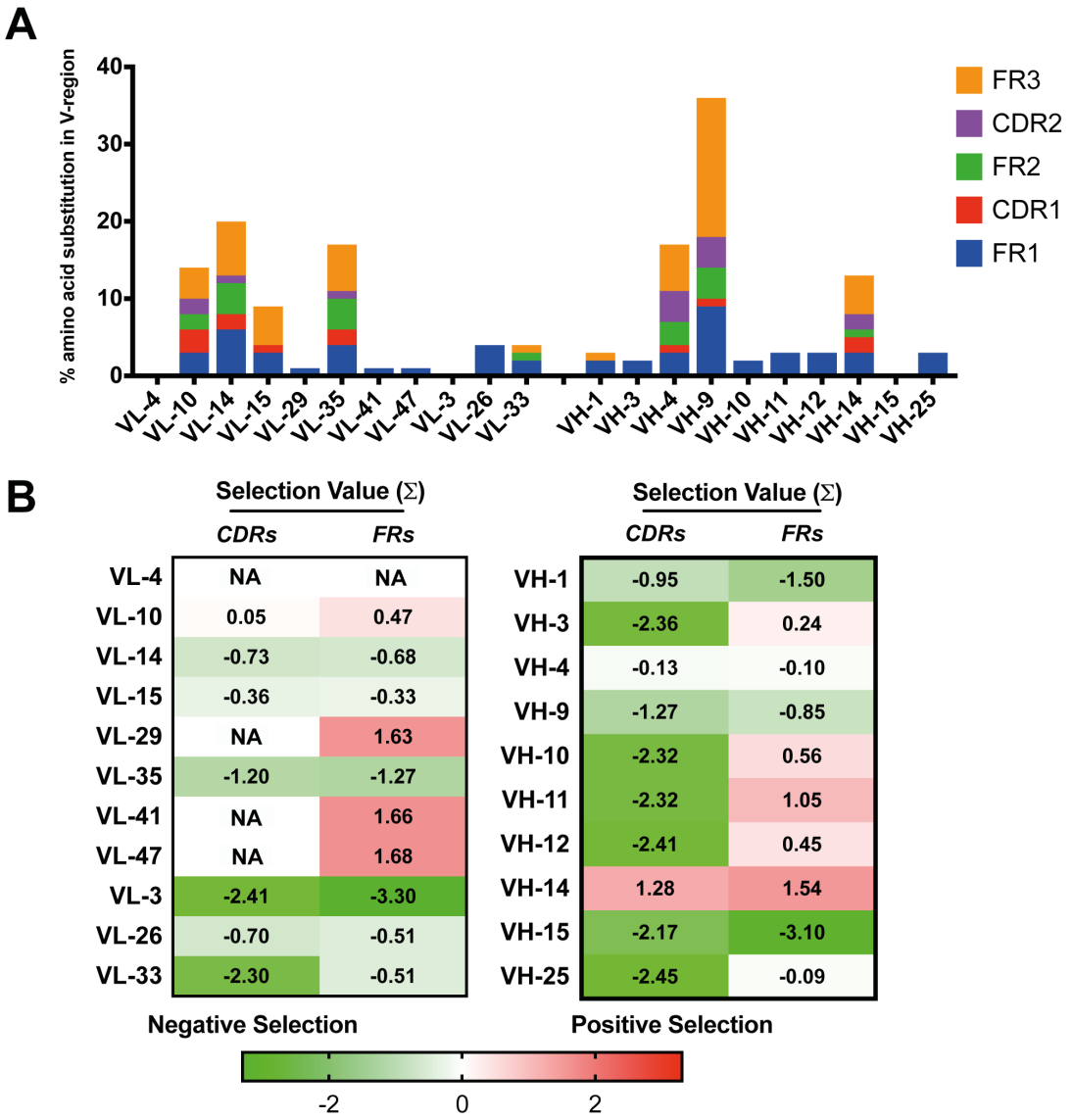

Figure 5.7 The selection pressure on the 5032-derived heavy and light chain sequences. (A) The level of somatic hypermutation in the V-region in 5032-derived V_L and V_H sequences (FR1-3 and CDR1-2). The percentage amino acid substitution was determined based on alignment with the closest germline V-region predicted by IMGT/V-QUEST (program v3.4.8, reference directory release: 201728-2). The percentage amino acid substitution in the V-region is calculated by (number of amino acid substitution)/(total number of residues in the V-region)×100. For the V_L and V_H sequences that shared low percentage identity to the predicted germline genes (e.g. VL-35 and VL-9), possible insertion(s) and deletion(s) of germline genes were searched, and none was found. (B) The selection values (∑s) of the available V_L and V_H sequences. The ∑ values were calculated using the BASELINe program (ver1.3) (http://selection.med.yale.edu/baseline/) (Uduman *et al.*, 2011; Yaari *et al.*, 2012). The CDR3 and FR4 sequence of each clone were not included for the ∑ calculation. Human S5F SHM targeting model and focused selection statistics were used in the calculation (Yaari *et al.*, 2013). The ∑s of V_L and V_H clones that have identical sequences to their designated germline CDRs and/or FRs were denoted as NA.

5.3.3 Biopanning of 5032-derived Fab repertoire

To further explore the antibody specificities against E2 elicited in chronic HCV and isolate HCV E2-specific Fabs from 5032, the Fab repertoire of 5032 was subjected to panning against E2 proteins. D123 was used as the panning target. As a recombinant HCV E2 RBD protein (G1a, H77c strain) with HVRs deleted, D123 represents the highly-conserved form of E2 core, and has an antigenic conformation that favours the exposure of cross-NAb epitopes on E2 and the generation of brNAb responses in small animals (Chapter 3) (Alhammad *et al.*, 2015a; McCaffrey *et al.*, 2007; Vietheer *et al.*, 2017). The HMWs of D123 in particular, elicited significantly higher titres of brNAbs in guinea pigs, suggesting that they are in configurations that more effectively engage BCRs to the conserved NAb epitopes on E2. Furthermore, high levels of IgG reactive against various forms of D123, including unfractionated, HMWs and monomeric forms, were observed in 5032 plasmas (Figure 5.2). Therefore, D123 was selected for the isolation of cross-reactive Fabs from 5032.

To ensure the maximum recovery of high-affinity, target-positive Fab clones, 5032 library I and II each underwent three rounds of panning with decreasing amounts of D123 protein (25μg, 10μg and 5μg), as shown in Table 5.5. In each round, the large input library was allowed to bind to immobilized D123, and any non-specific interaction was removed by stringent washes using detergent-containing buffers. The resulting output library was then amplified and subjected to the next round of panning. As shown in Table 5.5, a significant decrease in phage titres was observed following each round of panning. A total of ~150 phage clones were positively selected against D123 unfractionated proteins while few phages were reactive against both unfractionated D123 and D123 HMWs. The screening of randomly selected phage clones from the R3 output library showed no Fabs reactive to unfractionated D123 or D123 HMWs. Further analyses of the output library DNA using V_L/V_H-specific primers showed that the entire output library appeared to have lost Fab inserts following three rounds of panning. In summary, no D123-reactive Fab was isolated from 5032 libraries in this study.

Table 5.5 Biopanning of the 5032 Phage libraries (I and II) using D123 proteins[1].

	5032 (input PFUs/**output PFUs**)	
	Fab Library I	Fab Library II
R1 (**25µg** D123 mix)	$1.88x10^{11}$/ $\mathbf{8.25x10^{4}}$	$8.52x10^{9}$/$\mathbf{3.75x10^{5}}$
R2 (**10µg** D123mix)	$1.67x10^{12}$/**1240**	$2.56x10^{9}$/**80**
	Libraries Pooled after R2	
R3 (**5µg** D123 mix)	$1.14x10^{9}$/**150**	
R3 (**5µg** D123 HMWs)	$1.14x10^{9}$/**TFTC**	

[1]Selection of D123-specific Fabs was conducted with three rounds of panning (Round 1-3 or R1-3) with decreasing amounts of D123 proteins (25μg to 5μg). Phage libraries I and II were panned independently in R1 and R2 against unfractionated D123 (D123 mix) before being pooled and undergoing R3 selection against D123 mix or HMWs of D123. Number of phage clones before and after each round is indicated as input and output PFUs. PFUs: plaque-forming units. TFTC: too few to count. Results from one panning experiment, representative of the outcome of two independent panning experiments.

5.4 Discussion

It is proposed that the co-evolution of the B cell repertoire with antigenically diverse viruses such as HCV, HIV and influenza virus over an extended period of time will result in the proliferation of B cell clones that express affinity-matured, broadly-reactive antibodies (Burton *et al.*, 2012). Compared to HIV and influenza virus, HCV NAb studies have long been impeded by the lack of *in vitro* tools necessary for the screening of cross-NAbs or brNAbs. In this study, the breadth of NAb response in chronic HCV was assessed using 4 strains of HCV, either HCVcc or HCVpp, from G1 and G2. A small number of individuals, were found to develop potent cross-NAbs against G1 and G2a HCV after ≥6 months infection. Furthermore, the cross-NAb activity observed in this subset of chronically infected individuals cannot be explained by their plasma reactivity against peptide analogues of three known NAb regions on E2, 408-428, 430-451 and 523-549. It is possible that cross-NAbs to these regions were elicited in chronic HCV infection, but the exact conformation of these antigenic regions cannot be recapitulated in the solid-phase peptide binding assays. Alternatively, cross-NAbs elicited in chronic HCV may be directed towards discontinuous conformational regions, such as the AR3C binding region, and/or novel epitopes on E1 and E2.

The generation of broadly reactive antibodies against highly variable viruses are thought to be achieved through the repeated and prolonged exposure of viral antigens (Corti & Lanzavecchia, 2013). This allows for the selection of rare B cell lineages, or V(D)J recombinants, and/or extremely high levels of somatic hypermutation in the CDRs of V_H and V_L. To further investigate the changes of the B cell repertoire following chronic HCV, this chapter examined V_H and V_L repertoires of an individual (5032) who had been infected with HCV for >6 years. As discussed in Section 5.3.1, one of the prominent characteristics of the antibody repertoire of 5032 was the presence of a unique heavy chain sequence, VH-25. Amplified at noticeably high levels in the V_H pool during library construction, VH-25 appeared to originate from the germline V-gene IGHV5-51*03 (97.53% nucleotide identity, shown in Figure 5.5B), and a similar sequence has been described in a healthy human (100% amino acid identity in V-gene, CDR-H3 differs) [GenBank: LM646556.1] (Hansen *et al.*, 2015). In addition, the *BstE*II site observed in the FR3 of VH-25 can

be found in the germline sequence of IGHV5-51*03 as well as other alleles of the IGHV5-51 germline gene (IGHV5-51*03F, IGHV5-51*01F, IGHV5-51*04F, IGHV5-51*02F) and the IGHV5-10-1 germline gene (IGHV5-10-1*04F). Whilst the IGHV5-51 gene is utilized in 18 of 51 (~35%) neutralizing HMAbs targeting the V3 loop of HIV envelope gp120, its exact usage in HCV has not been documented (Gorny *et al.*, 2009). Nevertheless, the presence of IGHV5-51-derived B cell lineages clearly imposed a technical obstacle in the construction of phage library methods developed by de Haard (2002). Although the prevalence of this V-gene usage in HCV-infected individuals is not clear, alternative library vector or V_H cloning strategies may need to be employed for future phage library construction.

Another interesting V_H feature observed in 5032 is the use of IGHV1-69 gene in 2 of the 10 available V_H sequences (VH-10 and VH-11, with CDR-H3 lengths of 14 and 19 amino acids respectively). The V_H1-69 gene, also known as V_H 51p1, is reported in most of the HCV E2-specific HMAbs isolated to date, including HMAbs CBH-related antibodies (CBH-5, -7, -4B, -4D, -4G,-8E) (Chan *et al.*, 2001), all HC84-related antibodies (Krey *et al.*, 2013), AR3C (Kong *et al.*, 2013), as well as two recently reported HMAb panels isolated from acute resolvers, AT12-related antibodies (AT12-009, AT12-010, AT12-001, AT13-021) (Merat *et al.*, 2016) and HEPC-related antibodies (HEPC3, HEPC98, HEPC43, HEPC74) (Bailey *et al.*, 2017). It is also the V_H germline lineage prevalent in B cell clones isolated from HCV-associated B-lymphoproliferative disorders, in combination with the VL kv325 gene (Gasparotto *et al.*, 2002; Ivanovski *et al.*, 1998; Sasso *et al.*, 2001). Intriguingly, the usage of V_H1-69 gene has also been extensively described in HMAbs broadly reactive against two other antigenically diverse viruses, HIV and influenza virus (Corti *et al.*, 2010; Ekiert *et al.*, 2009; Ekiert *et al.*, 2011; Huang *et al.*, 2004; Kunert *et al.*, 2004; Luftig *et al.*, 2006; Morris *et al.*, 2011; Sui *et al.*, 2009; Throsby *et al.*, 2008; Wrammert *et al.*, 2011). Unique to this germline gene is a well conserved hydrophobic tip at its CDR-H2 (I^{H52}, F^{H55}) (Huang *et al.*, 2004). This hydrophobic CDR-H2 enables HIV-specific brNAb 17b to access the CD4-induced gp120 surface whilst anchoring the CDR-H3 to form intimate contact with gp120. For influenza virus brNAb CR6261, the V_H1-69-derived CDR-H1 and CDR-H2 are solely responsible for the antibody recognition of the conserved membrane proximal helical

stem of hemagglutinin (Ekiert *et al.*, 2011; Throsby *et al.*, 2008). Based on the crystal structures of HCV brNAbs HC84.27 and AR3C, it appears that this CDR-H2 plays a role in facilitating antibody access to the hydrophobic pocket at the putative fusion/CD81 binding helical structure G^{436}WLAGLFY (Drummer *et al.*, 2006; Kong *et al.*, 2013; Krey *et al.*, 2013). Nevertheless, in HCV infections, the exact ontogeny and role of V_H1-69-derived B cell lineages remains elusive. One study found that the usage of V_H1-69 in the naïve B cells of acute resolvers is significantly higher (~6-folds) than those of chronic HCV, although whether such usage is directly contributed by HCV is not known (Racanelli *et al.*, 2011). In the phage library candidate 5032, it is unclear whether the observed two V_H1-69 B cell clones were part of the inactivated, naïve B cell pool in the blood, or associated with chronic HCV, possibly responsible for the highly potent HCV-specific cross-NAbs. Additionally, limited clones were analyzed here using Sanger sequencing, and this may create some bias in clone frequency. Future quantitative studies investigating the ontogeny and evolution of HCV-specific V_H1-69 B cell lineages in acute and chronic HCV may answer this question and provide the insight in the potential role of specific B cell lineages in HCV control and prevention and aid the design of germline-specific immune interventions.

Despite the high titres of D123-reactive antibodies observed in 5032 plasma, no D123-binding Fabs were isolated from the phage libraries constructed from the concurrent PBMCs. This may be largely due to the low frequency of broadly reactive HCV-specific B cell clones found in the circulating blood. Flow cytometric analyses by others and our group showed that HCV E2 or D123-specific memory B cells only constitute 0.2-0.78% of total B cells in the circulating blood of chronic HCV patients (Boisvert *et al.*, 2016) (Ms Irene Boo and A/P Heidi Drummer, personal communication). The highly potent cross NAbs observed in some chronic HCV patients are therefore likely contributed by a very small number of HCV-activated B cells that express immunoglobulins at extremely high levels. In the case of 5032 whose PBMCs were collected after IFN-associated viral clearance, the absence of HCV-specific antigen simulation following clearance may additionally result in a gradual decay of such HCV-specific B cells, and this would further decrease the frequency of HCV-specific B cells available in PBMC samples. These corroborate

with the sequencing results of 5032 library Fab clones, as most of the available sequences did not appear to have undergone extensive antigen-driven somatic hypermutation, especially in the antigen-binding CDRs. For future HCV immune library construction or B cell studies, pooled PBMC samples from multiple chronic neutralizers and/or pre-sorting of HCV-specific B cells may be required to enrich for the rare HCV-specific B cells.

Here, the amplification and characterization of the 5032 antibody repertoire relied primarily on the primers described by de Haard (2002). Based on the knowledge on antibody genes and alleles at the time, the HC/LC primers were designed such that the HC and LC sequences from the V_H subgroups 1-7, Vk subgroups 1-6, and Vλ subgroups 1-7 can be amplified. Currently, there are 7 IGHV subgroups (159 genes and 422 alleles), 7 IGKV subgroups (77 genes and 114 alleles) and 16 IGLV subgroups (75 genes and 128 alleles) identified and deposited in the IMGT/GENE-DB database (Giudicelli *et al.*, 2005). It is therefore very likely that new degenerate primers need to be included to amplify some of the newly described or novel genes and/or alleles. Whilst the effects of PCR bias introduced by the primer library on the overall % distribution of HC and LC sequences is unclear, the recombination of HC/LC during the phage construction will ultimately influence the full recapitulation of the native BCR repertoire of 5032. Together, these further highlighted some of the technical limitations of phage display technique in the isolation of rare HCV-specific B cell clones. Future library construction may consider utilising up-to-date and optimised phage vector platforms from commercial sources such as the Creative Biolabs (Shirley, NY USA) or NeoClone (Madison, WI USA). Additionally, in this study, the isolation of HCV E2-reactive Fab clones utilised immobilized unfractionated D123 and D123 HMWs, as the two forms of E2 proteins demonstrated highly effective engagement of brNAb BCRs in a small animal model (Vietheer *et al.*, 2017). The recent mapping of the antigenic surface of different D123 species revealed that the HMW forms have an antigenic surface, distinctively different compared to the monomeric D123, at both the NAb and non-NAb faces (discussed in Chapter 3). D123 monomer may pose as an alternative panning target for isolating E2-specific brNAbs in the future.

In summary, the isolation and characterization of novel HCV-specific brNAbs is an ongoing challenge. Successful isolation of HCV brNAbs can only be achieved with the effective screening of individuals with potent brNAbs, the preparation of the B cell repertoire that not only incorporate rare, low-frequency BCR clones but also recapitulate the native B cell pool, as well as E2 antigen that enable the selection of broadly reactive HMAbs that recognize epitopes native on HCV E2. Future isolation and characterization of novel brNAbs in HCV will provide insights in the design and development of vaccine candidates that optimally engage B cell clones which offer broadly protective antibody response.

Chapter 6 General discussion and conclusion

Direct acting antivirals with high SVR rate of >95% have the ability to treat people with existing HCV infection and greatly reduce the number of people living with chronic HCV. However, to prevent new infection and reinfection, a universal vaccine for HCV is essential but has not been developed. An effective HCV vaccine should elicit potent and multi-specific T and B cell responses that provide protection against all circulating genotypes and subtypes of HCV with long-lasting immunity. To inform the design and development of the antibody generating component(s) of an HCV vaccine, this thesis explored the roles of antigenic domains on the HCV glycoprotein E2 in the generation and function of antibodies, particularly broadly reactive neutralizing antibodies.

A major finding of Chapter 3 was that the three HVRs on E2 modulate the antigenicity of conserved NAb epitopes as well as non-NAb epitopes on E2. Whilst the presence of the three HVRs greatly reduces the ability of both neutralizing MAbs and non-neutralizing MAbs to recognize E2 and inhibit E2-CD81 interaction, the deletion of HVRs enhances the immunogenicity of at least two major NAb epitopes on E2, the 408-428 region and the 530-549 region. In addition to HVRs, the intermolecular disulfide organization also plays a role in the antigenicity of NAb and non-NAb epitopes on E2. The HMW forms of both WT E2 and D123 were shown to elicit potent, pan-genotypic broadly neutralizing antibodies, effective against all 7 HCV genotypes, and demonstrated high immunogenicity towards all three NAb epitopes on E2. By contrast, the monomeric forms of WT E2 and D123, generated antibodies to non-NAb epitopes, especially within the 630-635 region. The brNAb specificities observed in D123 HMW forms is possibly contributed by the occlusion of the non-NAb face and the stabilization of the flexible NAb face on E2, which re-directs the antibody response from the non-NAb epitope on E2 to conserved and possibly stabilized NAb epitopes.

One main question in the design of D123-based immunogen remains unsolved: the exact folding and oligomeric arrangement of E2. The full-length E2 contains 18 cysteines (C1 to C18). The exact intramolecular and intermolecular pairing arrangement in the context of full-length E2 remains unclear. Given that free

thiols are found on both E1 and E2 and are required for HCVcc and HCVpp entry, cysteines on full-length E2 may contain flexible intramolecular and intermolecular disulfide pairing that is involved in disulfide reduction and/or isomerization during viral entry or fusion (Fraser *et al.*, 2011). While no studies to date have investigated the intermolecular disulfide connectivity of E2, the two crystal structures of E2 revealed different disulfide arrangement within the monomeric E2, possibly due to the different number of cysteines present in each E2 protein (Khan *et al.*, 2014; Kong *et al.*, 2013). The E2 from Khan's study formed exclusively monomers (14 cysteines, C3-C17), whereas Kong's E2 protein (16 cysteines, C1-C16) is expressed as monomers as well as "aggregates" and contains 7 disulfide bridges and two disordered cysteines (C3 and C4, flanking HVR2). In comparison, the E2 RBD construct used in this study contains the majority of cysteine(s) residues within E2 (17 cysteines, C1-C17). Vietheer *et al* (2017) showed that when HVRs are absent, structural differences between E2 RBD monomer and HMWs are found in the 424-428 and 630-635 regions, both of which are less accessible in HMW forms of these proteins. Given that the 424-428 and 630-635 regions are found adjacent to C1/C2 and C16/C17 in Kong's structure, these four cysteines (C1/C2, C16/C17) may therefore be implicated in the covalent association of E2 monomers. However, the possibility of the involvement of the two flexible cysteines, C3/C4, or a more dramatic reshuffling of cysteine pairing upon E2 oligomerization cannot be ruled out. Future studies are needed to determine the intermolecular disulfide pairing of E2 and D123 and the exact D123 oligomer optimal for inclusion in an HCV vaccine.

In addition to NAb epitope immunogenicity, another key question surrounding the efficacy of vaccines for the highly diverse HCV is whether the virus can escape from brNAbs. Chapter 4 showed that HCV rapidly acquires resistance against the brNAb MAb24 *in vitro*. Considered as a highly desirable antigenic component in HCV vaccines, the MAb24 recognition site (residues 412-423) is absent from the current high-resolution E2 structures and is predicted to be located distal to the NAb face of E2, adjacent to HVR1. Chapter 4 found that direct modifications at residue 415 confer MAb24 resistance but significantly compromise the immunological fitness of the virus, rendering it more sensitive to other brNAbs such as AR3C and HC84.27 that target the neutralizing face of E2. These findings reinforce the notions that D123

is a preferred vaccine candidate as it elicits a multi-specific NAb response (Chapter 3), greatly reducing the likelihood of selecting escape variants.

Whilst Chapter 4 demonstrated that direct changes at the epitope residue N415 affect MAb24 functions, several lines of evidence also suggested that the efficacy of MAb24-like brNAbs was influenced by the HVRs. For instance, the deletion of all three HVRs enhanced the ability of MAb24 to inhibit E2-CD81 binding, with a 12-fold decrease in IC_{50}s (Alhammad *et al.*, 2015a). In addition, HVR1 deletion resulted in increased sensitivity of HCVcc to AP33 and 3/11 whereas the replacement of HVRs derived from the sensitive HCV strain H77c with those of the resistant strain Con1 significantly reduced the ability of MAb24 to neutralize HCVpp (Meola *et al.*, 2015) (Mr Kevin te Wierik & A/P Heidi Drummer, unpublished data). These findings further highlighted the knowledge gap of the current E2 core structures where the structural details of this key brNAb epitope in the context of E2 or E1E2 heterodimer are missing. Structural studies into the links between the 412-423 region, and the NAb face and the HVRs are needed. Further studies are also required to determine whether the same resistance mechanism against MAb24 applies to other HCV genotypes (G3a-G7).

In natural HCV infections, the roles of antibodies in the control or the persistence of HCV remains elusive. Chapter 5 investigated the NAb response in chronic HCV which represents the majority of HCV infection, and is a key source of cross-NAbs as well as the target for a therapeutic vaccine. Although the attempt in isolating broadly reactive antibodies from a subject with chronic HCV (G6a) who had potent cross-NAbs was unsuccessful, the close examination of their total amplified B cell repertoire identified interesting B cell lineages, V_H1-69 and V_H5-51 genes. Utilised in most E2-specific HMAbs isolated to date, the V_H1-69 gene was also identified in HCV antigen-induced lymphoproliferative disease as a result of chronic HCV antigen activation (Ivanovski *et al.*, 1998). This restricted usage of V_H1-69 gene and over-proliferation of V_H1-69-derived B cells during chronic HCV may limit the antibody specificities generated in chronic infection, contributing to viral persistence. Alternatively, this exclusive usage of V_H1-69-derived B cells may be required for the production of brNAbs which clear HCV, and the delayed proliferation

and/or somatic hypermutation of such cells, as a result of genetic polymorphisms such as the varying copies of V_H1-69 alleles (1-4 copies), is associated with HCV persistence observed in some individuals but not others.

With limited tools for screening and isolating broadly reactive antibodies, most HCV antibody studies to date focus on the immunochemical characterization of the polyclonal antibodies elicited in chronic HCV. No studies have systematically examined the B cell repertoire in HCV. Future high throughput sequencing analyses of the circulating B cell transcripts during acute and chronic HCV infection may provide insight into the role of B lineages, such as V_H1-69 and V_H5-51, in infection outcomes, which may guide the design of a germline-targeted preventative and therapeutic vaccine for HCV. Bioinformatics analyses of the B cell transcripts, in combination with transcript sequence-based antibody expression and characterization may additionally identify new brNAbs that target novel brNAb epitopes on HCV.

Current efforts to develop an antibody-based vaccine for HCV focus primarily on identifying the ideal immunogen(s) (E2 alone or E1E2, as recombinant protein, or as HCV-VLPs, or encoded in viral vectors) and examining the immunogenicity of each candidate in small animal models and/or non-human primates. One of the best-characterized HCV glycoprotein-based immunogen is gpE1/gpE2 (G1a, strain HCV1). This recombinant E1E2 heterodimer (administered with MF59 as the adjuvant) has demonstrated immunogenicity in various animal models as well as healthy humans (Choo *et al.*, 1994; Law *et al.*, 2013; Wong *et al.*, 2014). Whilst the inclusion of E1 into the vaccine facilitates the generation of E1-specific antibodies, the expression of E1E2 heterodimer gpE1/gpE2 is retained in the ER, and can only be purified from cell lysates using GNA lectin (Law *et al.*, 2013). This poses a technical challenge to the large-scale production of such a vaccine. To address this issue, affinity purification tags such as human IgG1 Fc region or the FLAG tag have been introduced into the N or C-terminus of the HVR1 of E2 (Krapchev *et al.*, 2018; Logan *et al.*, 2017). Nevertheless, the intracellularly-expressed E1E2 heterodimer elicited high titres of type-specific anti-HVR1 antibodies and showed limited capacity to induce cross-reactive antibodies in humans (Law *et al.*, 2013; Ray *et al.*, 2010). In chimpanzees challenged with homologous virus, the gpE1/gpE2 immunization only

partially delayed viremia (Puig *et al.*, 2004). An alternative approach is the use of recombinant E2 protein, sE2 (residues 384-661, G1b, strain Con1, administered with either Alum, CpG or MPL as the adjuvant), which is expressed as a soluble protein allowing efficient purification from the tissue culture fluid of transiently or stably transfected cells (Li *et al.*, 2016). Mice immunized with insect cell derived sE2 in Alum, CpG or MPL produced high titres of cross NAbs, which neutralized all 7 genotypes of HCVcc *in vitro* (>50% neutralization at 1:40 dilution of the sera). Furthermore, prior immunization with sE2 protected humanized mice from infection by a heterologous virus (G2a). In rhesus macaques, immunization with sE2 elicited cross-NAbs as well as systemic and intrahepatic E2-specific memory T cells (Li *et al.*, 2017).

Similar to sE2, the vaccine candidate investigated in this thesis D123 is a soluble, affinity-purified E2-based immunogen, and in guinea pigs, its high molecular weight form elicited high titres of cross-reactive antibodies that can neutralize all 7 genotypes of HCV *in vitro*. Most importantly, D123 HMW generates a poly-specific broadly reactive antibody response, making it a promising candidate for a universal HCV vaccine. Future efforts to improve D123 efficacy should be directed to enhancing the immunogenicity of NAb epitopes on D123 such as modification of the intermolecular disulfide arrangement and glycan surface and high-efficiency, low-cost production. Alternatively, D123 may be produced in the context of E1E2 heterodimers. The incorporation of E1 in the expression and folding of E2 may provide structural constraints on the NAb face of E2, stabilizing the otherwise flexible and low/non-immunogenic NAb epitopes on monomeric D123. This may also enable the generation of broadly neutralizing antibodies specific to E1 (such as MAbs IGH526 and IGH520) and E1E2 heterodimers (such as MAbs AR4A and AR5A), which cannot be achieved with E2 immunogens alone. A major technical challenge to the production of such an immunogen is the expression of E1E2 heterodimers that are secreted and properly folded. The E1E2 heterodimer is stabilized through interactions mediated by their TMDs, stem regions and HVR2, whilst the TMDs of both E1 and E2 contain ER retention signals (Albecka *et al.*, 2011; Cocquerel *et al.*, 1998; Drummer & Poumbourios, 2004; McCaffrey *et al.*, 2011). Previous studies in the Baculovirus expression system showed that the replacement of the TMDs of E1E2

with the leucine zipper pair *jun* and *fos*, facilitates the heterodimerization and enables secretion of E1E2 heterodimers into extracellular space (Gu, 2010). Further studies into these Baculovirus-expressed E1E2 heterodimers with E2 HVRs replaced with longer linkers, especially around the large HVR2 region, may pave an alternative path for HCV vaccine development.

In conclusion, this thesis increased knowledge on the antigenic domains on HCV glycoprotein E2 and their roles in the generation and recognition of neutralizing antibodies. The findings will aid the design of a universal antibody-based HCV vaccine that have improved immunogenicity, with the ultimate goal of pan-genotypic efficacy and sterilising immunity.

Bibliography

Abe, K., Inchauspe, G., Shikata, T. & Prince, A. M. (1992). Three different patterns of hepatitis C virus infection in chimpanzees. *Hepatology* **15**, 690-695.

Acton, S., Rigotti, A., Landschulz, K. T., Xu, S. & et al. (1996). Identification of scavenger receptor SR-BI as a high density lipoprotein receptor. *Science* **271**, 518.

Afdhal, N. H. (2004). The natural history of hepatitis C. *Seminars in Liver Disease* **24**, 3-8.

Aitken, C. K., McCaw, R. F., Bowden, D. S., Tracy, S. L., Kelsall, J. G., Higgs, P. G., Kerger, M. J., Nguyen, H. & Crofts, J. N. (2004). Molecular epidemiology of hepatitis C virus in a social network of injection drug users. *The Journal of Infectious Diseases* **190**, 1586-1595.

Aitken, C. K., Lewis, J., Tracy, S. L., Spelman, T., Bowden, D. S., Bharadwaj, M., Drummer, H. & Hellard, M. (2008). High incidence of hepatitis C virus reinfection in a cohort of injecting drug users. *Hepatology* **48**, 1746-1752.

Akazawa, D., Moriyama, M., Yokokawa, H., Omi, N., Watanabe, N., Date, T., Morikawa, K., Aizaki, H., Ishii, K., Kato, T., Mochizuki, H., Nakamura, N. & Wakita, T. (2013). Neutralizing antibodies induced by cell culture–derived hepatitis C virus protect against infection in mice. *Gastroenterology* **145**, 447-455.e444.

Albecka, A., Montserret, R., Krey, T., Tarr, A. W., Diesis, E., Ball, J. K., Descamps, V., Duverlie, G., Rey, F., Penin, F. & Dubuisson, J. (2011). Identification of new functional regions in hepatitis C virus envelope glycoprotein E2. *Journal of Virology* **85**, 1777-1792.

Albecka, A., Belouzard, S., de Beeck, A. O., Descamps, V., Goueslain, L., Bertrand-Michel, J., Tercé, F., Duverlie, G., Rouillé, Y. & Dubuisson, J. (2012). Role of low-density lipoprotein receptor in the hepatitis C virus life cycle. *Hepatology* **55**, 998-1007.

Alhammad, Y., Gu, J., Boo, I., Harrison, D., McCaffrey, K., Vietheer, P. T., Edwards, S., Quinn, C., Coulibaly, F., Poumbourios, P. & Drummer, H. E. (2015a). Monoclonal antibodies directed toward the hepatitis C virus glycoprotein E2 detect antigenic differences modulated by the N-terminal hypervariable region 1 (HVR1), HVR2, and intergenotypic variable region. *Journal of Virology* **89**, 12245-12261.

Alhammad, Y. M. O., Maharajh, S., Butcher, R., Eden, J.-S., White, P. A., Poumbourios, P. & Drummer, H. E. (2015b). Longitudinal sequence and functional evolution within glycoprotein E2 in hepatitis C virus genotype 3a Infection. *PLoS One* **10**, e0126397.

Allander, T., Beyene, A., Jacobson, S. H., Grillner, L. & Persson, M. A. A. (1997). Patients infected with the same hepatitis C virus strain display different kinetics of the isolate-specific antibody response. *Journal of Infectious Diseases* **175**, 26-31.

Allander, T., Drakenberg, K., Beyene, A., Rosa, D., Abrignani, S., Houghton, M., Widell, A., Grillner, L. & Persson, M. A. A. (2000). Recombinant human monoclonal antibodies against different conformational epitopes of the E2 envelope glycoprotein of hepatitis C virus that inhibit its interaction with CD81. *Journal of General Virology* **81**, 2451-2459.

Alter, H., Holland, P., Purcell, R. & Popper, H. (1978). Transmissible agent in non-A, non-B hepatitis. *The Lancet* **311**, 459-463.

Alter, H. J. & Seeff, L. B. (2000). Recovery, persistence, and sequelae in hepatitis C virus infection: a perspective on long-term outcome. *Seminars in Liver Disease* **20**, 0017-0036.

André, P., Komurian-Pradel, F., Deforges, S., Perret, M., Berland, J. L., Sodoyer, M., Pol, S., Bréchot, C., Paranhos-Baccalà, G. & Lotteau, V. (2002). Characterization of low- and very-low-density hepatitis C virus RNA-containing particles. *Journal of Virology* **76**, 6919-6928.

Babcock, G. J., Iyer, S., Smith, H. L., Wang, Y., Rowley, K., Ambrosino, D. M., Zamore, P. D., Pierce, B. G., Molrine, D. C. & Weng, Z. (2014). High-throughput sequencing analysis of post-liver transplantation HCV E2 glycoprotein evolution in the presence and absence of neutralizing monoclonal antibody. *PLoS One* **9**, e100325.

Bailey, J. R., Flyak, A. I., Cohen, V. J., Li, H., Wasilewski, L. N., Snider, A. E., Wang, S., Learn, G. H., Kose, N., Loerinc, L., Lampley, R., Cox, A. L., Pfaff, J. M., Doranz, B. J., Shaw, G. M., Ray, S. C. & Crowe, J. E., Jr. (2017). Broadly neutralizing antibodies with few somatic mutations and hepatitis C virus clearance. *JCI Insight* **2**, e92872.

Bankwitz, D., Steinmann, E., Bitzegeio, J., Ciesek, S., Friesland, M., Herrmann, E., Zeisel, M. B., Baumert, T. F., Keck, Z.-y., Foung, S. K. H., Pécheur, E.-I. & Pietschmann, T. (2010). Hepatitis C virus hypervariable region 1 modulates receptor interactions, conceals the CD81 binding site, and protects conserved neutralizing epitopes. *Journal of Virology* **84**, 5751-5763.

Barnard, R., Chopra, A., James, I., Blinco, J., Watson, M. W., Jabara, C. B., Hazuda, D., Lemon, S. M., Mallal, S. & Gaudieri, S. (2016). Primer ID ultra-deep sequencing reveals dynamics of drug resistance-associated variants in breakthrough hepatitis C viruses: relevance to treatment outcome and resisatnce screening. *Antiviral Therapy* **21**, 567-577.

Barnes, E., Folgori, A., Capone, S., Swadling, L., Aston, S., Kurioka, A., Meyer, J., Huddart, R., Smith, K., Townsend, R., Brown, A., Antrobus, R., Ammendola, V., Naddeo, M., O'Hara, G., Willberg, C., Harrison, A., Grazioli, F., Esposito, M. L., Siani, L., Traboni, C., Oo, Y., Adams, D., Hill, A., Colloca, S., Nicosia, A., Cortese, R. & Klenerman, P. (2012). Novel adenovirus-based vaccines induce broad and sustained T cell responses to HCV in man. *Science Translational Medicine* **4**, 115ra111-115ra111.

Barth, H., Schäfer, C., Adah, M. I., Zhang, F., Linhardt, R. J., Toyoda, H., Kinoshita-Toyoda, A., Toida, T., van Kuppevelt, T. H., Depla, E., von Weizsäcker, F., Blum, H. E. & Baumert, T. F. (2003). Cellular binding of hepatitis C virus envelope glycoprotein E2 requires cell surface heparan sulfate. *Journal of Biological Chemistry* **278**, 41003-41012.

Bartosch, B., Bukh, J., Meunier, J.-C., Granier, C., Engle, R. E., Blackwelder, W. C., Emerson, S. U., Cosset, F.-L. & Purcell, R. H. (2003a). In vitro assay for neutralizing antibody to hepatitis C virus: evidence for broadly conserved neutralization epitopes. *Proceedings of the National Academy of Sciences of the United States of America* **100**, 14199-14204.

Bartosch, B., Dubuisson, J. & Cosset, F.-L. (2003b). Infectious hepatitis C virus pseudo-particles containing functional E1–E2 envelope protein complexes. *The Journal of Experimental Medicine* **197**, 633-642.

Bartosch, B., Vitelli, A., Granier, C., Goujon, C., Dubuisson, J., Pascale, S., Scarselli, E., Cortese, R., Nicosia, A. & Cosset, F.-L. (2003c). Cell entry of hepatitis C virus requires a set of co-receptors that include the CD81 tetraspanin and the SR-B1 scavenger receptor. *Journal of Biological Chemistry* **278**, 41624-41630.

Bartosch, B., Verney, G., Dreux, M., Donot, P., Morice, Y., Penin, F., Pawlotsky, J.-M., Lavillette, D. & Cosset, F.-L. (2005). An interplay between hypervariable region 1 of the hepatitis C virus E2 glycoprotein, the scavenger receptor BI, and high-density lipoprotein promotes both enhancement of infection and protection against neutralizing antibodies. *Journal of Virology* **79**, 8217-8229.

Bassett, S. E., Brasky, K. M. & Lanford, R. E. (1998). Analysis of hepatitis C virus-inoculated chimpanzees reveals unexpected clinical profiles. *Journal of Virology* **72**, 2589-2599.

Bassett, S. E., Guerra, B., Brasky, K., Miskovsky, E., Houghton, M., Klimpel, G. R. & Lanford, R. E. (2001). Protective immune response to hepatitis C virus in chimpanzees rechallenged following clearance of primary infection. *Hepatology* **33**, 1479-1487.

Basu, A., Beyene, A., Meyer, K. & Ray, R. (2004). The hypervariable region 1 of the E2 glycoprotein of hepatitis C virus binds to glycosaminoglycans, but this binding does not lead to infection in a pseudotype system. *Journal of Virology* **78**, 4478-4486.

Baumert, T. F., Ito, S., Wong, D. T. & Liang, T. J. (1998). Hepatitis C virus structural proteins assemble into virus-like particles in insect cells. *Journal of Virology* **72**, 3827-3836.

Beld, M., Penning, M., van Putten, M., Lukashov, V., van den Hoek, A., McMorrow, M. & Goudsmit, J. (1999). Quantitative antibody responses to structural (core) and nonstructural (NS3, NS4, and NS5) hepatitis C virus proteins among seroconverting injecting drug users: impact of epitope variation and relationship to detection of HCV RNA in blood. *Hepatology* **29**, 1288-1298.

Benedicto, I., Molina-Jiménez, F., Bartosch, B., Cosset, F.-L., Lavillette, D., Prieto, J., Moreno-Otero, R., Valenzuela-Fernández, A., Aldabe, R., López-Cabrera, M. & Majano, P. L. (2009). The tight junction-associated protein occludin is required for a postbinding step in hepatitis C virus entry and infection. *Journal of Virology* **83**, 8012-8020.

Bertaux, C. & Dragic, T. (2006). Different domains of CD81 mediate distinct stages of hepatitis C virus pseudoparticle entry. *Journal of Virology* **80**, 4940-4948.

Bharadwaj, M., Thammanichanond, D., Aitken, C. K., Moneer, S., Drummer, H. E., Tracy, S., Holdsworth, R., Bowden, S., Jackson, D., Hellard, M., Torresi, J. & McCluskey, J. (2009). TCD8 response in diverse outcomes of recurrent exposure to hepatitis C virus. *Immunology and Cell Biology* **87**, 464-472.

Bility, M. T., Zhang, L., Washburn, M. L., Curtis, T. A., Kovalev, G. I. & Su, L. (2012). Generation of a humanized mouse model with both human immune system and liver cells to model hepatitis C virus infection and liver immunopathogenesis. *Nature Protocols* **7**, 1608-1617.

Björkander, J., Cunningham-Rundles, C., Lundin, P., Olsson, R., Söderström, R. & Hanson, L. Å. (1988). Intravenous immunoglobulin prophylaxis causing

liver damage in 16 of 77 patients with hypogammaglobulinemia or IgG subclass deficiency. *The American Journal of Medicine* **84**, 107-111.

Bjoro, K., Froland, S. S., Yun, Z., Samdal, H. H. & Haaland, T. (1994). Hepatitis C infection in patients with primary hypogammaglobulinemia after treatment with contaminated immune globulin. *New England Journal of Medicine* **331**, 1607-1611.

Blanchard, E., Belouzard, S., Goueslain, L., Wakita, T., Dubuisson, J., Wychowski, C. & Rouillé, Y. (2006). Hepatitis C virus entry depends on clathrin-mediated endocytosis. *Journal of Virology* **80**, 6964-6972.

Blight, K. J., McKeating, J. A. & Rice, C. M. (2002). Highly permissive cell lines for subgenomic and genomic hepatitis C virus RNA replication. *Journal of Virology* **76**, 13001-13014.

Boisvert, M., Zhang, W., Elrod, E. J., Bernard, N. F., Villeneuve, J.-P., Bruneau, J., Marcotrigiano, J., Shoukry, N. H. & Grakoui, A. (2016). Novel E2 glycoprotein tetramer detects hepatitis C virus–specific memory B cells. *The Journal of Immunology* **197**, 4848-4858.

Boo, I., teWierik, K., Douam, F., Lavillette, D., Poumbourios, P. & Drummer, Heidi E. (2012). Distinct roles in folding, CD81 receptor binding and viral entry for conserved histidine residues of hepatitis C virus glycoprotein E1 and E2. *Biochemical Journal* **443**, 85-94.

Booth, J. C., Kumar, U., Webster, D., Monjardino, J. & Thomas, H. C. (1998). Comparison of the rate of sequence variation in the hypervariable region of E2/NS1 region of hepatitis C virus in normal and hypogammaglobulinemic patients. *Hepatology* **27**, 223-227.

Bradley, D., McCaustland, K., Krawczynski, K., Spelbring, J., Humphey, C. & Cook, E. H. (1991). Hepatitis C virus: buoyant density of the factor VIII-derived isolate in sucrose. *Journal of Medical Virology* **34**, 206-208.

Brazzoli, M., Helenius, A., Foung, S. K. H., Houghton, M., Abrignani, S. & Merola, M. (2005). Folding and dimerization of hepatitis C virus E1 and E2 glycoproteins in stably transfected CHO cells. *Virology* **332**, 438-453.

Brazzoli, M., Bianchi, A., Filippini, S., Weiner, A., Zhu, Q., Pizza, M. & Crotta, S. (2008). CD81 Is a central regulator of cellular events required for hepatitis C virus infection of human hepatocytes. *Journal of Virology* **82**, 8316-8329.

Brochet, X., Lefranc, M.-P. & Giudicelli, V. (2008). IMGT/V-QUEST: the highly customized and integrated system for IG and TR standardized V-J and V-D-J sequence analysis. *Nucleic Acids Research* **36**, W503-W508.

Broering, T. J., Garrity, K. A., Boatright, N. K., Sloan, S. E., Sandor, F., Thomas, W. D., Szabo, G., Finberg, R. W., Ambrosino, D. M. & Babcock, G. J. (2009). Identification and characterization of broadly neutralizing human monoclonal antibodies directed against the E2 envelope glycoprotein of hepatitis C virus. *Journal of Virology* **83**, 12473-12482.

Bukh, J. (2004). A critical role for the chimpanzee model in the study of hepatitis C. *Hepatology* **39**, 1469-1475.

Bukh, J., Thimme, R., Meunier, J.-C., Faulk, K., Spangenberg, H. C., Chang, K.-M., Satterfield, W., Chisari, F. V. & Purcell, R. H. (2008). Previously infected chimpanzees are not consistently protected against reinfection or persistent infection after reexposure to the identical hepatitis C virus strain. *Journal of Virology* **82**, 8183-8195.

Burioni, R., Plaisant, P., Manzin, A., Rosa, D., Carri, V. D., Bugli, F., Solforosi, L., Abrignani, S., Varaldo, P. E., Fadda, G. & Clementi, M. (1998).

Dissection of human humoral immune response against hepatitis C virus E2 glycoprotein by repertoire cloning and generation of recombinant Fab fragments. *Hepatology* **28**, 810-814.

Burton, D. R., Poignard, P., Stanfield, R. L. & Wilson, I. A. (2012). Broadly neutralizing antibodies present new prospects to counter highly antigenically diverse viruses. *Science* **337**, 183-186.

Callens, N., Ciczora, Y., Bartosch, B., Vu-Dac, N., Cosset, F.-L., Pawlotsky, J.-M., Penin, F. & Dubuisson, J. (2005). Basic residues in hypervariable region 1 of hepatitis C virus envelope glycoprotein E2 contribute to virus entry. *Journal of Virology* **79**, 15331-15341.

Caraux, G. & Pinloche, S. (2005). PermutMatrix: a graphical environment to arrange gene expression profiles in optimal linear order. *Bioinformatics* **21**, 1280-1281.

Catanese, M. T., Graziani, R., von Hahn, T., Moreau, M., Huby, T., Paonessa, G., Santini, C., Luzzago, A., Rice, C. M., Cortese, R., Vitelli, A. & Nicosia, A. (2007). High-avidity monoclonal antibodies against the human scavenger class B Type I receptor efficiently block hepatitis C virus infection in the presence of high-density lipoprotein. *Journal of Virology* **81**, 8063-8071.

Catanese, M. T., Ansuini, H., Graziani, R., Huby, T., Moreau, M., Ball, J. K., Paonessa, G., Rice, C. M., Cortese, R., Vitelli, A. & Nicosia, A. (2010). Role of scavenger receptor class B Type I in hepatitis C virus entry: kinetics and molecular determinants. *Journal of Virology* **84**, 34-43.

Catanese, M. T., Uryu, K., Kopp, M., Edwards, T. J., Andrus, L., Rice, W. J., Silvestry, M., Kuhn, R. J. & Rice, C. M. (2013). Ultrastructural analysis of hepatitis C virus particles. *Proceedings of the National Academy of Sciences of the United States of America* **110**, 9505-9510.

Catanese, M. T. & Dorner, M. (2015). Advances in experimental systems to study hepatitis C virus in vitro and in vivo. *Virology* **479–480**, 221-233.

Chan, C. H., Hadlock, K. G., Foung, S. K. H. & Levy, S. (2001). VH1-69 gene is preferentially used by hepatitis C virus–associated B cell lymphomas and by normal B cells responding to the E2 viral antigen. *Blood* **97**, 1023-1026.

Chatel-Chaix, L., Germain, M.-A., Götte, M. & Lamarre, D. (2012). Direct-acting and host-targeting HCV inhibitors: current and future directions. *Current Opinion in Virology* **2**, 588-598.

Chen, M., Sällberg, M., Sönnerborg, A., Weiland, O., Mattsson, L., Jin, L., Birkett, A., Peterson, D. & Milich, D. R. (1999). Limited humoral immunity in hepatitis C virus infection. *Gastroenterology* **116**, 135-143.

Chiba, H., Osanai, M., Murata, M., Kojima, T. & Sawada, N. (2008). Transmembrane proteins of tight junctions. *Biochimica et Biophysica Acta (BBA) - Biomembranes* **1778**, 588-600.

Choo, Q.-L., Kuo, G., Weiner, A. J., Overby, L. R., Bradley, D. W. & Houghton, M. (1989). Isolation of a cDNA clone derived from a blood-borne non-A, non-B viral hepatitis genome. *Science* **244**, 359-362.

Choo, Q. L., Richman, K. H., Han, J. H., Berger, K., Lee, C., Dong, C., Gallegos, C., Coit, D., Medina-Selby, R. & Barr, P. J. (1991). Genetic organization and diversity of the hepatitis C virus. *Proceedings of the National Academy of Sciences of the United States of America* **88**, 2451-2455.

Choo, Q. L., Kuo, G., Ralston, R., Weiner, A., Chien, D., Van Nest, G., Han, J., Berger, K., Thudium, K. & Kuo, C. (1994). Vaccination of chimpanzees

against infection by the hepatitis C virus. *Proceedings of the National Academy of Sciences of the United States of America* **91**, 1294-1298.

Choukhi, A., Ung, S., Wychowski, C. & Dubuisson, J. (1998). Involvement of endoplasmic reticulum chaperones in the folding of hepatitis C virus glycoproteins. *Journal of Virology* **72**, 3851-3858.

Christie, J. M. L., Healey, C. J., Watson, J., Wong, V. S., Duddridge, M., Snowden, N., Rosenberg, W. M. C., Fleming, K. A., Chapel, H. & Chapman, R. W. G. (1997). Clinical outcome of hypogammaglobulinaemic patients following outbreak of acute hepatitis C: 2 year follow up. *Clinical & Experimental Immunology* **110**, 4-8.

Chung, R. T., Gordon, F. D., Curry, M. P., Schiano, T. D., Emre, S., Corey, K., Markmann, J. F., Hertl, M., Pomposelli, J. J., Pomfret, E. A., Florman, S., Schilsky, M., Broering, T. J., Finberg, R. W., Szabo, G., Zamore, P. D., Khettry, U., Babcock, G. J., Ambrosino, D. M., Leav, B., Leney, M., Smith, H. L. & Molrine, D. C. (2013). Human monoclonal antibody MBL-HCV1 delays HCV viral rebound following liver transplantation: a randomized controlled study. *American Journal of Transplantation* **13**, 1047-1054.

Clayton, R. F., Owsianka, A., Aitken, J., Graham, S., Bhella, D. & Patel, A. H. (2002). Analysis of antigenicity and topology of E2 glycoprotein present on recombinant hepatitis C virus-like particles. *Journal of Virology* **76**, 7672-7682.

Cocquerel, L., Meunier, J.-C., Pillez, A., Wychowski, C. & Dubuisson, J. (1998). A retention signal necessary and sufficient for endoplasmic reticulum localization maps to the transmembrane domain of hepatitis C virus glycoprotein E2. *Journal of Virology* **72**, 2183-2191.

Cocquerel, L., Duvet, S., Meunier, J.-C., Pillez, A., Cacan, R., Wychowski, C. & Dubuisson, J. (1999). The transmembrane domain of hepatitis C virus glycoprotein E1 is a signal for static retention in the endoplasmic reticulum. *Journal of Virology* **73**, 2641-2649.

Cocquerel, L., Op de Beeck, A., Lambot, M., Roussel, J., Delgrange, D., Pillez, A., Wychowski, C., Penin, F. & Dubuisson, J. (2002). Topological changes in the transmembrane domains of hepatitis C virus envelope glycoproteins. *The EMBO Journal* **21**, 2893-2902.

Codran, A., Royer, C., Jaeck, D., Bastien-Valle, M., Baumert, T. F., Kieny, M. P., Pereira, C. A. & Martin, J.-P. (2006). Entry of hepatitis C virus pseudotypes into primary human hepatocytes by clathrin-dependent endocytosis. *Journal of General Virology* **87**, 2583-2593.

Connor, R. I., Chen, B. K., Choe, S. & Landau, N. R. (1995). Vpr is required for efficient replication of human immunodeficiency virus type-1 in mononuclear phagocytes. *Virology* **206**, 935-944.

Conrad, M. E. & Lemon, S. M. (1987). Prevention of endemic icteric viral hepatitis by administration of immune serum gamma globulin. *Journal of Infectious Diseases* **156**, 56-63.

Cooper, S., Erickson, A. L., Adams, E. J., Kansopon, J., Weiner, A. J., Chien, D. Y., Houghton, M., Parham, P. & Walker, C. M. (1999). Analysis of a successful immune response against hepatitis C virus. *Immunity* **10**, 439-449.

Cormier, E. G., Tsamis, F., Kajumo, F., Durso, R. J., Gardner, J. P. & Dragic, T. (2004). CD81 is an entry coreceptor for hepatitis C virus. *Proceedings of the*

National Academy of Sciences of the United States of America **101**, 7270-7274.

Corti, D., Suguitan, A. L., Jr., Pinna, D., Silacci, C., Fernandez-Rodriguez, B. M., Vanzetta, F., Santos, C., Luke, C. J., Torres-Velez, F. J., Temperton, N. J., Weiss, R. A., Sallusto, F., Subbarao, K. & Lanzavecchia, A. (2010). Heterosubtypic neutralizing antibodies are produced by individuals immunized with a seasonal influenza vaccine. *The Journal of Clinical Investigation* **120**, 1663-1673.

Corti, D. & Lanzavecchia, A. (2013). Broadly neutralizing antiviral antibodies. *Annual Review of Immunology* **31**, 705-742.

Cox, A. L., Netski, D. M., Mosbruger, T., Sherman, S. G., Strathdee, S., Ompad, D., Vlahov, D., Chien, D., Shyamala, V., Ray, S. C. & Thomas, D. L. (2005). Prospective evaluation of community-acquired acute-phase hepatitis C virus infection. *Clinical Infectious Diseases* **40**, 951-958.

Cribier, B., Schmitt, C., Kirn, A. & Stoll-Keller, F. (1998). Inhibition of hepatitis C virus adsorption to peripheral blood mononuclear cells by dextran sulfate. *Archives of Virology* **143**, 375-379.

Cukierman, L., Meertens, L., Bertaux, C., Kajumo, F. & Dragic, T. (2009). Residues in a highly conserved claudin-1 motif are required for hepatitis C virus entry and mediate the formation of cell-cell contacts. *Journal of Virology* **83**, 5477-5484.

Cunha, E. S., Sfriso, P., Rojas, A. L., Hospital, A., Orozco, M. & Abrescia, N. G. A. (2017). Mechanism of structural tuning of the hepatitis C virus human cellular receptor CD81 large extracellular loop. *Structure (London, England : 1993)* **25**, 53-65.

Dahari, H., Major, M., Zhang, X., Mihalik, K., Rice, C. M., Perelson, A. S., Feinstone, S. M. & Neumann, A. U. (2005). Mathematical modeling of primary hepatitis C infection: noncytolytic clearance and early blockage of virion production. *Gastroenterology* **128**, 1056-1066.

Dahari, H., Feinstone, S. M. & Major, M. E. (2010). Meta-analysis of hepatitis C virus vaccine efficacy in chimpanzees indicates an importance for structural proteins. *Gastroenterology* **139**, 965-974.

Day, C. L., Seth, N. P., Lucas, M., Appel, H., Gauthier, L., Lauer, G. M., Robbins, G. K., Szczepiorkowski, Z. M., Casson, D. R., Chung, R. T., Bell, S., Harcourt, G., Walker, B. D., Klenerman, P. & Wucherpfennig, K. W. (2003). Ex vivo analysis of human memory CD4 T cells specific for hepatitis C virus using MHC class II tetramers. *Journal of Clinical Investigation* **112**, 831-842.

de Jong, Y. P., Dorner, M., Mommersteeg, M. C., Xiao, J. W., Balazs, A. B., Robbins, J. B., Winer, B. Y., Gerges, S., Vega, K., Labitt, R. N., Donovan, B. M., Giang, E., Krishnan, A., Chiriboga, L., Charlton, M. R., Burton, D. R., Baltimore, D., Law, M., Rice, C. M. & Ploss, A. (2014). Broadly neutralizing antibodies abrogate established hepatitis C virus infection. *Science Translational Medicine* **6**, 254ra129-254ra129.

Deleersnyder, V., Pillez, A., Wychowski, C., Blight, K., Xu, J., Hahn, Y. S., Rice, C. M. & Dubuisson, J. (1997). Formation of native hepatitis C virus glycoprotein complexes. *Journal of Virology* **71**, 697-704.

Dhillon, S., Witteveldt, J., Gatherer, D., Owsianka, A. M., Zeisel, M. B., Zahid, M. N., Rychłowska, M., Foung, S. K. H., Baumert, T. F., Angus, A. G. N. & Patel, A. H. (2010). Mutations within a conserved region of the hepatitis C

virus E2 glycoprotein that influence virus-receptor interactions and sensitivity to neutralizing antibodies. *Journal of Virology* **84**, 5494-5507.

Dienstag, J., Bhan, A., Alter, H., Feinstone, S. & Purceli, R. (1979). Circulating immune complexes in non-A, non-B hepatitis: possible masking of viral antigen. *The Lancet* **313**, 1265-1267.

Diepolder, H. M., Zachoval, R., Hoffmann, R. M., Jung, M. C., Pape, G. R., Wierenga, E. A., Santantonio, T. & Eichenlaub, D. (1995). Possible mechanism involving T-lymphocyte response to non-structural protein 3 in viral clearance in acute hepatitis C virus infection. *The Lancet* **346**, 1006-1007.

Dorner, M., Horwitz, J. A., Robbins, J. B., Barry, W. T., Feng, Q., Mu, K., Jones, C. T., Schoggins, J. W., Catanese, M. T., Burton, D. R., Law, M., Rice, C. M. & Ploss, A. (2011). A genetically humanized mouse model for hepatitis C virus infection. *Nature* **474**, 208-211.

Dorner, M., Horwitz, J. A., Donovan, B. M., Labitt, R. N., Budell, W. C., Friling, T., Vogt, A., Catanese, M. T., Satoh, T., Kawai, T., Akira, S., Law, M., Rice, C. M. & Ploss, A. (2013). Completion of the entire hepatitis C virus life cycle in genetically humanized mice. *Nature* **501**, 237-241.

Douam, F., Lavillette, D. & Cosset, F.-L. (2015). Chapter Three - The mechanism of HCV entry into host cells. In *Progress in Molecular Biology and Translational Science*, vol. 129, pp. 63-107. Edited by P. J. Klasse: Academic Press.

Dowd, K. A., Netski, D. M., Wang, X. H., Cox, A. L. & Ray, S. C. (2009). Selection pressure from neutralizing antibodies drives sequence evolution during acute infection with hepatitis C virus. *Gastroenterology* **136**, 2377-2386.

Drane, D., Maraskovsky, E., Gibson, R., Mitchell, S., Barnden, M., Moskwa, A., Shaw, D., Gervase, B., Coates, S., Houghton, M. & Basser, R. (2009). Priming of CD4+ and CD8+ T cell responses using a HCV core ISCOMATRIX™ vaccine: a phase I study in healthy volunteers. *Human Vaccines* **5**, 151-157.

Dreux, M., Pietschmann, T., Granier, C., Voisset, C., Ricard-Blum, S., Mangeot, P.-E., Keck, Z., Foung, S., Vu-Dac, N., Dubuisson, J., Bartenschlager, R., Lavillette, D. & Cosset, F.-L. (2006). High density lipoprotein inhibits hepatitis C virus-neutralizing antibodies by stimulating cell entry via activation of the scavenger receptor BI. *Journal of Biological Chemistry* **281**, 18285-18295.

Dreux, M., Dao Thi, V. L., Fresquet, J., Guérin, M., Julia, Z., Verney, G., Durantel, D., Zoulim, F., Lavillette, D., Cosset, F.-L. & Bartosch, B. (2009). Receptor complementation and mutagenesis reveal SR-BI as an essential HCV entry factor and functionally imply its intra- and extra-cellular domains. *PLoS Pathogens* **5**, e1000310.

Drummer, H. E., Wilson, K. A. & Poumbourios, P. (2002). Identification of the hepatitis C virus E2 glycoprotein binding site on the large extracellular loop of CD81. *Journal of Virology* **76**, 11143-11147.

Drummer, H. E., Maerz, A. & Poumbourios, P. (2003). Cell surface expression of functional hepatitis C virus E1 and E2 glycoproteins. *FEBS Letters* **546**, 385-390.

Drummer, H. E. & Poumbourios, P. (2004). Hepatitis C virus glycoprotein E2 contains a membrane-proximal heptad repeat sequence that is essential for

E1E2 glycoprotein heterodimerization and viral entry. *Journal of Biological Chemistry* **279**, 30066-30072.

Drummer, H. E., Wilson, K. A. & Poumbourios, P. (2005). Determinants of CD81 dimerization and interaction with hepatitis C virus glycoprotein E2. *Biochemical and Biophysical Research Communications* **328**, 251-257.

Drummer, H. E., Boo, I., Maerz, A. L. & Poumbourios, P. (2006). A conserved Gly436-Trp-Leu-Ala-Gly-Leu-Phe-Tyr motif in hepatitis C virus glycoprotein E2 is a determinant of CD81 binding and viral entry. *Journal of Virology* **80**, 7844-7853.

Drummer, H. E., Boo, I. & Poumbourios, P. (2007). Mutagenesis of a conserved fusion peptide-like motif and membrane-proximal heptad-repeat region of hepatitis C virus glycoprotein E1. *Journal of General Virology* **88**, 1144-1148.

Dubuisson, J., Hsu, H. H., Cheung, R. C., Greenberg, H. B., Russell, D. G. & Rice, C. M. (1994). Formation and intracellular localization of hepatitis C virus envelope glycoprotein complexes expressed by recombinant vaccinia and Sindbis viruses. *Journal of Virology* **68**, 6147-6160.

Dubuisson, J. & Rice, C. M. (1996). Hepatitis C virus glycoprotein folding: disulfide bond formation and association with calnexin. *Journal of Virology* **70**, 778-786.

Duvet, S., Cocquerel, L., Pillez, A., Cacan, R., Verbert, A., Moradpour, D., Wychowski, C. & Dubuisson, J. (1998). Hepatitis C virus glycoprotein complex localization in the endoplasmic reticulum involves a determinant for retention and not retrieval. *Journal of Biological Chemistry* **273**, 32088-32095.

Ekiert, D. C., Bhabha, G., Elsliger, M.-A., Friesen, R. H. E., Jongeneelen, M., Throsby, M., Goudsmit, J. & Wilson, I. A. (2009). Antibody recognition of a highly conserved influenza virus epitope. *Science* **324**, 246-251.

Ekiert, D. C., Friesen, R. H. E., Bhabha, G., Kwaks, T., Jongeneelen, M., Yu, W., Ophorst, C., Cox, F., Korse, H. J. W. M., Brandenburg, B., Vogels, R., Brakenhoff, J. P. J., Kompier, R., Koldijk, M. H., Cornelissen, L. A. H. M., Poon, L. L. M., Peiris, M., Koudstaal, W., Wilson, I. A. & Goudsmit, J. (2011). A highly conserved neutralizing epitope on group 2 influenza A viruses. *Science* **333**, 843-850.

El Omari, K., Iourin, O., Kadlec, J., Fearn, R., Hall, D. R., Harlos, K., Grimes, J. M. & Stuart, D. I. (2014a). Pushing the limits of sulfur SAD phasing: de novo structure solution of the N-terminal domain of the ectodomain of HCV E1. *Acta Crystallographica Section D: Biological Crystallography* **70**, 2197-2203.

El Omari, K., Iourin, O., Kadlec, J., Sutton, G., Harlos, K., Grimes, J. M. & Stuart, D. I. (2014b). Unexpected structure for the N-terminal domain of hepatitis C virus envelope glycoprotein E1. *Nature Communications* **5**.

Ennishi, D., Terui, Y., Yokoyama, M., Mishima, Y., Takahashi, S., Takeuchi, K., Okamoto, H., Tanimoto, M. & Hatake, K. (2008). Monitoring serum hepatitis C virus (HCV) RNA in patients with HCV-infected CD20-positive B-cell lymphoma undergoing rituximab combination chemotherapy. *American Journal of Hematology* **83**, 59-62.

Eren, R., Landstein, D., Terkieltaub, D., Nussbaum, O., Zauberman, A., Ben-Porath, J., Gopher, J., Buchnick, R., Kovjazin, R., Rosenthal-Galili, Z., Aviel, S., Ilan, E., Shoshany, Y., Neville, L., Waisman, T., Ben-Moshe, O., Kischitsky, A., Foung, S. K. H., Keck, Z.-Y., Pappo, O., Eid, A., Jurim, O., Zamir, G., Galun, E. & Dagan, S. (2006). Preclinical evaluation of two

neutralizing human monoclonal antibodies against hepatitis C virus (HCV): a potential treatment to prevent HCV reinfection in liver transplant patients. *Journal of Virology* **80**, 2654-2664.

Evans, M. J., von Hahn, T., Tscherne, D. M., Syder, A. J., Panis, M., Wolk, B., Hatziioannou, T., McKeating, J. A., Bieniasz, P. D. & Rice, C. M. (2007). Claudin-1 is a hepatitis C virus co-receptor required for a late step in entry. *Nature* **446**, 801-805.

Falkowska, E., Kajumo, F., Garcia, E., Reinus, J. & Dragic, T. (2007). Hepatitis C virus envelope glycoprotein E2 glycans modulate entry, CD81 binding, and neutralization. *Journal of Virology* **81**, 8072-8079.

Falson, P., Bartosch, B., Alsaleh, K., Tews, B. A., Loquet, A., Ciczora, Y., Riva, L., Montigny, C., Montpellier, C., Duverlie, G., Pécheur, E.-I., le Maire, M., Cosset, F.-L., Dubuisson, J. & Penin, F. (2015). Hepatitis C virus envelope glycoprotein E1 forms trimers at the surface of the virion. *Journal of Virology* **89**, 10333-10346.

Farci, P., Alter, H. J., Wong, D., Miller, R. H., Shih, J. W., Jett, B. & Purcell, R. H. (1991). A long-term study of hepatitis C virus replication in non-A, non-B hepatitis. *New England Journal of Medicine* **325**, 98-104.

Farci, P., Alter, H. J., Govindarajan, S., Wong, D. C., Engle, R., Lesniewski, R. R., Mushahwar, I. K., Desai, S. M., Miller, R. H., Ogata, N. & Purcell, R. H. (1992). Lack of protective immunity against reinfection with hepatitis C virus. *Science* **258**, 135-139.

Farci, P., Alter, H. J., Wong, D. C., Miller, R. H., Govindarajan, S., Engle, R., Shapiro, M. & Purcell, R. H. (1994). Prevention of hepatitis C virus infection in chimpanzees after antibody-mediated in vitro neutralization. *Proceedings of the National Academy of Sciences of the United States of America* **91**, 7792-7796.

Farci, P., Shimoda, A., Wong, D., Cabezon, T., De Gioannis, D., Strazzera, A., Shimizu, Y., Shapiro, M., Alter, H. J. & Purcell, R. H. (1996). Prevention of hepatitis C virus infection in chimpanzees by hyperimmune serum against the hypervariable region 1 of the envelope 2 protein. *Proceedings of the National Academy of Sciences of the United States of America* **93**, 15394-15399.

Farci, P., Shimoda, A., Coiana, A., Diaz, G., Peddis, G., Melpolder, J. C., Strazzera, A., Chien, D. Y., Munoz, S. J., Balestrieri, A., Purcell, R. H. & Alter, H. J. (2000). The outcome of acute hepatitis C predicted by the evolution of the viral quasispecies. *Science* **288**, 339-344.

Feinstone, S. M., Kapikian, A. Z., Purcell, R. H., Alter, H. J. & Holland, P. V. (1975). Transfusion-associated hepatitis not due to viral hepatitis type A or B. *New England Journal of Medicine* **292**, 767-770.

Feinstone, S. M., Alter, H. J., Dienes, H. P., Shimizu, Y., Popper, H., Blackmore, D., Sly, D., London, W. T. & Purcell, R. H. (1981). Non-A, non-B hepatitis in chimpanzees and marmosets. *Journal of Infectious Diseases* **144**, 588-598.

Flint, M., Maidens, C., Loomis-Price, L. D., Shotton, C., Dubuisson, J., Monk, P., Higginbottom, A., Levy, S. & McKeating, J. A. (1999a). Characterization of hepatitis C virus E2 glycoprotein interaction with a putative cellular receptor, CD81. *Journal of Virology* **73**, 6235-6244.

Flint, M., Thomas, J. M., Maidens, C. M., Shotton, C., Levy, S., Barclay, W. S. & McKeating, J. A. (1999b). Functional analysis of cell surface-expressed hepatitis C virus E2 glycoprotein. *Journal of Virology* **73**, 6782-6790.

Flint, M., von Hahn, T., Zhang, J., Farquhar, M., Jones, C. T., Balfe, P., Rice, C. M. & McKeating, J. A. (2006). Diverse CD81 proteins support hepatitis C virus infection. *Journal of Virology* **80**, 11331-11342.

Fofana, I., Krieger, S. E., Grunert, F., Glauben, S., Xiao, F., Fafi–Kremer, S., Soulier, E., Royer, C., Thumann, C., Mee, C. J., McKeating, J. A., Dragic, T., Pessaux, P., Stoll–Keller, F., Schuster, C., Thompson, J. & Baumert, T. F. (2010). Monoclonal anti-claudin 1 antibodies prevent hepatitis C virus infection of primary human hepatocytes. *Gastroenterology* **139**, 953-964.e954.

Folgori, A., Capone, S., Ruggeri, L., Meola, A., Sporeno, E., Ercole, B. B., Pezzanera, M., Tafi, R., Arcuri, M., Fattori, E., Lahm, A., Luzzago, A., Vitelli, A., Colloca, S., Cortese, R. & Nicosia, A. (2006). A T-cell HCV vaccine eliciting effective immunity against heterologous virus challenge in chimpanzees. *Nature Medicine* **12**, 190-197.

Forns, X., Thimme, R., Govindarajan, S., Emerson, S. U., Purcell, R. H., Chisari, F. V. & Bukh, J. (2000). Hepatitis C virus lacking the hypervariable region 1 of the second envelope protein is infectious and causes acute resolving or persistent infection in chimpanzees. *Proceedings of the National Academy of Sciences of the United States of America* **97**, 13318-13323.

Fraser, J., Boo, I., Poumbourios, P. & Drummer, H. E. (2011). Hepatitis C virus (HCV) envelope glycoproteins E1 and E2 contain reduced cysteine residues essential for virus entry. *Journal of Biological Chemistry* **286**, 31984-31992.

Fukasawa, M., Nagase, S., Shirasago, Y., Iida, M., Yamashita, M., Endo, K., Yagi, K., Suzuki, T., Wakita, T., Hanada, K., Kuniyasu, H. & Kondoh, M. (2015). Monoclonal antibodies against extracellular domains of claudin-1 block hepatitis C virus infection in a mouse model. *Journal of Virology* **89**, 4866-4879.

Furuse, M., Itoh, M., Hirase, T., Nagafuchi, A., Yonemura, S., Tsukita, S. & Tsukita, S. (1994). Direct association of occludin with ZO-1 and its possible involvement in the localization of occludin at tight junctions. *The Journal of Cell Biology* **127**, 1617-1626.

Furuse, M., Fujita, K., Hiiragi, T., Fujimoto, K. & Tsukita, S. (1998). Claudin-1 and -2: novel integral membrane proteins localizing at tight junctions with no sequence similarity to occludin. *The Journal of Cell Biology* **141**, 1539-1550.

Gal-Tanamy, M., Keck, Z.-Y., Yi, M., McKeating, J. A., Patel, A. H., Foung, S. K. H. & Lemon, S. M. (2008). In vitro selection of a neutralization-resistant hepatitis C virus escape mutant. *Proceedings of the National Academy of Sciences of the United States of America* **105**, 19450-19455.

Gardner, J. P., Durso, R. J., Arrigale, R. R., Donovan, G. P., Maddon, P. J., Dragic, T. & Olson, W. C. (2003). L-SIGN (CD 209L) is a liver-specific capture receptor for hepatitis C virus. *Proceedings of the National Academy of Sciences of the United States of America* **100**, 4498-4503.

Garry, R. F. & Dash, S. (2003). Proteomics computational analyses suggest that hepatitis C virus E1 and pestivirus E2 envelope glycoproteins are truncated class II fusion proteins. *Virology* **307**, 255-265.

Gasparotto, D., De Re, V. & Boiocchi, M. (2002). Hepatitis C virus, B-cell proliferation and lymphomas. *Leukemia & Lymphoma* **43**, 747-751.

Gastaminza, P., Dryden, K. A., Boyd, B., Wood, M. R., Law, M., Yeager, M. & Chisari, F. V. (2010). Ultrastructural and biophysical characterization of hepatitis C virus particles produced in cell culture. *Journal of Virology* **84**, 10999-11009.

Gerlach, J. T., Diepolder, H. M., Jung, M. C., Gruener, N. H., Schraut, W. W., Zachoval, R., Hoffmann, R., Schirren, C. A., Santantonio, T. & Pape, G. R. (1999). Recurrence of hepatitis C virus after loss of virus-specific CD4+ T-cell response in acute hepatitis C. *Gastroenterology* **117**, 933-941.

Gerlach, J. T., Diepolder, H. M., Zachoval, R., Gruener, N. H., Jung, M.-C., Ulsenheimer, A., Schraut, W. W., Schirren, C. a., Waechtler, M., Backmund, M. & Pape, G. R. (2003). Acute hepatitis C: high rate of both spontaneous and treatment-induced viral clearance. *Gastroenterology* **125**, 80-88.

Germi, R., Crance, J.-M., Garin, D., Guimet, J., Lortat-Jacob, H., Ruigrok, R. W. H., Zarski, J.-P. & Drouet, E. (2002). Cellular glycosaminoglycans and low density lipoprotein receptor are involved in hepatitis C virus adsorption. *Journal of Medical Virology* **68**, 206-215.

Giang, E., Dorner, M., Prentoe, J. C., Dreux, M., Evans, M. J., Bukh, J., Rice, C. M., Ploss, A., Burton, D. R. & Law, M. (2012). Human broadly neutralizing antibodies to the envelope glycoprotein complex of hepatitis C virus. *Proceedings of the National Academy of Sciences of the United States of America* **109**, 6205-6210.

Giudicelli, V., Chaume, D. & Lefranc, M.-P. (2005). IMGT/GENE-DB: a comprehensive database for human and mouse immunoglobulin and T cell receptor genes. *Nucleic Acids Research* **33**, D256-D261.

Giudicelli, V., Brochet, X. & Lefranc, M.-P. (2011). IMGT/V-QUEST: IMGT Standardized Analysis of the Immunoglobulin (IG) and T Cell Receptor (TR) Nucleotide Sequences. *Cold Spring Harbor Protocols* **2011**, pdb.prot5633.

Glynn, S. A., Wright, D. J., Kleinman, S. H., Hirschkorn, D., Tu, Y., Heldebrant, C., Smith, R., Giachetti, C., Gallarda, J. & Busch, M. P. (2005). Dynamics of viremia in early hepatitis C virus infection. *Transfusion* **45**, 994-1002.

Goffard, A. & Dubuisson, J. (2003). Glycosylation of hepatitis C virus envelope proteins. *Biochimie* **85**, 295-301.

Goffard, A., Callens, N., Bartosch, B., Wychowski, C., Cosset, F.-L., Montpellier, C. & Dubuisson, J. (2005). Role of N-linked glycans in the functions of hepatitis C virus envelope glycoproteins. *Journal of Virology* **79**, 8400-8409.

Gorny, M. K., Wang, X.-H., Williams, C., Volsky, B., Revesz, K., Witover, B., Burda, S., Urbanski, M., Nyambi, P., Krachmarov, C., Pinter, A., Zolla-Pazner, S. & Nadas, A. (2009). Preferential use of the VH5-51 gene segment by the human immune response to code for antibodies against the V3 domain of HIV-1. *Molecular Immunology* **46**, 917-926.

Gottwein, J. M., Scheel, T. K. H., Jensen, T. B., Lademann, J. B., Prentoe, J. C., Knudsen, M. L., Hoegh, A. M. & Bukh, J. (2009). Development and characterization of hepatitis C virus genotype 1-7 cell culture systems: role of CD81 and scavenger receptor class B type I and effect of antiviral drugs. *Hepatology* **49**, 364-377.

Gower, E., Estes, C., Blach, S., Razavi-Shearer, K. & Razavi, H. (2014). Global epidemiology and genotype distribution of the hepatitis C virus infection. *Journal of Hepatology* **61**, S45-S57.

Grakoui, A., Wychowski, C., Lin, C., Feinstone, S. M. & Rice, C. M. (1993). Expression and identification of hepatitis C virus polyprotein cleavage products. *Journal of Virology* **67**, 1385-1395.

Grakoui, A., Shoukry, N. H., Woollard, D. J., Han, J.-H., Hanson, H. L., Ghrayeb, J., Murthy, K. K., Rice, C. M. & Walker, C. M. (2003). HCV

persistence and immune evasion in the absence of memory T cell help. *Science* **302**, 659-662.

Grebely, J., Conway, B., Raffa, J. D., Lai, C., Krajden, M. & Tyndall, M. W. (2006). Hepatitis C virus reinfection in injection drug users. *Hepatology* **44**, 1139-1145.

Grebely, J. & Dore, G. J. (2011). What is killing people with hepatitis C virus infection? *Seminars in Liver Disease* **31**, 331-339.

Grebely, J., Prins, M., Hellard, M., Cox, A. L., Osburn, W. O., Lauer, G., Page, K., Lloyd, A. R. & Dore, G. J. (2012). Hepatitis C virus clearance, reinfection, and persistence, with insights from studies of injecting drug users: towards a vaccine. *The Lancet Infectious Diseases* **12**, 408-414.

Grove, J., Huby, T., Stamataki, Z., Vanwolleghem, T., Meuleman, P., Farquhar, M., Schwarz, A., Moreau, M., Owen, J. S., Leroux-Roels, G., Balfe, P. & McKeating, J. A. (2007). Scavenger receptor BI and BII expression levels modulate hepatitis C virus infectivity. *Journal of Virology* **81**, 3162-3169.

Gu, J. (2010). *Expression and characterisation of recombinant soluble heterodimers of the Hepatitis C Virus glycoproteins E1 and E2*. Honours thesis, Monash University, Melbourne, Australia.

Gu, J., Hardy, J., Boo, I., Vietheer, P., McCaffrey, K., Alhammad, Y., Chopra, A., Gaudieri, S., Poumbourios, P., Coulibaly, F. & Drummer, H. E. (2018). Escape of Hepatitis C virus from epitope I neutralization increases sensitivity of other neutralization epitopes. *Journal of Virology* **92**, e02066-02017.

Guan, M., Wang, W., Liu, X., Tong, Y., Liu, Y., Ren, H., Zhu, S., Dubuisson, J., Baumert, T. F., Zhu, Y., Peng, H., Aurelian, L., Zhao, P. & Qi, Z. (2012). Three different functional microdomains in the hepatitis C virus hypervariable region 1 (HVR1) mediate entry and immune evasion. *Journal of Biological Chemistry* **287**, 35631-35645.

Hadlock, K. G., Lanford, R. E., Perkins, S., Rowe, J., Yang, Q., Levy, S., Pileri, P., Abrignani, S. & Foung, S. K. H. (2000). Human monoclonal antibodies that inhibit binding of hepatitis C virus E2 protein to CD81 and recognize conserved conformational epitopes. *Journal of Virology* **74**, 10407-10416.

Hajarizadeh, B., Grebely, J. & Dore, G. J. (2012). Case definitions for acute hepatitis C virus infection: a systematic review. *Journal of Hepatology* **57**, 1349-1360.

Hamada, H., Yatsuhashi, H., Yano, K., Daikoku, M., Arisawa, K., Inoue, O., Koga, M., Nakata, K., Eguchi, K. & Yano, M. (2002). Impact of aging on the development of hepatocellular carcinoma in patients with posttransfusion chronic hepatitis C. *Cancer* **95**, 331-339.

Han, J. H., Shyamala, V., Richman, K. H., Brauer, M. J., Irvine, B., Urdea, M. S., Tekamp-Olson, P., Kuo, G., Choo, Q. L. & Houghton, M. (1991). Characterization of the terminal regions of hepatitis C viral RNA: identification of conserved sequences in the 5' untranslated region and poly(A) tails at the 3' end. *Proceedings of the National Academy of Sciences of the United States of America* **88**, 1711-1715.

Hansen, T. Ø., Lange, A. B. & Barington, T. (2015). Sterile DJ_H rearrangements reveal that distance between gene segments on the human Ig H chain locus influences their ability to rearrange. *The Journal of Immunology* **194**, 973-982.

Harris, H. J., Davis, C., Mullins, J. G. L., Hu, K., Goodall, M., Farquhar, M. J., Mee, C. J., McCaffrey, K., Young, S., Drummer, H., Balfe, P. &

McKeating, J. A. (2010). Claudin association with CD81 defines hepatitis C virus entry. *Journal of Biological Chemistry* **285**, 21092-21102.

He, J., Choe, S., Walker, R., Di Marzio, P., Morgan, D. O. & Landau, N. R. (1995). Human immunodeficiency virus type 1 viral protein R (Vpr) arrests cells in the G2 phase of the cell cycle by inhibiting p34cdc2 activity. *Journal of Virology* **69**, 6705-6711.

Heim, M. H. (2013). Innate immunity and HCV. *Journal of Hepatology* **58**, 564-574.

Helle, F., Goffard, A., Morel, V., Duverlie, G., McKeating, J., Keck, Z.-Y., Foung, S., Penin, F., Dubuisson, J. & Voisset, C. (2007). The neutralizing activity of anti-hepatitis C virus antibodies is modulated by specific glycans on the E2 envelope protein. *Journal of Virology* **81**, 8101-8111.

Helle, F., Vieyres, G., Elkrief, L., Popescu, C.-I., Wychowski, C., Descamps, V., Castelain, S., Roingeard, P., Duverlie, G. & Dubuisson, J. (2010). Role of N-linked glycans in the functions of hepatitis C virus envelope proteins incorporated into infectious virions. *Journal of Virology* **84**, 11905-11915.

Higginbottom, A., Quinn, E. R., Kuo, C.-C., Flint, M., Wilson, L. H., Bianchi, E., Nicosia, A., Monk, P. N., McKeating, J. A. & Levy, S. (2000). Identification of amino acid residues in CD81 critical for interaction with hepatitis C virus envelope glycoprotein E2. *Journal of Virology* **74**, 3642-3649.

Hijikata, M., Shimizu, Y. K., Kato, H., Iwamoto, A., Shih, J. W., Alter, H. J., Purcell, R. H. & Yoshikura, H. (1993). Equilibrium centrifugation studies of hepatitis C virus: evidence for circulating immune complexes. *Journal of Virology* **67**, 1953-1958.

Hishiki, T., Shimizu, Y., Tobita, R., Sugiyama, K., Ogawa, K., Funami, K., Ohsaki, Y., Fujimoto, T., Takaku, H., Wakita, T., Baumert, T. F., Miyanari, Y. & Shimotohno, K. (2010). Infectivity of hepatitis C virus is influenced by association with apolipoprotein E isoforms. *Journal of Virology* **84**, 12048-12057.

Hoogenboom, H. R., de Bruïne, A. P., Hufton, S. E., Hoet, R. M., Arends, J.-W. & Roovers, R. C. (1998). Antibody phage display technology and its applications. *Immunotechnology* **4**, 1-20.

Hsu, M., Zhang, J., Flint, M., Logvinoff, C., Cheng-Mayer, C., Rice, C. M. & McKeating, J. A. (2003). Hepatitis C virus glycoproteins mediate pH-dependent cell entry of pseudotyped retroviral particles. *Proceedings of the National Academy of Sciences of the United States of America* **100**, 7271-7276.

Huang, C.-C., Venturi, M., Majeed, S., Moore, M. J., Phogat, S., Zhang, M.-Y., Dimitrov, D. S., Hendrickson, W. A., Robinson, J., Sodroski, J., Wyatt, R., Choe, H., Farzan, M. & Kwong, P. D. (2004). Structural basis of tyrosine sulfation and VH-gene usage in antibodies that recognize the HIV type 1 coreceptor-binding site on gp120. *Proceedings of the National Academy of Sciences of the United States of America* **101**, 2706-2711.

Ivanovski, M., Silvestri, F., Pozzato, G., Anand, S., Mazzaro, C., Burrone, O. R. & Efremov, D. G. (1998). Somatic hypermutation, clonal diversity, and preferential expression of the VH51p1/VLkv325 immunoglobulin gene combination in hepatitis C virus–associated immunocytomas. *Blood* **91**, 2433-2442.

Jabara, C. B., Jones, C. D., Roach, J., Anderson, J. A. & Swanstrom, R. (2011). Accurate sampling and deep sequencing of the HIV-1 protease gene using a

Primer ID. *Proceedings of the National Academy of Sciences of the United States of America* **108**, 20166-20171.

Johansson, D. X., Voisset, C., Tarr, A. W., Aung, M., Ball, J. K., Dubuisson, J. & Persson, M. A. A. (2007). Human combinatorial libraries yield rare antibodies that broadly neutralize hepatitis C virus. *Proceedings of the National Academy of Sciences of the United States of America* **104**, 16269-16274.

Kachko, A., Frey, S. E., Sirota, L., Ray, R., Wells, F., Zubkova, I., Zhang, P. & Major, M. E. (2015). Antibodies to an interfering epitope in hepatitis C virus E2 can mask vaccine-induced neutralizing activity. *Hepatology* **62**, 1670-1682.

Kanto, T., Hayashi, N., Takehara, T., Hagiwara, H., Mita, E., Naito, M., Kasahara, A., Fusamoto, H. & Kamada, T. (1994). Buoyant density of hepatitis C virus recovered from infected hosts: two different features in sucrose equilibrium density-gradient centrifugation related to degree of liver inflammation. *Hepatology* **19**, 296-302.

Kanto, T., Norio, H., Takehara, T., Hideki, H., Eiji, M., Masafumi, N., Akinori, K., Hideyuki, F. & Takenobu, K. (1995). Density analysis of hepatitis C virus particle population in the circulation of infected hosts: implications for virus neutralization or persistence. *Journal of Hepatology* **22**, 440-448.

Kapadia, S. B., Barth, H., Baumert, T., McKeating, J. A. & Chisari, F. V. (2007). Initiation of hepatitis C virus infection is dependent on cholesterol and cooperativity between CD81 and scavenger receptor B type I. *Journal of Virology* **81**, 374-383.

Kaplan, D. E., Sugimoto, K., Newton, K., Valiga, M. E., Ikeda, F., Aytaman, A., Nunes, F. A., Lucey, M. R., Vance, B. A., Vonderheide, R. H., Reddy, K. R., McKeating, J. A. & Chang, K. M. (2007). Discordant role of CD4 T-cell response relative to neutralizing antibody and CD8 T-cell responses in acute hepatitis C. *Gastroenterology* **132**, 654-666.

Kato, N., Ootsuyama, Y., Tanaka, T., Nakagawa, M., Nakazawa, T., Muraiso, K., Ohkoshi, S., Hijikata, M. & Shimotohno, K. (1992). Marked sequence diversity in the putative envelope proteins of hepatitis C viruses. *Virus Research* **22**, 107-123.

Kato, N., Sekiya, H., Ootsuyama, Y., Nakazawa, T., Hijikata, M., Ohkoshi, S. & Shimotohno, K. (1993). Humoral immune response to hypervariable region 1 of the putative envelope glycoprotein (gp70) of hepatitis C virus. *Journal of Virology* **67**, 3923-3930.

Kato, N., Ootsuyama, Y., Sekiya, H., Ohkoshi, S., Nakazawa, T., Hijikata, M. & Shimotohno, K. (1994). Genetic drift in hypervariable region 1 of the viral genome in persistent hepatitis C virus infection. *Journal of Virology* **68**, 4776-4784.

Kato, T., Furusaka, A., Miyamoto, M., Date, T., Yasui, K., Hiramoto, J., Nagayama, K., Tanaka, T. & Wakita, T. (2001). Sequence analysis of hepatitis C virus isolated from a fulminant hepatitis patient. *Journal of Medical Virology* **64**, 334-339.

Keck, Z.-Y., Op De Beeck, A., Hadlock, K. G., Xia, J., Li, T.-K., Dubuisson, J. & Foung, S. K. H. (2004a). Hepatitis C virus E2 has three immunogenic domains containing conformational epitopes with distinct properties and biological functions. *Journal of Virology* **78**, 9224-9232.

Keck, Z.-Y., Sung, V. M. H., Perkins, S., Rowe, J., Paul, S., Liang, T. J., Lai, M. M. C. & Foung, S. K. H. (2004b). Human monoclonal antibody to hepatitis C

virus E1 glycoprotein that blocks virus attachment and viral infectivity. *Journal of Virology* **78**, 7257-7263.

Keck, Z.-Y., Li, T.-K., Xia, J., Bartosch, B., Cosset, F.-L., Dubuisson, J. & Foung, S. K. H. (2005). Analysis of a highly flexible conformational immunogenic domain A in hepatitis C virus E2. *Journal of Virology* **79**, 13199-13208.

Keck, Z.-Y., Li, T.-K., Xia, J., Gal-Tanamy, M., Olson, O., Li, S. H., Patel, A. H., Ball, J. K., Lemon, S. M. & Foung, S. K. H. (2008). Definition of a conserved immunodominant domain on hepatitis C virus E2 glycoprotein by neutralizing human monoclonal antibodies. *Journal of Virology* **82**, 6061-6066.

Keck, Z.-Y., Saha, A., Xia, J., Wang, Y., Lau, P., Krey, T., Rey, F. A. & Foung, S. K. H. (2011). Mapping a region of hepatitis C virus E2 that is responsible for escape from neutralizing antibodies and a core CD81-binding region that does not tolerate neutralization escape mutations. *Journal of Virology* **85**, 10451-10463.

Keck, Z.-Y., Xia, J., Wang, Y., Wang, W., Krey, T., Prentoe, J., Carlsen, T., Li, A. Y.-J., Patel, A. H., Lemon, S. M., Bukh, J., Rey, F. A. & Foung, S. K. H. (2012). Human monoclonal antibodies to a novel cluster of conformational epitopes on HCV E2 with resistance to neutralization escape in a genotype 2a isolate. *PLoS Pathogens* **8**, e1002653.

Keck, Z.-Y., Wang, W., Wang, Y., Lau, P., Carlsen, T. H. R., Prentoe, J., Xia, J., Patel, A. H., Bukh, J. & Foung, S. K. H. (2013). Cooperativity in virus neutralization by human monoclonal antibodies to two adjacent regions located at the amino terminus of hepatitis C virus E2 glycoprotein. *Journal of Virology* **87**, 37-51.

Keck, Z.-Y., Angus, A. G. N., Wang, W., Lau, P., Wang, Y., Gatherer, D., Patel, A. H. & Foung, S. K. H. (2014). Non-random escape pathways from a broadly neutralizing human monoclonal antibody map to a highly conserved region on the hepatitis C virus E2 glycoprotein encompassing amino acids 412–423. *PLoS Pathogens* **10**, e1004297.

Keck, Z.-Y., Girard-Blanc, C., Wang, W., Lau, P., Zuiani, A., Rey, F. A., Krey, T., Diamond, M. S. & Foung, S. K. H. (2016). Antibody response to the hypervariable region-1 interferes with broadly neutralizing antibodies to hepatitis C virus. *Journal of Virology* **90**, 3112-3122.

Kelly, C., Swadling, L., Capone, S., Brown, A., Richardson, R., Halliday, J., von Delft, A., Oo, Y., Mutimer, D., Kurioka, A., Hartnell, F., Collier, J., Ammendola, V., Sorbo, M. D., Grazioli, F., Esposito, M. L., Marco, S. D., Siani, L., Traboni, C., Hill, A. V. S., Colloca, S., Nicosia, A., Cortese, R., Folgori, A., Klenerman, P. & Barnes, E. (2016). Chronic hepatitis C viral infection subverts vaccine-induced T-cell immunity in humans. *Hepatology* **63**, 1455-1470.

Khan, A. G., Whidby, J., Miller, M. T., Scarborough, H., Zatorski, A. V., Cygan, A., Price, A. A., Yost, S. A., Bohannon, C. D., Jacob, J., Grakoui, A. & Marcotrigiano, J. (2014). Structure of the core ectodomain of the hepatitis C virus envelope glycoprotein 2. *Nature* **509**, 381-384.

Kielian, M. & Rey, F. A. (2006). Virus membrane-fusion proteins: more than one way to make a hairpin. *Nature Reviews Microbiology* **4**, 67-76.

Kitadokoro, K., Bordo, D., Galli, G., Petracca, R., Falugi, F., Abrignani, S., Grandi, G. & Bolognesi, M. (2001). CD81 extracellular domain 3D structure:

insight into the tetraspanin superfamily structural motifs. *The EMBO Journal* **20**, 12-18.

Klade, C. S., Wedemeyer, H., Berg, T., Hinrichsen, H., Cholewinska, G., Zeuzem, S., Blum, H., Buschle, M., Jelovcan, S., Buerger, V., Tauber, E., Frisch, J. & Manns, M. P. (2008). Therapeutic vaccination of chronic hepatitis C nonresponder patients with the peptide vaccine IC41. *Gastroenterology* **134**, 1385-1395.e1381.

Knodell, R., Ginsberg, A., Conrad, M., Bell, C. & Flannery, E. P. (1976). Efficacy of prophylactic gamma-globulin in preventing non-A, non-B post-transfusion hepaptitis. *The Lancet* **307**, 557-561.

Kolykhalov, A. A., Feinstone, S. M. & Rice, C. M. (1996). Identification of a highly conserved sequence element at the 3' terminus of hepatitis C virus genome RNA. *Journal of Virology* **70**, 3363-3371.

Kong, L., Giang, E., Nieusma, T., Robbins, J. B., Deller, M. C., Stanfield, R. L., Wilson, I. A. & Law, M. (2012a). Structure of hepatitis C Virus envelope glycoprotein E2 antigenic site 412 to 423 in complex with antibody AP33. *Journal of Virology* **86**, 13085-13088.

Kong, L., Giang, E., Robbins, J. B., Stanfield, R. L., Burton, D. R., Wilson, I. A. & Law, M. (2012b). Structural basis of hepatitis C virus neutralization by broadly neutralizing antibody HCV1. *Proceedings of the National Academy of Sciences of the United States of America* **109**, 9499-9504.

Kong, L., Giang, E., Nieusma, T., Kadam, R. U., Cogburn, K. E., Hua, Y., Dai, X., Stanfield, R. L., Burton, D. R., Ward, A. B., Wilson, I. A. & Law, M. (2013). Hepatitis C virus E2 envelope glycoprotein core structure. *Science* **342**, 1090-1094.

Kong, L., Kadam, R. U., Giang, E., Ruwona, T. B., Nieusma, T., Culhane, J. C., Stanfield, R. L., Dawson, P. E., Wilson, I. A. & Law, M. (2015). Structure of hepatitis C virus envelope glycoprotein E1 antigenic site 314–324 in complex with antibody IGH526. *Journal of Molecular Biology* **427**, 2617-2628.

Kong, L., Lee, D. E., Kadam, R. U., Liu, T., Giang, E., Nieusma, T., Garces, F., Tzarum, N., Woods, V. L., Ward, A. B., Li, S., Wilson, I. A. & Law, M. (2016). Structural flexibility at a major conserved antibody target on hepatitis C virus E2 antigen. *Proceedings of the National Academy of Sciences of the United States of America* **113**, 12768-12773.

Krapchev, V. B., Rychłowska, M., Chmielewska, A., Zimmer, K., Patel, A. H. & Bieńkowska-Szewczyk, K. (2018). Recombinant Flag-tagged E1E2 glycoproteins from three hepatitis C virus genotypes are biologically functional and elicit cross-reactive neutralizing antibodies in mice. *Virology* **519**, 33-41.

Krause, G., Winkler, L., Mueller, S. L., Haseloff, R. F., Piontek, J. & Blasig, I. E. (2008). Structure and function of claudins. *Biochimica et Biophysica Acta (BBA) - Biomembranes* **1778**, 631-645.

Krawczynski, K., Alter, M. J., Tankersley, D. L., Beach, M., Robertson, B. H., Lambert, S., Kuo, G., Spelbring, J. E., Meeks, E., Sinha, S. & Carson, D. A. (1996). Effect of immune globulin on the prevention of experimental hepatitis C virus infection. *Journal of Infectious Diseases* **173**, 822-828.

Krey, T., d'Alayer, J., Kikuti, C. M., Saulnier, A., Damier-Piolle, L., Petitpas, I., Johansson, D. X., Tawar, R. G., Baron, B., Robert, B., England, P., Persson, M. A. A., Martin, A. & Rey, F. A. (2010). The disulfide bonds in

glycoprotein E2 of hepatitis C virus reveal the tertiary organization of the molecule. *PLoS Pathogens* **6**, e1000762.

Krey, T., Meola, A., Keck, Z.-y., Damier-Piolle, L., Foung, S. K. H. & Rey, F. A. (2013). Structural basis of HCV neutralization by human monoclonal antibodies resistant to viral neutralization escape. *PLoS Pathogens* **9**, e1003364.

Krieger, S. E., Zeisel, M. B., Davis, C., Thumann, C., Harris, H. J., Schnober, E. K., Mee, C., Soulier, E., Royer, C., Lambotin, M., Grunert, F., Dao Thi, V. L., Dreux, M., Cosset, F.-L., McKeating, J. A., Schuster, C. & Baumert, T. F. (2010). Inhibition of hepatitis C virus infection by anti-claudin-1 antibodies is mediated by neutralization of E2–CD81–Claudin-1 associations. *Hepatology* **51**, 1144-1157.

Kumar, U., Monjardino, J. & Thomas, H. C. (1994). Hypervariable region of hepatitis C virus envelope glycoprotein (E2/NS1) in an agammaglobulinemic patient. *Gastroenterology* **106**, 1072-1075.

Kunert, R., Wolbank, S., Stiegler, G., Weik, R. & Katinger, H. (2004). Characterization of molecular features, antigen-binding, and in vitro properties of IgG and IgM variants of 4E10, an anti-HIV type 1 neutralizing monoclonal antibody. *AIDS Research and Human Retroviruses* **20**, 755-762.

Kurosaki, M., Enomoto, N., Marumo, F. & Sato, C. (1993). Rapid sequence variation of the hypervariable region of hepatitis C virus during the course of chronic infection. *Hepatology* **18**, 1293-1299.

Laemmli, U. K. (1970). Cleavage of structural proteins during the assembly of the head of bacteriophage T4. *Nature* **227**, 680-685.

Lanford, R. E., Guerra, B., Chavez, D., Bigger, C., Brasky, K. M., Wang, X.-H., Ray, S. C. & Thomas, D. L. (2004). Cross-genotype immunity to hepatitis C virus. *Journal of Virology* **78**, 1575-1581.

Lauer, G. M., Barnes, E., Lucas, M., Timm, J., Ouchi, K., Kim, A. Y., Day, C. L., Robbins, G. K., Casson, D. R., Reiser, M., Dusheiko, G., Allen, T. M., Chung, R. T., Walker, B. D. & Klenerman, P. (2004). High resolution analysis of cellular immune responses in resolved and persistent hepatitis C virus infection. *Gastroenterology* **127**, 924-936.

Lavillette, D., Morice, Y., Germanidis, G., Donot, P., Soulier, A., Pagkalos, E., Sakellariou, G., Intrator, L., Bartosch, B., Pawlotsky, J.-M. & Cosset, F.-L. (2005a). Human serum facilitates hepatitis C virus infection, and neutralizing responses inversely correlate with viral replication kinetics at the acute phase of hepatitis C virus infection. *Journal of Virology* **79**, 6023-6034.

Lavillette, D., Tarr, A. W., Voisset, C., Donot, P., Bartosch, B., Bain, C., Patel, A. H., Dubuisson, J., Ball, J. K. & Cosset, F.-L. (2005b). Characterization of host-range and cell entry properties of the major genotypes and subtypes of hepatitis C virus. *Hepatology* **41**, 265-274.

Lavillette, D., Bartosch, B., Nourrisson, D., Verney, G., Cosset, F.-L., Penin, F. & Pécheur, E.-I. (2006). Hepatitis C virus glycoproteins mediate low pH-dependent membrane fusion with liposomes. *Journal of Biological Chemistry* **281**, 3909-3917.

Lavillette, D., Pécheur, E.-I., Donot, P., Fresquet, J., Molle, J., Corbau, R., Dreux, M., Penin, F. & Cosset, F.-L. (2007). Characterization of fusion determinants points to the involvement of three discrete regions of both E1 and E2 glycoproteins in the membrane fusion process of hepatitis C virus. *Journal of Virology* **81**, 8752-8765.

Law, J. L. M., Chen, C., Wong, J., Hockman, D., Santer, D. M., Frey, S. E., Belshe, R. B., Wakita, T., Bukh, J., Jones, C. T., Rice, C. M., Abrignani, S., Tyrrell, D. L. & Houghton, M. (2013). A hepatitis C virus (HCV) vaccine comprising envelope glycoproteins gpE1/gpE2 derived from a single isolate elicits broad cross-genotype neutralizing antibodies in humans. *PLoS One* **8**, e59776.

Law, M., Maruyama, T., Lewis, J., Giang, E., Tarr, A. W., Stamataki, Z., Gastaminza, P., Chisari, F. V., Jones, I. M., Fox, R. I., Ball, J. K., McKeating, J. A., Kneteman, N. M. & Burton, D. R. (2008). Broadly neutralizing antibodies protect against hepatitis C virus quasispecies challenge. *Nature Medicine* **14**, 25-27.

Lechner, F., Gruener, N. H., Urbani, S., Uggeri, J., Santantonio, T., Kammer, A. R., Cerny, A., Phillips, R., Ferrari, C., Pape, G. R. & Klenerman, P. (2000a). CD8+ T lymphocyte responses are induced during acute hepatitis C virus infection but are not sustained. *European Journal of Immunology* **30**, 2479-2487.

Lechner, F., Wong, D. K. H., Dunbar, P. R., Chapman, R., Chung, R. T., Dohrenwend, P., Robbins, G., Phillips, R., Klenerman, P. & Walker, B. D. (2000b). Analysis of successful immune responses in persons infected with hepatitis C virus. *The Journal of Experimental Medicine* **191**, 1499-1512.

Leroux-Roels, G., Depla, E., Hulstaert, F., Tobback, L., Dincq, S., Desmet, J., Desombere, I. & Maertens, G. (2004). A candidate vaccine based on the hepatitis C E1 protein: tolerability and immunogenicity in healthy volunteers. *Vaccine* **22**, 3080-3086.

Leroux-Roels, G., Batens, A.-H., Desombere, I., Steen, B. V. D., Stichele, C. V., Maertens, G. & Hulstaert, F. (2005). Immunogenicity and tolerability of intradermal administration of an HCV E1-based vaccine candidate in healthy volunteers and patients with resolved or ongoing chronic HCV infection. *Human Vaccines* **1**, 61-65.

Li, D., von Schaewen, M., Wang, X., Tao, W., Zhang, Y., Li, L., Heller, B., Hrebikova, G., Deng, Q., Ploss, A., Zhong, J. & Huang, Z. (2016). Altered glycosylation patterns increase immunogenicity of a subunit hepatitis C virus vaccine, inducing neutralizing antibodies which confer protection in mice. *Journal of Virology* **90**, 10486-10498.

Li, D., Wang, X., von Schaewen, M., Tao, W., Zhang, Y., Heller, B., Hrebikova, G., Deng, Q., Sun, Q., Ploss, A., Zhong, J. & Huang, Z. (2017). Immunization with a subunit hepatitis C virus vaccine elicits pan-genotypic neutralizing antibodies and intrahepatic T-cell responses in nonhuman primates. *The Journal of Infectious Diseases* **215**, 1824-1831.

Li, H.-F., Huang, C.-H., Ai, L.-S., Chuang, C.-K. & Chen, S. S. (2009). Mutagenesis of the fusion peptide-like domain of hepatitis C virus E1 glycoprotein: involvement in cell fusion and virus entry. *Journal of Biomedical Science* **16**, 1-18.

Li, Y. & Modis, Y. (2014). A novel membrane fusion protein family in Flaviviridae? *Trends in Microbiology* **22**, 176-182.

Li, Y., Pierce, B. G., Wang, Q., Keck, Z.-Y., Fuerst, T. R., Foung, S. K. H. & Mariuzza, R. A. (2015a). Structural basis for penetration of the glycan shield of hepatitis C virus E2 glycoprotein by a broadly neutralizing human antibody. *Journal of Biological Chemistry* **290**, 10117-10125.

Li, Y.-P., Ramirez, S., Jensen, S. B., Purcell, R. H., Gottwein, J. M. & Bukh, J. (2012). Highly efficient full-length hepatitis C virus genotype 1 (strain TN) infectious culture system. *Proceedings of the National Academy of Sciences of the United States of America* **109**, 19757-19762.

Li, Y.-P., Ramirez, S., Mikkelsen, L. & Bukh, J. (2015b). Efficient infectious cell culture systems of the hepatitis C virus (HCV) prototype strains HCV-1 and H77. *Journal of Virology* **89**, 811-823.

Lindenbach, B. D., Evans, M. J., Syder, A. J., Wölk, B., Tellinghuisen, T. L., Liu, C. C., Maruyama, T., Hynes, R. O., Burton, D. R., McKeating, J. A. & Rice, C. M. (2005). Complete replication of hepatitis C virus in cell culture. *Science* **309**, 623-626.

Lindenbach, B. D., Meuleman, P., Ploss, A., Vanwolleghem, T., Syder, A. J., McKeating, J. A., Lanford, R. E., Feinstone, S. M., Major, M. E., Leroux-Roels, G. & Rice, C. M. (2006). Cell culture-grown hepatitis C virus is infectious in vivo and can be recultured in vitro. *Proceedings of the National Academy of Sciences of the United States of America* **103**, 3805-3809.

Lindenbach, B. D. & Rice, C. M. (2013). The ins and outs of hepatitis C virus entry and assembly. *Nature Reviews Microbiology* **11**, 688-700.

Liu, L., Fisher, B. E., Dowd, K. A., Astemborski, J., Cox, A. L. & Ray, S. C. (2010a). Acceleration of hepatitis C virus envelope evolution in humans is consistent with progressive humoral immune selection during the transition from acute to chronic infection. *Journal of Virology* **84**, 5067-5077.

Liu, S., Yang, W., Shen, L., Turner, J. R., Coyne, C. B. & Wang, T. (2009). Tight junction proteins claudin-1 and occludin control hepatitis C virus entry and are downregulated during infection to prevent superinfection. *Journal of Virology* **83**, 2011-2014.

Liu, S., Kuo, W., Yang, W., Liu, W., Gibson, G. A., Dorko, K., Watkins, S. C., Strom, S. C. & Wang, T. (2010b). The second extracellular loop dictates occludin-mediated HCV entry. *Virology* **407**, 160-170.

Logan, M., Law, J., Wong, J. A. J.-X., Hockman, D., Landi, A., Chen, C., Crawford, K., Kundu, J., Baldwin, L., Johnson, J., Dahiya, A., LaChance, G., Marcotrigiano, J., Law, M., Foung, S., Tyrrell, L. & Houghton, M. (2017). Native folding of a recombinant gpE1/gpE2 heterodimer vaccine antigen from a precursor protein fused with Fc IgG. *Journal of Virology* **91**.

Logvinoff, C., Major, M. E., Oldach, D., Heyward, S., Talal, A., Balfe, P., Feinstone, S. M., Alter, H., Rice, C. M. & McKeating, J. A. (2004). Neutralizing antibody response during acute and chronic hepatitis C virus infection. *Proceedings of the National Academy of Sciences of the United States of America* **101**, 10149-10154.

Lozach, P.-Y., Lortat-Jacob, H., De Lacroix De Lavalette, A., Staropoli, I., Foung, S., Amara, A., Houlès, C., Fieschi, F., Schwartz, O., Virelizier, J.-L., Arenzana-Seisdedos, F. & Altmeyer, R. (2003). DC-SIGN and L-SIGN are high affinity binding receptors for hepatitis C virus glycoprotein E2. *Journal of Biological Chemistry* **278**, 20358-20366.

Lozach, P.-Y., Amara, A., Bartosch, B., Virelizier, J.-L., Arenzana-Seisdedos, F., Cosset, F.-L. & Altmeyer, R. (2004). C-type lectins L-SIGN and DC-SIGN capture and transmit infectious hepatitis C virus pseudotype particles. *Journal of Biological Chemistry* **279**, 32035-32045.

Lucas, M., Ulsenheimer, A., Pfafferot, K., Heeg, M. H. J., Gaudieri, S., Grüner, N., Rauch, A., Gerlach, J. T., Jung, M.-C., Zachoval, R., Pape, G. R.,

Schraut, W., Santantonio, T., Nitschko, H., Obermeier, M., Phillips, R., Scriba, T. J., Semmo, N., Day, C., Weber, J. N., Fidler, S., Thimme, R., Haberstroh, A., Baumert, T. F., Klenerman, P. & Diepolder, H. M. (2007). Tracking virus-specific CD4+ T cells during and after acute hepatitis C virus infection. *PLoS One* **2**, e649.

Luftig, M. A., Mattu, M., Di Giovine, P., Geleziunas, R., Hrin, R., Barbato, G., Bianchi, E., Miller, M. D., Pessi, A. & Carfi, A. (2006). Structural basis for HIV-1 neutralization by a gp41 fusion intermediate-directed antibody. *Nature Structural and Molecular Biology* **13**, 740-747.

Lupberger, J., Zeisel, M. B., Xiao, F., Thumann, C., Fofana, I., Zona, L., Davis, C., Mee, C. J., Turek, M., Gorke, S., Royer, C., Fischer, B., Zahid, M. N., Lavillette, D., Fresquet, J., Cosset, F.-L., Rothenberg, S. M., Pietschmann, T., Patel, A. H., Pessaux, P., Doffoel, M., Raffelsberger, W., Poch, O., McKeating, J. A., Brino, L. & Baumert, T. F. (2011). EGFR and EphA2 are host factors for hepatitis C virus entry and possible targets for antiviral therapy. *Nature Medicine* **17**, 589-595.

Ly, K. N., Hughes, E. M., Jiles, R. B. & Holmberg, S. D. (2016). Rising mortality associated with hepatitis C virus in the United States, 2003–2013. *Clinical Infectious Diseases* **62**, 1287-1288.

Lynch, S. V. & Balderson, G. A. (2014). ANZLT Registry Report 2014. Brisbane, QLD Australia: Australia and New Zealand Liver Transplant Registry.

Maertens, G., Bosman, F., De, M. G. & Buyse, M. A. (1996). Purified hepatitis C virus envelope proteins for diagnostic and therapeutic use. Edited by US Patent 6, 134.

Mailly, L., Xiao, F., Lupberger, J., Wilson, G. K., Aubert, P., Duong, F. H. T., Calabrese, D., Leboeuf, C., Fofana, I., Thumann, C., Bandiera, S., Lutgehetmann, M., Volz, T., Davis, C., Harris, H. J., Mee, C. J., Girardi, E., Chane-Woon-Ming, B., Ericsson, M., Fletcher, N., Bartenschlager, R., Pessaux, P., Vercauteren, K., Meuleman, P., Villa, P., Kaderali, L., Pfeffer, S., Heim, M. H., Neunlist, M., Zeisel, M. B., Dandri, M., McKeating, J. A., Robinet, E. & Baumert, T. F. (2015). Clearance of persistent hepatitis C virus infection in humanized mice using a claudin-1-targeting monoclonal antibody. *Nature Biotechnology* **33**, 549-554.

Major, M. E., Mihalik, K., Fernandez, J., Seidman, J., Kleiner, D., Kolykhalov, A. A., Rice, C. M. & Feinstone, S. M. (1999). Long-term follow-up of chimpanzees inoculated with the first infectious clone for hepatitis C virus. *Journal of Virology* **73**, 3317-3325.

Major, M. E., Mihalik, K., Puig, M., Rehermann, B., Nascimbeni, M., Rice, C. M. & Feinstone, S. M. (2002). Previously infected and recovered chimpanzees exhibit rapid responses that control hepatitis C virus replication upon rechallenge. *Journal of Virology* **76**, 6586-6595.

Mancini, N., Diotti, R. A., Perotti, M., Sautto, G., Clementi, N., Nitti, G., Patel, A. H., Ball, J. K., Clementi, M. & Burioni, R. (2009). Hepatitis C virus (HCV) infection may elicit neutralizing antibodies targeting epitopes conserved in all viral genotypes. *PLoS One* **4**, e8254.

Martin, D. N. & Uprichard, S. L. (2013). Identification of transferrin receptor 1 as a hepatitis C virus entry factor. *Proceedings of the National Academy of Sciences of the United States of America* **110**, 10777-10782.

Marukian, S., Jones, C. T., Andrus, L., Evans, M. J., Ritola, K. D., Charles, E. D., Rice, C. M. & Dustin, L. B. (2008). Cell culture–produced hepatitis C

virus does not infect peripheral blood mononuclear cells. *Hepatology* **48**, 1843-1850.

Masciopinto, F., Freer, G., Burgio, V. L., Levy, S., Galli-Stampino, L., Bendinelli, M., Houghton, M., Abrignani, S. & Uematsu, Y. (2002). Expression of human CD81 in transgenic mice does not confer susceptibility to hepatitis C virus infection. *Virology* **304**, 187-196.

McCafferty, J., Griffiths, A. D., Winter, G. & Chiswell, D. J. (1990). Phage antibodies: filamentous phage displaying antibody variable domains. *Nature* **348**, 552-554.

McCaffrey, K., Boo, I., Poumbourios, P. & Drummer, H. E. (2007). Expression and characterization of a minimal hepatitis C virus glycoprotein E2 core domain that retains CD81 binding. *Journal of Virology* **81**, 9584-9590.

McCaffrey, K., Gouklani, H., Boo, I., Poumbourios, P. & Drummer, H. E. (2011). The variable regions of hepatitis C virus glycoprotein E2 have an essential structural role in glycoprotein assembly and virion infectivity. *Journal of General Virology* **92**, 112-121.

McCaffrey, K., Boo, I., Tewierek, K., Edmunds, M. L., Poumbourios, P. & Drummer, H. E. (2012). Role of conserved cysteine residues in hepatitis C virus glycoprotein E2 folding and function. *Journal of Virology* **86**, 3961-3974.

McCaffrey, K., Boo, I., Owczarek, C. M., Hardy, M. P., Perugini, M. A., Fabri, L., Scotney, P., Poumbourios, P. & Drummer, H. E. (2017). An optimized hepatitis C virus E2 glycoprotein core adopts a functional homodimer that efficiently blocks virus entry. *Journal of Virology* **91**, e01668.

McKeating, J. A., Zhang, L. Q., Logvinoff, C., Flint, M., Zhang, J., Yu, J., Butera, D., Ho, D. D., Dustin, L. B., Rice, C. M. & Balfe, P. (2004). Diverse hepatitis C virus glycoproteins mediate viral infection in a CD81-dependent manner. *Journal of Virology* **78**, 8496-8505.

Mehta, S. H., Cox, A., Hoover, D. R., Wang, X.-H., Mao, Q., Ray, S., Strathdee, S. A., Vlahov, D. & Thomas, D. L. (2002). Protection against persistence of hepatitis C. *The Lancet* **359**, 1478-1483.

Meola, A., Tarr, A. W., England, P., Meredith, L. W., McClure, C. P., Foung, S. K. H., McKeating, J. A., Ball, J. K., Rey, F. A. & Krey, T. (2015). Structural flexibility of a conserved antigenic region in hepatitis C virus glycoprotein E2 recognized by broadly neutralizing antibodies. *Journal of Virology* **89**, 2170-2181.

Merat, S. J., Molenkamp, R., Wagner, K., Koekkoek, S. M., van de Berg, D., Yasuda, E., Böhne, M., Claassen, Y. B., Grady, B. P., Prins, M., Bakker, A. Q., de Jong, M. D., Spits, H., Schinkel, J. & Beaumont, T. (2016). Hepatitis C virus broadly neutralizing monoclonal antibodies isolated 25 years after spontaneous clearance. *PLoS One* **11**, e0165047.

Mercer, D. F., Schiller, D. E., Elliott, J. F., Douglas, D. N., Hao, C., Rinfret, A., Addison, W. R., Fischer, K. P., Churchill, T. A., Lakey, J. R. T., Tyrrell, D. L. J. & Kneteman, N. M. (2001). Hepatitis C virus replication in mice with chimeric human livers. *Nature Medicine* **7**, 927-933.

Merz, A., Long, G., Hiet, M.-S., Brügger, B., Chlanda, P., Andre, P., Wieland, F., Krijnse-Locker, J. & Bartenschlager, R. (2011). Biochemical and morphological properties of hepatitis C virus particles and determination of their lipidome. *Journal of Biological Chemistry* **286**, 3018-3032.

Messina, J. P., Humphreys, I., Flaxman, A., Brown, A., Cooke, G. S., Pybus, O. G. & Barnes, E. (2015). Global distribution and prevalence of hepatitis C virus genotypes. *Hepatology* **61**, 77-87.

Meuleman, P., Hesselgesser, J., Paulson, M., Vanwolleghem, T., Desombere, I., Reiser, H. & Leroux-Roels, G. (2008). Anti-CD81 antibodies can prevent a hepatitis C virus infection in vivo. *Hepatology* **48**, 1761-1768.

Meuleman, P., Bukh, J., Verhoye, L., Farhoudi, A., Vanwolleghem, T., Wang, R. Y., Desombere, I., Alter, H., Purcell, R. H. & Leroux-Roels, G. (2011). In vivo evaluation of the cross-genotype neutralizing activity of polyclonal antibodies against hepatitis C virus. *Hepatology* **53**, 755-762.

Meunier, J.-C., Engle, R. E., Faulk, K., Zhao, M., Bartosch, B., Alter, H., Emerson, S. U., Cosset, F.-L., Purcell, R. H. & Bukh, J. (2005). Evidence for cross-genotype neutralization of hepatitis C virus pseudo-particles and enhancement of infectivity by apolipoprotein C1. *Proceedings of the National Academy of Sciences of the United States of America* **102**, 4560-4565.

Meunier, J.-C., Russell, R. S., Goossens, V., Priem, S., Walter, H., Depla, E., Union, A., Faulk, K. N., Bukh, J., Emerson, S. U. & Purcell, R. H. (2008). Isolation and characterization of broadly neutralizing human monoclonal antibodies to the E1 glycoprotein of hepatitis C virus. *Journal of Virology* **82**, 966-973.

Meunier, J.-C., Gottwein, J. M., Houghton, M., Russell, R. S., Emerson, S. U., Bukh, J. & Purcell, R. H. (2011). Vaccine-induced cross-genotype reactive neutralizing antibodies against hepatitis C virus. *The Journal of Infectious Diseases* **204**, 1186-1190.

Meunier, J. C., Fournillier, A., Choukhi, A., Cahour, A., Cocquerel, L., Dubuisson, J. & Wychowski, C. (1999). Analysis of the glycosylation sites of hepatitis C virus (HCV) glycoprotein E1 and the influence of E1 glycans on the formation of the HCV glycoprotein complex. *Journal of General Virology* **80**, 887-896.

Micallef, J. M., Kaldor, J. M. & Dore, G. J. (2006). Spontaneous viral clearance following acute hepatitis C infection: a systematic review of longitudinal studies. *Journal of Viral Hepatitis* **13**, 34-41.

Micallef, J. M., Macdonald, V., Jauncey, M., Amin, J., Rawlinson, W., Van Beek, I., Kaldor, J. M., White, P. A. & Dore, G. J. (2007). High incidence of hepatitis C virus reinfection within a cohort of injecting drug users. *Journal of Viral Hepatitis* **14**, 413-418.

Michalak, J. P., Wychowski, C., Choukhi, A., Meunier, J. C., Ung, S., Rice, C. M. & Dubuisson, J. (1997). Characterization of truncated forms of hepatitis C virus glycoproteins. *Journal of General Virology* **78**, 2299-2306.

Michta, M. L., Hopcraft, S. E., Narbus, C. M., Kratovac, Z., Israelow, B., Sourisseau, M. & Evans, M. J. (2010). Species-specific regions of occludin required by hepatitis C virus for cell entry. *Journal of Virology* **84**, 11696-11708.

Minsky, A., Summers, R. G. & Knowles, J. R. (1986). Secretion of beta-lactamase into the periplasm of *Escherichia coli*: evidence for a distinct release step associated with a conformational change. *Proceedings of the National Academy of Sciences of the United States of America* **83**, 4180-4184.

Miyamoto, H., Okamoto, H., Sato, K., Tanaka, T. & Mishiro, S. (1992). Extraordinarily low density of hepatitis C virus estimated by sucrose density

gradient centrifugation and the polymerase chain reaction. *Journal of General Virology* **73**, 715-718.

Modis, Y., Ogata, S., Clements, D. & Harrison, S. C. (2004). Structure of the dengue virus envelope protein after membrane fusion. *Nature* **427**, 313-319.

Molina, S., Castet, V., Fournier-Wirth, C., Pichard-Garcia, L., Avner, R., Harats, D., Roitelman, J., Barbaras, R., Graber, P., Ghersa, P., Smolarsky, M., Funaro, A., Malavasi, F., Larrey, D., Coste, J., Fabre, J.-M., Sa-Cunha, A. & Maurel, P. (2007). The low-density lipoprotein receptor plays a role in the infection of primary human hepatocytes by hepatitis C virus. *Journal of Hepatology* **46**, 411-419.

Molina, S., Castet, V., Pichard-Garcia, L., Wychowski, C., Meurs, E., Pascussi, J.-M., Sureau, C., Fabre, J.-M., SaCunha, A., Larrey, D., Dubuisson, J., Coste, J., McKeating, J., Maurel, P. & Fournier-Wirth, C. (2008). Serum-derived hepatitis C virus infection of primary human hepatocytes is tetraspanin CD81 dependent. *Journal of Virology* **82**, 569-574.

Monazahian, M., Böhme, I., Bonk, S., Koch, A., Scholz, C., Grethe, S. & Thomssen, R. (1999). Low density lipoprotein receptor as a candidate receptor for hepatitis C virus. *Journal of Medical Virology* **57**, 223-229.

Morin, T. J., Broering, T. J., Leav, B. A., Blair, B. M., Rowley, K. J., Boucher, E. N., Wang, Y., Cheslock, P. S., Knauber, M., Olsen, D. B., Ludmerer, S. W., Szabo, G., Finberg, R. W., Purcell, R. H., Lanford, R. E., Ambrosino, D. M., Molrine, D. C. & Babcock, G. J. (2012). Human monoclonal antibody HCV1 effectively prevents and treats HCV infection in chimpanzees. *PLoS Pathogens* **8**, e1002895.

Morris, L., Chen, X., Alam, M., Tomaras, G., Zhang, R., Marshall, D. J., Chen, B., Parks, R., Foulger, A., Jaeger, F., Donathan, M., Bilska, M., Gray, E. S., Abdool Karim, S. S., Kepler, T. B., Whitesides, J., Montefiori, D., Moody, M. A., Liao, H.-X. & Haynes, B. F. (2011). Isolation of a human anti-HIV gp41 membrane proximal region neutralizing antibody by antigen-specific single B cell sorting. *PLoS One* **6**, e23532.

Nascimbeni, M., Mizukoshi, E., Bosmann, M., Major, M. E., Mihalik, K., Rice, C. M., Feinstone, S. M. & Rehermann, B. (2003). Kinetics of CD4+ and CD8+ memory T-cell responses during hepatitis C virus rechallenge of previously recovered chimpanzees. *Journal of Virology* **77**, 4781-4793.

Netski, D. M., Mosbruger, T., Depla, E., Maertens, G., Ray, S. C., Hamilton, R. G., Roundtree, S., Thomas, D. L., McKeating, J. & Cox, A. (2005). Humoral immune response in acute hepatitis C virus infection. *Clinical Infectious Diseases* **41**, 667-675.

Neumann, A. U., Lam, N. P., Dahari, H., Gretch, D. R., Wiley, T. E., Layden, T. J. & Perelson, A. S. (1998). Hepatitis C viral dynamics in vivo and the antiviral efficacy of interferon-α therapy. *Science* **282**, 103-107.

Neumann-Haefelin, C. & Thimme, R. (2013). Adaptive immune responses in hepatitis C virus infection. In *Hepatitis C Virus: From Molecular Virology to Antiviral Therapy* (Current Topics in Microbiology and Immunology), vol. 369, pp. 243-262. Edited by R. Bartenschlager: Springer Berlin Heidelberg.

Nevens, F., Roskams, T., Van Vlierberghe, H., Horsmans, Y., Sprengers, D., Elewaut, A., Desmet, V., Leroux-Roels, G., Quinaux, E., Depla, E., Dincq, S., Stichele, C. V., Maertens, G. & Hulstaert, F. (2003). A pilot study of therapeutic vaccination with envelope protein E1 in 35 patients with chronic hepatitis C. *Hepatology* **38**, 1289-1296.

Nielsen, S. U., Bassendine, M. F., Burt, A. D., Martin, C., Pumeechockchai, W. & Toms, G. L. (2006). Association between hepatitis C virus and very-low-density lipoprotein (VLDL)/LDL analyzed in iodixanol density gradients. *Journal of Virology* **80**, 2418-2428.

Nikolaeva, L. I., Blokhina, N. P., Tsurikova, N. N., Voronkova, N. V., Miminoshvili, M. I., Braginsky, D. M., Yastrebova, O. N., Booynitskaya, O. B., Isaeva, O. V., Michailov, M. I. & Archakov, A. I. (2002). Virus-specific antibody titres in different phases of hepatitis C virus infection. *Journal of Viral Hepatitis* **9**, 429-437.

Ogata, N., Alter, H. J., Miller, R. H. & Purcell, R. H. (1991). Nucleotide sequence and mutation rate of the H strain of hepatitis C virus. *Proceedings of the National Academy of Sciences of the United States of America* **88**, 3392-3396.

Op De Beeck, A., Montserret, R., Duvet, S., Cocquerel, L., Cacan, R., Barberot, B., Le Maire, M., Penin, F. & Dubuisson, J. (2000). The transmembrane domains of hepatitis C virus envelope glycoproteins E1 and E2 play a major role in heterodimerization. *Journal of Biological Chemistry* **275**, 31428-31437.

Op De Beeck, A., Voisset, C., Bartosch, B., Ciczora, Y., Cocquerel, L., Keck, Z., Foung, S., Cosset, F.-L. & Dubuisson, J. (2004). Characterization of functional hepatitis C virus envelope glycoproteins. *Journal of Virology* **78**, 2994-3002.

Osburn, W. O., Fisher, B. E., Dowd, K. A., Urban, G., Liu, L., Ray, S. C., Thomas, D. L. & Cox, A. L. (2010). Spontaneous control of primary hepatitis C virus infection and immunity against persistent reinfection. *Gastroenterology* **138**, 315-324.

Owsianka, A., Clayton, R. F., Loomis-Price, L. D., McKeating, J. A. & Patel, A. H. (2001). Functional analysis of hepatitis C virus E2 glycoproteins and virus-like particles reveals structural dissimilarities between different forms of E2. *Journal of General Virology* **82**, 1877-1883.

Owsianka, A., Tarr, A. W., Juttla, V. S., Lavillette, D., Bartosch, B., Cosset, F.-L., Ball, J. K. & Patel, A. H. (2005). Monoclonal antibody AP33 defines a broadly neutralizing epitope on the hepatitis C virus E2 envelope glycoprotein. *Journal of Virology* **79**, 11095-11104.

Owsianka, A. M., Timms, J. M., Tarr, A. W., Brown, R. J. P., Hickling, T. P., Szwejk, A., Bienkowska-Szewczyk, K., Thomson, B. J., Patel, A. H. & Ball, J. K. (2006). Identification of conserved residues in the E2 envelope glycoprotein of the hepatitis C virus that are critical for CD81 binding. *Journal of Virology* **80**, 8695-8704.

Owsianka, A. M., Tarr, A. W., Keck, Z.-Y., Li, T.-K., Witteveldt, J., Adair, R., Foung, S. K. H., Ball, J. K. & Patel, A. H. (2008). Broadly neutralizing human monoclonal antibodies to the hepatitis C virus E2 glycoprotein. *Journal of General Virology* **89**, 653-659.

Pacheco, B., Gómez-Gutiérrez, J., Yélamos, B., Delgado, C., Roncal, F., Albar, J. P., Peterson, D. & Gavilanes, F. (2006). Membrane-perturbing properties of three peptides corresponding to the ectodomain of hepatitis C virus E2 envelope protein. *Biochimica et Biophysica Acta (BBA) - Biomembranes* **1758**, 755-763.

Paciello, R., Urbanowicz, R. A., Riccio, G., Sasso, E., McClure, P. C., Zambrano, N., Ball, J. K., Cortese, R., Nicosia, A. & De Lorenzo, C. (2016). Novel

human anti-claudin 1 monoclonal antibodies inhibit HCV infection and may synergize with anti-SRB1 mAb. *Journal of General Virology* **97**, 82-94.

Pantua, H., Diao, J., Ultsch, M., Hazen, M., Mathieu, M., McCutcheon, K., Takeda, K., Date, S., Cheung, T. K., Phung, Q., Hass, P., Arnott, D., Hongo, J.-A., Matthews, D. J., Brown, A., Patel, A. H., Kelley, R. F., Eigenbrot, C. & Kapadia, S. B. (2013). Glycan shifting on hepatitis C virus (HCV) E2 glycoprotein is a mechanism for escape from broadly neutralizing antibodies. *Journal of Molecular Biology* **425**, 1899-1914.

Patel, A. H., Wood, J., Penin, F., Dubuisson, J. & McKeating, J. A. (2000). Construction and characterization of chimeric hepatitis C virus E2 glycoproteins: analysis of regions critical for glycoprotein aggregation and CD81 binding. *Journal of General Virology* **81**, 2873-2883.

Patel, J., Patel, A. H. & McLauchlan, J. (1999). Covalent interactions are not required to permit or stabilize the non-covalent association of hepatitis C virus glycoproteins E1 and E2. *Journal of General Virology* **80**, 1681-1690.

Patel, J., Patel, A. H. & McLauchlan, J. (2001). The transmembrane domain of the hepatitis C virus E2 glycoprotein is required for correct folding of the E1 glycoprotein and native complex formation. *Virology* **279**, 58-68.

Pawlotsky, J. M., Chevaliez, S. & McHutchison, J. G. (2007). The hepatitis C virus life cycle as a target for new antiviral therapies. *Gastroenterology* **132**, 1979-1998.

Penin, F., Combet, C., Germanidis, G., Frainais, P.-O., Deléage, G. & Pawlotsky, J.-M. (2001). Conservation of the conformation and positive charges of hepatitis C virus E2 envelope glycoprotein hypervariable region 1 points to a role in cell attachment. *Journal of Virology* **75**, 5703-5710.

Pérez-Berná, A. J., Moreno, M. R., Guillén, J., Bernabeu, A. & Villalaín, J. (2006). The membrane-active regions of the hepatitis C virus E1 and E2 envelope glycoproteins. *Biochemistry* **45**, 3755-3768.

Pérez-Berná, A. J., Pabst, G., Laggner, P. & Villalaín, J. (2009). Biophysical characterization of the fusogenic region of HCV envelope glycoprotein E1. *Biochimica et Biophysica Acta (BBA) - Biomembranes* **1788**, 2183-2193.

Perotti, M., Mancini, N., Diotti, R. A., Tarr, A. W., Ball, J. K., Owsianka, A., Adair, R., Patel, A. H., Clementi, M. & Burioni, R. (2008). Identification of a broadly cross-reacting and neutralizing human monoclonal antibody directed against the hepatitis C virus E2 protein. *Journal of Virology* **82**, 1047-1052.

Pestka, J. M., Zeisel, M. B., Bläser, E., Schürmann, P., Bartosch, B., Cosset, F.-L., Patel, A. H., Meisel, H., Baumert, J., Viazov, S., Rispeter, K., Blum, H. E., Roggendorf, M. & Baumert, T. F. (2007). Rapid induction of virus-neutralizing antibodies and viral clearance in a single-source outbreak of hepatitis C. *Proceedings of the National Academy of Sciences of the United States of America* **104**, 6025-6030.

Petit, M.-A., Lièvre, M., Peyrol, S., De Sequeira, S., Berthillon, P., Ruigrok, R. W. H. & Trépo, C. (2005). Enveloped particles in the serum of chronic hepatitis C patients. *Virology* **336**, 144-153.

Petracca, R., Falugi, F., Galli, G., Norais, N., Rosa, D., Campagnoli, S., Burgio, V., Di Stasio, E., Giardina, B., Houghton, M., Abrignani, S. & Grandi, G. (2000). Structure-function analysis of hepatitis C virus envelope-CD81 binding. *Journal of Virology* **74**, 4824-4830.

Pietschmann, T., Kaul, A., Koutsoudakis, G., Shavinskaya, A., Kallis, S., Steinmann, E., Abid, K., Negro, F., Dreux, M., Cosset, F.-L. &

Bartenschlager, R. (2006). Construction and characterization of infectious intragenotypic and intergenotypic hepatitis C virus chimeras. *Proceedings of the National Academy of Sciences of the United States of America* **103**, 7408-7413.

Pileri, P., Uematsu, Y., Campagnoli, S., Galli, G. & et al. (1998). Binding of hepatitis C virus to CD81. *Science* **282**, 938-941.

Ploss, A., Evans, M. J., Gaysinskaya, V. A., Panis, M., You, H., de Jong, Y. P. & Rice, C. M. (2009). Human occludin is a hepatitis C virus entry factor required for infection of mouse cells. *Nature* **457**, 882-886.

Pöhlmann, S., Zhang, J., Baribaud, F., Chen, Z., Leslie, G. J., Lin, G., Granelli-Piperno, A., Doms, R. W., Rice, C. M. & McKeating, J. A. (2003). Hepatitis C virus glycoproteins interact with DC-SIGN and DC-SIGNR. *Journal of Virology* **77**, 4070-4080.

Polakos, N. K., Drane, D., Cox, J., Ng, P., Selby, M. J., Chien, D., O'Hagan, D. T., Houghton, M. & Paliard, X. (2001). Characterization of hepatitis C virus core-specific immune responses primed in rhesus macaques by a nonclassical ISCOM vaccine. *The Journal of Immunology* **166**, 3589-3598.

Post, J. J., Pan, Y., Freeman, A. J., Harvey, C. E., White, P. A., Palladinetti, P., Haber, P. S., Marinos, G., Levy, M. H., Kaldor, J. M., Dolan, K. A., Ffrench, R. A., Lloyd, A. R., Rawlinson, W. D., Incidence, H. C. & Group, T. i. P. S. (2004). Clearance of hepatitis C viremia associated with cellular immunity in the absence of seroconversion in the hepatitis C incidence and transmission in prisons study cohort. *Journal of Infectious Diseases* **189**, 1846-1855.

Potter, J. A., Owsianka, A. M., Jeffery, N., Matthews, D. J., Keck, Z.-Y., Lau, P., Foung, S. K. H., Taylor, G. L. & Patel, A. H. (2012). Toward a hepatitis C virus vaccine: the structural basis of hepatitis C virus neutralization by AP33, a broadly neutralizing antibody. *Journal of Virology* **86**, 12923-12932.

Prentoe, J., Jensen, T. B., Meuleman, P., Serre, S. B. N., Scheel, T. K. H., Leroux-Roels, G., Gottwein, J. M. & Bukh, J. (2011). Hypervariable region 1 differentially impacts viability of hepatitis C virus strains of genotypes 1 to 6 and impairs virus neutralization. *Journal of Virology* **85**, 2224-2234.

Prentoe, J., Serre, S. B. N., Ramirez, S., Nicosia, A., Gottwein, J. M. & Bukh, J. (2014). Hypervariable region 1 deletion and required adaptive envelope mutations confer decreased dependency on scavenger receptor class B type I and low-density lipoprotein receptor for hepatitis C virus. *Journal of Virology* **88**, 1725-1739.

Prentoe, J., Verhoye, L., Velázquez Moctezuma, R., Buysschaert, C., Farhoudi, A., Wang, R., Alter, H., Meuleman, P. & Bukh, J. (2016). HVR1-mediated antibody evasion of highly infectious in vivo adapted HCV in humanised mice. *Gut* **65**, 1988-1997.

Prince, A. M., Brotman, B., Huima, T., Pascual, D., Jaffery, M. & Genevieve, I. (1992). Immunity in hepatitis C infection. *Journal of Infectious Diseases* **165**, 438-443.

Prince, A. M., Brotman, B., Lee, D.-H., Pfahler, W., Tricoche, N., Andrus, L. & Shata, M. T. (2005). Protection against chronic hepatitis C virus infection after rechallenge with homologous, but not heterologous, genotypes in a chimpanzee model. *Journal of Infectious Diseases* **192**, 1701-1709.

Prokunina-Olsson, L., Muchmore, B., Tang, W., Pfeiffer, R. M., Park, H., Dickensheets, H., Hergott, D., Porter-Gill, P., Mumy, A., Kohaar, I.,

Chen, S., Brand, N., Tarway, M., Liu, L., Sheikh, F., Astemborski, J., Bonkovsky, H. L., Edlin, B. R., Howell, C. D., Morgan, T. R., Thomas, D. L., Rehermann, B., Donnelly, R. P. & O'Brien, T. R. (2013). A variant upstream of IFNL3 (IL28B) creating a new interferon gene IFNL4 is associated with impaired clearance of hepatitis C virus. *Nature Genetics* **45**, 164-171.

Puig, M., Major, M. E., Mihalik, K. & Feinstone, S. M. (2004). Immunization of chimpanzees with an envelope protein-based vaccine enhances specific humoral and cellular immune responses that delay hepatitis C virus infection. *Vaccine* **22**, 991-1000.

Racanelli, V., Brunetti, C., De Re, V., Caggiari, L., De Zorzi, M., Leone, P., Perosa, F., Vacca, A. & Dammacco, F. (2011). Antibody Vh repertoire differences between resolving and chronically evolving hepatitis C virus infections. *PLoS One* **6**, e25606.

Radziewicz, H., Ibegbu, C. C., Hon, H., Osborn, M. K., Obideen, K., Wehbi, M., Freeman, G. J., Lennox, J. L., Workowski, K. A., Hanson, H. L. & Grakoui, A. (2008). Impaired hepatitis C virus (HCV)-specific effector CD8+ T cells undergo massive apoptosis in the peripheral blood during acute HCV infection and in the liver during the chronic phase of infection. *Journal of Virology* **82**, 9808-9822.

Raghuraman, S., Park, H., Osburn, W. O., Winkelstein, E., Edlin, B. R. & Rehermann, B. (2012). Spontaneous clearance of chronic hepatitis C virus infection is associated with appearance of neutralizing antibodies and reversal of T-cell exhaustion. *Journal of Infectious Diseases* **205**, 763-771.

Ralston, R., Thudium, K., Berger, K., Kuo, C., Gervase, B., Hall, J., Selby, M., Kuo, G., Houghton, M. & Choo, Q. L. (1993). Characterization of hepatitis C virus envelope glycoprotein complexes expressed by recombinant vaccinia viruses. *Journal of Virology* **67**, 6753-6761.

Ramirez, S., Li, Y.-P., Jensen, S. B., Pedersen, J., Gottwein, J. M. & Bukh, J. (2014). Highly efficient infectious cell culture of three hepatitis C virus genotype 2b strains and sensitivity to lead protease, nonstructural protein 5A, and polymerase inhibitors. *Hepatology* **59**, 395-407.

Rauch, A., Kutalik, Z., Descombes, P., Cai, T., Di Iulio, J., Mueller, T., Bochud, M., Battegay, M., Bernasconi, E., Borovicka, J., Colombo, S., Cerny, A., Dufour, J. F., Furrer, H., Günthard, H. F., Heim, M., Hirschel, B., Malinverni, R., Moradpour, D., Müllhaupt, B., Witteck, A., Beckmann, J. S., Berg, T., Bergmann, S., Negro, F., Telenti, A. & Bochud, P. Y. (2010). Genetic variation in IL28B is associated with chronic hepatitis C and treatment failure: a genome-wide association study. *Gastroenterology* **138**, 1338-1345.e1337.

Ray, R., Meyer, K., Banerjee, A., Basu, A., Coates, S., Abrignani, S., Houghton, M., Frey, S. E. & Belshe, R. B. (2010). Characterization of antibodies induced by vaccination with hepatitis C virus envelope glycoproteins. *Journal of Infectious Diseases* **202**, 862-866.

Rehermann, B. (2009). Hepatitis C virus versus innate and adaptive immune responses: a tale of coevolution and coexistence. *The Journal of Clinical Investigation* **119**, 1745-1754.

Rein, D. B., Smith, B. D., Wittenborn, J. S., Lesesne, S. B., Wagner, L. D., Roblin, D. W., Patel, N., Ward, J. W. & Weinbaum, C. M. (2012). The

cost-effectiveness of birth-cohort screening for hepatitis C antibody in U.S. primary care settings. *Annals of Internal Medicine* **156**, 263-270.

Rey, F. A., Heinz, F. X., Mandl, C., Kunz, C. & Harrison, S. C. (1995). The envelope glycoprotein from tick-borne encephalitis virus at 2Å resolution. *Nature* **375**, 291-298.

Roccasecca, R., Ansuini, H., Vitelli, A., Meola, A., Scarselli, E., Acali, S., Pezzanera, M., Ercole, B. B., McKeating, J., Yagnik, A., Lahm, A., Tramontano, A., Cortese, R. & Nicosia, A. (2003). Binding of the hepatitis C virus E2 glycoprotein to CD81 is strain specific and is modulated by a complex interplay between hypervariable regions 1 and 2. *Journal of Virology* **77**, 1856-1867.

Rodrigo, C., Walker, M. R., Leung, P., Eltahla, A. A., Grebely, J., Dore, G. J., Applegate, T., Page, K., Dwivedi, S., Bruneau, J., Morris, M. D., Cox, A. L., Osburn, W., Kim, A. Y., Schinkel, J., Shoukry, N. H., Lauer, G. M., Maher, L., Hellard, M., Prins, M., Luciani, F., Lloyd, A. R. & Bull, R. A. (2017). Limited naturally occurring escape in broadly neutralizing antibody epitopes in hepatitis C glycoprotein E2 and constrained sequence usage in acute infection. *Infection, Genetics and Evolution* **49**, 88-96.

Rothwangl, K. B., Manicassamy, B., Uprichard, S. L. & Rong, L. (2008). Dissecting the role of putative CD81 binding regions of E2 in mediating HCV entry: putative CD81 binding region 1 is not involved in CD81 binding. *Virology Journal* **5**, 1-12.

Sabo, M. C., Luca, V. C., Prentoe, J., Hopcraft, S. E., Blight, K. J., Yi, M., Lemon, S. M., Ball, J. K., Bukh, J., Evans, M. J., Fremont, D. H. & Diamond, M. S. (2011). Neutralizing monoclonal antibodies against hepatitis C virus E2 protein bind discontinuous epitopes and inhibit infection at a postattachment step. *Journal of Virology* **85**, 7005-7019.

Saeed, M., Andreo, U., Chung, H.-Y., Espiritu, C., Branch, A. D., Silva, J. M. & Rice, C. M. (2015). SEC14L2 enables pan-genotype HCV replication in cell culture. *Nature* **524**, 471-475.

Sainz, B., Barretto, N., Martin, D. N., Hiraga, N., Imamura, M., Hussain, S., Marsh, K. A., Yu, X., Chayama, K., Alrefai, W. A. & Uprichard, S. L. (2012). Identification of the Niemann-Pick C1-like 1 cholesterol absorption receptor as a new hepatitis C virus entry factor. *Nature Medicine* **18**, 281-285.

Sanchez-Quijano, A., Lissen, E., Diaz-Torres, M. A., Rivera, F., Pineda, J. A., Leal, M., Garcia de Pesquera, F., Castro, R. & Muñoz, J. (1988). Prevention of post-transfusion non-A, non-B hepatitis by non-specific immunoglobulin in heart surgery patients. *The Lancet* **331**, 1245-1249.

Sasso, E. H., Ghillani, P., Musset, L., Piette, J. C. & Cacoub, P. (2001). Effect of 51p1-related gene copy number (V1–69 locus) on production of hepatitis C-associated cryoglobulins. *Clinical & Experimental Immunology* **123**, 88-93.

Scarselli, E., Ansuini, H., Cerino, R., Roccasecca, R. M., Acali, S., Filocamo, G., Traboni, C., Nicosia, A., Cortese, R. & Vitelli, A. (2002). The human scavenger receptor class B type I is a novel candidate receptor for the hepatitis C virus. *The EMBO Journal* **21**, 5017-5025.

Schofield, D. J., Bartosch, B., Shimizu, Y. K., Allander, T., Alter, H. J., Emerson, S. U., Cosset, F.-L. & Purcell, R. H. (2005). Human monoclonal antibodies that react with the E2 glycoprotein of hepatitis C virus and possess neutralizing activity. *Hepatology* **42**, 1055-1062.

Schoggins, J. & Rice, C. (2013). Innate immune responses to hepatitis C virus. In *Hepatitis C Virus: From Molecular Virology to Antiviral Therapy* (Current Topics in Microbiology and Immunology), vol. 369, pp. 219-242. Edited by R. Bartenschlager: Springer Berlin Heidelberg.

Schulze zur Wiesch, J., Ciuffreda, D., Lewis-Ximenez, L., Kasprowicz, V., Nolan, B. E., Streeck, H., Aneja, J., Reyor, L. L., Allen, T. M., Lohse, A. W., McGovern, B., Chung, R. T., Kwok, W. W., Kim, A. Y. & Lauer, G. M. (2012). Broadly directed virus-specific CD4+ T cell responses are primed during acute hepatitis C infection, but rapidly disappear from human blood with viral persistence. *The Journal of Experimental Medicine* **209**, 61-75.

Scott, J. D., McMahon, B. J., Bruden, D., Sullivan, D., Homan, C., Christensen, C. & Gretch, D. R. (2006). High rate of spontaneous negativity for hepatitis c virus RNA after establishment of chronic infection in Alaska natives. *Clinical Infectious Diseases* **42**, 945-952.

Scull, M. A., Shi, C., de Jong, Y. P., Gerold, G., Ries, M., von Schaewen, M., Donovan, B. M., Labitt, R. N., Horwitz, J. A., Gaska, J. M., Hrebikova, G., Xiao, J. W., Flatley, B., Fung, C., Chiriboga, L., Walker, C. M., Evans, D. T., Rice, C. M. & Ploss, A. (2015). Hepatitis C virus infects rhesus macaque hepatocytes and simianized mice. *Hepatology* **62**, 57-67.

Seaberg, E. C., Witt, M. D., Jacobson, L. P., Detels, R., Rinaldo, C. R., Margolick, J. B., Young, S., Phair, J. P. & Thio, C. L. (2015). Spontaneous clearance of the hepatitis C virus among men who have sex with men. *Clinical Infectious Diseases* **61**, 1381-1388.

Seeff, L. B. (2002). Natural history of chronic hepatitis C. *Hepatology* **36**, S35-S46.

Seeff, L. B. (2009). The history of the "natural history" of hepatitis C (1968–2009). *Liver International* **29**, 89-99.

Shimizu, Y. K., Weiner, A. J., Rosenblatt, J., Wong, D. C., Shapiro, M., Popkin, T., Houghton, M., Alter, H. J. & Purcell, R. H. (1990). Early events in hepatitis C virus infection of chimpanzees. *Proceedings of the National Academy of Sciences of the United States of America* **87**, 6441-6444.

Shimizu, Y. K., Hijikata, M., Iwamoto, A., Alter, H. J., Purcell, R. H. & Yoshikura, H. (1994). Neutralizing antibodies against hepatitis C virus and the emergence of neutralization escape mutant viruses. *Journal of Virology* **68**, 1494-1500.

Shin, E. C., Park, S. H., DeMino, M., Nascimbeni, M., Mihalik, K., Major, M., Veerapu, N. S., Heller, T., Feinstone, S. M., Rice, C. M. & Rehermann, B. (2011). Delayed induction, not impaired recruitment, of specific CD8+ T cells causes the late onset of acute hepatitis C. *Gastroenterology* **141**, 686-695.e681.

Shoukry, N. H., Grakoui, A., Houghton, M., Chien, D. Y., Ghrayeb, J., Reimann, K. A. & Walker, C. M. (2003). Memory CD8+ T cells are required for protection from persistent hepatitis C virus infection. *The Journal of Experimental Medicine* **197**, 1645-1655.

Simmonds, P., Bukh, J., Combet, C., Deléage, G., Enomoto, N., Feinstone, S., Halfon, P., Inchauspé, G., Kuiken, C., Maertens, G., Mizokami, M., Murphy, D. G., Okamoto, H., Pawlotsky, J.-M., Penin, F., Sablon, E., Shin-I, T., Stuyver, L. J., Thiel, H.-J., Viazov, S., Weiner, A. J. & Widell, A. (2005). Consensus proposals for a unified system of nomenclature of hepatitis C virus genotypes. *Hepatology* **42**, 962-973.

Slater-Handshy, T., Droll, D. A., Fan, X., Di Bisceglie, A. M. & Chambers, T. J. (2004). HCV E2 glycoprotein: mutagenesis of N-linked glycosylation sites and its effects on E2 expression and processing. *Virology* **319**, 36-48.

Smith, B. D., Morgan, R. L., Beckett, G. A., Falck-Ytter, Y., Holtzman, D., Teo, C.-G., Jewett, A., Baack, B., Rein, D. B., Patel, N., Alter, M., Yartel, A. & Ward, J. W. (2012). Recommendations for the identification of chronic Hepatitis C virus infection among persons born during 1945-1965. *MMWR Recommendations and Reports* **61**, 1-32.

Smith, D. B., Bukh, J., Kuiken, C., Muerhoff, A. S., Rice, C. M., Stapleton, J. T. & Simmonds, P. (2014). Expanded classification of hepatitis C virus into 7 genotypes and 67 subtypes: updated criteria and genotype assignment web resource. *Hepatology* **59**, 318-327.

Smith, G. (1985). Filamentous fusion phage: novel expression vectors that display cloned antigens on the virion surface. *Science* **228**, 1315-1317.

Stamataki, Z., Coates, S., Abrignani, S., Houghton, M. & McKeating, J. A. (2011). Immunization of human volunteers with hepatitis C virus envelope glycoproteins elicits antibodies that cross-neutralize heterologous virus strains. *Journal of Infectious Diseases* **204**, 811-813.

Sugg, U., Schneider, W., Hoffmeister, H. E., Huth, C. H., Stephan, W., Lissner, R. & Haase, W. (1985). Hepatitis B immue globulin to prevent non-A, non-B post-transfuison hepatitis. *The Lancet* **325**, 405-406.

Sui, J., Hwang, W. C., Perez, S., Wei, G., Aird, D., Chen, L.-m., Santelli, E., Stec, B., Cadwell, G., Ali, M., Wan, H., Murakami, A., Yammanuru, A., Han, T., Cox, N. J., Bankston, L. A., Donis, R. O., Liddington, R. C. & Marasco, W. A. (2009). Structural and functional bases for broad-spectrum neutralization of avian and human influenza A viruses. *Nature Structural and Molecular Biology* **16**, 265-273.

Swadling, L., Capone, S., Antrobus, R. D., Brown, A., Richardson, R., Newell, E. W., Halliday, J., Kelly, C., Bowen, D., Fergusson, J., Kurioka, A., Ammendola, V., Del Sorbo, M., Grazioli, F., Esposito, M. L., Siani, L., Traboni, C., Hill, A., Colloca, S., Davis, M., Nicosia, A., Cortese, R., Folgori, A., Klenerman, P. & Barnes, E. (2014). A human vaccine strategy based on chimpanzee adenoviral and MVA vectors that primes, boosts, and sustains functional HCV-specific T cell memory. *Science Translational Medicine* **6**, 261ra153-261ra153.

Swadling, L., Halliday, J., Kelly, C., Brown, A., Capone, S., Ansari, M., Bonsall, D., Richardson, R., Hartnell, F., Collier, J., Ammendola, V., Del Sorbo, M., Von Delft, A., Traboni, C., Hill, A., Colloca, S., Nicosia, A., Cortese, R., Klenerman, P., Folgori, A. & Barnes, E. (2016). Highly-immunogenic virally-vectored T-cell vaccines cannot overcome subversion of the T-cell response by HCV during chronic infection. *Vaccines* **4**, 27.

Syder, A. J., Lee, H., Zeisel, M. B., Grove, J., Soulier, E., Macdonald, J., Chow, S., Chang, J., Baumert, T. F., McKeating, J. A., McKelvy, J. & Wong-Staal, F. (2011). Small molecule scavenger receptor BI antagonists are potent HCV entry inhibitors. *Journal of Hepatology* **54**, 48-55.

Tanaka, Y., Nishida, N., Sugiyama, M., Kurosaki, M., Matsuura, K., Sakamoto, N., Nakagawa, M., Korenaga, M., Hino, K., Hige, S., Ito, Y., Mita, E., Tanaka, E., Mochida, S., Murawaki, Y., Honda, M., Sakai, A., Hiasa, Y., Nishiguchi, S., Koike, A., Sakaida, I., Imamura, M., Ito, K., Yano, K., Masaki, N., Sugauchi, F., Izumi, N., Tokunaga, K. & Mizokami, M.

(2009). Genome-wide association of IL28B with response to pegylated interferon-alpha and ribavirin therapy for chronic hepatitis C. *Nature Genetics* **41**, 1105-1109.

Tarr, A., Khera, T., Hueging, K., Sheldon, J., Steinmann, E., Pietschmann, T. & Brown, R. (2015). Genetic diversity underlying the envelope glycoproteins of hepatitis C virus: structural and functional consequences and the implications for vaccine design. *Viruses* **7**, 3995-4046.

Tarr, A. W., Owsianka, A. M., Timms, J. M., McClure, C. P., Brown, R. J. P., Hickling, T. P., Pietschmann, T., Bartenschlager, R., Patel, A. H. & Ball, J. K. (2006). Characterization of the hepatitis C virus E2 epitope defined by the broadly neutralizing monoclonal antibody AP33. *Hepatology* **43**, 592-601.

Tarr, A. W., Owsianka, A. M., Jayaraj, D., Brown, R. J. P., Hickling, T. P., Irving, W. L., Patel, A. H. & Ball, J. K. (2007). Determination of the human antibody response to the epitope defined by the hepatitis C virus-neutralizing monoclonal antibody AP33. *Journal of General Virology* **88**, 2991-3001.

Tarr, A. W., Urbanowicz, R. A., Hamed, M. R., Albecka, A., McClure, C. P., Brown, R. J. P., Irving, W. L., Dubuisson, J. & Ball, J. K. (2011). Hepatitis C patient-derived glycoproteins exhibit marked differences in susceptibility to serum neutralizing antibodies: genetic subtype defines antigenic but not neutralization serotype. *Journal of Virology* **85**, 4246-4257.

Tarr, A. W., Urbanowicz, R. A., Jayaraj, D., Brown, R. J. P., McKeating, J. A., Irving, W. L. & Ball, J. K. (2012). Naturally occurring antibodies that recognize linear epitopes in the amino terminus of the hepatitis C virus E2 protein confer noninterfering, additive neutralization. *Journal of Virology* **86**, 2739-2749.

Tester, I., Smyk-Pearson, S., Wang, P., Wertheimer, A., Yao, E., Lewinsohn, D. M., Tavis, J. E. & Rosen, H. R. (2005). Immune evasion versus recovery after acute hepatitis C virus infection from a shared source. *The Journal of Experimental Medicine* **201**, 1725-1731.

Thein, H.-H., Yi, Q., Dore, G. J. & Krahn, M. D. (2008). Estimation of stage-specific fibrosis progression rates in chronic hepatitis C virus infection: a meta-analysis and meta-regression. *Hepatology* **48**, 418-431.

Thimme, R., Oldach, D., Chang, K.-M., Steiger, C., Ray, S. C. & Chisari, F. V. (2001). Determinants of viral clearance and persistence during acute hepatitis C virus infection. *The Journal of Experimental Medicine* **194**, 1395-1406.

Thimme, R., Bukh, J., Spangenberg, H. C., Wieland, S., Pemberton, J., Steiger, C., Govindarajan, S., Purcell, R. H. & Chisari, F. V. (2002). Viral and immunological determinants of hepatitis C virus clearance, persistence, and disease. *Proceedings of the National Academy of Sciences of the United States of America* **99**, 15661-15668.

Thomas, D. L., Thio, C. L., Martin, M. P., Qi, Y., Ge, D., O/'hUigin, C., Kidd, J., Kidd, K., Khakoo, S. I., Alexander, G., Goedert, J. J., Kirk, G. D., Donfield, S. M., Rosen, H. R., Tobler, L. H., Busch, M. P., McHutchison, J. G., Goldstein, D. B. & Carrington, M. (2009). Genetic variation in IL28B and spontaneous clearance of hepatitis C virus. *Nature* **461**, 798-801.

Thomssen, R., Bonk, S., Propfe, C., Heermann, K. H., Köchel, H. G. & Uy, A. (1992). Association of hepatitis C virus in human sera with β-lipoprotein. *Med Microbiol Immunol* **181**, 293-300.

Thomssen, R., Bonk, S. & Thiele, A. (1993). Density heterogeneities of hepatitis C virus in human sera due to the binding of β-lipoproteins and immunoglobulins. *Med Microbiol Immunol* **182**, 329-334.

Throsby, M., van den Brink, E., Jongeneelen, M., Poon, L. L. M., Alard, P., Cornelissen, L., Bakker, A., Cox, F., van Deventer, E., Guan, Y., Cinatl, J., Meulen, J. t., Lasters, I., Carsetti, R., Peiris, M., de Kruif, J. & Goudsmit, J. (2008). Heterosubtypic neutralizing monoclonal antibodies cross-protective against H5N1 and H1N1 recovered from human IgM+ memory B cells. *PLoS One* **3**, e3942.

Tillmann, H. L., Thompson, A. J., Patel, K., Wiese, M., Tenckhoff, H., Nischalke, H. D., Lokhnygina, Y., Kullig, U., Göbel, U., Capka, E., Wiegand, J., Schiefke, I., Güthoff, W., Grüngreiff, K., König, I., Spengler, U., McCarthy, J., Shianna, K. V., Goldstein, D. B., McHutchison, J. G., Timm, J. & Nattermann, J. (2010). A polymorphism near IL28B is associated with spontaneous clearance of acute hepatitis C virus and jaundice. *Gastroenterology* **139**, 1586-1592.e1581.

Torresi, J. (2017). The rationale for a preventative HCV virus-like particle (VLP) vaccine. *Frontiers in Microbiology* **8**.

Triyatni, M., Vergalla, J., Davis, A. R., Hadlock, K. G., Foung, S. K. H. & Liang, T. J. (2002). Structural features of envelope proteins on hepatitis C virus-like particles as determined by anti-envelope monoclonal antibodies and CD81 binding. *Virology* **298**, 124-132.

Troesch, M., Meunier, I., Lapierre, P., Lapointe, N., Alvarez, F., Boucher, M. & Soudeyns, H. (2006). Study of a novel hypervariable region in hepatitis C virus (HCV) E2 envelope glycoprotein. *Virology* **352**, 357-367.

Tsai, S., Liaw, Y., Chen, M., Huang, C. & Kuo, G. C. (1997). Detection of type 2-like T-helper cells in hepatitis C virus infection: implications for hepatitis C virus chronicity. *Hepatology* **25**, 449-458.

Tscherne, D. M., Jones, C. T., Evans, M. J., Lindenbach, B. D., McKeating, J. A. & Rice, C. M. (2006). Time- and temperature-dependent activation of hepatitis C virus for low-pH-triggered entry. *Journal of Virology* **80**, 1734-1741.

Uduman, M., Yaari, G., Hershberg, U., Stern, J. A., Shlomchik, M. J. & Kleinstein, S. H. (2011). Detecting selection in immunoglobulin sequences. *Nucleic Acids Research* **39**, W499-W504.

Ulsenheimer, A., Lucas, M., Seth, N. P., Gerlach, J. T., Gruener, N. H., Loughry, A., Pape, G. R., Wucherpfennig, K. W., Diepolder, H. M. & Klenerman, P. (2006). Transient immunological control during acute hepatitis C virus infection: ex vivo analysis of helper T-cell responses. *Journal of Viral Hepatitis* **13**, 708-714.

Urbani, S., Amadei, B., Tola, D., Massari, M., Schivazappa, S., Missale, G. & Ferrari, C. (2006). PD-1 expression in acute hepatitis C virus (HCV) infection is associated with HCV-specific CD8 exhaustion. *Journal of Virology* **80**, 11398-11403.

van de Laar, T. J. W., Molenkamp, R., van den Berg, C., Schinkel, J., Beld, M. G. H. M., Prins, M., Coutinho, R. A. & Bruisten, S. M. (2009). Frequent HCV reinfection and superinfection in a cohort of injecting drug users in Amsterdam. *Journal of Hepatology* **51**, 667-674.

Vanwolleghem, T., Bukh, J., Meuleman, P., Desombere, I., Meunier, J.-C., Alter, H., Purcell, R. H. & Leroux-Roels, G. (2008). Polyclonal immunoglobulins

from a chronic hepatitis C virus patient protect human liver–chimeric mice from infection with a homologous hepatitis C virus strain. *Hepatology* **47**, 1846-1855.

Verstrepen, B. E., Depla, E., Rollier, C. S., Mares, G., Drexhage, J. A. R., Priem, S., Verschoor, E. J., Koopman, G., Granier, C., Dreux, M., Cosset, F. L., Maertens, G. & Heeney, J. L. (2011). Clearance of genotype 1b hepatitis C virus in chimpanzees in the presence of vaccine-induced E1-neutralizing antibodies. *The Journal of Infectious Diseases* **204**, 837-844.

Vietheer, P. T., Boo, I., Gu, J., McCaffrey, K., Edwards, S., Owczarek, C., Hardy, M. P., Fabri, L., Center, R. J., Poumbourios, P. & Drummer, H. E. (2017). The core domain of hepatitis C virus glycoprotein E2 generates potent cross-neutralizing antibodies in guinea pigs. *Hepatology* **65**, 1117-1131.

Vieyres, G., Thomas, X., Descamps, V., Duverlie, G., Patel, A. H. & Dubuisson, J. (2010). Characterization of the envelope glycoproteins associated with infectious hepatitis C virus. *Journal of Virology* **84**, 10159-10168.

Vieyres, G., Dubuisson, J. & Patel, A. H. (2011). Characterization of antibody-mediated neutralization directed against the hypervariable region 1 of hepatitis C virus E2 glycoprotein. *The Journal of General Virology* **92**, 494-506.

Voisset, C., Callens, N., Blanchard, E., Op De Beeck, A., Dubuisson, J. & Vu-Dac, N. (2005). High density lipoproteins facilitate hepatitis C virus entry through the scavenger receptor class B type I. *Journal of Biological Chemistry* **280**, 7793-7799.

von Hahn, T., Yoon, J. C., Alter, H., Rice, C. M., Rehermann, B., Balfe, P. & McKeating, J. A. (2007). Hepatitis C virus continuously escapes from neutralizing antibody and T-cell responses during chronic infection in vivo. *Gastroenterology* **132**, 667-678.

Wahid, A., Helle, F., Descamps, V., Duverlie, G., Penin, F. & Dubuisson, J. (2013). Disulfide bonds in hepatitis C virus glycoprotein E1 control the assembly and entry functions of E2 glycoprotein. *Journal of Virology* **87**, 1605-1617.

Wakita, T., Pietschmann, T., Kato, T., Date, T., Miyamoto, M., Zhao, Z., Murthy, K., Habermann, A., Krausslich, H.-G., Mizokami, M., Bartenschlager, R. & Liang, T. J. (2005). Production of infectious hepatitis C virus in tissue culture from a cloned viral genome. *Nature Medicine* **11**, 791-796.

Walewski, J. L., Keller, T. R., Stump, D. D. & Branch, A. D. (2001). Evidence for a new hepatitis C virus antigen encoded in an overlapping reading frame. *RNA* **7**, 710-721.

Wang, W., Guan, M., Liu, Y., Xu, Q., Peng, H., Liu, X., Tang, Z., Zhu, Y., Wu, D., Ren, H., Zhao, P. & Qi, Z. (2014). Alanine scanning mutagenesis of hepatitis C virus E2 cysteine residues: insights into E2 biogenesis and antigenicity. *Virology* **448**, 229-237.

Washburn, M. L., Bility, M. T., Zhang, L., Kovalev, G. I., Buntzman, A., Frelinger, J. A., Barry, W., Ploss, A., Rice, C. M. & Su, L. (2011). A humanized mouse model to study hepatitis C virus infection, immune response, and liver disease. *Gastroenterology* **140**, 1334-1344.

Watanabe, H., Saito, T., Shinzawa, H., Okumoto, K., Hattori, E., Adachi, T., Takeda, T., Sugahara, K., Ito, J.-i., Saito, K., Togashi, H., Suzuki, R., Hayashi, M., Miyamura, T., Matsuura, Y. & Kawata, S. (2003).

Spontaneous elimination of serum hepatitis C virus (HCV) RNA in chronic HCV carriers: a population-based cohort study. *Journal of Medical Virology* **71**, 56-61.

Wedemeyer, H., He, X.-S., Nascimbeni, M., Davis, A. R., Greenberg, H. B., Hoofnagle, J. H., Liang, T. J., Alter, H. & Rehermann, B. (2002). Impaired effector function of hepatitis C virus-specific CD8+ T cells in chronic hepatitis C virus infection. *The Journal of Immunology* **169**, 3447-3458.

Wedemeyer, H., Schuller, E., Schlaphoff, V., Stauber, R. E., Wiegand, J., Schiefke, I., Firbas, C., Jilma, B., Thursz, M., Zeuzem, S., Hofmann, W. P., Hinrichsen, H., Tauber, E., Manns, M. P. & Klade, C. S. (2009). Therapeutic vaccine IC41 as late add-on to standard treatment in patients with chronic hepatitis C. *Vaccine* **27**, 5142-5151.

Weiner, A. J., Brauer, M. J., Rosenblatt, J., Richman, K. H., Tung, J., Crawford, K., Bonino, F., Saracco, G., Choo, Q.-L., Houghton, M. & Han, J. H. (1991). Variable and hypervariable domains are found in the regions of HCV corresponding to the flavivirus envelope and NS1 proteins and the pestivirus envelope glycoproteins. *Virology* **180**, 842-848.

Weiner, A. J., Geysen, H. M., Christopherson, C., Hall, J. E., Mason, T. J., Saracco, G., Bonino, F., Crawford, K., Marion, C. D. & Crawford, K. A. (1992). Evidence for immune selection of hepatitis C virus (HCV) putative envelope glycoprotein variants: potential role in chronic HCV infections. *Proceedings of the National Academy of Sciences of the United States of America* **89**, 3468-3472.

Weiner, A. J., Paliard, X., Selby, M. J., Medina-Selby, A., Coit, D., Nguyen, S., Kansopon, J., Arian, C. L., Ng, P., Tucker, J., Lee, C.-T., Polakos, N. K., Han, J., Wong, S., Lu, H.-H., Rosenberg, S., Brasky, K. M., Chien, D., Kuo, G. & Houghton, M. (2001). Intrahepatic genetic inoculation of hepatitis C virus RNA confers cross-protective immunity. *Journal of Virology* **75**, 7142-7148.

Whidby, J., Mateu, G., Scarborough, H., Demeler, B., Grakoui, A. & Marcotrigiano, J. (2009). Blocking hepatitis C virus infection with recombinant form of envelope protein 2 ectodomain. *Journal of Virology* **83**, 11078-11089.

WHO (2016). Guidelines for the screening, care and treatment of persons with chronic Hepatitis C infection. Edited by W. H. Organization.

WHO (2017). Global hepatitis Report, 2017. Edited by W. H. Organization. Geneva.

Wong, J. A. J.-X., Bhat, R., Hockman, D., Logan, M., Chen, C., Levin, A., Frey, S. E., Belshe, R. B., Tyrrell, D. L., Law, J. L. M. & Houghton, M. (2014). Recombinant hepatitis C virus envelope glycoprotein vaccine elicits antibodies targeting multiple epitopes on the envelope glycoproteins associated with broad cross-neutralization. *Journal of Virology* **88**, 14278-14288.

Workowski, K. A. & Bolan, G. A. (2015). Emerging issues: Hepatitis C. *Sexcually Transmitted Diseases Treatment Guidelines, 2015, MMWR Recommendations and Reports* **64**, 17-20.

Wrammert, J., Koutsonanos, D., Li, G.-M., Edupuganti, S., Sui, J., Morrissey, M., McCausland, M., Skountzou, I., Hornig, M., Lipkin, W. I., Mehta, A., Razavi, B., Del Rio, C., Zheng, N.-Y., Lee, J.-H., Huang, M., Ali, Z., Kaur, K., Andrews, S., Amara, R. R., Wang, Y., Das, S. R., O'Donnell, C. D., Yewdell, J. W., Subbarao, K., Marasco, W. A., Mulligan, M. J., Compans, R., Ahmed, R. & Wilson, P. C. (2011). Broadly cross-reactive antibodies

dominate the human B cell response against 2009 pandemic H1N1 influenza virus infection. *The Journal of Experimental Medicine* **208**, 181-193.

Yaari, G., Uduman, M. & Kleinstein, S. H. (2012). Quantifying selection in high-throughput Immunoglobulin sequencing data sets. *Nucleic Acids Research* **40**, e134-e134.

Yaari, G., Vander Heiden, J. A., Uduman, M., Gadala-Maria, D., Gupta, N., Stern, J. N. H., O'Connor, K. C., Hafler, D. A., Laserson, U., Vigneault, F. & Kleinstein, S. H. (2013). Models of somatic hypermutation targeting and substitution based on synonymous mutations from high-throughput immunoglobulin sequencing data. *Frontiers in Immunology* **4**, 358.

Yagnik, A. T., Lahm, A., Meola, A., Roccasecca, R. M., Ercole, B. B., Nicosia, A. & Tramontano, A. (2000). A model for the hepatitis C virus envelope glycoprotein E2. *Proteins: Structure, Function, and Bioinformatics* **40**, 355-366.

Yamaguchi, N., Tokushige, K., Yamauchi, K. & Hayashi, N. (2000). Humoral immune response in Japanese acute hepatitis patients with hepatitis C virus infection. *Canadian Journal of Gastroenterology & Hepatology* **14**, 593 - 598.

Yang, W., Qiu, C., Biswas, N., Jin, J., Watkins, S. C., Montelaro, R. C., Coyne, C. B. & Wang, T. (2008). Correlation of the tight junction-like distribution of claudin-1 to the cellular tropism of hepatitis C virus. *Journal of Biological Chemistry* **283**, 8643-8653.

Youn, J.-W., Hu, Y.-W., Tricoche, N., Pfahler, W., Shata, M. T., Dreux, M., Cosset, F.-L., Folgori, A., Lee, D.-H., Brotman, B. & Prince, A. M. (2008). Evidence for protection against chronic hepatitis C virus infection in chimpanzees by immunization with replicating recombinant vaccinia virus. *Journal of Virology* **82**, 10896-10905.

Yutani, S., Komatsu, N., Shichijo, S., Yoshida, K., Takedatsu, H., Itou, M., Kuromatu, R., Ide, T., Tanaka, M., Sata, M., Yamada, A. & Itoh, K. (2009). Phase I clinical study of a peptide vaccination for hepatitis C virus-infected patients with different human leukocyte antigen-class I-A alleles. *Cancer Science* **100**, 1935-1942.

Zaltron, S., Spinetti, A., Biasi, L., Baiguera, C. & Castelli, F. (2012). Chronic HCV infection: epidemiological and clinical relevance. *BMC Infectious Diseases* **12**, 1-7.

Zeisel, M. B., Koutsoudakis, G., Schnober, E. K., Haberstroh, A., Blum, H. E., Cosset, F.-L., Wakita, T., Jaeck, D., Doffoel, M., Royer, C., Soulier, E., Schvoerer, E., Schuster, C., Stoll-Keller, F., Bartenschlager, R., Pietschmann, T., Barth, H. & Baumert, T. F. (2007). Scavenger receptor class B type I is a key host factor for hepatitis C virus infection required for an entry step closely linked to CD81. *Hepatology* **46**, 1722-1731.

Zhang, J., Randall, G., Higginbottom, A., Monk, P., Rice, C. M. & McKeating, J. A. (2004). CD81 is required for hepatitis C virus glycoprotein-mediated viral infection. *Journal of Virology* **78**, 1448-1455.

Zhang, P., Wu, C. G., Mihalik, K., Virata-Theimer, M. L., Yu, M.-y. W., Alter, H. J. & Feinstone, S. M. (2007). Hepatitis C virus epitope-specific neutralizing antibodies in Igs prepared from human plasma. *Proceedings of the National Academy of Sciences of the United States of America* **104**, 8449-8454.

Zhang, P., Zhong, L., Struble, E. B., Watanabe, H., Kachko, A., Mihalik, K., Virata-Theimer, M. L., Alter, H. J., Feinstone, S. & Major, M. (2009).

Depletion of interfering antibodies in chronic hepatitis C patients and vaccinated chimpanzees reveals broad cross-genotype neutralizing activity. *Proceedings of the National Academy of Sciences of the United States of America* **106**, 7537-7541.

Zhong, J., Gastaminza, P., Cheng, G., Kapadia, S., Kato, T., Burton, D. R., Wieland, S. F., Uprichard, S. L., Wakita, T. & Chisari, F. V. (2005). Robust hepatitis C virus infection in vitro. *Proceedings of the National Academy of Sciences of the United States of America* **102**, 9294-9299.

Zibert, A., Meisel, H., Kraas, W., Schulz, A., Jung, G. & Roggendorf, M. (1997). Early antibody response against hypervariable region 1 is associated with acute self-limiting infections of hepatitis C virus. *Hepatology* **25**, 1245-1249.